MICROFLUIDIC PLATFORM FOR BILAYER EXPERIMENTATION

FROM A RESEARCH TOOL TOWARDS DRUG SCREENING

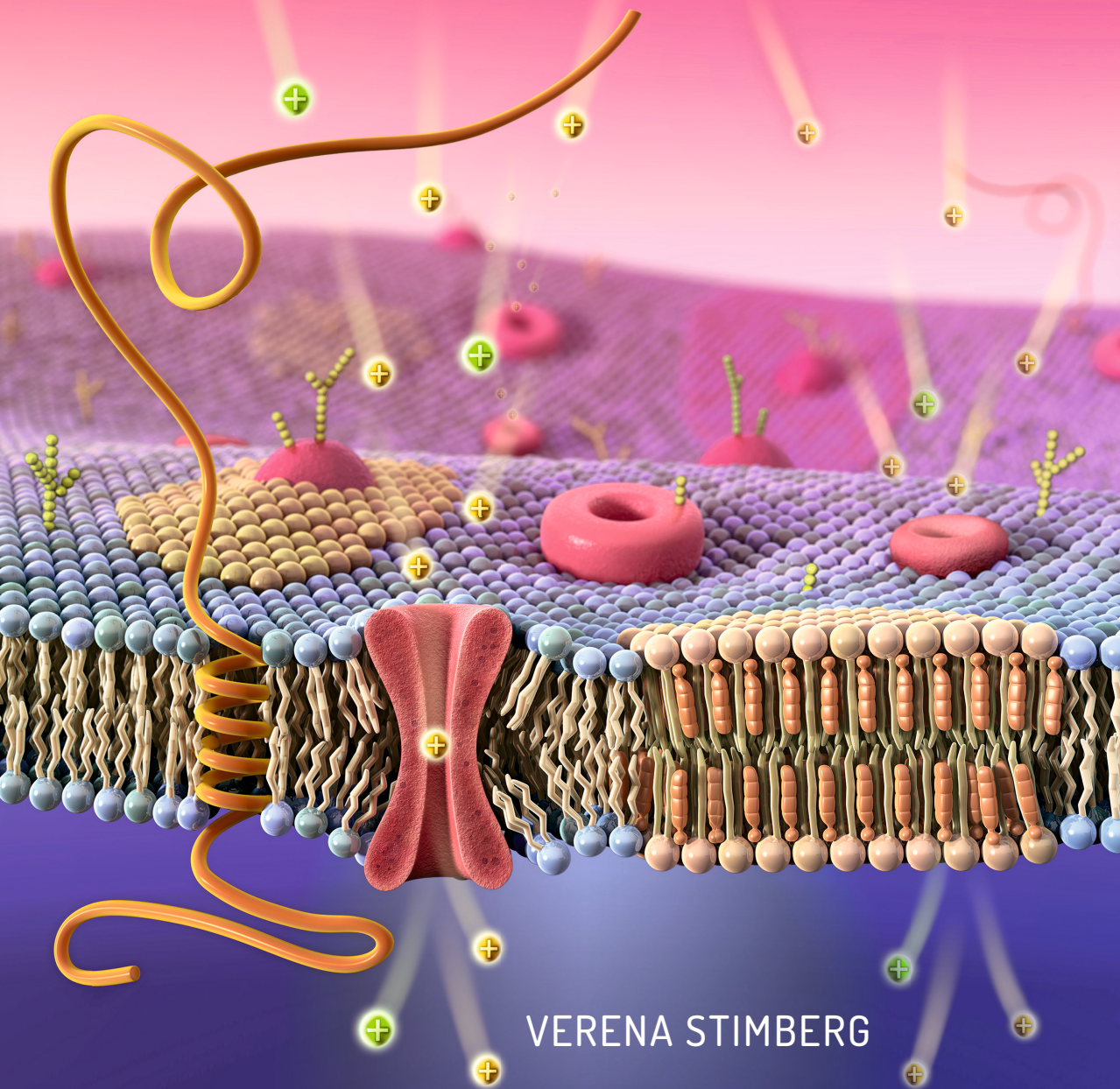

VERENA STIMBERG

MICROFLUIDIC PLATFORM FOR BILAYER EXPERIMENTATION

FROM A RESEARCH TOOL TOWARDS DRUG SCREENING

Verena Stimberg

The research described in this thesis was performed at the BIOS – Lab on a Chip group, which is part of MESA+ Institute for Nanotechnology, and MIRA Institute for Biomedical Technology and Technical Medicine, at the University of Twente. This thesis is part of NanoNextNL, a micro and nanotechnology innovation consortium of the Government of the Netherlands and 130 partners from academia and industry. More information on www.nanonextnl.nl.

Members of the committee:

Chairman	Prof. dr. H. Wallinga	University of Twente
Promotor	Prof. dr. ir. A. van den Berg	University of Twente
Assistant promotor	Dr. ir. S. Le Gac	University of Twente
Members	Prof. dr. ir. P. Jonkheijm	University of Twente
	Prof. dr. V. Subramaniam	FOM Institute AMOLF, University of Twente
	Prof. dr. ir. Harro van Lente	University of Utrecht
	Dr. A. Koçer	University of Groningen
	Prof. dr. O.S. Andersen	Weill Cornell Medical College

Title:	Microfluidic platform for bilayer experimentation – From a research tool towards drug screening
Author:	Verena Stimberg
ISBN:	978-90-365-3741-4
DOI:	10.3990/1.9789036537414
Publisher:	Wöhrmann Print Service, Zutphen, The Netherlands
Cover images:	Nymus 3D. Picture of the membrane has been published as cover in Stimberg et al., "High Yield, Reproducible and Quasi-Automated Bilayer Formation in a Microfluidic Format.", Small, 2013, 9, 1076. Copyright Wiley-VCH Verlag GmbH & Co. KGaA, reproduced with permission.
Cover design:	Simon Stimberg

MICROFLUIDIC PLATFORM FOR BILAYER EXPERIMENTATION

FROM A RESEARCH TOOL TOWARDS DRUG SCREENING

PROEFSCHRIFT

ter verkrijging van
de graad van doctor aan de Universiteit Twente,
op gezag van de rector magnificus,
prof.dr. H. Brinksma,
volgens besluit van het College voor Promoties
in het openbaar te verdedigen
op vrijdag 10 oktober 2014 om 14:45 uur

door

Verena Carolin Stimberg
geboren op 9 februari 1985
te Münster, Duitsland

Dit proefschrift is goedgekeurd door:

Promotor:	Prof. dr. ir. A. van den Berg
Assistant promotor:	Dr. ir. S. Le Gac

To Stephan

who always puts a smile on my face

Table of Contents

Chapter 1

Aim and outline of the thesis

The aim of this thesis, which is the development of a microfluidic platform for bilayer experimentation with the potential for drug screening on ion channels, is introduced in this chapter. After a short presentation of the field of drug screening, an outline of this thesis is given, together with a brief summary of the different chapters.

1.1 Drug screening on ion channels

Ion channels are located in the membrane of a cell, and they are responsible for a number of basic and highly diverse physiological processes such as muscle and nerve excitation, regulation of the blood pressure, learning, memory, fertilization or cell death.[1] As Ashcroft nicely said, "your ability to read and understand this page depends on the activity of ion channels in your eye and brain".[1] Consequently, the mutation in ion channel genes resulting in alteration of ion channel function has a huge impact on these basic but essential processes. These mutations lead to diseases, the so-called channelopathies, such as cystic fibrosis, epilepsy, and cardiac dysfunction.[2,3] For these reasons, ion channels are attractive targets for drug development, and ~13% of the known drugs exert their therapeutic action on these proteins.[4]

Nonetheless, drug screening on ion channels is highly challenging due to the complexity of these proteins and their high degree of structural diversity, and, interestingly, current ion channel drugs have been discovered by serendipity during traditional pharmacological methods.[4] Currently, fluorescent-based assays are applied for high throughput screening, where the ion flux is measured indirectly via, e.g., ion sensitive dyes. These techniques however, are prone to artefacts leading to the risk of missing high quality hits.[4,5] Alternatively, ion channel function is studied in detail with the patch clamp technique.[6] Even though this technique provides high content information on the single ion channel behavior, patch clamping is a manual and tedious procedure, and requires a highly skilled operator.[7] Therefore, this technique is not amenable to high throughput, and screening of a large amount of drugs on ion channel activity. Automation of the patch clamp technique has brought a certain increase in throughput while providing the same quality of information as manual patch-clamp.[8] However, the throughput of automated patch clamp (APC) techniques cannot compete with optical methods, and additionally, costs associated with APC are very high. Furthermore, all these assays work on cell models, which is a limitation in itself.[9] Currently, pharmaceutical companies are embedding new technologies to improve the success of the final drug.[5] At the same time, recordings using cell-free systems such as bilayer lipid membranes (BLMs) are gaining more and more interest.[9]

Bilayer lipid membranes are planar and simplified models of the cell membrane, which are conventionally formed across a vertical microaperture, machined in a hydrophobic partition, and sandwiched between two mL-sized reservoirs with buffer solution.[10] Ion channels are inserted in the bilayers, for instance by fusion of proteoliposomes,[11] to be studied in a tailored lipidic environment. The conventional bilayer set up however is not suitable for high throughput applications, and furthermore, standard protocols for bilayer formation are not user-friendly, neither reproducible, require close monitoring

and manual intervention, and suffer from a low success yield, all these aspects being essential for automation.[12] Additionally, multiplexing is not favorable, and large volumes are handled. Recently, the field of microfabrication has brought a number of advantages for bilayer experimentation to overcome these issues. For instance, the use of smaller structures decreases the volumes and results in faster assays and improved bilayer stability, whereas the microfluidic format is ideal for automation and multiplexing. Furthermore, the horizontal arrangement of the aperture in most of these systems, favors the implementation of other characterization schemes than electrophysiology, such as optical techniques including high-resolution microscopy. So far, a number of microfluidic and miniaturized bilayer platforms have been reported, including half-open, fully-closed and DIB systems, as recently reviewed by others.[12,13]

The goal of this PhD project was to develop an alternative platform for bilayer experimentation and drug screening on ion channels. In this context, a versatile microfluidic device has been realized which exhibits key features for drug screening applications and high content information. The work has been performed in the BIOS – Lab on a Chip group, which is part of MESA+ Institute for Nanotechnnology, and MIRA Institute for Biomedical Technology and Technical Medicine, at the University of Twente. This PhD project is funded by NanoNextNL, a micro and nanotechnology innovation consortium of the Government of the Netherlands and 130 partners from academia and industry. This project is part of the subprogram "Nanoscale biomolecular interactions in disease" led by Prof. Vinod Subramaniam. More information on www.nanonextnl.nl.

1.2 Thesis outline

An outline of the thesis with a brief introduction to the content of all chapters is provided below.

First, the process of drug screening on ion channels is presented, together with a detailed overview of currently utilized techniques for this purpose, as well as a critical discussion on their advantages and limitations (chapter 2). As an alternative to the cell model, bilayer lipid membranes (BLMs) are introduced. A number of membrane models such as vesicles, suspended, supported and droplet bilayers, are reviewed in terms of formation techniques and bilayer characteristics. The alternative use of BLMs instead of cell models for drug screening is proposed, and advantages brought by miniaturization and microfluidics in this field are highlighted. Finally, existing miniaturized bilayer platforms are discussed for their amenability to automation and

high throughput screening, as well as their potential as future drug screening platforms.

We have developed a fully closed microfluidic device for bilayer experimentation, which is presented in chapter 3. In this device, bilayers are formed across one experimentation site in a quasi-automated way, and with a high success yield. Bilayers are subsequently characterized using optical - bright field microscopy - and electrophysiological techniques. Additionally, recordings on single pore forming species (α-hemolysin and gramicidin) are presented. Finally, a potential drug-screening assay is proposed, where changes in the gramicidin activity are sensed electrophysiologically after exposure of the membrane to external soluble factors (ethanol & acetylsalicylic acid).

As demonstrated in chapter 3, bilayers can be imaged using bright field microscopy. This approach enables to monitor the process of bilayer formation, and only provides macroscopic information, e.g., on the surface area. However, knowledge on the molecular scale is lacking. Therefore, the platform is adapted for high-resolution confocal microscopy, allowing visualization of phase separation processes in ternary membranes. In a next step, confocal imaging is utilized to study phospholipid diffusion in the membrane to assess the membrane fluidity. Finally, the optical bilayer characterization (thickness and fluidity) is combined with electrophysiological measurements on the gramicidin activity to demonstrate the potential of the platform for multi-parametric detection schemes (chapter 4).

Next to the direct interaction of a drug compound with an ion channel, non-specific effects of drugs can occur, through changes in the bilayer properties, which can in turn indirectly influence ion channel activity.[14] To investigate this, the combination of the confocal and electrophysiological measurement approach proposed in chapter 4 is applied to study the influence of cholesterol on the bilayer properties, and the indirect impact of its presence on ion channel activity. BLMs are characterized in terms of thickness and fluidity, as before, while at the same time the gramicidin activity is recorded for membranes supplemented with cholesterol (15 and 40%) or not (chapter 5).

Key requirements for high throughput drug-screening applications are automation and multiplexing. Multiplexing of the microfluidic device is explored, by proposing two designs with up to four experimentation sites in parallel. Additionally, the bilayer formation procedure is adapted to reduce the number of liquid handling steps, towards automation of the process. In a series of preliminary experiments, bilayers are characterized in the two designs, and gramicidin activity is recorded electrophysiologically (chapter 6).

Chapter 7 focuses on technology assessment of the herein presented microfluidic platform. For that purpose, a workshop is organized gathering people with a variety of backgrounds to define a possible road map for commercialization of the microfluidic bilayer platform, and to discuss factors that may play an important role during this process. Following this, four possible applications of the platform are selected, and their innovation pathways are discussed in terms of possible hurdles and opportunities, as well as their impact on society.

In the last chapter, first the results described in this thesis are summarized, followed by an outlook for future developments and other possible applications for the microfluidic platform developed in this work (chapter 8).

1.3 References

1. Ashcroft, F. M., From molecule to malady. *Nature* **2006,** *440* (7083), 440-447.
2. Filmore, D., It's a GPCR world. *Modern Drug Discovery* **2004,** *7* (11), 24-28.
3. Hübner, C. A.; Jentsch, T. J., Ion channel diseases. *Human Molecular Genetics* **2002,** *11* (20), 2435-2445.
4. Clare, J. J., Targeting ion channels for drug discovery. *Discovery medicine* **2010,** *9* (46), 253-260.
5. Möller, C.; Slack, M., Impact of new technologies for cellular screening along the drug value chain. *Drug Discovery Today* **2010,** *15* (9–10), 384-390.
6. Hamill, O. P.; Marty, A.; Neher, E.; Sakmann, B.; Sigworth, F. J., Improved patch-clamp techniques for high-resolution current recording from cells and cell-free membrane patches. *Pflugers Arch* **1981,** *391* (2), 85-100.
7. Xu, J.; Wang, X.; Ensign, B.; Li, M.; Wu, L.; Guia, A.; Xu, J., Ion-channel assay technologies: quo vadis? *Drug Discovery Today* **2001,** *6* (24), 1278-1287.
8. Steller, L.; Kreir, M.; Salzer, R., Natural and artificial ion channels for biosensing platforms. *Anal Bioanal Chem* **2012,** *402* (1), 209-230.
9. Farre, C.; Fertig, N., HTS techniques for patch clamp-based ion channel screening – advances and economy. *Expert Opinion on Drug Discovery* **2012,** *7* (6), 515-524.
10. Montal, M.; Mueller, P., Formation of Bimolecular Membranes from Lipid Monolayers and a Study of their Electrical Properties. *Proceedings of the National Academy of Sciences of the United States of America* **1972,** *69* (12), 3561-3566.
11. Cohen, F. S., Fusion of Liposomes to Planar Bilayers. In *Ion Channel Reconstitution*, Miller, C., Ed. Plenum Press: New York, **1986**.
12. Zagnoni, M., Miniaturised technologies for the development of artificial lipid bilayer systems. *Lab on a Chip* **2012,** *12* (6), 1026-1039.
13. Kongsuphol, P.; Fang, K. B.; Ding, Z., Lipid bilayer technologies in ion channel recordings and their potential in drug screening assay. *Sensors and Actuators B: Chemical* **2013,** *185* (0), 530-542.

14. Lundbaek, J. A., Lipid bilayer-mediated regulation of ion channel function by amphiphilic drugs. *Journal of General Physiology* **2008,** *131* (5), 421-429.

Miniaturized bilayer platforms for drug screening on ion channels

Ion channels are involved in a large variety of diseases and consequently, they are prominent targets for the development of new drugs. In this chapter, the process of drug screening on ion channels is shortly described, and currently utilized screening techniques are presented, together with their advantages and limitations. As an alternative to the currently widely used cells, bilayer lipid membrane (BLM) models are proposed as alternative format for drug screening, and various types of bilayer models such as vesicles, suspended, supported and droplet bilayers are briefly introduced. Next, the advantages brought by miniaturization and microfluidics in this field are highlighted and existing platforms are discussed for their amenability to automated and stable bilayer formation, and multiplexing. Finally, the potential of these miniaturized bilayer platforms for drug screening on ion channels is considered.[1]

[1] Manuscript in preparation

2.1 Introduction

Ion channels, which are transmembrane proteins, are present in all cell types throughout the human body, and are encoded by more than 300 human genes.[1,2] These proteins are responsible for the passive and selective transport of different kinds of ions via a central pore across the membrane, and often are specific for one type of ions (Na^+, K^+, Ca^{2+}, or Cl^-).[2-3] The ion flux, which is associated with the creation of an electrical current through the membrane, is triggered through gating, which causes activation of the ion channel via conformational rearrangements, resulting in opening and closing of the pore. Possible gating mechanisms include binding of a ligand, a local change in the potential across the membrane, mechanical stimuli, or a change in temperature.[3,4] At the scale of the organisms, ion channels are responsible for instance for a number of basic yet essential physiological processes allowing us to move, feel, think and learn.[1] Mutations in genes encoding ion channels may modify their function (loss- or gain-of-function) and cause diseases, the so called channelopathies, or a great variety of disorders such as epilepsy, myotonia, ataxia, or cardiac arrhythmia.[1,5]

Due to their central role, ion channels are promising candidates for the development of new drugs. Currently, 13-15% of the drugs on the market target these proteins, which corresponds to worldwide sales of several billion dollars.[6] However, it is worth noticing that ion channels have been under-targeted so far, mostly due to a lack of structural information until recently, and the difficulty to assess the efficiency of drugs on those proteins.[1] Furthermore, in the last decades, a number of drugs approved by the US Food and Drug Administration (FDA) turned out to present side effects such as induction of prolonged cardiac repolarization (long QT), associated with a severe type of cardiac arrhythmia, that leads to sudden death.[5] The drugs had to be withdrawn from the market, and in addition to this, the FDA introduced new regulations to screen all drug candidates on cardiac ion channels to assess possible risks of arrhythmia.[7,8] Therefore, pharmaceutical companies urgently had to implement dedicated assays for safety screening on hERG, a cardiac potassium channel central in this long QT process. Altogether, not only ion channels have become major targets for the design of new drugs for the pharmaceutical industries, but cardiac ion channels must now also be included in any drug screening process for safety purposes.

In general, drug screening on ion channels proceeds as for any other drug, and is described in detail elsewhere.[8-10] Briefly, first a molecular target is selected in the *basic research* stage, which remains the most important step,[10] followed by a *primary screening* where a compound library is tested on the identified target, this requiring a

throughput of >100 000 compounds per day. [9,11] Next, the most promising lead compounds are further optimized during the *secondary screening* (ideal throughput of 10-100 compounds per day).[9] Additionally, the potential drug is tested on cardiac ion channels such as hERG in the *safety screening* phase (similar throughput as for the *secondary screening*).[5,8] As recalled by Xu et al., drug screening on ion channels must fulfill a number of key-requirements, which are: throughput, sensitivity, specificity, information content, robustness, flexibility, cost, and physiological relevance,[8] those being slightly different for the different screening segments. Those criteria will be used in the rest of this chapter to assess the different technologies discussed.

In this chapter, existing and routinely used technologies to test drugs on ion channel proteins are presented, and their strengths and weaknesses critically assessed. Miniaturized bilayer platforms are introduced, which have been proposed as promising alternatives to the currently used cell-based assays, after a short description of the structure of the cell membrane and a presentation of artificial bilayer models. Next, essential features microfluidic bilayer platforms must present before they can be utilized in the field of drug screening on ion channels are discussed, those comprising automation of the membrane formation, stability of the bilayer structure, multiplexing, and possible recording on relevant ion channels including drug screening assays. Finally, the current and future place of these microfluidic bilayer platforms in the drug screening market segment is evaluated. It should be noted that the goal of this chapter is not to review microfluidic bilayer platforms, for which interested readers are referred to excellent recent articles,[12-14] but more to focus on a number of key features for reliable and high throughput drug screening on membrane proteins.

2.2 Current drug screening assays for ion channels

Various approaches and techniques currently dominate the field of drug screening on ion channels. On one hand, the patch clamp technique directly measures ion channel activity by recording currents across cell membranes, and, on the other hand, indirect assays examine flux of ions or local changes in the membrane potential. The latter techniques are lacking information on the ion channel function, and only assess the effect of tested compounds in a yes-or-no manner, whereas the former approach suffers from a low throughput. Automated patch clamp platforms have been developed for increased throughput while granting direct information on ion channel activity. Both direct approaches and one indirect assay are presented in **Figure 2.1** and in the following section, with a discussion on their performance and limitations.

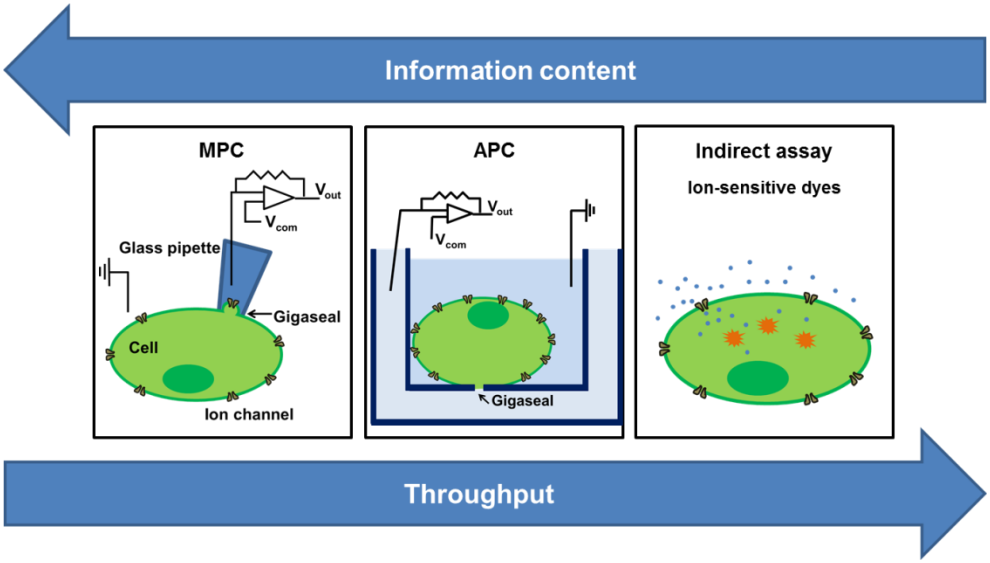

Figure 2.1. Drug screening on ion channels. Assays currently applied for drug screening offer various performances in terms of information content and throughput. The manual patch clamp technique (left) directly measures the ion channel activity with respect to the target compound using electrophysiology, yet in a low-throughput manner. Alternatively, the flux of ions is measured with a high throughput but indirectly with, e.g., ion-sensitive fluorescent dyes (right). Finally, automated patch clamp platforms (APC, middle) allow high-quality electrophysiological recordings on ion channels, with a medium throughput.

2.2.1 Patch clamp technique

Patch clamp technique, which has been introduced in the 70's by Neher and Sackmann,[15] is the gold standard for ion channel measurements.[16] Manual patch clamp technique (MPC) relies on the establishment of a tight seal (so called gigaseal) between a glass pipette with a tip of a few micrometer diameter and the membrane of a cell. One electrode is inserted in the pipette buffer, and a second one in the bath solution surrounding the cell enabling high resolution electrophysiological recordings across the cell membrane. The cleanliness of the pipette tip and the precise shape of the apertures are crucial for the creation of such a gigaseal, and, in turn, for low noise recordings,[16] which is essentially the key to study the activity of individual ion channels with a sub-picoampere and sub-millisecond resolution.[16] This powerful approach provides plethora information on ion channel activity, down to the single ion channel level: (i) the conductance and possible sub-conductance states of a single pore, the latter being either natural or induced intermediate states; (ii) the open probability and the respective durations of the open and closed states, revealing thereby single channel kinetics; as well as (iii) insight into the channel gating mechanism.[17]

In terms of drug screening, the activity of the targeted ion channel, which has been over-expressed, is recorded while exposing the cell to drug candidates. Ideally, a range of concentrations is tested to yield an IC_{50} curve. Manual patch clamp provides a direct readout of the response of individual ion channels to drug candidates, with high quality and high fidelity information, as well as great degree of flexibility in the experiments, with various recording configurations (e.g., cell-attached, whole-cell, perforated patch, inside-out, and outside-out).[17,18] However, the downside is that patch clamp is a labor-intensive technique, demanding a highly skilled operator, and subsequently, it suffers from an extremely low throughput of only 10's of compounds per week, and high costs.[11] Therefore, it is mainly applied in the *basic research* step and for target validation in the *secondary screen*ing, where data quality is more important than throughput.[9,11]

2.2.2 High-throughput drug screening assays

Due to these limitations encountered with MPC in terms of throughput and user-friendliness, other assays, which are faster and easier to implement, while however providing indirect information on the ion channel activity, are preferred for the *primary screening*. These assays examine for instance the ion-flux, as well as binding events, as discussed in detail in excellent reviews,[8] and shortly recalled here. In a first strategy, the amount of ions flown through the membrane is quantified in the intracellular compartment, using fluorescent or radioactive probes. Cells are loaded with ion-sensitive dyes, mostly targeting Ca^{2+}, and changes in fluorescence are detected for instance using Fluorometric Imaging Plate Reader (FLIPR™, Molecular Devices, Sunnyvale, CA).[8,9] Alternatively, cells are incubated with $^{86}Rb^{+}$ ions, whose efflux through potassium or non-selective cationic channels is monitored by radioactive counting.[10] Along a different principle, fluorescent voltage sensor probes are attached to the cell membrane. Upon depolarization of the membrane, the fluorescent emission is shifted if FRET probes are used, or the fluorescence intensity increases upon binding of the dye to intracellular structures.[9,10] Finally, interaction of the targeted compound to the ion channel is monitored in a so-called binding assay.[8]

These alternative assays provide very high throughput (up to 10^5 compounds per day),[9] they are very cheap, while being straightforward,[8,9] which justifies that they are routinely applied for *primary screening*. However, the readout is indirect, which, on one hand, is associated with a high risk of false negatives and positives,[8] and, on the other hand, provides little information on the effect of the tested compound (low temporal resolution, ion channel kinetics). Additionally, most assays are specific to certain types of ions, which limits their flexibility. Last, signals are collected from whole cells, and no information on the single channel behavior is available. In conclusion, indirect

assays meet the set requirements for *primary screening* in terms of high throughput and low costs, but not those of sensitivity, selectivity, flexibility, and robustness.[8,11]

2.2.3 Automated patch clamp

In the last decade, another approach has emerged with the development of automated patch-clamp systems (APC), to preserve the high information content of electrophysiological measurements, while increasing the analysis throughput and additionally reducing the level of technicality.[11] In most automated patch clamp (APC) platforms, the glass micropipette is replaced by a planar substrate comprising a micrometer-sized aperture, as realized for the first time 12 years ago.[19] Using this configuration, cells are patched automatically, which suppresses the need for a skilled operator, and apertures can easily be arrayed for parallelization of the experiments. Since the introduction of the first APC platform, the field has evolved very rapidly, with an increase in the number of experimentation sites, reaching a number of 384 today. Additionally, diverse platforms have been developed with add-on capabilities, increased parallelization, higher levels of automation, a dedicated surrounding infrastructure, and software for analyzing large amounts of data.[11] Currently, several APC systems are commercially available, as thoroughly described in recent reviews.[7, 11, 18, 20, 21] Here, only some of the key features offered by specific platforms are briefly presented.

Today, a throughput of around 6250 compounds/day and 6000 data points/hour has been reported for the IonWorks Barracuda (Molecular Devices, www.moleculardevices.com), comprising 384 recording sites. However, this record throughput comes with a reduction in data quality, due to a decreased seal resistance, lack of continuous voltage clamp, or poor fluidic performance.[11] Two platforms (SyncroPatch 96 (Nanion) and the QPatch HT/HTX (Sophion)) have a slightly lower throughput (96 and 48 parallel recording sites compared to 384 in the IonWorks Barracuda), which is compensated with increased experimental versatility. While APC measurements are conventionally conducted on stable cell lines which are transfected to over-express the ion channel of interest, these two platforms allow recordings on stem cells or primary cells, which are physiologically more relevant.[22] Additionally, the SyncroPatch 96 permits intracellular perfusion, which is key to resolve the kinetics of the channel activity, and allows controlling the temperature, to test drugs under physiological conditions. The temperature has proven to be essential for hERG, while testing Erythromycin, a hERG blocker which is 6-fold less potent at room temperature than at a physiological temperature.[4] Finally, the concept of population patch clamp (PPC) (Ion Works Barracuda and IonFlux HT (Fluxion Bioscience), has

been introduced to record simultaneously a cell population and to correct for cell-cell variability (www.moleculardevices.com).

APC systems have opened a new avenue in the field of drug screening on ion channels, with a throughput ~1000 times higher than MPC,[21] which is extremely valuable for *secondary* and *safety screening*, while providing high quality data. However, APC systems do not reach yet the desired throughput level for *primary screening*. The limiting step, as pointed out by Farre and Fertig, now is not anymore the parallelization of the experiments, but the level of robotization.[11] Manual intervention is still regularly needed for APC measurements, and the typical "walk-away" time is limited to a few hours.[23]

On other aspects, the cost per data point is still extremely high for APC, this being accounted for by, on one hand, the price of the consumables, which are microfabricated devices and, on the other hand, the need for personnel to take care of the steps not yet included in the automation.[11]

Another series of limitations come from the fact that APC utilize cell models. Therefore, a dedicated infrastructure or so-called "cell hotel" is required,[22] where cells are cultured and prepared for each experimental run. In APC, the inherent cell-to-cell variability translates into poor reproducibility of the data, which has been addressed with PPC systems. Additionally, the sealing quality of the cells is essential for the measurements.[18] To alleviate this, standard cell lines (e.g., HEK-293 or CHO cells) that have been validated for APC recordings are mostly utilized,[18] for which protocols have also been optimized for the over-expression of the ion channels of interest.[18] A novel trend, especially for *safety screening*, consists of working with primary cells or stem cell-derived cardiomyocytes, which are however more challenging: they have a lower ion channel density; the formation of a gigaseal is more difficult;[4] and they are available in lower amounts.[22]

So far, three techniques currently dominate the field of drug screening on ion channels, manual patch-clamp, indirect assays, and automated patch-clamp, which all present certain limitations (**Figure 2.1**). Therefore, most of the time, a compromise must be found between data quality and reliability, throughput and costs. Finally, all three approaches rely on the use of cells, which brings additional limitations. Altogether, there is room for a new technology not utilizing cells while offering both high throughput and high quality data.

2.3 Bilayer lipid membranes

Artificial bilayers have been proposed as powerful models to study ion channels[24] and the effect of drug candidates. In the following section, the main characteristics of a natural cell membrane are recalled, followed by a short description of existing artificial bilayer models, and their advantages compared to cells are discussed for drug screening purposes. Finally, the concept of miniaturization is introduced for bilayer experimentation.

2.3.1 Cell membrane

The cell membrane is an impermeable barrier, through which the flux of ions is regulated by membrane proteins such as ion channels (**Figure 2.2**). These ion exchange processes are central to cell homeostasis, and they are also involved in the cell communication with its environment.[3]

The plasma membrane is made from building blocks or phospholipids, which mostly comprise one hydrophilic head and one or two hydrophobic tails. These amphiphatic molecules self-assemble into two molecule thick structures in aqueous solution, with the polar heads facing the solution while the phospholipid tails, which are non-polar and insoluble in water, organize themselves in clustered structures where the tails are facing each other while avoiding contact to aqueous solution.

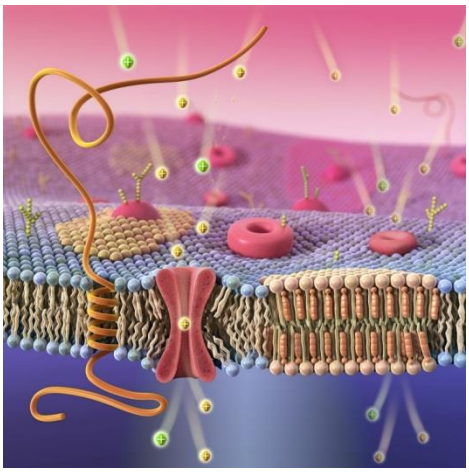

Figure 2.2. Cell membrane. The graphic illustrates part of a plasma membrane, to highlight its complex structure. The cell membrane is built from a variety of phospholipids and proteins, and local differences in its composition can lead to phase separation and local changes in membrane thickness and fluidity. A number of proteins are present, such as ion channels, and the transport of ions across the membrane through these channel proteins is shown. Image: Nymus 3D.

Membranes comprise various types of phospholipids such as phosphatidylcholine (PC), phosphatidylethanolamine (PE), phosphatidylserine (PS), phosphatidylglycerol (PG), phosphatidic acid (PA), phosphatidylinositols (PI) or cardiolipin, while PE and PS are predominant in the inner leaflet. Additionally, in the outer leaflet of the membrane, glycolipids and sphingomyelin are present.[3,25] These phospholipids differ

from each other in terms of head group size and charge, chain length, and in the number of unsaturations present in the hydrophobic tails, altogether dictating the shape of the phospholipids.[3, 25] The shape of the phospholipid also has an influence on the membrane properties. For instance unsaturation introduce a kink in the hydrocarbon chain, which makes it more difficult for the lipids to pack, resulting in a more fluid membrane. In contrast, lipid tails that contain no saturations are arranged in a regular way and are more closely packed. The lateral fluidity of the lipid molecules in the leaflets of the membrane thus depends on the lipid shape and composition.[3] Additionally, the overall membrane properties are modulated by cholesterol, which is a small molecule with a rigid planar steroid ring structure that fills the spaces between neighboring phospholipid molecules, and is present in concentrations between 30 – 50% mol in eukaryotic membranes.[26]

Next to lipids and cholesterol, membrane proteins are present in the bilayer and account for about 50% of the membrane mass.[3] Ion channels are one type of transport proteins and consist of one to a few protein molecules, and form an aqueous pore in the center which allows for ions to pass through with a high rate of more than 10^7 ions per second.[17, 27] Ion channels can be selective to certain types of ions, e.g., calcium, or less selective allowing several ion groups to be transported across the membrane.[3, 17, 27] Next to outer membrane proteins, ion channels can also be found in the membrane of intracellular organelles such as the endoplasmic reticulum or the mitochondria.[5]

In conclusion, the cell membrane is a highly complex structure, this being caused not only by the lipidic composition, but also by the presence of proteins, such as ion channels, which are crucial for basic physiological functions.[1]

2.3.2 Bilayer lipid membrane models

Bilayer lipid membrane models are proposed for studying ion channel function in a controlled and simplified model of the cell membrane. A number of artificial membranes are developed, such as vesicles, supported, suspended, and droplet bilayers, which are shown in **Figure 2.3**. In the following, the different membrane models are shortly discussed in terms of their typical characteristics, and their advantages and limitations.

Vesicles

One type of model bilayers consists of vesicles or liposomes, which are made of a lipid membrane that encloses aqueous solution. Vesicles have for instance been utilized to image phase separation phenomena in the bilayer with respect to the lipid composition.[28] While their round shape resembles the shape of the cell better than

planar models, the intracellular compartment is not directly accessible for both solution replenishment and electrophysiological measurements.

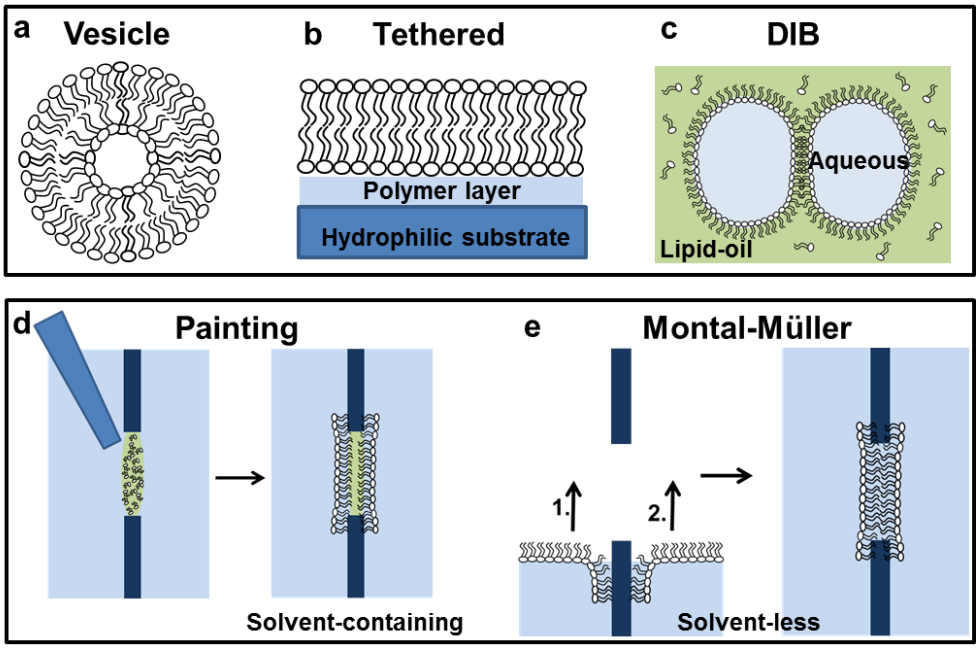

Figure 2.3. Bilayer lipid membranes. Summary of various bilayer models such as, a) vesicles, b) tethered bilayers which are supported on a substrate but separated from it with a hydrophilic polymer layer, c) droplet interface bilayers (DIBs), d) painted solvent-containing bilayers, and e) Montal-Müller BLMs, which are solvent-less, the latter ones being created across a vertical aperture.

Supported and tethered

Supported bilayer lipid membranes (sBLMs) are formed on a solid substrate which results in a high bilayer stability. These sBLMs are typically made with the Langmuir-Blodgett or Langmuir-Schaefer procedure allowing the formation of asymmetrical bilayers. Alternatively, bilayers can be created simply by bursting vesicles onto a smooth and hydrophilic substrate.[29] In general, sBLMs are separated from the solid substrate only by a 1-2 nm thin water layer, and interactions of transmembrane proteins with the surface can alter their mobility and function.[21,29] To increase the distance between the BLM and the substrate, a hydrophilic spacer can be inserted between the membrane and the solid support. These bilayers are called tethered BLMs.[21] Supported bilayers are characterized by their high stability (5-10 days),[30] however only one side of the bilayer is accessible which influences protein studies, prohibits the control of buffer solution on both sides, and complicates electrophysiological recordings.

Suspended

In order to allow the accessibility to both sides of the BLM, suspended bilayers are formed across a vertical and hydrophobic substrate with a micrometer-sized aperture (typically 50-500 μm in diameter), surrounded by aqueous buffer solution on both sides. A number of techniques have been developed for the formation of suspended bilayers, and a few are discussed in the following. More detailed information on all techniques can be found elsewhere.[21, 30-31]

In the painting or Müller-Rudin technique, a bilayer is made by spreading lipids, dissolved in an organic solvent such as n-decane, across a microaperture with a brush.[32] Drainage of the solvent leads to spontaneous thinning of the lipid droplet in the aperture and to bilayer formation. The membrane is stabilized by bulk lipid solution at the edge of the aperture, the so called annulus. Since the lipids are dissolved in non-volatile solution, a layer of solvent remains between the two leaflets after membrane formation with this technique.

Alternatively, solvent-less membranes can be created with the Montal-Mueller technique.[24] First, a monolayer of lipids is formed on the buffer solution in both reservoirs, by letting volatile solvent of the lipid solution, such as hexane, evaporate. In a next step, the water levels on both sides are raised subsequently above the aperture, allowing the lipid molecules to come in contact with each other at the aperture and to assemble into a bilayer structure. The hydrophobic substrate supports the adhesion of the lipid tails to the aperture. Here, no solvent is present between the two leaflets of the bilayer, and additionally, this techniques allows to make asymmetrical bilayers.

Finally, a suspended bilayer can be formed by flushing aqueous solution containing vesicles across a hydrophilic substrate including apertures (e.g., 1 μm in diameter). The vesicles rupture spontaneously leading to bilayer formation across the aperture.[33,34] The membranes made with this method are also solvent-free, and additionally, proteins can be incorporated in the vesicles, which will be present in the final bilayer.

One great advantage of suspended bilayers, is the accessibility to both sides of the membrane which allows straight forward electrophysiological measurements by simply inserting the electrodes in both reservoirs. Additionally, the buffer can easily be controlled on both sides, which gives the flexibility to change the composition of the aqueous solutions during the experiment. This step is especially interesting after the insertion of an ion channel in the bilayer via proteoliposome fusion, or to test the action of a drug compound. The ion channel function can be characterized with electrophysiology, yielding comparable information to the patch clamp technique. One general drawback of suspended bilayers, is their limited stability, which typically lasts several hours.

Droplet interface bilayer

Droplet interface bilayers (DIBs) are created by adding an aqueous droplet to an oil-lipid mixture, and by bringing two droplets into contact. A bilayer is created from the two monolayers, which are spontaneously formed at the oil-water interface of each droplet. Alternatively, the aqueous droplets can be filled with lipid vesicles, which spontaneously fuse with the oil-water interface to form a monolayers, and finally asymmetric bilayers. Alternatively, droplet-on-hydrogel bilayers (DHBs) have been reported where one droplet is replaced by a planar hydrophilic substrate covered with a lipid monolayer. DIBs are characterized by extremely high stabilities of days to weeks, and their automatable bilayer formation. One major drawback in these systems, is the accessibility of the solution in the droplet. More information on recent work can be found in an excellent review.[14]

In conclusion, BLMs mimic the cell membrane and reduce their complexity, while at the same time, they can serve as a matrix for ion channels. As potential cell-free platforms, suspended and droplet-based bilayers are considered most promising concepts for drug screening on ion channels, due to the membrane accessibility or their high stability, respectively. In general, bilayers offer a number of advantages compared to cells, which is discussed below.

2.3.3 Microfluidics for bilayer experimentation

A particularly interesting format to conduct experimentation on bilayers is microfluidics. These miniaturized devices exhibit key advantages for drug screening in general, due to their high level of integration, easy parallelization of the assays, compatibility with automated interfaces, the sub-µL internal volumes, and subsequently reduced costs of the assays.[35] Some APC platforms are actually already utilizing a microfluidic format, for all these reasons, and for fast perfusion of the extracellular solution. Miniaturized devices also bring about additional advantages for bilayer experimentation. Smaller apertures, which are conceivable using micro and nanofabrication approaches, translate into enhanced stabilities for suspended bilayers and a reduced noise level.[36] More importantly, in a microfluidic format, suspended bilayers can be prepared with a horizontal configuration, which allows combined measurements using orthogonal techniques such as (high-resolution) imaging and electrophysiology.

2.3.4 Cell-based platforms vs. bilayer systems

Current drug screening assays on ion channels are conducted using cells, which is ideal to keep the proteins in their physiological and natural environment. However, culturing cells is expensive, time-consuming and is an inherent limitation to

automation of the assays. Cellular assays often suffer from a poor reproducibility, due to inter-cell variability. The over-expression of the protein of interest in the cell membrane, which is commonly done for APC experiments, can lead to additional problems.[6] On other aspects, a cell is highly complex, which makes it difficult to isolate a specific ion channel and associated pathways to assess the effect of a drug. Similarly, a drug can have an indirect effect on an ion channel, for instance, via alteration of the membrane properties,[26] a mechanism which is not accessible using cell models. Multiple ion channels can be patched and recorded simultaneously, which complicates as well the analysis and interpretation of the data. Finally, depending on the drug screening approach, not both cellular environments are easily accessible, while ion channels can also be regulated from the intra-cellular side. Altogether, working with cells is obviously highly demanding, and brings a number of limitations while an artificial membrane-like environment is sufficient to study ion channels and their activity, and this approach presents additional advantages.

Additionally, experimentation using bilayer membrane models only requires a lipid solution and buffer, which is much cheaper and easier to manipulate than cells. Compared to cells, artificial bilayers bring about a higher level of flexibility and full control on various experimental parameters such as the bilayer lipid composition, the extra- and intracellular solutions, and ion channels. The lipidic environment of an ion channel is known to have an influence on its activity, by variation in, e.g., thickness, fluidity, compressibility, or surface charge distribution.[26] Using bilayer models, this relationship can be elucidated by systematically varying the membrane composition. Similarly, indirect effects of a drug on an ion channel linked to changes in the membrane properties, which is another approach to target ion channels,[37] can be detected. In a bilayer set-up, both the *cis*- and *trans*-compartments can be used for perfusion, and for the stimulation of ion channels from the intra and extracellular sides. Finally, in a bilayer model, ion channels are introduced through the fusion of proteoliposomes preferably containing only the protein of interest, which provides better focus on the experiments. Furthermore, intracellular ion channels can also be reconstituted and studied in a bilayer matrix, which is more challenging using patch-clamp in general and some indirect assays. For instance, the ryanodine receptor (RyR) is an intracellular calcium channel involved in cardiovascular diseases, which is located in the membrane of the sarcoplasmic reticulum (ER).[38] This ion channel has been studied in a bilayer format for its electrophysiological characterization,[39] which has brought better insight into its function, through single RyR channel recordings. Measurements conducted on cells using a fluorescence approach only provide collective data on a channel population, with possible influence of RyR protein channels on each other.[39] However, a limiting step found in the bilayer approach is the reconstitution of the ion channels in the bilayer matrix. For that essential step, proteins are most of the time first expressed in a cell system, for which still a

dedicated cell culture facility is required. Recently, cell-free protein expression protocols have been developed,[40] and a number of kits are currently commercially available, which is likely to facilitate this essential step of protein reconstitution in a bilayer model.

2.4 Miniaturized bilayer platforms for drug screening

A number of miniaturized and microfluidic devices have been developed in the last decade, with a primary focus on drug screening applications. However, a number of issues must be carefully addressed before the technology can enter that targeted market, such as: (i) automation, particularly of the membrane formation step; (ii) reproducibility of the experiments; (iii) stability of the bilayer; and (iv) true multiplexing of the devices. Next, microfluidic bilayer platforms must be validated on relevant ion channels, from a pharmaceutical point of view, and finally through drug screening. These aspects are the point of focus of recent developments, and, the integration of the following aspects of multiplexing, automation, bilayer stability, and measurements on ion channels including drug screening assays in miniaturized BLM platforms are presented, with a particular focus on suspended and droplet bilayers.

2.4.1 Membrane formation and stability

The core element of the bilayer platform is the bilayer model itself, and one widely acknowledged weakness of this model is its lack of robustness. First, the conventional techniques employed to form suspended bilayers are in most cases entirely manual and tedious, not reproducible, and the stability of the bilayer structures is limited (several hours), which is an issue if drugs must be tested on proteins.

Membrane formation - Automation

Traditional approaches to form suspended bilayers such as the Mueller-Rudin[32] and Montal-Mueller[24] techniques cannot be readily applied in microfluidic and miniaturized devices due to rearrangement of the aperture and the liquid reservoirs. Therefore, novel approaches have been proposed to create suspended bilayer models in microapertures integrated in a miniaturized or microfluidic format, such as the air-exposure technique,[41] solvent-evaporation approach,[42] and pressure induced thinning.[43] In general, an essential aspect towards automation is the ability to monitor the formation process or, to utilize a spontaneous process to eventually reach a 100% formation yield. Typically, thinning of a "lipid plug" created through "painting" or flow-based deposition in an aperture, proceeds in two steps, with first drainage of the solvent to yield a plug with a thickness of ~100 nm, followed by spontaneous zipping into a bilayer structure.[44,45]

Direct spontaneous thinning occurs provided the aperture-containing substrate is thin enough, as reported by Le Pioufle et al. for 20 μm thick parylene.[46] In an alternative approach, but using a vertical configuration and no aperture, a bilayer was formed via solvent evaporation through PDMS, benefiting from the porosity of the material which was used to build the microchannels.[42] Finally, in another report, the lipid plug was frozen prior to thinning, and spontaneously formed a bilayer upon thawing, with a success yield of up to 50%.[47]

In contrast, if the aperture-containing substrate is thicker, thinning must be assisted by applying an external force. For instance, hydrostatic pressure was employed to induce thinning of a lipid plug deposited in a 47-μm thick PMMA substrate (100-μm diameter aperture), reaching a success yield of 90%.[43] Alternatively, in the air exposure technique, the lipid plug thins down when it is brought in contact with air, after removal of the buffer in the top compartment.[41] In an attempt to automate membrane formation in an array of 12 bilayers, Zagnoni et al. calibrated the air exposure cycles, and reported a 50% formation yield against 80% when BLMs were formed separately.[48] In a second attempt and using the same platform, another approach was tested, using falling droplets on a phospholipid monolayer, to reach a 95% success rate.[12] Using a similar approach, Poulos et al. were able to produce arrays of >2200 bilayers within 3 h, with a success yield of 95%, and full automation of the process using a pipetting robot (**Figure 2.4** a).[49]

DIBs and DHBs, which have been introduced much later in the bilayer field, are created along the same principle by contacting a droplet to either another droplet or a lipid monolayer,[50] and they can easily be formed using an automated process utilizing liquid handling robots.[51]

In a fully different approach, Baaken et al. presented a modified painting technique to create a series of bilayers on top of an array of microcavities (**Figure 2.4** b).[52] For that purpose, instead of using a micropipette tip, a Teflon-coated metal bar is employed, which is magnetically actuated, allowing the creation of 16 bilayers in a few seconds and with a success yield exceeding 90%, just by pushing on a button, from the operator point of view.[53]

Finally, bursting of vesicles on a hydrophilic substrate containing an aperture, which has been successfully implemented in fully microfluidic devices[33] requires minimal monitoring and is subsequently a method of choice for automated membrane formation. Interestingly, this approach has not been adopted to form arrays of bilayers in multiplexed devices.

Membrane stability - lifetime

An often-highlighted advantage of microfabrication for bilayer platforms is the possibility to create smaller apertures, since the stability of suspended membranes inversely scales with the size of the aperture supporting the bilayers. For instance, lifetimes of 15 h were reported for apertures with a diameter of 15-50 µm produced in a 20 µm thick parylene film,[46] this being extended to up to 120 h for sub-micrometer apertures (**Figure 2.4** c),[54] and a record of 10 days has been reached for 20-µm size apertures made in TMMF material.[55] However, it is worth mentioning that not only the size of the aperture matters, but also the ratio between the height and the diameter plays an important role for bilayer formation.[56] Furthermore, monitoring bilayer formation in too small structures becomes challenging, since the bilayer capacitance compares with the stray capacitance of the device,[54] and the BLM is not visible anymore.[46] Lastly, working with too small bilayers is not ideal for the fusion of proteoliposomes for protein reconstitution in the bilayers.

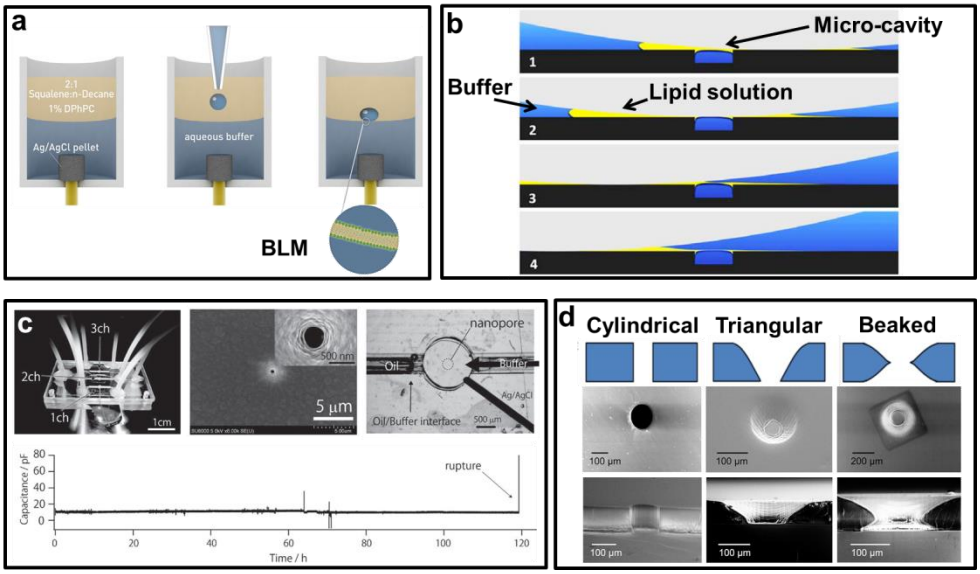

Figure 2.4. Automation of bilayer formation and stability. a) Bilayer formation using a liquid handling robot: an aqueous droplet is pipetted in a lipid-oil phase, onto a buffer solution. A bilayer is formed at the interface between the droplet and the buffer (*right*). Adapted from [49]. b) To form bilayers across microcavity arrays, the lipid solution (yellow) is painted automatically across the array surface utilizing a Teflon coated metal bar (grey) which is magnetically actuated. Adapted from [53]. c) Fully closed microfluidic device with three nanopores in parallel, as shown in the middle top picture, across which highly stable bilayers are formed (stability of up to 120 hours as illustrated by the lifetime recording). Adapted from [54]. d) The aperture shape is an important parameter for the bilayer mechanical stability and for its lifetime. Here, three aperture shapes are fabricated in SU8 and presented in a sketch (*top*), together with SEM images of a top- (*middle*) and side view (*bottom*). Adapted from [57].

On other aspects, micromachining provides unique opportunities to tailor the shape of the aperture, which has proven to be a second main strategy to increase the bilayer quality through stabilization of the annulus and enhanced sealing of the phospholipids. Kalsi et al. explored this stabilization approach, and compared 60-µm diameter apertures with different shapes made from the photoresist SU-8, as presented in **Figure 2.4** d.[57] They found that tapered apertures provided lifetimes longer than 20 h together with greater mechanical stability. Similarly, 3D apertures were produced in the same material using photolithography and tilted illumination; the lifetime was however limited to a few hours only for 50-µm apertures.[58]

Finally, supporting the bilayer with hydrogel (DHB) or a droplet (DIB) greatly increases the bilayer mechanical stability and lifetimes, those being extended to days to weeks.[14,51]

2.4.2 Multiplexing and integration

The second main element is the platform itself, its architecture, its suitability for parallelization and multiplexing of the experiments, and the integration of add-on capabilities such as integrated electrodes. A handful of architectures have been proposed to realize miniaturized and microfluidic platforms for bilayer experimentation, all comprising the same main features: the two *cis*- and *trans*- fluidic compartments, which are separated by the bilayers possibly formed across a microaperture.

In a first approach, one compartment becomes a cavity, the bilayer being formed on top of the cavity, and the other compartment is a large reservoir (**Figure 2.5** a).[52,55] This architecture can easily be scaled up by arraying the cavities and the bilayer, the top reservoir being common for all experimentation sites, and devices with up to 16 cavities were reported.[52] Electrodes were integrated in the cavities for electrophysiological recordings, and fabricated from Ag/AgCl.[52,55] However, in this configuration solutions cannot easily be replaced, since the cavities are not accessible and all bilayers must be tested under the same experimental conditions.

In a second architecture, the bottom fluidic compartment is a microchannel, and the top one a microwell to provide access to the bilayer (**Figure 2.5** b). [41, 43] There again, multiplexing was easily demonstrated through parallelization and arraying of the apertures[46,48,59] to yield platforms with up to 96 wells, though each well contained arrays of 9 BLMs.[60] Ag/AgCl electrodes were also integrated in the device.[48] For drug testing applications, this platform allows quick replenishment of the solutions, for instance from the microchannel side.

The last possible architecture is a fully microfluidic platform, where both fluidic compartments are replaced by microchannels and the micrometer-sized aperture is machined in an intermediate substrate.[61] This architecture seems to be less popular since the BLM is not accessible at all, and fewer examples are found using this approach. However, one multiplexed device has been reported with 3 experimentation sites which are connected via the same channels, as shown in **Figure 2.5** c.[54]

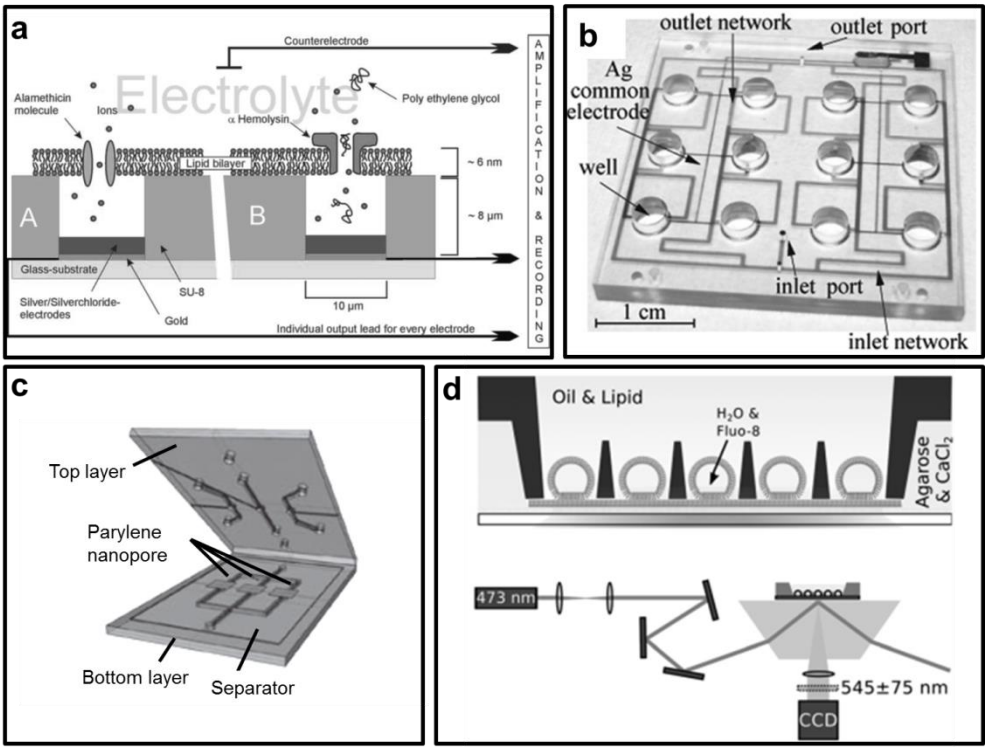

Figure 2.5. Multiplexed devices. Various approaches have been presented for the multiplexing of miniaturized bilayer platforms with a horizontal bilayer configuration. a) Bilayers are formed on top of a microcavity array, with integrated Ag/AgCl electrodes in every cavity. Adapted from [52]. b) In a half-open system, the bilayer sites are connected to one top reservoir and one microfluidic channel; here 12 bilayers can be formed in parallel. Adapted from [48]. c) Multiplexing in a fully closed microfluidic device is achieved by 3 experimentation sites which are connected via one common channel. Adapted from [54]. d) Array of droplets on a hydrogel layer (DHB bilayer), which are applied for high resolution optical measurements (TIRFM). Adapted from [67].

In DIB platforms, both fluidic compartments consist of droplets, and the bilayer is defined as the interface between the two droplets,[14] while in an alternative variant, one droplet is in contact with a lipid monolayer[12], e.g., supported by a hydrogel (DHB).[62] Electrodes are inserted in the droplets, and the bilayers can easily be arrayed or parallelized (**Figure 2.5** d).[63] A main bottleneck found with these models is the

difficulty to perfuse liquid in the *cis*- and *trans*- compartments, to introduce drugs for instance. Two solutions have however recently been proposed, either by connecting the droplets to independent microfluidic channels enabling solution replacement within less than 20 s,[64] or by separating the droplets and reconnecting them to other droplets filled with a different buffer solution, for instance by the split-and-contact process.[65]

A last but essential element of the bilayer set-up, which has not been integrated so far in the microfabricated device, is the patch amplifier. Most of the time, in multiplexed devices, successive measurements are conducted on the different bilayers.[49] Thei et al. worked on the miniaturization and multiplexing of the patch-amplifier,[66] and recently demonstrated simultaneous measurements on 4 independent bilayers created in a 4-cavity array.[55]

2.4.3 Ion channel recordings and drug screening

Ion channel recordings

The last essential element is to demonstrate the capability of these microfluidic bilayer platforms (MBPs) for measurements on relevant ion channels, and for drug screening assays. These devices have mainly been tested in using model pore-forming species such as alamethicin, gramicidin and alpha-hemolysin,[12, 33, 42, 47-48, 51, 62-63, 68] for proof-of-concept ion channel recordings, which can simply be added to the buffer solution and self-insert in the bilayers. The reconstitution of relevant ion channels in a bilayer require more delicate protocols, e.g., after their solubilization in a detergent-rich solution, or through the fusion of a proteoliposome in which they are contained, using a salt gradient or a fusogenic peptide, for instance. So far, using these approaches, a variety of K+ channels such as KcsA,[12, 51, 69] hBK,[51] or Kcv,[63] as well as TRPM8,[70] the mammalian cold and menthol receptor have successfully been recorded in suspended bilayers or DIBs, in miniaturized and microfluidic devices. Furthermore, more recently, using cell-free expression approaches, ion channels were also synthesized *in situ* and directly incorporated in DIB and DHB bilayers for recordings.[63]

Drug screening

After the insertion of the ion channel in the bilayer, they have been exposed to various soluble factors susceptible to modulate their activity. For instance, the bacterial toxin alpha-hemolysin has been exploited for the analysis of polymers such as PEG[72] and DNA,[59] or for the development of biosensors for the detection of cocaine (**Figure 2.6** a)[51] or based on a beta-CD cavity.[54, 66] Ompf has served to study translocation events of polyamines and antibiotics.[73] In terms of real "drug screening" assays, the response of potassium channels to modulators has been assessed, and in particular, Syeda et al. were able to test 9 different compounds within one hour on the Kcv potassium

channel.[63] Finally, and most importantly, several recent articles have demonstrated the capability of droplet interface platforms for the establishment of IC_{50} curves, using potassium channels such as hBK[51] and TRPM8[70], which is the ultimate evidence that this microfluidic bilayer approach can be utilized for drug screening application on ion channels (**Figure 2.6** b,c).

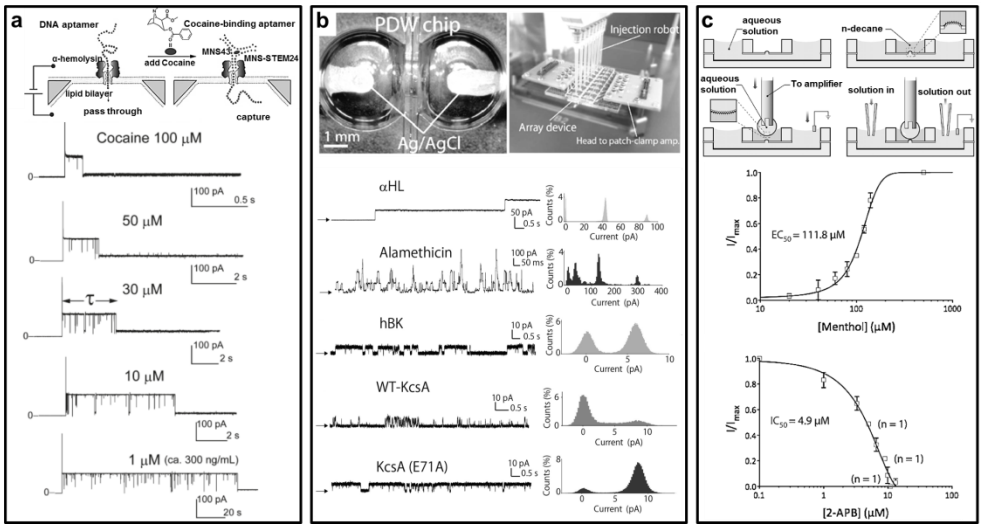

Figure 2.6. Ion channel recordings and drug screening. a) Suspended bilayers in a half-open system are utilized for the detection of low concentrations of cocaine coupled to a DNA aptamer applying the model ion channel α-hemolysin. Adapted from [71]. Cocaine is monitored upon addition of different concentrations. b) 16 DIBs are formed automatically using a liquid handling system, followed by simultaneous electrophysiological recordings. Here, measurements of various ion channels are presented such as model species like α-hemolysin and alamethicin, and potassium ion channels (hBK & KcsA). Adapted from [51]. c) A single droplet bilayer is formed across an aperture and utilized for drug screening on TRPM8 ion channel with menthol (agonist) and 2-APB (antagonist), with the establishment of IC_{50} and EC_{50} curves. Adapted from [70].

2.5 Outlook

Drug screening on ion channels relies on the use of a handful well-established technologies, which are manual patch-clamp, indirect fluorescence-based assays, and automated patch-clamp. However, none of these technologies satisfy all criteria such as high throughput, low cost and sensitive recording quality, to only name the most important ones (**Figure 2.7**). Consequently, a choice must be made between throughput (indirect assays) and data quality (patch-clamp). APC platforms have considerably improved the situation, but their current throughput is limited, and remains too low for *primary screening*. Therefore, there exists a niche for novel

technologies combining these key features, and ideally working with a cell-free model. Miniaturized bilayer platforms perfectly fit in this niche, and different types of bilayer models have been proposed recently. On one hand, suspended bilayers have been implemented in microfluidic devices with different architectures, characterized among others by different levels of accessibility to the bilayers, while being all compatible with electrophysiological measurements, alone or in combination with high resolution optical techniques. On the other hand, droplet based platforms have more recently been developed with horizontal (DHB) or vertical (DIB) configurations of the bilayer. All these platforms working with droplet-based or suspended bilayers do meet the key requirements of automation, membrane stability, and multiplexing. They have also been successfully applied for recording on ion channels and drug screening assays, although some platforms are more advanced in terms of development, which makes them more attractive at a first sight. For instance, some capability remains to be demonstrated for suspended bilayers, while IC_{50} curves have already been established using droplet-based bilayers, the latter being a true milestone to raise interest from the pharmaceutical industries.

Initially, a number of key-requirements that must be fulfilled by drug screening platforms, have been mentioned which are namely sensitivity, specificity, robustness, flexibility, cost, information content and throughput. The sensitivity and specificity of microfluidic bilayer platforms (MBPs) are assumed to be similar to that of patch clamp approaches (MPC & APC), provided the sealing of the bilayer is good, at least for suspended bilayers. The robustness relates to the bilayer itself, its stability and the automation of its formation. Records in terms of bilayer lifetimes exceed what is required for the establishment of an IC_{50} curve, and a number of approaches have proven to be suitable for automated bilayer formation. Furthermore, flexibility of the experimentation is even higher using a bilayer model compared to patch clamp measurements, since its lipidic environment can be tailored, and recordings of intracellular channels are easily possible. The cost of the assay for MBPs is expected to be lower than for APC platforms: the infrastructure is less demanding than for cell experimentation, and one could argue that only a pipetting robot is necessary. Furthermore, MBPs provide comparable information as the conventionally utilized patch clamp techniques, since they also apply electrophysiological measurements (**Figure 2.7**). Finally, in terms of throughput, one platform with a few thousand bilayers has been reported so far, although electrophysiological recordings are not yet truly multiplexed, and are conducted successively.

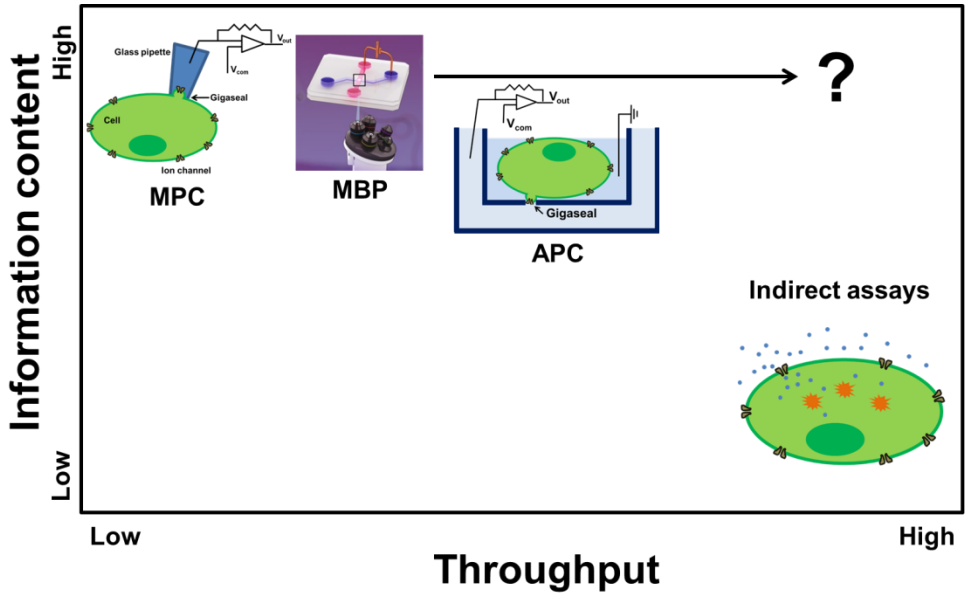

Figure 2.7. Current and potential drug screening platforms. The currently applied platforms for drug screening on ion channels such as MPC, APC and indirect assays, are presented in terms of throughput and information content, together with that of MBPs (microfluidic bilayer platforms). The capability of MBPs is estimated to be comparable in terms of information content with that of MPC, while providing a higher throughput. With respect to APC systems, the throughput of MBPs is lower, although the same number of experimentation sites of ca. 384 has been reported for both approaches. The potential of MBPs as drug screening tools has recently been demonstrated, without clear indication of the throughput they could achieve; however, future developments are likely to lead to increased throughput, as indicated by the arrow, to reach the ideal and desired high throughput/high information content area of the graph..

Altogether, the so far demonstrated performance of MBPs proves their suitability for drug screening on ion channels, for the different segments of the process, which are the *primary*, *secondary*, *safety screening*, and *basic research*, although data on the performance of MBP platforms in terms of drug screening and high throughput are still lacking. Interestingly, APC platforms have evolved at a rapid pace in the last 12 years, starting from devices with one experimentation site to up to 384 today (**Figure 2.8**), with additional developments in terms of infrastructure and accompanying robotization. This development can be directly compared with MBPs, where a similar trend is found in terms of experimentation sites, as presented in **Figure 2.8**, while further multiplexing is still expected. Interestingly, MBPs could benefit from elements developed for APC, such as dedicated software for recording and data analysis, robotic interface for, e.g., liquid handling, and parallelized electrophysiological measurement set-ups. Another important aspect for future developments, is the miniaturization of the latter, as already demonstrated,[66] and its possible integration in

the MBP device will be a key aspect not only for truly parallelized measurements but also to reduce the size of the complete set-up. A point that still requires attention is the expression and reconstitution of the ion channel in the bilayer. The most commonly used protocols for ion channel insertion rely on, e.g., a salt gradient created across the bilayer, and these techniques are tedious and endanger the bilayer lifetime. Additionally, folding of complex ion channels comprising different subunit remains a challenge. In that respect, current developments regarding cell free protein expression and protein insertion in bilayers are of great interest, and the availability of commercial kits is expected to help addressing these issues.[40]

At the moment, only few bilayer platforms are on the market, based on suspended (www.nanion.de) and droplet-based bilayers (www.librede.com), while most of the developments take place in an academic environment. However, in a recent review one of the owners of a market-leading APC company stated that "ion channel recordings in cell-free membranes are gaining more and more interest, since it allows investigating ion channels residing in, for example, inaccessible organelle", which confirms there is a bright future for microfluidic bilayer platforms for drug screening applications.[11]

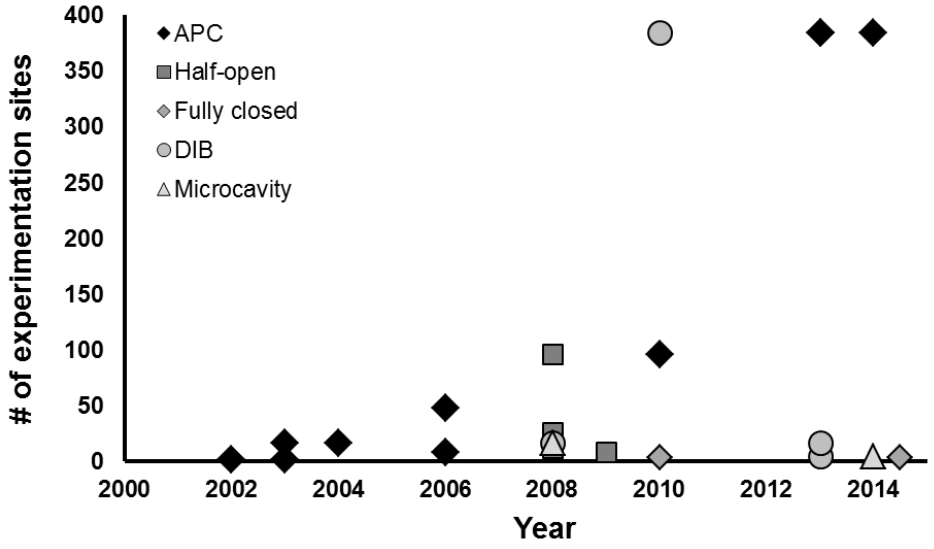

Figure 2.8. Multiplexing trend for APC and MBP devices. The number of experimentation sites for various APC and bilayer platforms is plotted over time. Black diamonds represent the experimentation sites available in various systems of three APC companies (Molecular devices, Nanion, and Sophion) and the approximate release date of their platforms. The number of experimentation sites reported for multiplexed MBPs are shown in grey for different platform architectures (half-open (square), fully closed (diamond), DIB (circle) and microcavity (triangle) systems).

2.6 References

1. Ashcroft, F. M., From molecule to malady. *Nature* **2006,** *440* (7083), 440-447.
2. Hille, B., *Ion Channels of Excitable Membranes*. Third ed.; Sunauer Associates, Inc.: Sunderland, MA, USA, **2001**.
3. Alberts, B., *Molecular Biology of the Cell*. Garland Publishing, Inc., New York, USA: **1989**.
4. Stoelzle, S.; Obergrussberger, A.; Bruggemann, A.; Haarmann, C.; George, M.; Kettenhofen, R. F.; Fertig, N., State-of-the-art automated patch clamp devices: Heat activation, action potentials and high throughput in ion channel screening. *Frontiers in Pharmacology* **2011,** *2*.
5. Hübner, C. A.; Jentsch, T. J., Ion channel diseases. *Human Molecular Genetics* **2002,** *11* (20), 2435-2445.
6. Clare, J. J., Targeting ion channels for drug discovery. *Discovery medicine* **2010,** *9* (46), 253-260.
7. Möller, C.; Slack, M., Impact of new technologies for cellular screening along the drug value chain. *Drug Discovery Today* **2010,** *15* (9–10), 384-390.
8. Xu, J.; Wang, X.; Ensign, B.; Li, M.; Wu, L.; Guia, A.; Xu, J., Ion-channel assay technologies: quo vadis? *Drug Discovery Today* **2001,** *6* (24), 1278-1287.
9. Zheng, W.; Spencer, R. H.; Kiss, L., High throughput assay technologies for ion channel drug discovery. *Assay and Drug Development Technologies* **2004,** *2* (5), 543-552.
10. McManus, O. B., HTS assays for developing the molecular pharmacology of ion channels. *Current Opinion in Pharmacology* **2014,** *15* (0), 91-96.
11. Farre, C.; Fertig, N., HTS techniques for patch clamp-based ion channel screening – advances and economy. *Expert Opinion on Drug Discovery* **2012,** *7* (6), 515-524.
12. Zagnoni, M.; Sandison, M.; Marius, P.; Morgan, H., Bilayer lipid membranes from falling droplets. *Anal Bioanal Chem* **2009,** *393* (6-7), 1601-1605.
13. Kongsuphol, P.; Fang, K. B.; Ding, Z., Lipid bilayer technologies in ion channel recordings and their potential in drug screening assay. *Sensors and Actuators B: Chemical* **2013,** *185* (0), 530-542.
14. Bayley, H.; Cronin, B.; Heron, A.; Holden, M. A.; Hwang, W. L.; Syeda, R.; Thompson, J.; Wallace, M., Droplet interface bilayers. *Molecular BioSystems* **2008,** *4* (12), 1191-1208.
15. Neher, E.; Sakmann, B., Single-Channel Currents Recorded from Membrane of Denervated Frog Muscle-Fibers *Nature* **1976,** *260* (5554), 799-802.
16. Hamill, O. P.; Marty, A.; Neher, E.; Sakmann, B.; Sigworth, F. J., Improved patch-clamp techniques for high-resolution current recording from cells and cell-free membrane patches. *Pflugers Arch.* **1981,** *391* (2), 85-100.
17. Aidley, D. J.; Stanfield, P. R., *Ion Channels*. Cambridge University Press: Cambridge, **1996**.
18. Dunlop, J.; Bowlby, M.; Peri, R.; Vasilyev, D.; Arias, R., High-throughput electrophysiology: an emerging paradigm for ion-channel screening and physiology. *Nat Rev Drug Discov* **2008,** *7* (4), 358-368.
19. Fertig, N.; Blick, R. H.; Behrends, J. C., Whole Cell Patch Clamp Recording Performed on a Planar Glass Chip. *Biophysical Journal* **2002,** *82* (6), 3056-3062.

20. Wood, C.; Williams, C.; Waldron, G. J., Patch clamping by numbers. *Drug Discovery Today* **2004,** *9* (10), 434-441.
21. Steller, L.; Kreir, M.; Salzer, R., Natural and artificial ion channels for biosensing platforms. *Anal Bioanal Chem* **2012,** *402* (1), 209-230.
22. Becker, N.; Stoelzle, S.; Göpel, S.; Guinot, D.; Mumm, P.; Haarmann, C.; Malan, D.; Bohlen, H.; Kossolov, E.; Kettenhofen, R.; George, M.; Fertig, N.; Brüggemann, A., Minimized cell usage for stem cell-derived and primary cells on an automated patch clamp system. *Journal of Pharmacological and Toxicological Methods* **2013,** *68* (1), 82-87.
23. Mathes C, F. S., Finley M, Liu Y., QPatch: the missing link between HTS and ion channel drug discovery. *Comb Chem High Throughput Screen* **2009,** *12* (1), 78-95.
24. Montal, M.; Mueller, P., Formation of Bimolecular Membranes from Lipid Monolayers and a Study of their Electrical Properties *Proceedings of the National Academy of Sciences of the United States of America* **1972,** *69* (12), 3561-3566.
25. Heimburg, T., *Thermal Biophysics of Membranes*. Wiley-VCH Verlag GmbH & Co. KgaA: Weinheim, **2007**.
26. Tillman, T.; Cascio, M., Effects of membrane lipids on ion channel structure and function. *Cell Biochem Biophys* **2003,** *38* (2), 161-190.
27. Trezise, D.; Dale, T.; Main, M., Ion channels. Principles, terminology and methodology. In *Ion channels: From structure to function.*, Second ed.; Kew, J.; Davies, C., Eds. Oxford University Press: Oxford, **2010**.
28. Veatch, S. L.; Keller, S. L., Separation of liquid phases in giant vesicles of ternary mixtures of phospholipids and cholesterol. *Biophysical Journal* **2003,** *85* (5), 3074-3083.
29. Castellana, E. T.; Cremer, P. S., Solid supported lipid bilayers: From biophysical studies to sensor design. *Surface Science Reports* **2006,** *61* (10), 429-444.
30. Zagnoni, M., Miniaturised technologies for the development of artificial lipid bilayer systems. *Lab on a Chip* **2012,** *12* (6), 1026-1039.
31. Hirano-Iwata, A.; Niwano, M.; Sugawara, M., The design of molecular sensing interfaces with lipid-bilayer assemblies. *TrAC Trends in Analytical Chemistry* **2008,** *27* (6), 512-520.
32. Mueller, P.; Wescott, W. C.; Rudin, D. O.; Tien, H. T., Methods for Formation of Single Bimolecular Lipid Membranes in Aqueous Solution *Journal of Physical Chemistry* **1963,** *67* (2), 534-535.
33. Mach, T.; Chimerel, C.; Fritz, J.; Fertig, N.; Winterhalter, M.; Fuetterer, C., Miniaturized planar lipid bilayer: increased stability, low electric noise and fast fluid perfusion. *Anal Bioanal Chem* **2008,** *390* (3), 841-846.
34. Schmidt, C.; Mayer, M.; Vogel, H., A Chip-Based Biosensor for the Functional Analysis of Single Ion Channels. *Angewandte Chemie International Edition* **2000,** *39* (17), 3137-3140.
35. Whitesides, G. M., The origins and the future of microfluidics. *Nature* **2006,** *442* (7101), 368-373.

36. Mayer, M.; Kriebel, J. K.; Tosteson, M. T.; Whitesides, G. M., Microfabricated teflon membranes for low-noise recordings of ion channels in planar lipid bilayers. *Biophysical Journal* **2003,** *85* (4), 2684-2695.
37. Lundbæk, J. A.; Andersen, O. S., Cholesterol Regulation of Membrane Protein Function by Changes in Bilayer Physical Properties—An Energetic Perspective. In *Cholesterol Regulation of Ion Channels and Receptors*, John Wiley & Sons, Inc.: **2012**; pp 27-44.
38. Zhou, Q.; Xiao, J. M.; Jiang, D. W.; Wang, R. W.; Vembaiyan, K.; Wang, A. X.; Smith, C. D.; Xie, C. H.; Chen, W. Q.; Zhang, J. Q.; Tian, X. X.; Jones, P. P.; Zhong, X. W.; Guo, A.; Chen, H. Y.; Zhang, L.; Zhu, W. Z.; Yang, D. M.; Li, X. D.; Chen, J.; Gillis, A. M.; Duff, H. J.; Cheng, H. P.; Feldman, A. M.; Song, L. S.; Fill, M.; Back, T. G.; Chen, S. R. W., Carvedilol and its new analogs suppress arrhythmogenic store overload-induced Ca2+ release. *Nat. Med.* **2011,** *17* (8), 1003-U126.
39. Porta, M.; Zima, A. V.; Nani, A.; Diaz-Sylvester, P. L.; Copello, J. A.; Ramos-Franco, J.; Blatter, L. A.; Fill, M., Single Ryanodine Receptor Channel Basis of Caffeine's Action on Ca2+ Sparks. *Biophysical Journal* **2011,** *100* (4), 931-938.
40. Katzen, F.; Peterson, T. C.; Kudlicki, W., Membrane protein expression: no cells required. *Trends in Biotechnology* **2009,** *27* (8), 455-460.
41. Sandison, M. E.; Zagnoni, M.; Morgan, H., Air-exposure technique for the formation of artificial lipid bilayers in microsystems. *Langmuir* **2007,** *23* (15), 8277-8284.
42. Malmstadt, N.; Nash, M. A.; Purnell, R. F.; Schmidt, J. J., Automated formation of lipid-bilayer membranes in a microfluidic device. *Nano Letters* **2006,** *6* (9), 1961-1965.
43. Suzuki, H.; Tabata, K. V.; Noji, H.; Takeuchi, S., Highly reproducible method of planar lipid bilayer reconstitution in polymethyl methacrylate microfluidic chip. *Langmuir* **2006,** *22* (4), 1937-1942.
44. Fujiwara, H.; Fujihara, M.; Ishiwata, T., Dynamics of the spontaneous formation of a planar phospholipid bilayer: A new approach by simultaneous electrical and optical measurements. *Journal of Chemical Physics* **2003,** *119* (13), 6768-6775.
45. Tien, H. T.; Dawidowi.Ea, Black Lipid Films in Aqueous Media - A New Type of Interfacial Phenomenon - Experimental Techniques and Thickness Measurements *Journal of Colloid and Interface Science* **1966,** *22* (5), 438-453.
46. Le Pioufle, B.; Suzuki, H.; Tabata, K. V.; Noji, H.; Takeuchi, S., Lipid bilayer microarray for parallel recording of transmembrane ion currents. *Analytical Chemistry* **2008,** *80* (1), 328-332.
47. Jeon, T.-J.; Poulos, J. L.; Schmidt, J. J., Long-term storable and shippable lipid bilayer membrane platform. *Lab on a Chip* **2008,** *8* (10), 1742-1744.
48. Zagnoni, M.; Sandison, M. E.; Morgan, H., Microfluidic array platform for simultaneous lipid bilayer membrane formation. *Biosensors & Bioelectronics* **2009,** *24* (5), 1235-1240.
49. Poulos, J. L.; Jeon, T.-J.; Damoiseaux, R.; Gillespie, E. J.; Bradley, K. A.; Schmidt, J. J., Ion channel and toxin measurement using a high throughput lipid membrane platform. *Biosensors and Bioelectronics* **2009,** *24* (6), 1806-1810.

50. Funakoshi, K.; Suzuki, H.; Takeuchi, S., Lipid Bilayer Formation by Contacting Monolayers in a Microfluidic Device for Membrane Protein Analysis. *Analytical Chemistry* **2006,** *78* (24), 8169-8174.
51. Kawano, R.; Tsuji, Y.; Sato, K.; Osaki, T.; Kamiya, K.; Hirano, M.; Ide, T.; Miki, N.; Takeuchi, S., Automated Parallel Recordings of Topologically Identified Single Ion Channels. *Sci. Rep.* **2013,** *3*.
52. Baaken, G.; Sondermann, M.; Schlemmer, C.; Ruehe, J.; Behrends, J. C., Planar microelectrode-cavity array for high-resolution and parallel electrical recording of membrane ionic currents. *Lab on a Chip* **2008,** *8* (6), 938-944.
53. Juan M. del Rio Martinez; Ekaterina Zaitseva; Sönke Petersen; Baaken, G.; Behrends, J. C., Automated Formation of Lipid Membrane Microarrays for Ionic Single Molecule Sensing with Protein Nanopores. *Small* **2014**.
54. Kawano, R.; Osaki, T.; Sasaki, H.; Takeuchi, S., A Polymer-Based Nanopore-Integrated Microfluidic Device for Generating Stable Bilayer Lipid Membranes. *Small* **2010,** *6* (19), 2100-2104.
55. Saha, S. C.; Thei, F.; de Planque, M. R. R.; Morgan, H., Scalable micro-cavity bilayer lipid membrane arrays for parallel ion channel recording. *Sensors and Actuators B: Chemical* **2014,** *199* (0), 76-82.
56. White, S. H., Analysis of Torus Surrounding Planar Lipid Bilayer Membranes. *Biophysical Journal* **1972,** *12* (4), 432-&.
57. Kalsi, S.; Powl, Andrew M.; Wallace, B. A.; Morgan, H.; de Planque, Maurits R. R., Shaped Apertures in Photoresist Films Enhance the Lifetime and Mechanical Stability of Suspended Lipid Bilayers. *Biophysical Journal* **2014,** *106* (8), 1650-1659.
58. Baker, C. A.; Bright, L. K.; Aspinwall, C. A., Photolithographic Fabrication of Microapertures with Well-Defined, Three-Dimensional Geometries for Suspended Lipid Membrane Studies. *Analytical Chemistry* **2013,** *85* (19), 9078-9086.
59. Osaki, T.; Suzuki, H.; Le Pioufle, B.; Takeuchi, S., Multichannel Simultaneous Measurements of Single-Molecule Translocation in alpha-Hemolysin Nanopore Array. *Analytical Chemistry* **2009,** *81* (24), 9866-9870.
60. Suzuki, H.; Le Pioufle, B.; Takeuhci, S., Ninety-six-well planar lipid bilayer chip for ion channel recording Fabricated by hybrid stereolithography. *Biomedical Microdevices* **2009,** *11* (1), 17-22.
61. Sandison, M. E.; Morgan, H., Rapid fabrication of polymer microfluidic systems for the production of artificial lipid bilayers. *Journal of Micromechanics and Microengineering* **2005,** *15* (7), S139.
62. Heron, A. J.; Thompson, J. R.; Cronin, B.; Bayley, H.; Wallace, M. I., Simultaneous Measurement of Ionic Current and Fluorescence from Single Protein Pores. *Journal of the American Chemical Society* **2009,** *131* (5), 1652-1653.
63. Syeda, R.; Holden, M. A.; Hwang, W. L.; Bayley, H., Screening Blockers Against a Potassium Channel with a Droplet Interface Bilayer Array. *Journal of the American Chemical Society* **2008,** *130* (46), 15543-15548.
64. Tsuji, Y.; Kawano, R.; Osaki, T.; Kamiya, K.; Miki, N.; Takeuchi, S., Droplet-based lipid bilayer system integrated with microfluidic channels for solution exchange. *Lab on a Chip* **2013,** *13* (8), 1476-1481.

65. Tsuji, Y.; Kawano, R.; Osaki, T.; Kamiya, K.; Miki, N.; Takeuchi, S., Droplet Split-and-Contact Method for High-Throughput Transmembrane Electrical Recording. *Analytical Chemistry* **2013,** *85* (22), 10913-10919.
66. Thei, F.; Rossi, M.; Bennati, M.; Crescentini, M.; Lodesani, F.; Morgan, H.; Tartagni, M., Parallel Recording of Single Ion Channels: A Heterogeneous System Approach. *Ieee Transactions on Nanotechnology* **2010,** *9* (3), 295-312.
67. Castell, O. K.; Berridge, J.; Wallace, M. I., Quantification of Membrane Protein Inhibition by Optical Ion Flux in a Droplet Interface Bilayer Array. *Angewandte Chemie International Edition* **2012,** *51* (13), 3134-3138.
68. Osaki, T.; Watanabe, Y.; Kawano, R.; Sasaki, H.; Takeuchi, S., Electrical Access to Lipid Bilayer Membrane Microchambers for Transmembrane Analysis. *Microelectromechanical Systems, Journal of* **2011,** *20* (4), 797-799.
69. Leptihn, S.; Thompson, J. R.; Ellory, J. C.; Tucker, S. J.; Wallace, M. I., In Vitro Reconstitution of Eukaryotic Ion Channels Using Droplet Interface Bilayers. *Journal of the American Chemical Society* **2011,** *133* (24), 9370-9375.
70. El-Arabi, A. M.; Salazar, C. S.; Schmidt, J. J., Ion channel drug potency assay with an artificial bilayer chip. *Lab on a Chip* **2012,** *12* (13), 2409-2413.
71. Kawano, R.; Osaki, T.; Sasaki, H.; Takinoue, M.; Yoshizawa, S.; Takeuchi, S., Rapid Detection of a Cocaine-Binding Aptamer Using Biological Nanopores on a Chip. *Journal of the American Chemical Society* **2011,** *133* (22), 8474-8477.
72. Baaken, G.; Ankri, N.; Schuler, A.-K.; Ruehe, J.; Behrends, J. C., Nanopore-Based Single-Molecule Mass Spectrometry on a Lipid Membrane Microarray. *Acs Nano* **2011,** *5* (10), 8080-8088.
73. Kreir, M.; Farre, C.; Beckler, M.; George, M.; Fertig, N., Rapid screening of membrane protein activity: electrophysiological analysis of OmpF reconstituted in proteoliposomes. *Lab on a Chip* **2008,** *8* (4), 587-595.

Microfluidic platform for high-yield bilayer formation, in-depth membrane characterization, and experimentation on pore-forming species

In this chapter, a fully closed microfluidic bilayer platform is proposed, consisting of two channels fabricated in glass, and separated by a Teflon foil with a micrometer-sized aperture (50-100 μm in diameter), which is located at the channel intersection. Bilayers are formed across this aperture by successive flushing of lipid and buffer solutions through both channels, resulting in spontaneous and instantaneous thinning of the lipid plug deposited in the aperture into a bilayer. This quasi-automated approach gives a success yield of ~100%, and bilayers with various lipid compositions are characterized in depths by utilizing a combination of optical and electrophysiological techniques. In a next step, the activity of model pore-forming species (α-hemolysin and gramicidin) is recorded, with a single channel resolution. Finally, a potential drug screening assay is proposed, where changes in the gramicidin activity are sensed electrophysiologically after exposure of the bilayer to external soluble factors (ethanol & acetylsalicylic acid).[1]

[1] Modified from: V.C. Stimberg, J.G. Bomer, I. van Uitert, A. van den Berg, and S. Le Gac, "High Yield, Reproducible and Quasi-Automated Bilayer Formation in a Microfluidic Format", *Small,* 2013, 9 (7), 1076–1085. **Cover article**

3.1 Introduction

Bilayer lipid membranes (BLMs) are simplified models of the cell membrane. Conventionally, planar BLMs are formed across a vertical micro-aperture fabricated in a hydrophobic material, and sandwiched between two mL-sized buffer reservoirs that correspond to the intra- and extracellular environment of the cell.[1] One major advantage of BLM experimentation compared to cell studies is the accessibility of the membrane from two sides which is particularly suitable for electrophysiological measurements across the membrane and for the individual control of the buffer environment on both sides. Additionally, the lipid composition of the bilayer can be modified for fundamental studies on bilayer properties with respect to the lipidic environment. Finally, the BLM is an excellent matrix for experimentation on membrane proteins with various applications: on one hand, the approach is well suited for fundamental studies on protein function due to the controlled environment and reduced complexity of the membrane and the elimination of the cell itself, and, on the other hand, for drug screening on membrane proteins. Membrane proteins, as for instance ion channels, are involved in several diseases, e.g., channelopathies, neurodegenerative or cardiovascular diseases. Therefore, they find increasing interest by the pharmaceutical industry as drug targets.[2] Next to drug screening, bilayer systems can also be applied for testing engineered proteins,[3] DNA sequencing,[4-6] polymer analysis,[7,8] and fundamental studies on protein-membrane[9] and nanoparticle-membrane interactions.[10]

The conventional bilayer set-up however, makes use of large sample volumes, it is mainly restricted to electrical measurements due to the vertical orientation of the aperture, and it has a low potential for multiplexing and automation. Consequently, new bilayer platforms are desired for the above mentioned applications. In this context, microfluidics offers various advantages: i) the microliter volumes of the compartments on both sides of the bilayer reduce experimentation costs and increase assay speed, ii) the possibility to produce smaller apertures down to the nanometer scale results in enhancement of both the membrane stability and the sensitivity of electrical measurements, iii) the integration of additional characterization schemes such as optical (confocal) techniques provides additional information for bilayer and protein studies, and iv) the microfluidic format is ideal for automation and multiplexing.

Such microfluidic platforms for membrane-related studies find increasing interest in the literature, and various devices have been described, including semi-microfluidic[7,8,11-21] and fully microfluidic[22-27] systems. The former comprise one microfluidic channel combined with mostly a milli-fluidic reservoir, whereas the latter

make use of two fully closed microfluidic compartments. Additionally, alternative systems are developed such as droplet-interface-bilayers (DIBs).[28] A detailed summary of most microfluidic bilayer platforms can be found in a recent review by Zagnoni.[29]

In this chapter, a versatile platform in a fully closed microfluidic format is described that enables: i) high yield bilayer formation, ii) dual optical and electrical in-depth bilayer characterization, iii) electrical measurements on single pore-forming species, and iv) drug screening as illustrated here by a gramicidin-based assay to indirectly sense changes in the membrane environment.

3.2 Experimental Section

3.2.1 Materials

Potassium chloride (KCl), (4-(2-hydroxyethyl)-1-piperazineethanesulfonic acid (HEPES), dichloromethane, chloroform, sulfuric acid, acetylsalicylic acid, gramicidin (mixture of species with ~80% gramicidin A) and α-hemolysin (αHL) are purchased from Sigma Aldrich (Zwijndrecht, The Netherlands). Solvents such as n-decane, hydrogen peroxide and ethanol are ordered from Fluka (Steinheim, Germany), Merck (Darmstadt, Germany) and Assink Chemie (Enschede, The Netherlands), respectively. Lipids (1,2-diphytanoyl-*sn*-glycero-3-phosphocholine (DPhPC), 1,2-dioleoyl-*sn*-glycero-3-phosphoethanolamine-N-(lissamine rhodamine B sulfonyl) (DOPE), L-α-phosphatidylcholine (Heart, Bovine, PC)) are purchased from Avanti polar lipids (Alabaster, AL, USA) as solutions together with cholesterol as a powder. For the preparation of all aqueous solutions, deionized water is used (MilliQ system, Millipore, Billerica, MA, USA). All experiments are carried out at room temperature.

3.2.2 Fabrication

The microfluidic device contains three layers: two glass substrates, each with one independent microfluidic channel, which are separated by a Teflon foil comprising a micro-aperture (**Figures 3.1** a,b), located at the channel intersection (**Figure 3.1** c), and across which bilayers are formed (**Figures 3.1** d,e).
The fabrication of the platform is described in detail below. First, the two glass substrates comprising microfluidic channels and fluidic reservoirs are processed. Next, the structures (aperture and reservoirs) are etched in the Teflon foil and finally, the three layers are assembled. The full fabrication is illustrated in **Figure 3.2**.

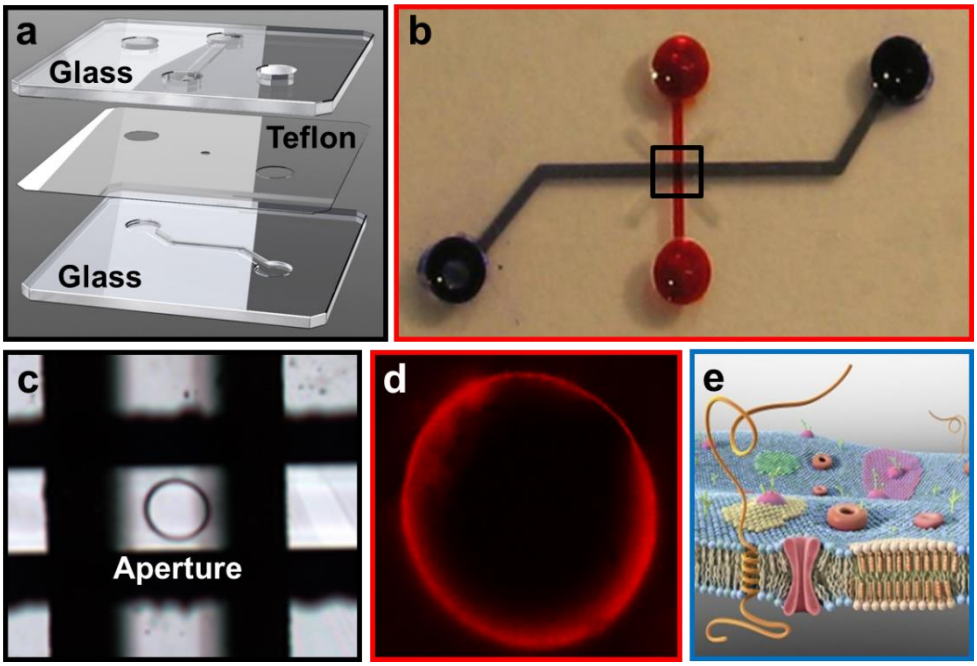

Figure 3.1. Microfluidic platform for bilayer experimentation. Open view (a) and photograph (b) of the device consisting of a glass-Teflon-glass sandwich structure. The two channels (height: 100 μm, width: 300 μm) are filled with ink for visualization purposes (red = top channel, blue = bottom channel). c) A small aperture (diameter: 100 μm) is located at the intersection of the channels for the formation of a bilayer (d) in the device, here visualized by supplementing the lipid solution with fluorescently labeled phospholipids. e) Schematic representation of a cell membrane to be recapitulated in the microfluidic device (sketches a & e @ Nymus 3D).

Glass substrates

The microfluidic channels are wet-etched in glass wafers (Borofloat 33, 100-mm diameter, 500-μm thickness) (**Figure 3.2** a). Therefore, a chromium-gold layer (Cr 30 nm, Au 150 nm) is sputtered on the glass wafers and subsequently patterned using photolithography and dedicated etchants (commercial Chrome Etch №1, Technic France, and home-made Au etchant (1 part I_2, 4 parts KI and 40 parts H_2O)). The patterned Cr/Au layer acts as a mask for wet-etching the glass channels (100-μm height; 300-μm width) using hydrofluoric acid (approx. 33% in concentration). The remaining photoresist and metal layers are subsequently removed in acetone (VLSI 100038, BASF) and the metal etchants, respectively. Following this, access holes are produced in the top glass substrate using powder-blasting (**Figure 3.2** a, *bottom*).

For this, a photosensitive foil (Ordyl, BF410) is employed as a masking layer. The reservoir patterns are defined in that foil using standard photolithography technique,

and subsequently developed in a 0.2% sodium carbonate solution. Following this, the substrate is exposed to Al_2O_3 powder (29 µm grain size) to realize the reservoirs, and the photosensitive foil is removed in acetone for 5 min. The resulting substrate is ultrasonically rinsed in deionized water for 10 min and in fuming nitric acid for 5 min. Finally, the glass wafers are diced into 1 cm x 2 cm pieces using dedicated equipment (Disco DAD321, blade-type TC 300, spindle rev. 25.000 rpm, feed 4 mm/s).

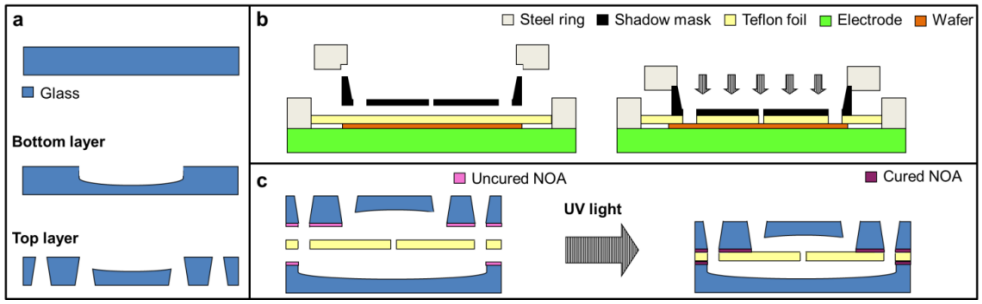

Figure 3.2. Device fabrication. a) Processing of the glass substrates with successive wet-etching of the microfluidic channels (100-µm height; 300-µm width) and powder-blasting of access holes (1600-µm diameter) in the top substrate. b) Patterning of the FEP foil using reactive ion etching (RIE) and a shadow mask to produce the micro-apertures (100-µm diameter) and the access holes. The shadow mask is placed on the FEP foil which is secured on a carbon electrode to prevent any wrinkling (*left*), and the mask is kept in close contact with the foil using stainless steel rings. The desired structures are opened by etching (*right*). c) Device bonding using an optical adhesive (NOA81), which is applied on both glass substrates with a roller and subsequently cured using UV light. Drawings courtesy of Iris van Uitert.

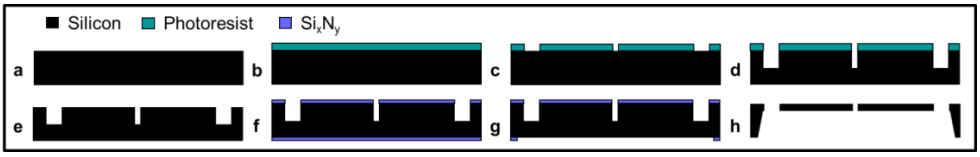

Figure 3.3. Process flow for the fabrication of the silicon-based shadow mask. a) Wafer cleaning in 100% HNO_3. b) Deposition of a photoresist layer. c) Patterning of the photoresist. d) DRIE of silicon. e) Removal of the photoresist. f) LPCVD of a silicon nitride (Si_xN_y) layer (ca. 100 nm). g) Patterning of the backside of the Si_xN_y layer. h) Etching of the silicon and removal of the Si_xN_y. Drawings courtesy of Iris van Uitert.

Teflon foil

The apertures (50 or 100 µm) and access holes are etched in the Teflon FEP foil (Sabic BV Snij-Unie HiFi, Enkhuizen) using RIE (reactive ion etching) and a silicon-based shadow mask (**Figure 3.2** b).

For the fabrication of the shadow mask (**Figure 3.3**), a silicon wafer (CZ-silicon, 100-mm diameter, 525-µm thickness, Okmetic, Vantaa, Finland) is cleaned for 10 min in an oxygen plasma (Tepla, barrel-etcher; **Figure 3.3** a). Subsequently, this wafer is

patterned using a standard photolithography process (**Figure 3.3** b,c), and 100-μm deep structures defining the aperture and the access holes, are etched using deep reactive ion etching (DRIE, Adixen SE; standard Bosch process, **Figure 3.2** d). Following this, the wafer is cleaned for 10 min in oxygen plasma and subsequently for 10 min in piranha solution (2:1 H_2SO_4:H_2O_2) at 120°C (**Figure 3.3** e). A thin layer of silicon-rich nitride (Si_xN_y, ~100 nm thick) is grown on top of the silicon using LPCVD techniques (low pressure chemical vapor deposition, Amtech tempress diffusion system) as a protection during wet-etching (**Figure 3.3** f). The nitride layer is patterned on the backside of the wafer using a RIE process (Elektrotech Twin system Plasmafab (PF340), **Figure 3.3** g) to give a hard mask for the last wet-etching step. The backside is wet-etched with 25% KOH at 75°C until a thin layer (50 μm) is left. The resulting shadow mask is rinsed with deionized water and dried. The residual silicon-rich nitride on the bottom of the holes is etched by RIE in the same way as described above to yield the final shadow mask employed for patterning the FEP foil (**Figure 3.3** h).

For patterning the Teflon, the FEP foil is secured on a carbon electrode with tape and a stainless steel ring to facilitate the manipulation and to prevent the FEP foil from wrinkling. To protect the carbon electrode, a dummy wafer is placed below the Teflon (**Figure 3.2** b, *left*). The shadow mask is placed on the FEP foil, and pushed against the Teflon with a second stainless steel ring (**Figure 3.2** b, *right*). The apertures and access holes are subsequently dry-etched (Elektrotech Twin system Plasmafab (PF340), 20 sccm O_2, 15 sccm N_2, and 2 sccm CHF_3 at 100 mTorr and 80 W; etching speed of about 300 nm/min) in the FEP foil. For apertures of 100 μm diameter, an etch-time of 45 min is sufficient, while it must be extended to 60 min to open up smaller apertures.

Device assembly

The devices are assembled at the chip level using an optical adhesive, as previously described.[30] The glass substrates are first cleaned in hot piranha solution (3:1 H_2SO_4:H_2O_2) for 10 min, rinsed thoroughly in deionized water and dried. Following this, NOA81 is applied on a cover slip, spin coated (30s at 500 rpm, 30s at 5000 rpm) to achieve a thin layer and pre-cured under UV light for 10-15 s (Konrad Benda Laborgeräte, Wiesloch, Germany, λ = 366 nm). The remaining uncured glue from the cover slip is transferred on the two glass substrates using a roller (**Figure 3.2** c, *left*). The Teflon foil is cut into pieces of 1 cm x 2 cm, cleaned in ethanol, rolled on a clean cover slip and placed on the heating plate of an in-house built aligner, which is set to 25ºC to facilitate an evenly spread glue layer. The aperture is carefully aligned to the bottom glass substrate with the help of alignment marks and by moving the plate of the aligner in the x and y directions. Subsequently, the top glass substrate is aligned.

NOA81 is cured under UV light for ~2 min under atmospheric conditions to bond the 3 layers (**Figure 3.2** c, *right*).
For recycling, the devices are immersed in dichloromethane or acetone for ca. one night to disassemble the layers. The FEP sheet is discarded while the two glass substrates are thoroughly rinsed with acetone and cleaned in piranha solution before they are re-used.

3.2.3 Aperture characterization

The edges of the microaperture are characterized using bright field microscopy (Leica DMI 5000M) and scanning electron microscopy (SEM, JEOL JSM 5610), as shown in **Figures 3.4** a-d. The shape of the aperture is characterized using white light interferometry (WLI) and laser scanning confocal microscopy (LSCM) to get some insight into the 3D shape of the aperture (**Figures 3.4** e,f). For WLI measurements (PSV-400 scanning vibrometer, Polytec, Antwerpen, Belgium), the aperture is placed on a polystyrene (PS) microscope slide (Thermo Fisher Scientific, Rochester, NY, USA), and the topography of the surface is determined based on the interference pattern obtained during a scan along the vertical axis. A 3D reconstruction of the aperture is thereafter created using TMS 2.1 software (Polytec), as shown in **Figure 3.4** e. For the LSCM measurements, the aperture is included in the microfluidic device, as for BLM experimentation, and both channels are filled with 1 mM aqueous fluorescein sodium salt solution (Sigma, Zwijndrecht, The Netherlands). A z-stack of the area surrounding the aperture is carried out using an inverted confocal microscope (LSM510, Zeiss, Argon laser, λ = 488 nm, LD-Achroplan 40x objective, LP 530 filter and HFT UV/488/543/633 beam splitter). An orthogonal profile is made from the z-stack using ImageJ (open source software from NIH), as shown in **Figure 3.4** f.

3.2.4 Experimental set-up

For the experiments, the assembled microfluidic chip is placed into an in-house built chip-holder which fits in the stage of a microscope (Leica DMI 5000M, Rijswijk, The Netherlands, **Figure 3.5** a,b). Fluorescent and bright field images are recorded with a CCD camera (DFC310FX, Leica, Rijswijk, The Netherlands) coupled to both the computer and the microscope. External Ag/AgCl electrodes (Molecular devices, Sunnyvale, CA, USA) are inserted in the reservoirs of the chip-holder and connected to an Axopatch 200b amplifier equipped with a CV 203 BU headstage (Molecular devices, Sunnyvale, CA, USA). The headstage and the electrodes are shielded by a faraday cage placed on top of the microscope. Data for the electrical measurements

are acquired using LabVIEW and a PCI-6259 data acquisition card (National Instruments, Austin, TX, USA).

3.2.5 Bilayer experimentation

All phospholipids are purchased as chloroform-based solutions at a concentration of 10 mg/mL whereas cholesterol is dissolved in chloroform to yield a concentration of 25 mg/mL. The lipid solutions (DPhPC or L-α-PC/Ch) are prepared by letting chloroform evaporate in a vacuum chamber for at least 30 min. This residue is dissolved in n-decane to a final concentration of 25 mg/mL for BLM experimentation. For fluorescence measurements, the lipid solution is supplemented with 1% vol fluorescently labeled DOPE.

For bilayer formation, both channels of the microchips are manually filled with 0.2 μL of lipid solution using a conventional micropipette. Subsequently, 30 μL of buffer (1 M KCl, 10 mM Hepes, pH 7.4) is added in the bottom channel to replace the lipid solution, followed by 20 μL of buffer in the top channel, as soon as the buffer meniscus reaches the aperture. While the buffer in the top channel passes the aperture, spontaneous and instantaneous thinning of the lipid solution in the aperture down to a bilayer is observed, without any external intervention. In case this process is not successful, reflushing steps are implemented where the remaining lipid solution in one channel is pushed back across the aperture to initiate again the process of membrane formation.

3.2.6 Electrical measurements

Prior to the measurements, the microfluidic chip is characterized in terms of noise, electrical resistance and stray capacitance. For all measurements, a Teflon film without any aperture is employed and assembled in a microfluidic device. The device is placed in the chip holder, the channels filled with buffer solution (1 M KCl, 10 mM Hepes, pH 7.4), and Ag/AgCl electrodes inserted in the reservoirs. For all electrical measurements a 1 kHz low-pass Bessel filter is used. In order to determine the noise of the system, the current is measured at zero voltage. The rms of the current noise corresponds to 0.24 pA rms @ 10 kHz sampling rate and 1 kHz filter which is similar to previously reported values.[8,19] The resistance is determined by measuring the current while applying dc voltages (0–100 mV, in 20 mV steps), and a value of 388 ± 332 GΩ (n = 3) is found, which is comparable to the resistance reported by Mayer et al. for a bare 60-μm thick Teflon film.[31] When the device includes an aperture, the resistance is found to be 26.77 ± 0.06 kΩ (n = 3) for 100 μm apertures. The capacitance is determined using an ac voltage (triangular wave, 50 Hz, 75 mV pp) and

by recording the current response. The capacitance is derived from the measured current value, after thorough calibration of the system with solid state capacitors (1–22 pF). The system has a stray capacitance of 3.34 ± 0.16 pF (n=3). The resistance and capacitance of BLMs are determined in the same way, and for all capacitance measurements, the stray capacitance of the device is subtracted, and the values are corrected for eventual leakage current (**Appendix I**).

3.2.7 Pore forming species

For the αHL measurements, the protein is added to the top channel after bilayer formation (L-α-PC with 35% mol Ch) to yield a final concentration of 13 μg/mL, and protein insertion is monitored by applying a dc voltage of 50 mV (10 Hz sample rate). To measure the gramicidin activity, 0.6 μL of a 25 mg/mL peptide solution in ethanol is added to the top channel after bilayer formation using L-α-PC and 30% mol Ch supplemented with 2% vol ethanol and 1% vol fluorescently labeled DOPE (80 mV dc voltage, 50 kHz sample rate). For the drug screening assay, the peptide is added directly to the lipid solution (DPhPC) prior to bilayer formation to yield a peptide/lipid ratio of ~$7 \cdot 10^{-8}$, and the current response is recorded (80 mV dc voltage, 10 kHz sampling rate). Data are filtered and analyzed using an in-house written Matlab routine in terms of channel appearance rate, number of channels, and average channel lifetime. In this set of experiments, the average of all channel lifetimes is calculated for one condition, not taking into account longer open times due to multiple channels. For all measurements the same buffer is applied (1 M KCl, 10 mM Hepes, pH 7.4).

3.3 Results and Discussion

3.3.1 Microfluidic platform

Design

The microfluidic device is designed to resemble a conventional BLM set-up. The independent microfluidic channels in the two glass substrates represent the *trans*- and *cis*-compartments, while the intermediate Teflon layer corresponds to the hydrophobic partition with a micrometer-sized aperture (**Figure 3.1** a). The two channels are arranged in a perpendicular configuration (**Figure 3.1** b), with the aperture located at their intersection (**Figures 3.1** b,c).

Material choice

The device is fabricated from materials conventionally applied in microfabrication which are as well compatible with bilayer experimentation. After assembly of the three

layers the device must be suitable for optical (bright field, fluorescence) and sensitive electrophysiological detection: the materials i) are transparent, ii) have no background fluorescence and (iii) are electrically insulating.
The layers comprising the channels are fabricated from glass, which fulfills all the requirements mentioned above. Compared to most polymer materials, glass is inert to a large amount of solvents and chemicals, and its manufacturing employs standard fabrication processes such as wet-etching. Teflon is the most commonly employed substrate to produce hydrophobic partitions for BLM experimentation. Teflon guarantees high adhesion of the lipid molecules around the aperture supporting the GΩ seal, which is crucial for single protein experiments. Furthermore, Teflon has excellent insulating properties, which suppresses issues associated with stray capacitances and leakage currents. Finally, the Teflon foil is transparent and chemically inert.

Aperture fabrication

Conventionally apertures are realized in Teflon substrates by mechanical punching or with a heated wire.[32] Although these approaches yield clean apertures, they are not easily amenable to wafer-scale fabrication of apertures. Alternatively, Mayer et al. reported an original process for the production of aperture arrays relying on spin-coating of liquid Teflon on a structured PDMS substrate.[31] This methodology allows fast and reproducible production of aperture arrays outside a clean room environment (**Figure 3.4** a), although closer investigation of the aperture under the SEM reveals rough edges (**Figure 3.4** a, *inset*). Furthermore, due to wetting phenomena, the resulting Teflon sheet is not fully planar around the features, which precludes leakage-free assembly of the devices.
Consequently, a new wafer-scale fabrication technology is developed to pattern a 12.5-μm thin Teflon FEP substrate, as described in detail in the experimental section. This wafer-scale fabrication process is highly reliable and allows the production of well-defined and "clean" features (**Figure 3.4** c,d). Apertures with diameters down to 15 μm have been realized. However, the size of the aperture is probably limited by the thickness of the foil, and such apertures presented a more conical profile (**Figure 3.4** b). Next to the aperture diameter, a crucial parameter in this fabrication process is the distance between the shadow mask and the Teflon. Close contact between them is required to prevent under-etching phenomena and to obtain a straight profile.
The dimensions and shape of the dry-etched apertures are characterized using a number of imaging techniques (bright field microscopy, WLI, and LSCM). This comprehensive characterization first reveals that the size of the aperture is slightly larger than expected (120.0 ± 7.5 μm (n = 7) and 54.7 ± 3.2 μm (n = 4) for 100 and 50 μm designs, respectively). The edges of the 100-μm apertures, which have mainly

been used for bilayer experimentation, are vertical, yielding a well-defined cylindrical structure, as can be seen in **Figure 3.4** e,f.

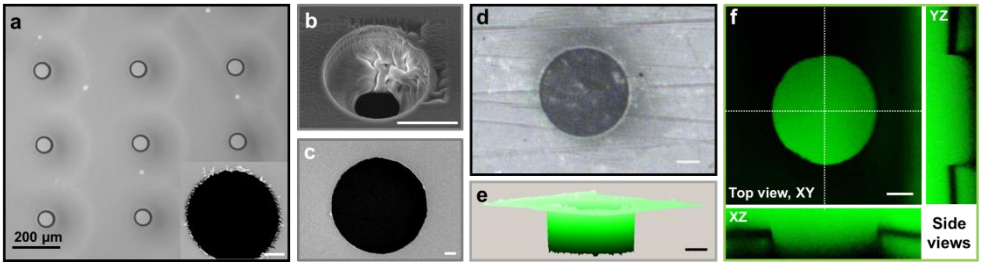

Figure 3.4. Aperture fabrication and characterization. a) Aperture array formed from liquid Teflon. The inset shows a SEM picture of such an aperture. b) SEM image of a 15-µm aperture fabricated by RIE of a 12.5-µm thin Teflon foil. c) SEM image of a 50-µm aperture formed with the same technique. d) Bright-field microscopy picture of a 100-µm dry-etched aperture in the Teflon foil. e) Shape of the same aperture determined using WLI. f) Confocal imaging of the shape of the same aperture after inclusion of the dry-etched Teflon foil in a microfluidic system; channels are filled with a fluorescein solution (1 mM) and a z-stack is done to determine the precise shape of the aperture in the Teflon foil, seen here as dark areas. Pictures of the x-y plane and of the side views (y-z and x-z) of the aperture along the dashed lines are presented. Scale bars in inset in a-c: 10 µm; d-f: 25 µm.

Device assembly

For the assembly of the device, two routes have been considered: clamping of the three layers,[17] or physical bonding. As the alignment of the three layers is crucial to ensure the aperture is located at the channel intersection, the first option has not been pursued. A number of strategies have been reported for bonding Teflon and glass;[33-35] however, these techniques involve numerous steps, and they mostly require clean-room facilities. Therefore, another approach has been chosen based on a technique previously developed in our lab,[30] where the three layers are glued together utilizing a UV-curable adhesive (NOA81).

The process is straightforward while being conducted in a conventional wet-lab, and it has proven to assemble a great variety of materials, including glass and Teflon. Additionally, the cured adhesive can be chemically dissolved for recycling of the device. Crucial aspects in the bonding process are the proper straightening of the foil, application of a thin layer of glue, and alignment of the aperture to the microchannels. First, the thin FEP foil tends to wrinkle, which prevents leakage-free bonding of the device. Therefore, the foil is cut to the size of a chip, cleaned in ethanol and rolled out on a cover slip. This procedure keeps the Teflon straight during bonding and the ethanol evaporates so that it does not influence bonding. Second, it is important to apply a thin layer of glue to the glass substrates to prevent clogging of the channels, but to have enough glue to yield proper bonding. To achieve this, the glue is spin-coated on a cover slip, and shortly exposed to UV light (pre-curing) to only cure the

bottom part of the glue on the cover slip, which further reduces the thickness of the "active" uncured glue layer. The remaining glue is applied to the glass with a roller. In order to remove the right amount of uncured glue, the pre-curing times are adapted to 15 s for the bottom and 10 s for the top part, the latter requiring more glue for proper bonding. Finally, the three layers are aligned with the help of dedicated marks etched in the bottom glass substrate and by matching the fluidic accesses in the three layers. The use of an in-house built aligner with micrometer precision in the *x*-, *y*-, and *z*-direction improves the alignment precision compared to alignment by hand, from 17 ± 13 µm to 7 ± 5 µm (both n=3) for a channel width of ~300 µm.

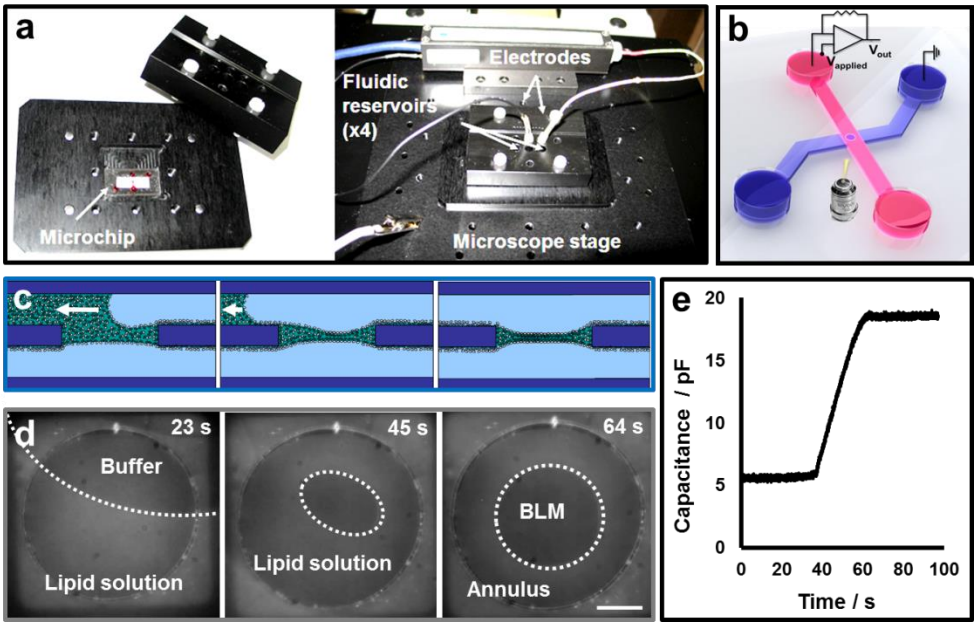

Figure 3.5. Simultaneous electrical and optical monitoring of BLM experimentation. a) Picture of the chip-holder developed for BLM experimentation in its open (left) and closed (right) configuration; the chip-holder includes a niche in which the device precisely fits, and in which a window is machined for optical measurements, as well as reservoirs in its top part for fluidic access and connection to a patch-amplifier via Ag/AgCl electrodes. b) Schematic representation of the experimentation approach where microscopy and electrical measurements are combined to monitor membrane formation and to characterize the membrane properties (Sketch of the chip @ Nymus 3D). c) Drawings showing the process of membrane formation at the molecular scale, and viewed from the side (not drawn at scale). Three main steps are identified in the process of membrane formation: flushing of buffer in both channels to replace the previously introduced lipid solution; instantaneous thinning of the lipid solution in the partition into a bilayer, stabilization of the bilayer ~64 s after the buffer front in the top channel has reached the channel intersection (which is defined as t = 0). d) Bright microscopy pictures illustrating the same three steps, and e) electrical monitoring of the process by following the changes in the capacitance as a function of time; here again three regions are found in the graph that correspond to the three steps presented in c) and d). Scale bar in d) 25 µm.

3.3.2 Bilayer experimentation

Membrane formation

Bilayers are formed in the closed microfluidic device by successively flushing the lipid solution in n-decane and buffer (1 M KCl, 10 mM Hepes, pH 7.4) in both microchannels (**Figure 3.5** c). Upon flushing with buffer solution, the lipid solution instantaneously and spontaneously thins down into a bilayer in the 100-µm aperture without any intervention of the experimenter. In 96% of the cases (43 out of 45), a stable bilayer is directly formed. If the process is not successful, i.e., if the membrane is not stable, the procedure is repeated and the remaining lipid solution is flushed again across the aperture. Including 1–3 reflushing steps, we measure a 100% membrane formation yield. Furthermore, the resulting membranes are stable for up to 36 h, with an average stability of 10–15 h (n = 5). To the best of our knowledge, such a quasi-automated approach for bilayer formation with a nearly 100% yield has not been reported previously. A key-feature in our device for easy and reproducible bilayer formation is the micrometer-sized aperture in the Teflon layer. We believe that both the aperture shape and dimensions contribute to the instantaneous thinning and the zipping of the phospholipids in the aperture into a bilayer without any external intervention, as well as to the reproducibility of the process. As already described above, the aperture has a well-defined geometry, which is essential to control the amount of lipid deposited in the aperture.[15,20] On other aspects, spontaneous thinning has been reported for substrates thinner than 20-µm,[12,25] while external help is required to trigger membrane formation for 47-µm[20] or 125-µm[15] thick substrates. Here, we believe that the spontaneous and instantaneous thinning of the lipid solution into a bilayer is accounted for by the 12.5-µm thin partition. More specifically, the volume of the aperture - which is defined by the substrate thickness and the aperture diameter - seems to be crucial for efficient BLM formation in the aperture: if a smaller aperture (50-µm diameter) is used under the same experimental conditions (similar flow rate and identical lipid solution) instantaneous thinning of the lipid solution is less often observed. Specifically, BLMs only form in 57% of the cases (n = 7) and only 43% instantaneously, they are much smaller (7 ± 5% of the aperture vs. 55 ± 15% in a 100-µm aperture) and more likely to go back to a lipid plug state within ~15 min. In combination with the aperture shape and dimensions, the flow is likely to assist the drainage of the solution in the aperture to give a ca. 100-nm thick lipid plug, which is the first main step proposed for the formation of a bilayer.[36,37] In the next step, fluctuations in this thinner lipid film bring phospholipids in both leaflets in contact, which initiates their self-organization and zipping into a bilayer structure.[36,37] Here again, we reason that the buffer flow in both channels promotes the perturbation of the thin lipid film, causing immediate initiation of the bilayer formation upon flushing of the buffer in both channels. Therefore, we endeavor ourselves to determine the

flow in the channels in the vicinity of the aperture during membrane formation, and to correlate this to the process of membrane formation. Assessment of the flow speed around the aperture shows values in the 2–27 μm/s range (n = 8) when thinning is successful. On the contrary, higher flow speed (36 ± 3.5 μm/s, n = 3) results in breaking of the lipid plug during membrane formation, which we attribute to a too high shear on the lipid film in the aperture.
Altogether, the nearly 100% membrane formation yield and the reproducibility of the process are accounted for by the aperture shape and dimensions, together with the presence of a moderate flow in the channel that assists the thinning process.

Monitoring membrane formation process

The process of membrane formation is monitored both electrically and optically (**Figure 3.5** a,b). The displacement of the solutions and the thinning process are followed using bright field (**Figure 3.5** d) or fluorescence microscopy. Simultaneously, a triangular voltage (50 Hz, 75 mV pp) is applied, while the current response is recorded (10 kHz sampling rate). The BLM capacitance C_m is derived from the measured current after calibration of the system (see experimental section), and plotted as a function of the time (**Figure 3.5** e). First, until the buffer front has passed ~70% of the aperture (n = 3), the measured capacitance is stable (**Figure 3.5** e, t < 35 s). Thereafter, instantaneous thinning is observed (**Figures 3.5** c–e); this is accompanied by a progressive increase of the capacitance (**Figure 3.5** e, 35 s < t < 64 s) since this parameter is inversely proportional to the membrane thickness. It should be noted that the bilayer is growing at a constant rate, as reported previously.[36,37] Finally, the measured capacitance reaches a plateau (**Figure 3.5** e, t > 64 s) around 20–30 pF, which indicates successful formation of a membrane. Simultaneously, the bilayer is visualized as a 'black' area in the center of the aperture (**Figure 3.5** d). The black color originates from the thickness of the bilayer which is much smaller than the wavelength of the light: subsequently, destructive interferences are obtained between the light reflected from the two sides of the bilayers.[36,37,1] In the annulus that surrounds the bilayer a series of fringes is observed, corresponding to successive constructive and destructive interferences (data not shown). It is worth noticing, that the two optical and electrical characterization schemes are fully independent and can be employed separately.

In-depth bilayer characterization

Membranes are characterized in the microfluidic platform in terms of seal resistance (R_m), capacitance (C_m), and surface area (A_{BLM}) using the same combination of electrical and optical measurements (**Table 3.1**). This complete set of information which is not accessible using conventional bilayer set-ups not only enables in-depth

characterization of the membranes, but also brings a better insight into the membrane preparation technique.

Table 3.1. Membrane properties. Bilayers are formed with DPhPC in n-decane, DPhPC in n-decane supplemented with 2% vol ethanol and 70/30 L-α-PC/Ch (cholesterol) in n-decane supplemented with 2% vol ethanol. The BLMs are characterized in terms of seal resistance (R_m), capacitance (C_m), surface area (A_{BLM}), specific capacitance (C_s) and thickness (d). To calculate the thickness, a dielectric constant of 2.7 is used for all measurements.[38]

Lipids (in *n*-decane)	R_m **[GΩ]**	C_m **[pF]**[a]	A_{BLM} **[%]**	C_s **[μF/cm²]**	d **[nm]**
DPhPC	9 ± 5[b]	24 ± 5[c]	55 ± 15[c]	0.54 ± 0.06[c]	4.43 ± 0.40[c]
DPhPC+EtOH	10 ± 3[b]	21 ± 6[d]	44 ± 17[d]	0.62 ± 0.11[d]	3.86 ± 0.27[d]
L-α-*PC/Ch +EtOH*	30 ± 12[b]	27 ± 8[d]	56 ± 16[d]	0.60 ± 0.10[d]	3.98 ± 0.24[d]

[a] corrected for the stray capacitance of the device b: n=5 c: n=9 d: n=11

First, DPhPC BLMs are employed to characterize the membrane formation technique. A GΩ seal resistance (R_m = 9 ± 5 GΩ (n = 5)) is measured, which is essential for high-quality electrical measurements, and the capacitance equals C_m = 24 ± 5 pF (n = 5). Concomitantly, the surface area of the bilayer is determined using bright field microscopy (ImageJ software): BLMs typically cover 55 ± 15% of the aperture. Using this together with the membrane capacitance, the specific capacitance (C_s) which is defined as a capacitance per unit area is calculated. For DPhPC membranes, we found C_s = 0.54 ± 0.06 μF/cm². Interestingly, this parameter indicates whether the BLM contains solvent, and to which extent. Membranes prepared by the painting technique,[1] which are defined as solvent containing membranes, are characterized by C_s ≈ 0.45 μF/cm² against 0.9 μF/cm² and 1.0 μF/cm² for solvent-less and cell membranes, respectively.[39] The value found here suggests that the membranes formed in our microfluidic device may contain less solvent than those prepared with the painting technique. Following this, the thickness of the membrane is derived using $d=\varepsilon_0\varepsilon_r/C_s$ where ε_r is the dielectric constant (relative permittivity) of the bilayer and ε_0 the permittivity of free space. The membrane thickness is assessed to be 4.43 ± 0.40 nm using a dielectric constant equal to 2.7, as reported in the literature for solvent-free DPhPC bilayers.[38] As the dielectric constant for n-decane is similar (2.0-2.1),[38,40] this value of 2.7 can be used in a first approximation for DPhPC membranes, although it might result in slightly higher values for the bilayer thickness.

Subsequently, the composition of the lipid solution is varied, both in terms of solvent and lipid mixture and the impact of these changes on the membrane properties is measured, as summarized in **Table 3.1**. First, the lipid solution (DPhPC in n-decane) is supplemented with 2% vol ethanol. A slightly higher C_s = 0.62 ± 0.11 μF/cm² (n = 9) is measured, which translates in a thinner membrane (3.86 ± 0.27 nm) using again ε_r = 2.7. These results suggest that the presence of alcohol in the lipid mixture promotes thinning of the bilayer.[11] Subsequently, the lipid composition of the membrane is altered. DPhPC is a synthetic lipid and for this reason, it cannot serve as a good model for experimentation on natural membranes. Mammalian cells are mainly built from another glycerophospholipid, L-α-phosphatidylcholine (L-α-PC), and they comprise ca. 30% mol cholesterol (Ch).[41] Therefore, a 70:30 L-α-PC/Ch mixture in n-decane supplemented with 2% vol ethanol is subsequently employed. For L-α-PC/Ch membranes (n = 11), C_s = 0.60 ± 0.10 μF/cm² and d = 3.98 ± 0.24 nm are found, using the same ε_r value in a first approximation.[38]

This set of experiments demonstrates the versatility of our platform for the preparation of membranes having various compositions, followed by their thorough characterization. This combined optical and electrophysiological approach is highly attractive for screening various lipid/solvent compositions towards the formulation of solvent-less bilayers and closer models of the cell membrane. Furthermore, this versatility is essential to conduct experiments on membrane proteins which often require a specific lipidic environment for proper functioning,[42] and which may be sensitive to the presence of solvent in the bilayer.

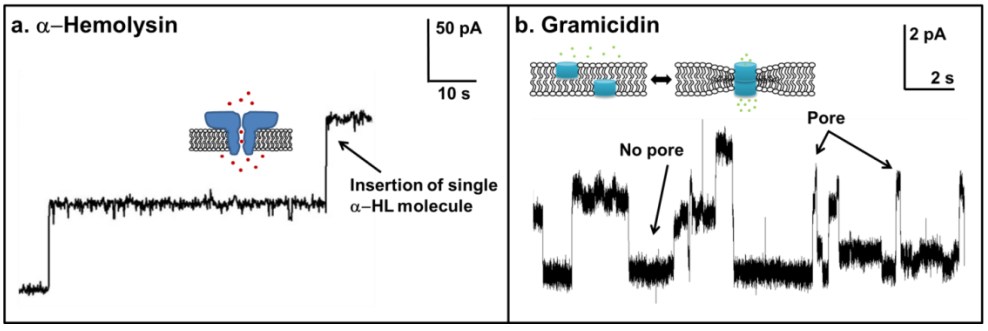

Figure 3.6. Single nanopore measurement. (a) Electrical monitoring of the insertion of individual α-hemolysin proteins (applied dc voltage 50 mV, sampling rate 10 Hz). **(b)** Electrical recording of the gramicidin channel activity (applied dc voltage 80 mV, sampling rate 50 kHz). In both cases, bilayers are formed with L-α-PC/Ch in n-decane, and a 1 M KCl buffer is used for the measurements.

3.3.3 Studies on natural nanopores

Pore-forming species

The applicability of the microfluidic platform is finally demonstrated for single molecule measurements using the membrane pore-forming species α-hemolysin (αHL) and gramicidin. Insertion of these proteins in a BLM is considered as a routine assay to confirm successful bilayer formation, and this demonstrates as well the capability of BLM experimentation platforms for single protein measurements.[11,25] After bilayer formation using L-α-PC/Ch, the pore-forming species are added in the top channel of the device while applying a dc voltage across the membrane to monitor protein insertion in the bilayer and to measure the current through the pore (dc voltage of 50 or 80 mV; sampling rate 10 Hz or 50 kHz for αHL and gramicidin, respectively). Every single αHL protein insertion gives rise to a current jump of 56 ± 19 pA (**Figure 3.6** a), and the corresponding pore conductance value of 1.03 ± 0.35 nS (n = 6) is in good agreement with previously reported values (1 nS, same buffer conditions).[43] Gramicidin is a linear peptide and forms pores upon trans-bilayer dimerization of two monomers present in the different leaflets of the BLM.[44] This process is highly dynamic and monomers continuously associate and dissociate in the bilayer, as shown in **Figure 3.6** b. Single pore events (ca. 2 pA) are successfully detected. The measured pore conductance is on average 24 pS (n = 37), which is comparable to the 21 pS value reported by Borisenko et al. for gramicidin A alone in DPhPC membranes.[45] However, the values measured here are spread (18–27 pS) as a mixture of species (gramicidin A, B, and C) is employed. It is worth noticing that the lifetime of the bilayer is not affected by the presence of pore-forming species, and that gramicidin-containing bilayers are stable for up to 23 h. Furthermore, the noise in the electrical signal is as low as 0.4 pA rms in those measurements.

Gramicidin assay for sensing membrane properties

Gramicidin dimer formation involves compression and bending of the bilayer and the dynamics of gramicidin pore formation are influenced by the bilayer properties (e.g., thickness, curvature, stiffness, and fluidity) due to a change in equilibrium between the monomeric and the dimeric forms.[44,46-48] This phenomenon is exploited here to indirectly compare the properties of membranes prepared from (1) DPhPC in n-decane, (2) DPhPC in n-decane supplemented with 2% vol ethanol, and (3) DPhPC in n-decane exposed to acetylsalicylic acid (1 μM in 1 M KCl buffer) (**Figure 3.7** a–c). For this set of experiments, the peptide is directly added to the lipid mixture prior to bilayer formation to keep the peptide/lipid ratio constant ($\sim 7 \cdot 10^{-8}$). The peptide activity is measured as before (80 mV dc voltage; 10 kHz sampling rate; 1 M KCl buffer), and characterized in terms of channel appearance rate, the number of

channels, and average channel lifetime (data are filtered and analyzed using an in-house written Matlab routine). For every condition, the assay is repeated at least twice, until the total amount of recorded channels exceeds 800. First, in presence of ethanol, the channel appearance rate highly increases (~209 versus ~19 channels per min without ethanol) as well as the number of channels (up to 8 simultaneously detected open channels with ethanol versus 4 in absence of ethanol). This may be accounted for by two reasons: i) an increase in membrane fluidity,[49,50] which favors the dimerization process and ii) a decrease in membrane thickness, as suggested earlier in this article, which has been reported to increase the probability of pore formation.[52] The gramicidin pore has a hydrophobic length of 2.17 nm, which is smaller than the hydrophobic thickness of the bilayers formed in our device (~4.43 nm and ~3.86 nm for BLMs without and with ethanol, respectively). Therefore, the bilayer must deform locally to enable the dimerization of two gramicidin sub-units and the formation of a pore.[51] For thinner membranes, the energetic cost required for the membrane deformation is lower, and this consequently translates into a higher probability of pore formation and an increased number of channels,[52] as seen here for the ethanol-containing bilayer. Additionally, the average channel lifetime is decreased for BLMs with ethanol (0.14 s *vs.* 0.51 s for BLMs without ethanol) as already reported for long-chain alcohols and n-decanol.[51,52] The latter is reported to contribute to a decrease in channel lifetime through a decrease in the surface tension; we presume that ethanol has a similar action on DPhPC membranes, which accounts for the shorter lifetimes we observe.[52]

In a second step, the bilayer properties are studied under exposure of amphiphilic drugs such as acetylsalicylic acid. Interestingly, the opposite is observed, and the channel appearance rate is slightly lower (~10 channels per min) as well as the number of channel events whereas the average channel lifetime becomes longer (0.80 s). This change in gramicidin activity is likely to be attributed to the adsorption of the amphiphilic drug on the bilayer. Thereby, the interactions between the headgroups of neighboring lipids and the packing density of the molecules is increased which leads to a reduction in membrane fluidity, as described on vesicles prepared from dipalmitoyl phosphatidic acid (DPPA)[53] or using another amphiphilic drug, ibuprofen on phosphatidylcholine (PC) monolayers.[54]

These preliminary experiments demonstrate the potential of our platform to indirectly probe membrane properties and their variations upon exposure to external factors using the natural nanopore gramicidin.

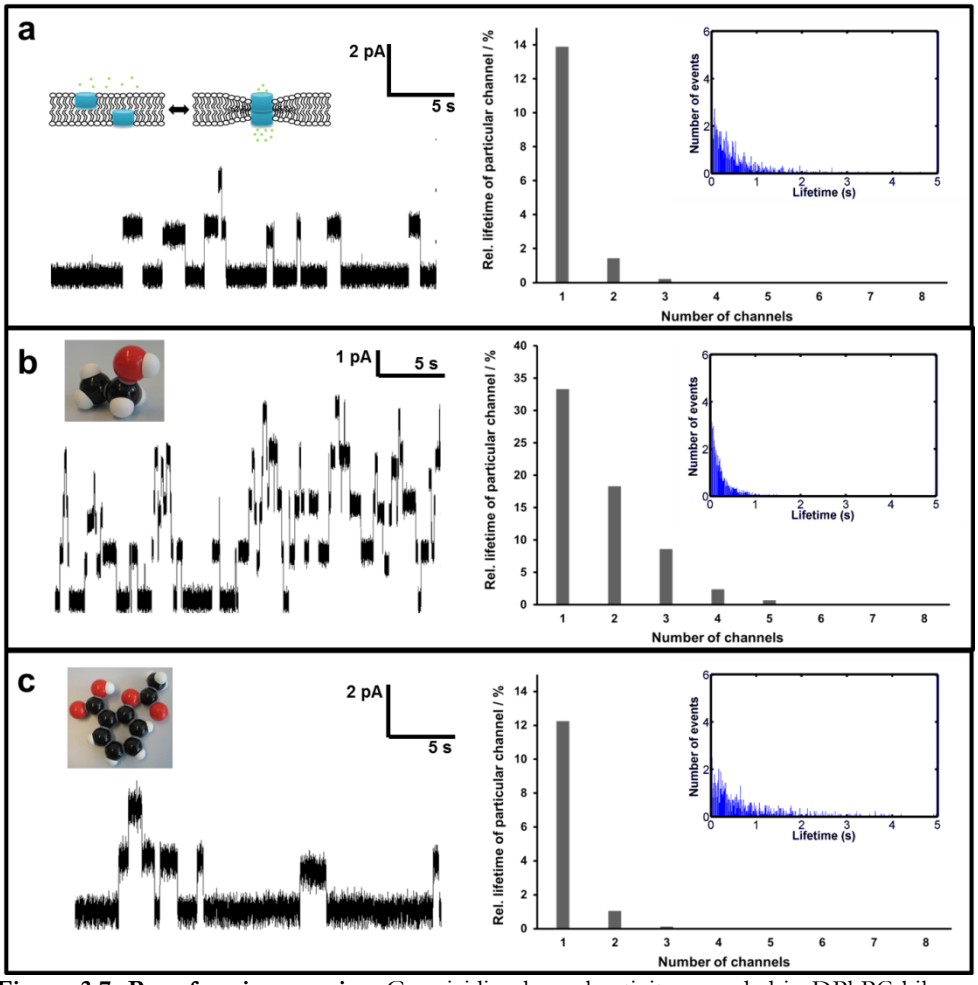

Figure 3.7. Pore-forming species. Gramicidin channel activity recorded in DPhPC bilayers a), in DPhPC bilayers with 2% vol ethanol b), and in DPhPC bilayers exposed to 1 µM acetylsalicylic acid c) (applied dc voltage 80 mV, sampling rate 10 kHz). The experiments are analyzed in terms of channel appearance rate (a–c, *left*), number of open channels (a–c, *right*) and average channel lifetime (a–c, *inset right*, bin size 0.01 s). The gramicidin activity is determined for all conditions through at least two experiments until ~800 channels in total are recorded, i.e., for ~66 min (a), ~16 min (b), and ~88 min (c). In a), an activity of 19 channels/min is recorded, against 209 channels/min in b), and 10 channels/min in c). For all measurements, a 1 M KCl buffer with 10 mM Hepes (pH 7.4) is employed. Note that the scale of the graphs in the right column is different for better visualization of the measurements.

3.4 Conclusion

In this chapter, a microfluidic platform is presented for reproducible bilayer formation with a nearly 100% success yield. The platform performance is demonstrated by the

in-depth characterization of membranes comprising synthetic and natural phospholipids while employing a dual optical and electrical measurement scheme. Electrophysiological measurements of the pore-forming species α-hemolysin and gramicidin confirm high electrical resolution on the single molecule level, and a gramicidin-based assay illustrates the potential of our platform to indirectly probe alterations in the bilayer properties after exposure to external stimuli.
Altogether, these experiments validate the capability of our platform for several applications including fundamental studies on membrane properties and eventually, for drug development or screening. Additionally, the optical and electrophysiological measurement scheme can be further extended towards high-resolution imaging, such as confocal microscopy, as discussed in the next chapter.

3.5 Acknowledgements

I would like to thank Johan Bomer for his great support in the clean room, Hans de Boer for the fabrication of the chip-holder and the alignment setup, Adithya Sridhar who kindly performed WLI imaging of the apertures, Lennart de Vreede for SEM pictures of the apertures, and Mathieu Odijk for his help with data analysis.

3.6 References

1. Mueller, P.; Wescott, W. C.; Rudin, D. O.; Tien, H. T., Methods for formation of single bimolecular lipid membranes in aqueous solution. *Journal of Physical Chemistry* **1963**, *67* (2), 534-535.
2. Wei Zheng, R. H. S., Laszlo Kiss, High throughput assay technologies for ion channel drug discovery. *ASSAY and Drug Development Technologies* **2004**, *2* (5), 543-552.
3. Kocer, A.; Walko, M.; Meijberg, W.; Feringa, B. L., A light-actuated nanovalve derived from a channel protein. *Science* **2005**, *309* (5735), 755-758.
4. Howorka, S.; Movileanu, L.; Braha, O.; Bayley, H., Kinetics of duplex formation for individual DNA strands within a single protein nanopore. *Proc. Natl. Acad. Sci. U. S. A.* **2001**, *98* (23), 12996–13001.
5. Clarke, J.; Wu, H.-C.; Jayasinghe, L.; Patel, A.; Reid, S.; Bayley, H., Continuous base identification for single-molecule nanopore DNA sequencing. *Nat. Nanotechnol.* **2009**, *4* (4), 265-270.
6. Hall, A. R.; Scott, A.; Rotem, D.; Mehta, K. K.; Bayley, H.; Dekker, C., Hybrid pore formation by directed insertion of alpha-haemolysin into solid-state nanopores. *Nat. Nanotechnol.* **2010**, *5* (12), 874-877.
7. Baaken, G.; Ankri, N.; Schuler, A.-K.; Ruehe, J.; Behrends, J. C., Nanopore-Based Single-Molecule Mass Spectrometry on a Lipid Membrane Microarray. *Acs Nano* **2011**, *5* (10), 8080-8088.

8. Baaken, G.; Sondermann, M.; Schlemmer, C.; Ruehe, J.; Behrends, J. C., Planar microelectrode-cavity array for high-resolution and parallel electrical recording of membrane ionic currents. *Lab on a Chip* **2008**, *8* (6), 938-944.
9. Lundbaek, J. A.; Birn, P.; Hansen, A. J.; Søgaard, R.; Nielsen, C.; Girshman, J.; Bruno, M. J.; Tape, S. E.; Egebjerg, J.; Greathouse, D. V.; Mattice, G. L.; II, R. E. K.; Andersen, O. S., Regulation of Sodium Channel Function by Bilayer Elasticity: The Importance of Hydrophobic Coupling. Effects of Micelle-forming Amphiphiles and Cholesterol. *The Journal of General Physiology* **2004**, *123* (5), 599-621.
10. de Planque, M. R. R.; Aghdaei, S.; Roose, T.; Morgan, H., Electrophysiological Characterization of Membrane Disruption by Nanoparticles. *Acs Nano* **2011**, *5* (5), 3599-3606.
11. Osaki, T.; Suzuki, H.; Le Pioufle, B.; Takeuchi, S., Multichannel Simultaneous Measurements of Single-Molecule Translocation in alpha-Hemolysin Nanopore Array. *Analytical Chemistry* **2009**, *81* (24), 9866-9870.
12. Le Pioufle, B.; Suzuki, H.; Tabata, K. V.; Noji, H.; Takeuchi, S., Lipid bilayer microarray for parallel recording of transmembrane ion currents. *Analytical Chemistry* **2008**, *80* (1), 328-332.
13. Suzuki, H.; Le Pioufle, B.; Takeuhci, S., Ninety-six-well planar lipid bilayer chip for ion channel recording Fabricated by hybrid stereolithography. *Biomedical Microdevices* **2009**, *11* (1), 17-22.
14. Sandison, M. E.; Malleo, D.; Holmes, D.; Berry, R.; Morgan, H., Artificial bilayer lipid membranes (BLMs) on-chip for single molecule sensing. In *Nanotechnology II*, Lugli, P. K. L. B. M. J., Ed. **2005**; Vol. 5838, pp 252-257.
15. Sandison, M. E.; Zagnoni, M.; Morgan, H., Air-exposure technique for the formation of artificial lipid bilayers in microsystems. *Langmuir* **2007**, *23* (15), 8277-8284.
16. Sandison, M. E.; Zagnoni, M.; Abu-Hantash, M.; Morgan, H., Micromachined glass apertures for artificial lipid bilayer formation in a microfluidic system. *Journal of Micromechanics and Microengineering* **2007**, *17* (7), S189-S196.
17. Zagnoni, M.; Sandison, M. E.; Morgan, H., Microfluidic array platform for simultaneous lipid bilayer membrane formation. *Biosensors & Bioelectronics* **2009**, *24* (5), 1235-1240.
18. Zagnoni, M.; Sandison, M.; Marius, P.; Morgan, H., Bilayer lipid membranes from falling droplets. *Analytical and Bioanalytical Chemistry* **2009**, *393* (6-7), 1601-1605.
19. Suzuki, H.; Tabata, K. V.; Noji, H.; Takeuchi, S., Electrophysiological recordings of single ion channels in planar lipid bilayers using a polymethyl methacrylate microfluidic chip. *Biosensors & Bioelectronics* **2007**, *22* (6), 1111-1115.
20. Suzuki, H.; Tabata, K. V.; Noji, H.; Takeuchi, S., Highly reproducible method of planar lipid bilayer reconstitution in polymethyl methacrylate microfluidic chip. *Langmuir* **2006**, *22* (4), 1937-1942.
21. Hromada, L. P.; Nablo, B. J.; Kasianowicz, J. J.; Gaitan, M. A.; DeVoe, D. L., Single molecule measurements within individual membrane-bound ion

channels using a polymer-based bilayer lipid membrane chip. *Lab on a Chip* **2008**, *8* (4), 602-608.
22. Sandison, M. E.; Morgan, H., Rapid fabrication of polymer microfluidic systems for the production of artificial lipid bilayers. *Journal of Micromechanics and Microengineering* **2005**, *15* (7), S139-S144.
23. Shao, C.; Kendall, E. L.; DeVoe, D. L., Electro-optical BLM chips enabling dynamic imaging of ordered lipid domains. *Lab on a Chip* **2012**, *12* (17), 3142-3149.
24. Kawano, R.; Osaki, T.; Sasaki, H.; Takinoue, M.; Yoshizawa, S.; Takeuchi, S., Rapid Detection of a Cocaine-Binding Aptamer Using Biological Nanopores on a Chip. *Journal of the American Chemical Society* **2011**, *133* (22), 8474-8477.
25. Kawano, R.; Osaki, T.; Sasaki, H.; Takeuchi, S., A Polymer-Based Nanopore-Integrated Microfluidic Device for Generating Stable Bilayer Lipid Membranes. *Small* **2010**, *6* (19), 2100-2104.
26. Mach, T.; Chimerel, C.; Fritz, J.; Fertig, N.; Winterhalter, M.; Fuetterer, C., Miniaturized planar lipid bilayer: increased stability, low electric noise and fast fluid perfusion. *Analytical and Bioanalytical Chemistry* **2008**, *390* (3), 841-846.
27. Malmstadt, N.; Nash, M. A.; Purnell, R. F.; Schmidt, J. J., Automated formation of lipid-bilayer membranes in a microfluidic device. *Nano Letters* **2006**, *6* (9), 1961-1965.
28. Bayley, H.; Cronin, B.; Heron, A.; Holden, M. A.; Hwang, W. L.; Syeda, R.; Thompson, J.; Wallace, M., Droplet interface bilayers. *Molecular BioSystems* **2008**, *4* (12), 1191-1208.
29. Zagnoni, M., Miniaturised technologies for the development of artificial lipid bilayer systems. *Lab on a Chip* **2012**, *12* (6), 1026-1039.
30. Arayanarakool, R.; Le Gac, S.; van den Berg, A., Low-temperature, simple and fast integration technique of microfluidic chips by using a UV-curable adhesive. *Lab on a Chip* **2010**, *10* (16), 2115-2121.
31. Mayer, M.; Kriebel, J. K.; Tosteson, M. T.; Whitesides, G. M., Microfabricated teflon membranes for low-noise recordings of ion channels in planar lipid bilayers. *Biophysical Journal* **2003**, *85* (4), 2684-2695.
32. Montal, M.; Mueller, P., Formation of bimolecular membranes from lipid monolayers and a study of their electrical properties. *Proc. Natl. Acad. Sci. U. S. A.* **1972**, *69* (12), 3561-3566.
33. Im, S. G.; Bong, K. W.; Lee, C.-H.; Doyle, P. S.; Gleason, K. K., A conformal nano-adhesive via initiated chemical vapor deposition for microfluidic devices. *Lab on a Chip* **2009**, *9* (3), 411-416.
34. Bart, J.; Tiggelaar, R.; Yang, M.; Schlautmann, S.; Zuilhof, H.; Gardeniers, H., Room-temperature intermediate layer bonding for microfluidic devices. *Lab on a Chip* **2009**, *9* (24), 3481-3488.
35. Grover, W. H.; von Muhlen, M. G.; Manalis, S. R., Teflon films for chemically-inert microfluidic valves and pumps. *Lab on a Chip* **2008**, *8* (6), 913-918.
36. Fujiwara, H.; Fujihara, M.; Ishiwata, T., Dynamics of the spontaneous formation of a planar phospholipid bilayer: A new approach by simultaneous

electrical and optical measurements. *Journal of Chemical Physics* **2003**, *119* (13), 6768-6775.

37. Tien, H. T.; Dawidowi, E. A., Black lipid films in aqueous media - A new type of interfacial phenomenon. Experimental techniques and thickness measurements. *Journal of Colloid and Interface Science* **1966**, *22* (5), 438-453.
38. Plant, A. L.; Gueguetchkeri, M.; Yap, W., Supported phospholipid/alkanethiol biomimetic membranes - insulating properties. *Biophysical Journal* **1994**, *67* (3), 1126-1133.
39. Nikolelis, D. P.; Krull, U. J.; Ottova, A. L.; Tien, H. T., Bilayer lipid membranes and other lipid-based methods. In *Handbook of chemical and biological sensors*, Taylor, r.; schultz, j., Eds. Institute of physics publishing: Bristol, **1996**; pp 221-256.
40. Dilger, J. P.; McLaughlin, S. G. A.; McIntosh, T. J.; Simon, S. A., Dielectric-constant of phospholipid-bilayers and the permeability of membranes to ions. *Science* **1979**, *206* (4423), 1196-1198.
41. Alberts, B., *Molecular Biology of the Cell*. Garland Publishing, Inc., New York, USA: **1989**.
42. van Rooijen, B. D.; Claessens, M. M. A. E.; Subramaniam, V., Membrane Permeabilization by Oligomeric alpha-Synuclein: In Search of the Mechanism. *Plos One* **2010**, *5* (12).
43. Krasilnikov, O. V.; Ternovsky, V. I.; Tashmukhamedov, B. A., Properties of alpha-staphylotoxin-induced conductivity channels in bilayer phospholipid-membranes. *Biofizika* **1981**, *26* (2), 271-276.
44. Lundbaek, J. A.; Collingwood, S. A.; Ingolfsson, H. I.; Kapoor, R.; Andersen, O. S., Lipid bilayer regulation of membrane protein function: gramicidin channels as molecular force probes. *Journal of the Royal Society Interface* **2010**, *7* (44), 373-395.
45. Borisenko, V.; Lougheed, T.; Hesse, J.; Fureder-Kitzmuller, E.; Fertig, N.; Behrends, J. C.; Woolley, G. A.; Schutz, G. J., Simultaneous optical and electrical recording of single gramicidin channels. *Biophysical Journal* **2003**, *84* (1), 612-622.
46. Ingolfsson, H. I.; Andersen, O. S., Screening for Small Molecules' Bilayer-Modifying Potential Using a Gramicidin-Based Fluorescence Assay. *Assay and Drug Development Technologies* **2010**, *8* (4), 427-436.
47. Woolley, G. A.; Wallace, B. A., Model ion channels - Gramicidin and alamethicin. *Journal of Membrane Biology* **1992**, *129* (2), 109-136.
48. Andersen, O. S.; Koeppe, R. E., II, Bilayer thickness and membrane protein function: An energetic perspective. *Annual Review of Biophysics and Biomolecular Structure* **2007**, *36*, 107-130.
49. Elliott, J. R.; Haydon, D. A., The influence of n-alkanols on the capacity per unit area of planar lipid bilayers. *Biochimica Et Biophysica Acta* **1984**, *773* (1), 165-168.
50. Ly, H. V.; Longo, M. L., The influence of short-chain alcohols on interfacial tension, mechanical properties, area/molecule, and permeability of fluid lipid bilayers. *Biophysical Journal* **2004**, *87* (2), 1013-1033.

51. Lundbaek, J. A., Lipid bilayer-mediated regulation of ion channel function by amphiphilic drugs. *J. Gen. Physiol.* **2008**, *131* (5), 421-429.
52. Elliott, J. R.; Needham, D.; Dilger, J. P.; Haydon, D. A., The effects of bilayer thickness and tension on gramicidin single-channel lifetime. *Biochimica Et Biophysica Acta* **1983**, *735* (1), 95-103.
53. Panicker, L., Interaction of benzoic acid, aspirin and para-hydroxy benzoic acid with dipalmitoyl phosphatidic acid vesicles. *Thermochimica Acta* **2006**, *451* (1-2), 174-180.
54. Jablonowska, E.; Bilewicz, R., Interactions of ibuprofen with Langmuir monolayers of membrane lipids. *Thin Solid Films* **2007**, *515* (7-8), 3962-3966.

Chapter 4

Microfluidic bilayer platform for high-resolution confocal imaging in combination with electrophysiological measurements

---

Bright field microscopy provides macroscopic information on the bilayer characteristics, without any insight on the molecular scale. To achieve high resolution imaging using confocal microscopy, the microfluidic device is adapted by thinning down the bottom glass substrate to ~200 μm. The confocal capability is exploited to visualize phase separation in bilayers prepared from a ternary lipid mixture (L-α-phosphatidylcholine, sphingomyelin and cholesterol). Following, the confocal measurements are combined with electrophysiological recordings to characterize POPC bilayers supplemented with two probes (NBD-PE and/or gramicidin). The bilayers are studied in terms of thickness and fluidity, and at the same time the gramicidin activity is recorded. These combined measurements reveal that NBD-PE has no effect on the bilayer thickness, while gramicidin induces thinning of the membrane. Additionally, in BLMs with both probes, a reduction in gramicidin open probability is observed compared to BLMs with gramicidin only, suggesting an influence of NBD-PE on the (mechanical) bilayer properties. Conversely, no influence of gramicidin on the membrane fluidity could be observed. Altogether, these experiments demonstrate the applicability of our platform for multi-parametric measurements.[1,2]

---

[1] Partly modified from: V.C. Stimberg, J.G. Bomer, I. van Uitert, A. van den Berg, and S. Le Gac, "High Yield, Reproducible and Quasi-Automated Bilayer Formation in a Microfluidic Format", *Small,* 2013, 9 (7), 1076–1085. **Cover article**

[2] Manuscript in preparation

4.1 Introduction

Ion channels are widely studied in bilayer lipid membranes, which are simplified and planar models of the cell membrane, while their activity is recorded with electrophysiology and a patch clamp amplifier. This approach provides high content information on single channel behavior with a sub-picoampere and sub-millisecond resolution, as well as insight into gating mechanisms of a single channel, and whether, for instance, the open and closed states of a given channel are triggered upon ligand binding, by applying a voltage across the membrane or by a mechanical stimulus.[1] Furthermore, conductance and sub-conductance states of a single pore can be characterized.[1] Finally, the open probability of the protein is accessible, as well as the duration of the open and closed events, which reveals information on ion channel kinetics.[2] Even though bilayer electrophysiology is a highly powerful technique to elucidate the behavior of individual ion channels, it is blind to the nature of the ions, which are transported through the pore, unless the buffer composition is varied to include one type of ions only.[1] Additionally, membrane properties, which can be regulated locally by a variety of physical or soluble factors, and which have been reported to significantly influence ion channel activity,[3] can only be assessed globally using electrophysiological recordings and bilayer models, while local changes in the bilayer are not accessible. To obtain this missing information, complementary strategies coupling lipid bilayer electrophysiology with an orthogonal method are needed. In that context, high resolution imaging techniques are highly attractive as they give access to the aforementioned missing information, while being easily combinable to electrophysiology.

Förster Resonance Energy Transfer (FRET) for instance yields information on interactions between two molecules such as a target compound and an ion channel if they are spaced apart less than 10 nm, by detecting transfer in the fluorescence signal.[4] Next, Fluorescence Recovery After Photobleaching (FRAP) is widely employed to assess the mobility of lipids or proteins in a membrane by locally photobleaching a defined region and monitoring its fluorescence recovery. Both FRET and FRAP techniques are typically based on confocal microscopy. Finally, Total Internal Reflection Fluorescence (TIRF) microscopy is utilized to characterize molecules close to the specimen surface.[5] All the aforementioned techniques yield valuable information on the bilayer organization, together with fundamental insight into ion channel activity, as well as complementary information to electrophysiological techniques. In a conventional bilayer set up however, membranes have a vertical orientation and are sandwiched between two relatively large reservoirs, which precludes high resolution imaging, even though a number of attempts in that direction have been reported.[6,7]

In that context, microfluidics offers new possibilities for multi-parametric measurements on bilayers, mainly due to the horizontal orientation of the aperture. Furthermore, the height of the microstructures can be adjusted to decrease the distance between the bilayer and the objective. Mainly two formats have been proposed to control the distance between the bilayer and the objective: in a first approach, the lower fluidic compartment is replaced by a shallow microfluidic channel, to facilitate the exchange of solutions below the bilayer. Alternatively, a bilayer is formed on a thin (<100 μm)[8] agarose layer providing mechanical support to the BLM and increasing thereby its lifetime. Utilizing the microfluidic format, phase separation phenomena were successfully imaged, and these studies provided additional insight into the growth and dynamics of liquid-ordered domains,[9] the temperature dependence of the process,[10] or even its influence on gramicidin activity, after coupling of confocal microscopy to electrophysiological measurements.[10] Alternatively, gramicidin dimer formation was investigated in agarose-supported bilayers using monomers tagged with different fluorophores and FRET, while recording electrophysiologically gramicidin activity. This combined approach allowed studying structural rearrangements of the gramicidin dimers, and correlating it to the peptide activity.[8] TIRF microcopy was also utilized to monitor the motion of single fluorescently labeled lipid molecules, as well as the fusion process between liposomes and a bilayer supported by an agarose layer, using a combination of optical and electrophysiological recordings.[11] In the future, this approach could notably yield fundamental understanding of the process governing liposome fusion. Finally, the ion flux across α-hemolysin pores was measured using TIRF in a droplet hydrogel bilayer (DHB) platform, while recording electrophysiologically the ion channel current, yielding comprehensive information on ion channel activity.[12] Altogether, these previous works have demonstrated the potential of high resolution imaging, and its combination with electrophysiological measurements to yield complementary information on bilayers.

In chapter 3 of this thesis, we conducted a gramicidin assay where bilayer properties were modified upon addition of soluble factors (aspirin & ethanol), and we hypothesized that the changes we recorded in gramicidin activity were caused either by changes in the bilayer or in its fluidity. Here, we extend this gramicidin assay, and combine electrophysiological measurements with the assessment of various bilayer properties, such as its thickness and fluidity. While the former parameter is accessible using electrophysiological measurements and bright-field imaging, the latter requires confocal microscopy and FRAP measurements.

To implement this dual measurement approach, we adapt our fully closed microfluidic device for high resolution imaging by thinning down the bottom glass substrate to ~200 μm, and we subsequently demonstrate the potential of the resulting device to

study bilayer properties and their influence on ion channel activity by confocal microscopy. First, phase separation is introduced in suspended bilayers prepared from a ternary lipid mixture (L-α-phosphatidylcholine, sphingomyelin and cholesterol), and visualized with confocal microscopy. In a next step, bilayers are characterized in terms of thickness and fluidity, while recording at the same time the gramicidin peptide activity (open probability, number of channels, single channel lifetime and conductance) in POPC bilayers supplemented with one or two probes, gramicidin and NBD-PE, necessary for the gramicidin and FRAP measurements, respectively.

4.2 Experimental Section

4.2.1 Materials

Membranes are prepared from DPhPC (1,2-diphytanoyl-*sn*-glycero-3-phosphocholine), L-α-PC (L-α-phosphatidylcholine (Heart, Bovine), SM (Egg sphingomyelin), Ch (Cholesterol), and rhodamine labeled DOPE (1,2-dioleoyl-*sn*-glycero-3-phosphoethanolamine-N-(lissamine rhodamine B sulfonyl)), POPC (1-palmitoyl-2-oleoyl-*sn*-glycero-3-phosphocholine), and NBD-PE (1,2-dioleoyl-*sn*-glycero-3-phosphoethanolamine-N-(7-nitro-2-1,3-benzoxadiazol-4-yl) (ammonium salt)), which are all purchased from Avanti Polar lipids (Alabaster, AL, USA) as solutions in chloroform, and cholesterol as powder. Potassium chloride (KCl), (4-(2-hydroxyethyl)-1-piperazineethanesulfonic acid (Hepes), chloroform, and gramicidin (mixture of species with ~80% gramicidin A) are obtained from Sigma Aldrich (Zwijndrecht, The Netherlands), n-decane from Fluka (Steinheim, Germany), and ethanol from Assink Chemie (Enschede, The Netherlands). Deionized water (MilliQ system, Millipore, Billerica, MA, USA) is used for the preparation of all aqueous solutions. All experiments are carried out at room temperature, but without any precise temperature control in the device.

4.2.2 Microfluidic device

The microfluidic device utilized in this chapter is described in detail in chapter 3, with two microfluidic channels (100 μm deep, 300 μm wide) and an aperture (100 μm diameter) located at the channel intersection. However, the initial thickness of the bottom glass substrate of 500 μm is not suitable for confocal imaging. Therefore, it is thinned down to ~200 μm by manual polishing (Vanhespen optics, Borne, The Netherlands) after processing the glass at the wafer-scale, and before bonding at the chip level. Furthermore, the bonding procedure is slightly adapted due to the higher fragility of the thinned substrate. Therefore, the Teflon layer is first bonded to the top

glass substrate, after careful alignment, and thereafter, the thinned bottom substrate is assembled. The pre-curing times for the top and bottom layers are, respectively, ~15 s and ~10 s. Since the resulting device is thinner, it does not fit tightly in the chip-holder presented in chapter 3. Therefore, a PDMS packaging is developed to prevent evaporation. In one series of experiments, PDMS rings are fabricated from thin (~50 μm) PDMS films, and subsequently placed around the reservoirs in the top glass chip (**Figure 4.1** a). In a second series of experiments, PDMS reservoirs (~3.4 mm diameter) are punched in a thicker slab of PDMS (~4.4 mm thickness, **Figure 4.1** b), which is subsequently bonded to the microfluidic device after activation by oxygen plasma (Harrick Scientific Products, NY, USA).

4.2.3 Dedicated experimental set-up for combined confocal and electrophysiological measurements

For the combined confocal and electrophysiological measurement, a dedicated chip holder that fits on the stage of an inverted confocal microscope is developed in-house (**Figure 4.1** c,d). The microfluidic device is placed in a matching cavity with clamps and an opening to allow contact between the bottom surface of the device and the oil-immersion objective (**Figure 4.1** e). A metal bar in the bottom plate of the holder enables to fix the CV 203 BU head stage of the Axopatch 200B amplifier (both Molecular devices, Sunnyvale, CA, USA), and for electrical measurements Ag/AgCl electrodes (Molecular devices, Sunnyvale, CA, USA) are connected to the head stage and inserted in the PDMS reservoirs. The head stage and the electrodes are shielded by a faraday cage for electrophysiological measurements. Data are acquired using a LabView program and a PCI-6259 data acquisition card (National Instruments, Austin, TX, USA).

4.2.4 BLM visualization and domain formation

BLM visualization

In a first series of experiments, the microfluidic device is placed on top of the microscope stage without any chip-holder or PDMS rings for a proof-of-concept experiment, to demonstrate that bilayer lipid membranes can be imaged using confocal microscopy. Bilayers are formed using a similar technique as described in chapter 3, by adding 0.2 μL of lipid solution (25 mg/mL DPhPC in n-decane, supplemented with 1% vol fluorescently labeled DOPE) to each channel, followed by 5 μL buffer solution (1 M KCl, 10 mM Hepes, pH 7.4). The BLM is imaged vertically along a *x*-*z* plane roughly in its middle, using an Evotec Insight Cell 3d microscope

(DPSS Nd:YAG laser, λ = 532 nm). These initial measurements are carried out at Ionovation GmbH (www.ionovation.com, Osnabrück, Germany).

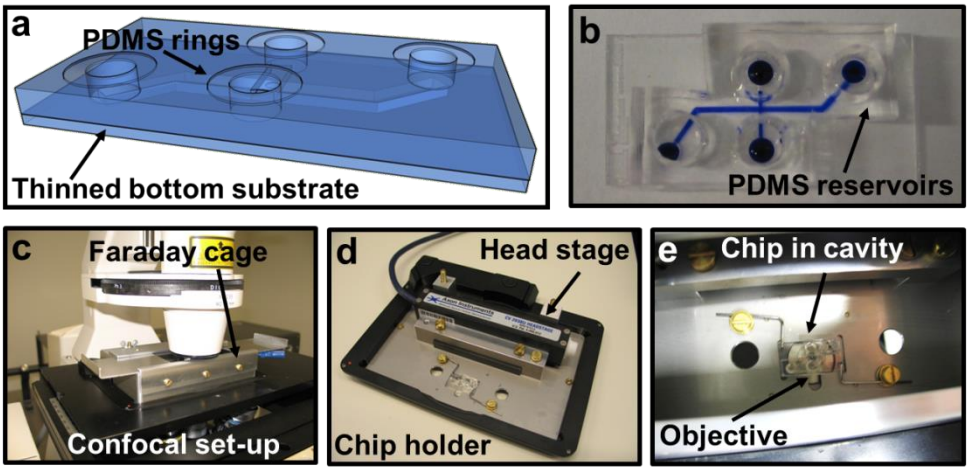

Figure 4.1. Confocal set-up. a) Microfluidic device adapted for confocal microscopy by thinning the bottom substrate to ~200 μm, and with PDMS rings placed on the glass surface to prevent evaporation (not at scale). b) PDMS reservoirs are bonded to the devices to further limit evaporation issues for longer measurements. c) Complete confocal set-up with the faraday cage for electrophysiological measurements, an in-house built chip holder with fixed head stage (d) and a cavity for the chip allowing contact of the oil-immersion objective with the chip (e).

Domain formation

In a second series of experiments using confocal imaging only, thin PDMS rings are added around the reservoirs of the device to limit evaporation phenomena. Droplets of buffer on the hydrophobic PDMS surface are round, and they are subsequently less prone to evaporation than spread droplets on the hydrophilic glass surface. BLMs are prepared using the same approach as described above, but from a ternary lipid mixture (L-α-PC:SM:Ch, 2:1:1 or 1:1:1) with 1% vol fluorescently labeled DOPE (25 mg/mL lipid solution in n-decane, supplemented with 1% vol ethanol). Images are obtained with an inverted confocal laser scanning microscope (LSM510 Zeiss, HeNe laser, λ=543 nm, plan-apochromat 63x/1.4 oil DIC objective, BP 563–615 IR filter and HFT KP 700/543 beam splitter).

4.2.5 Combined confocal and electrophysiological measurements

Bilayer formation

For the combined measurements, thicker PDMS reservoirs are bonded on the microfluidic device for longer experimentation times, and the device is placed in the previously described dedicated chip holder. As before, BLMs are formed by adding 0.5 μL lipid solution (25 mg/mL POPC in n-decane, supplemented with 1% mol NBD-PE and/or 1 nM gramicidin) in both channels, and subsequently 30 and 20 μL of buffer solution (1 M KCl, 10 mM Hepes, pH 7.4) are injected in the bottom and top channel, respectively. The lipid solution is replaced by buffer, and spontaneous and instantaneous bilayer formation is observed, as discussed previously (chapter 3).

Characterization of the bilayer properties

After BLM formation and after the experiment, a wide field picture is taken of the BLM using the confocal microscope to assess its surface area (Image J, open source software from NIH). At the same time, the capacitance is determined electrically, as explained in chapter 3. Briefly, an ac voltage (50 Hz, 75 mV pp) is applied, and the value from the current response is calculated after calibration of the system with solid-state capacitors (2.2-56 pF). The capacitance values are corrected for stray capacitance measured in a chip filled with lipid solution (0.84 ± 0.27 pF, n=2) by subtracting the corresponding values from the curve, and for eventual leakage current (more detailed description in **Appendix I**). To determine the seal resistance, a dc voltage (10 mV, ~5 s) is applied, the current response recorded, and finally R_m is calculated with $R_m = V_{applied} / (I_{applied\ voltage} - I_{voltage=0})$.

FRAP measurements

The BLM is imaged with a laser scanning confocal microscope (LSCM, LSM510 Zeiss, Argon laser, λ = 488 nm, plan-apochromat 63x/1.4 oil DIC objective, LP 505 filter and HFT 488 beam splitter) by zooming in at the center of the BLM (zoom of 3.5x). Two regions of interest (ROIs), a measurement region and a reference region, are defined in this zoom (15 μm diameter, 10 μm spacing in the *x*-direction, same *y*-position), and the focus is adjusted until the highest intensity is reached. Following this, a FRAP protocol is applied resulting in a bleach of ~22%, followed by full recovery. This protocol includes in total 500 imaging cycles, 20 cycles before bleaching, a bleach step at 100% laser intensity with 5 iterations, a bleach time of 1.322 s, and 0.22 s scan time per image. The FRAP protocol is repeated at least twice per BLM, and a detailed scheme of this process is found in **Appendix II**. After the experiment, the BLM is ruptured with a high voltage pulse and the same imaging protocol is applied without BLM to determine the background fluorescence. The diffusion coefficient (*D*) is calculated using the software FRAPAnalyser (freeware from the University of Luxemburg, http://actinsim.uni.lu/eng).

Gramicidin activity

For the gramicidin experiment, the peptide is dissolved in ethanol (100 nM) and added to the lipid solution prior to BLM formation to yield a final concentration of 1 nM (gramicidin/lipid molar ratio ~$3 \cdot 10^{-8}$). Gramicidin activity is measured by applying a dc voltage of 80 mV and recording the current response (1 kHz Low-pass Bessel filter, 10 kHz sampling rate). Data are filtered and analyzed using an in-house written Matlab routine to determine the open probability, number of channels, average single channel lifetime and conductance. In these experiments, multiple channels simultaneously occur; in that case, data analysis is more challenging to assess the exact lifetime of individual channels. More information can be found in **Appendix III**. Altogether, the chosen analysis approach may give slightly underestimated values for the channel lifetime.

Combined and control measurements

For the combined experiments, the bilayers are formed and characterized as described above. After selecting the ROIs in the bilayer for the FRAP measurements, a dc voltage of 80 mV is applied and the FRAP protocol is started. At the same time, the current is recorded to determine the gramicidin activity. At the end of each experiment, the bilayer is ruptured to determine the background fluorescence for the FRAP analysis. In the control measurements with only NBD-PE, the same amount of ethanol is added as for the gramicidin-containing bilayers, and a dc voltage of 80 mV is applied during the FRAP recordings to keep the conditions constant.

4.3 Results and discussion

4.3.1 BLM visualization and domain formation

Although standard electrophysiological set-ups have been combined with conventional optical microscopy (fluorescence and bright field),[13] this approach is limited to the "macro" scale. For instance, it only allows monitoring bilayer formation and estimating the surface area of the bilayer, as described in chapter 3. To get closer insight into processes at the molecular scale, and to investigate for instance lipid organization in the membrane and membrane diffusion phenomena, high resolution imaging techniques such as confocal microscopy are required. For that purpose, the bottom glass substrate of our microfluidic device is thinned down to ~200 μm.

BLM visualization

In a first series of experiments, bilayers prepared from DPhPC (in n-decane) supplemented with 1% vol fluorescently labeled DOPE are imaged using confocal microscopy in the *x*-*z* plane to yield a cross section of the membrane (**Figure 4.2** a).

Interestingly, spontaneous fluctuations of the BLM in the z-direction are observed during imaging (**Figure 4.2** b), which eventually leads to rupture of the membrane. In this experiment, no chip holder is used and buffer evaporates quickly from the reservoirs, which most probably results in the creation of a flow in the microfluidic channel explaining the spontaneous bending observed here.

Domain formation

After confirmation that confocal microscopy could be applied in our device, we decided to image domain formation and phospholipid organization in bilayers prepared from a ternary mixture. For these experiments, PDMS rings are placed around the reservoirs of the chip to solve the evaporation issues encountered previously, and to increase the bilayer stability. Here, bilayers are prepared from a ternary mixture of a saturated sphingolipid (sphingomyelin), an unsaturated phospholipid (L-α-phosphatidylcholine) and cholesterol, in ratios reported to separate into a liquid ordered (l_o) phase and a liquid disordered (l_d) phase.[14-16] Phase separation occurs upon preferences of the cholesterol for saturated phospholipids (here SM), while cholesterol is found to have an even stronger preference for SM rich areas.[15] As before, BLMs are supplemented with 1% vol fluorescently labeled DOPE for visualization of the domains that will partition in the L-α-PC-rich phase. The SM/Ch clusters form l_o rich-phases, seen as dark areas in the L-α-PC-rich l_d matrix which comprises the fluorescently labeled DOPE (**Figures 4.2** c,d). Next to the phase separation, the influence of the temperature on the domain size is observed. Specifically, larger and less numerous domains are detected when the lipid solution has been stored on ice prior to bilayer formation (data not shown), as also reported by Honigman et al.[10]

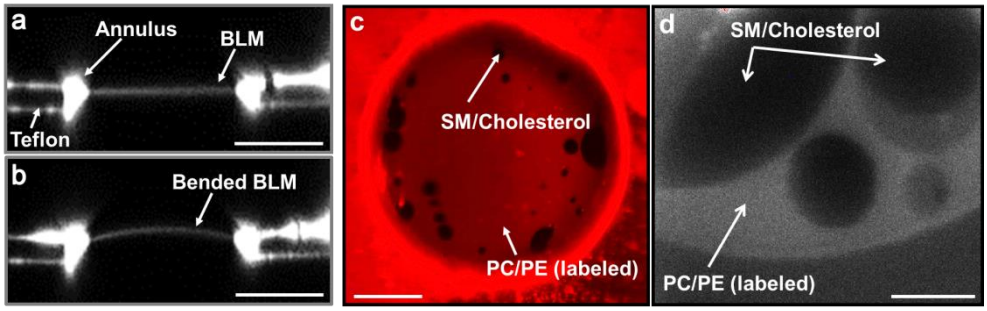

Figure 4.2. BLM visualization and domain formation. a) Side-view of an aperture in the Teflon substrate showing the free-standing BLM surrounded by a bright annulus (50-μm aperture). The DPhPC lipid solution in n–decane has been supplemented with 1% vol DOPE labeled with rhodamine B. b) Spontaneous bending of the same bilayer. c) Phase separation in a BLM formed from a ternary 2:1:1 and d) 1:1:1 L-α-PC/SM/Ch mixture, also supplemented with 1% vol DOPE labeled with rhodamine B at room temperature. Scale bars: 25 μm (a-c) and 5 μm (d).

4.3.2 Combined confocal and electrophysiological measurements

The cell membrane can present local variations in terms of thickness or fluidity, and these changes can impact the function and activity of certain proteins.[3] To assess the membrane thickness and fluidity and to correlate these properties to protein activity, a combination of (confocal) imaging and electrophysiology is utilized. Specifically, the bilayer properties are fully characterized using wide field imaging and electrophysiological measurements, as already reported in chapter 3, while the bilayer fluidity is assessed with FRAP measurements and confocal microscopy, and the activity of a model ion channel, gramicidin, is recorded simultaneously. For these experiments, POPC bilayers (25 mg/mL in n-decane) are utilized, supplemented with 1% mol NBD-PE and/or 1 nM gramicidin for fluidity assessment and/or ion channel measurements, respectively.

Bilayer characterization

First, all bilayers are characterized in terms of seal resistance (R_m), capacitance (C_m) and surface area (A_{BLM}), as summarized in **Table 4.1**. Next to POPC BLMs with both NBD-PE and gramicidin probes, BLMs prepared from plain POPC, and POPC supplemented with either probe (1% mol NBD-PE or 1 nM gramicidin) are characterized as controls to determine the influence of the probes (NBD-PE and gramicidin) on the bilayer properties, if any effect is present.

Table 4.1. Properties POPC BLMs. Bilayers are formed with POPC (25 mg/mL) in n-decane, supplemented with only NBD-PE (1% mol), only gramicidin (1 nM, gramicidin/lipid molar ratio ~$3{\cdot}10^{-8}$), and both NBD-PE and gramicidin (same concentrations). The BLMs are characterized in terms of seal resistance (R_m), capacitance (C_m), surface area (A_{BLM}), specific capacitance (C_s) and thickness (d). To calculate the thickness, a dielectric constant of 2.09 is used for all measurements.[17] a: n=6; b: n=5; c: n=4, ±SD

POPC BLM	R_m (GΩ)	C_m (pF)	A_{BLM} (%)	C_s (μF/cm²)	d (nm)
Plain[a] 25 mg/mL, n-decane	54 ± 33	28 ± 4	67 ± 9	0.54 ± 0.02	3.45 ± 0.16
+ NBD-PE (1%mol)[b]	24 ± 25	25 ± 5	60 ± 7	0.52 ± 0.10	3.65 ± 0.64
+ gramicidin (1 nM)[c]	63 ± 55	29 ± 4	58 ± 9	0.65 ± 0.03	2.86 ± 0.15
+ NBD-PE (1% mol) [b] + gramicidin (1 nM)	34 ± 24	27 ± 4	60 ± 13	0.57 ± 0.03	3.28 ± 0.18

The seal resistance of the membranes is determined after bilayer formation, prior to the FRAP and gramicidin measurements. Bilayers show a seal resistance typically in the GΩ range (between 24 and 63 GΩ in average), which is in a similar range as previously measured values in our microfluidic device (~10 GΩ for DPhPC bilayers, chapter 3),[18] and variations observed for R_m for the different conditions are within the error bars. The capacitance of the BLMs is determined after the experiment, and, in average, values between 25 and 29 pF are found, as expected (chapter 3).[18] Simultaneously, the surface area of the bilayer is assessed, revealing coverage of the aperture between 58 and 67%. Altogether, and as summarized in **Table 4.1**, no clear difference is observed in terms of seal resistance, capacitance and surface area between the four types of POPC membranes suggesting that the two probes, NBD-PE (1% mol) and gramicidin (1 nM), do not influence significantly these bilayer properties under the present experimental conditions.

In a next step, the specific capacitance (C_s) is determined from the values of the membrane capacitance and surface area ($C_s = C_m/A_{BLM}$). For plain POPC BLMs, a value of 0.54 ± 0.02 μF/cm² (n = 6) is obtained, which is comparable to previously measured values for DPhPC membranes in our device. As already discussed, this value is slightly higher than values reported for solvent-containing BLMs formed using the painting method (C_s = 0.45 μF/cm²)[19] while being lower than that of solvent-less membranes (0.9 μF/cm², see chapter 3).[19] Altogether, this value indicates that solvent (n-decane) is present in the membrane between the two leaflets of phospholipids. Following this, the thickness of the bilayers is derived using $d=\varepsilon_0\varepsilon_r/C_s$, where ε_0 is the permittivity of free space and ε_r the dielectric constant (relative permittivity). Here, a value of 2.09 is used for ε_r, as previously reported for phosphatidylcholine membranes in n-decane.[17] The thickness of plain POPC BLMs is assessed to be 3.45 ± 0.16 nm, indicating thinner BLMs compared to conventional solvent-containing membranes (4.8 nm for BLMs of egg yolk phosphatidylcholine with a variety of chain lengths, in n-decane).[17] Following this, the specific capacitance of NBD-PE containing BLMs without and with gramicidin is calculated, yielding C_s values of 0.52 ± 0.10 and 0.57 ± 0.03 μF/cm² (both n = 5), respectively, which corresponds to thicknesses of 3.65 ± 0.64 and 3.28 ± 0.18 nm, respectively, using the same ε_r value as above. Altogether, the specific capacitance and thickness of these membranes are not significantly different, and similar to those of plain POPC BLMs.

Interestingly, BLMs containing only gramicidin exhibit a significantly higher specific capacitance (0.65 ± 0.03 μF/cm², n = 4) compared to plain POPC membranes. This higher value seems to indicate a decrease in membrane thickness from 3.45 ± 0.16 nm (n = 6) for plain POPC BLMs to 2.86 ± 0.15 nm (n = 4) for gramicidin containing BLMs, when using the same ε_r value. As reported previously, the presence of gramicidin does not significantly affect the dielectric properties of the bilayer.[20]

Subsequently, the same value for ε_r can be used for gramicidin containing membranes, even though during pore formation, the ε_r value changes locally to the one of aqueous solution (10 or 80), which is neglected here.[20] One possible explanation for the increase in C_s is that open channels during the capacitance measurements would distort the recorded current, and lead to an over-estimation of the capacitance. However, the capacitance values are corrected for possible leakage currents to compensate for this potential effect, as described in detail in **Appendix I**. Therefore, another factor plays a role here. Upon dimerization of two gramicidin monomers to form a conductive pore, the membrane locally thins down if it is thicker than the hydrophobic length of the gramicidin channel (2.17 nm).[21] In solvent-containing BLMs, this phenomenon of membrane deformation is accompanied by expulsion of the solvent out of the membrane, followed by compression of the hydrocarbon chains of the phospholipid in close proximity to the channel.[22, 23] As a result, the bilayer thickness in the direct vicinity of the gramicidin channel is close to the thickness of solvent-free membranes.[24] Altogether, one possible hypothesis is that this local reduction in bilayer thickness, caused by the expulsion of n-decane upon pore formation, would result in a global decrease in the bilayer thickness, while keeping in mind that only a low gramicidin/lipid concentration (~$3 \cdot 10^{-8}$) is present.

Interestingly, this trend is not observed for bilayers supplemented with both gramicidin and NBD-PE, which exhibit a thickness comparable to bilayers containing NBD-PE only (3.28 ± 0.18 nm (n = 5) and 3.65 ± 0.64 nm (n = 5) for POPC bilayers containing NBD-PE, with and without gramicidin, respectively). Since the decrease in thickness for gramicidin containing bilayers is accounted for by expulsion of the n-decane upon gramicidin dimerization, these results suggest that NBD-PE could modulate gramicidin activity, by changing other bilayer properties than its thickness. In a next stage, this hypothesis is tested by combining the dual membrane characterization with electrophysiological measurements.

In summary, the NBD-PE and gramicidin probes have no significant effect on the seal resistance, capacitance and surface area of POPC membranes. However, the presence of gramicidin alone correlates with an increase in the specific capacitance, reflecting plausible thinning of the bilayer. Interestingly, if both probes are added, this effect is not observed, suggesting that PE could have an impact on the bilayer properties.

FRAP measurements

Fluorescence recovery after photobleaching (FRAP) is generally used to determine kinetic parameters such as the diffusion constant and mobile fraction of small molecules such as lipids in a membrane. Additionally, the transport, binding and dissociation rates of proteins in a cell or an artificial bilayer lipid membrane can be

accessed.[25] FRAP relies on selective and irreversible photobleaching of a fluorophore in a specified region (region of interest, ROI) with a high-intensity laser beam,[26] followed by monitoring over time the fluorescence recovery in this ROI (**Figure 4.3** a).[25] The rate of recovery directly reflects the diffusion process, and allows assessing the diffusion coefficient *(D)* of the imaged species.[26] Furthermore, the respective amounts of mobile and immobile fractions in the membrane can be determined from the final recovery level compared to the pre-bleach intensity, as illustrated on **Figure 4.3** b.[26] Incomplete fluorescence recovery indicates the existence of an immobile fraction in the target.[25] Next to the bleach ROI, a reference region is simultaneously imaged under the same conditions to correct for unspecific photobleaching (**Figure 4.3** b). Last, a background measurement provides the so-called zero intensity, which allows characterizing the bleaching amount of the ROI.

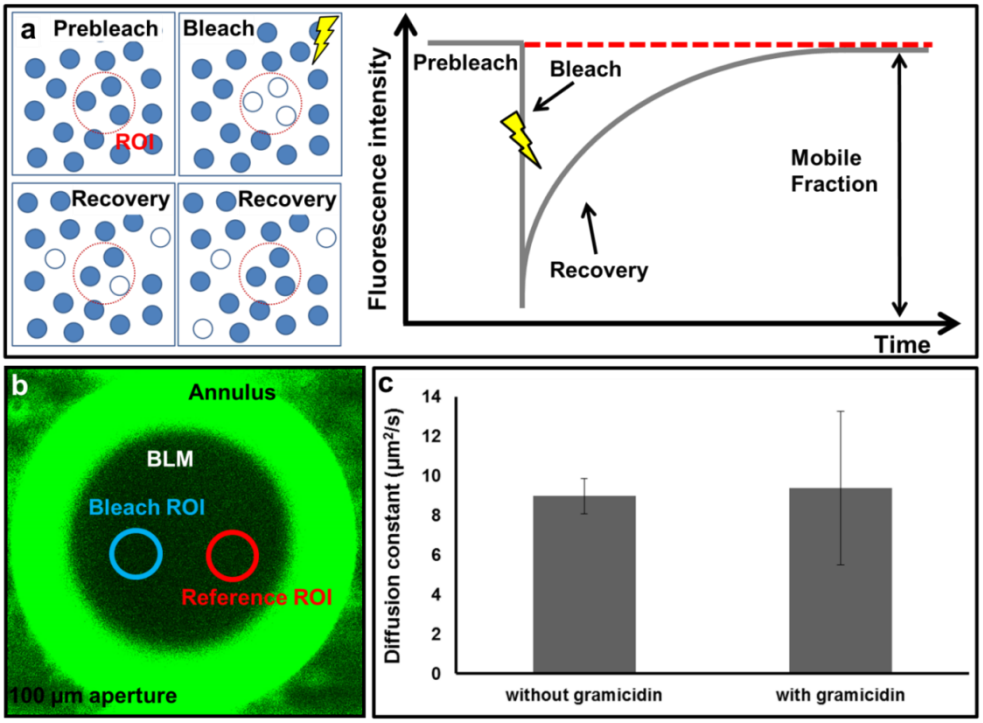

Figure 4.3. FRAP measurements. a) Schematic process of a typical FRAP measurement: a region of interest (ROI) is defined, and the fluorescence intensity in this ROI is monitored, prior to the bleach by a high intensity laser pulse, as well as the recovery of fluorescence after bleach. The blue circles represent fluorescently labeled molecules. b) A bilayer formed with fluorescently labeled NBD-PE in a 100-µm aperture. The bleach and reference ROIs (15 µm in diameter) are positioned in the center of the BLM and separated by 10 µm. c) Experimentally determined diffusion coefficients (*D*) for bilayers formed from POPC in n-decane, supplemented with 1% mol NBD-PE without (*left*) and with (*right*) gramicidin present (gramicidin/lipid ratio ~$3 \cdot 10^{-8}$).

In a first instance, we have optimized the protocol for reliable FRAP measurements of POPC membranes by varying the diameter of the ROIs, the number of iterations for the bleach and the confocal settings (e.g., zoom and scan time).

After optimization, the protocol is applied to estimate the fluidity of POPC membranes supplemented or not with gramicidin, by deriving the diffusion coefficient (*D*) of NBD-PE phospholipids added to the POPC matrix. This coefficient is assessed to be 8.97 ± 0.90 $\mu m^2/s$ (n=5) for BLMs without gramicidin, which is similar to previously reported data in the literature. For instance, higher values around 12 and 13 $\mu m^2/s$ have been mentioned for suspended PC BLMs with 1% mol NBD-PE.[27,7] This difference can be attributed to the use of altered experimental conditions and changes in the measurement protocol such as the size of the ROI or the temperature, which is not accurately regulated in our experiments, but assessed as ca. 21°C in the room. Next to this, our *D* values are slightly higher than that found for supported POPC BLMs at a temperature of 25°C (4.2 ± 0.4 $\mu m^2/s$),[28] as expected, since diffusion is decreased by the presence of a solid substrate below the bilayer as in the case of supported bilayers. The diffusion coefficient upon addition of 1 nM gramicidin is found to be 9.37 ± 3.88 $\mu m^2/s$ (n=5), as shown in **Figure 4.3** c, which is not significantly different from membranes without any gramicidin. It should be noted, that earlier reports in the literature also show no direct influence of gramicidin on the membrane properties, determined as an electroporation threshold, at concentrations even higher than utilized here.[29]

Gramicidin measurements

The gramicidin activity is measured in POPC BLMs in n-decane without (n = 4) and with 1% mol NBD-PE (n = 5), and it is characterized in terms of open probability (t_{open}/t_{total}), number of channels (f), average single channel lifetime (τ), and conductance (g) using an in-house written Matlab routine. In general, data are acquired for a total recording time of 1209 and 2327 s, which corresponds to a total number of channels of 365 and 368, for BLMs without and with NBD-PE, respectively.

The open probability describes the complete time where channels are open divided by the total recording time per experiment, while the number of channels (f) represents the total amount of channels open simultaneously, which is presented here as percentage of the total lifetime for the particular number of simultaneous channels. Here, open probabilities of 0.37 ± 0.06 and 0.13 ± 0.11 for BLMs without and with NBD-PE are measured, respectively, as shown in **Figure 4.4** a, and the number of channels amounts to up to 4 and 3 for BLMs without and with NBD-PE, respectively (**Figure 4.4** b). Next, the single channel lifetime is plotted for both conditions (**Figure 4.4** c). The number of channels with various lifetimes is plotted as *N(t)*

defined as the total number of channels with a lifetime longer than *t*, and normalized with *N(0)*. This distribution is fitted using Matlab and an exponential fit, and the average single channel lifetime τ is derived from $N(t)/N(0) = \exp(-t/\tau)$.[30] For the two data sets, average single channel lifetime values of 1.22 and 0.74 s are found for BLMs without and with NBD-PE, respectively. Last, the single channel conductance (*g*) is examined for both types of experiments, and the distribution of *g* for both conditions is found to be similar, as presented in **Figure 4.4** d. The distribution is fitted with a Gaussian curve, resulting in average conductance values of 16.4 pS and 16.7 pS for BLMs without and with NBD-PE, respectively. These values are in the same range as previously reported by others and by us.[8,18] The spread in the conductance is likely to be caused by the fact that we use a mixture of various types of gramicidin, which present different single channel conductance states.[31] All these results for the gramicidin activity in POPC bilayers, with both probes (NBD-PE and gramicidin) as well as only one probe are presented in **Table 4.2**, together with the FRAP experiments.

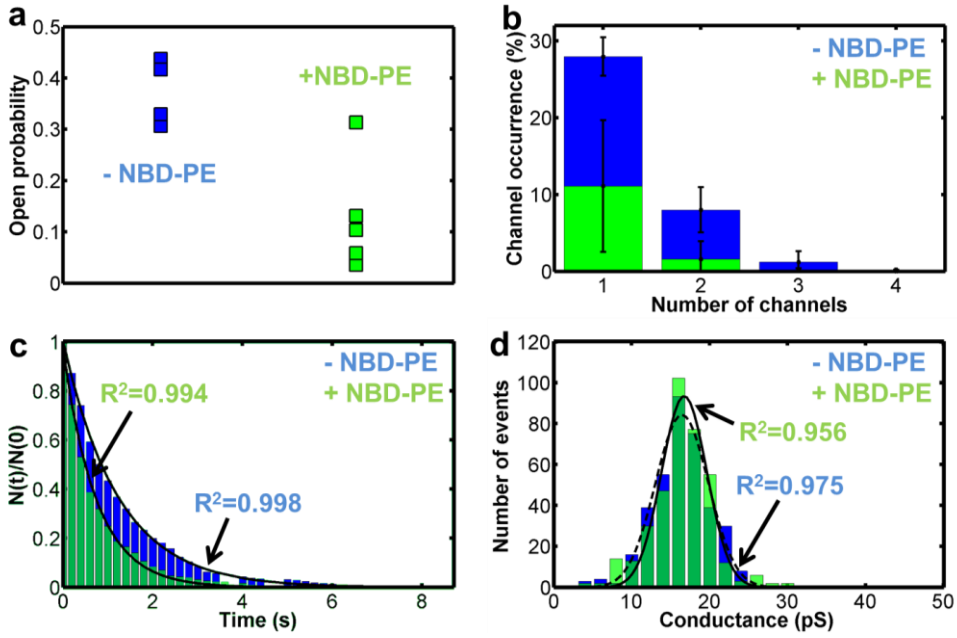

Figure 4.4. Gramicidin activity. a) Open probability (t_{open}/t_{total}) for gramicidin (1 nM) in POPC bilayers (25 mg/mL in n-decane) without (blue) and with (green) NBD-PE (1% mol). b) Number of simultaneous channels plotted as their occurrence in percentage of the total lifetime of a particular channel number for both conditions. c) Single channel lifetime, normalized to the total number of channels (*N(0)*) and fitted with $N(t)/N(0) = \exp(-t/\tau)$ with *N(t)* the number of channels with a lifetime larger than *t* and τ the average lifetime (bin size = 0.2 s). d) Single channel conductance for both conditions (bin size = 2 pS), fitted with Matlab for BLMs without (dashed line) and with (solid line) NBD-PE (1% mol). The experiments are carried out in 1 M KCl buffer and while applying a dc voltage of 80 mV and using a sampling rate of 10 kHz. The peptide/lipid molar ratio is ~$3 \cdot 10^{-8}$.

Table 4.2: BLM properties and gramicidin activity. The bilayer thickness (*d*) and its fluidity (*D*) are illustrated, as well as the gramicidin activity in terms of open probability (t_{open}/t_{total}), simultaneous maximum number of channels (f_{max}), the average single channel lifetime (τ), and the single channel conductange (*g*). Bilayers are formed with POPC (25 mg/mL) in n-decane, supplemented with gramicidin (gramicidin/lipid molar ratio ~$3 \cdot 10^{-8}$) and NBD-PE (1% mol) or only one of the two probes. a: n=5, b: n=4; ± SD.

POPC BLM	*d* (nm)	*D* (μm²/s)	t_{open}/t_{total}	f_{max}	τ (s)	*g* (pS)
+ NBD-PE[a]	3.65 ± 0.64	8.97 ± 0.90	-	-	-	-
+gramicidin[b]	2.86 ± 0.15	-	0.37 ± 0.06	4	1.22	16.4
+ NBD-PE[a] **+ gramicidin**	3.28 ± 0.18	9.37 ± 3.88	0.13 ± 0.11	3	0.74	16.7

In general, the addition of the NBD-PE probe to the membrane translates in a change in gramicidin activity. Specifically, the open probability and the total number of channels decrease, while the lifetime becomes shorter. At the same time, no significant difference is detected for the single channel conductance, as discussed in the following.

Gramicidin activity is easily modulated depending on the properties of the bilayer, such as its fluidity, thickness as well as its mechanical properties (stiffness, curvature, bending and compression modulus).[30,32] In our experimental approach, we have access to both the bilayer thickness and fluidity, but not to its mechanical properties. The bilayer thickness as discussed earlier, is not changed upon addition of NBD-PE. The fluidity is assessed using FRAP measurements, which however require the presence of NBD-PE in the bilayer in our experimental settings, so that the influence of this probe on the bilayer fluidity cannot be examined here. Therefore, we focus on the possible influence of NBD-PE on other bilayer properties, keeping in mind that only 1% mol of the probe is added to the bilayers. First of all, the NBD moiety is attached to the head group of PE, and in a first approximation, a possible influence of the fluorophore on the bilayer properties is neglected, and therefore only PE is examined in this discussion. PE possesses a small head group, which is known to cause closer packing of the lipids.[33] However, this effect should be accompanied by an increase in bilayer thickness, which we don't observe here (**Table 4.1**). Additionally, PE presents a conical shape due to its small head group, which confers a negative curvature to the bilayer. Importantly, this change in monolayer curvature is known to affect gramicidin activity, with lower channel open probability and shorter lifetime,[30,33] as we observe here.

Last, no significant variation is detected in the single channel conductance for the different sets of experiments. According to the literature, gramicidin conductance is not affected by the bilayer properties but by the dipole potential of the lipids,[34] a positive dipole potential leading to a decrease in conductance whereas similar conductance values indicate comparable surface charge densities.[24] In our case, the head groups for PE and PC are equivalent from a charge point of view, and the NBD group attached to the head of PE molecules has an overall neutral charge. Therefore, no change in the conductance is to be expected, as observed here.

4.4 Conclusion

Here, we have demonstrated the potential of our microfluidic platform for high-resolution optical imaging, and combined electrophysiological and confocal measurements. In a first instance, after adapting the device and its chip-holder for high resolution imaging by thinning down the bottom glass substrate to ~200 μm, we have proven its suitability for confocal microscopy by imaging a suspended bilayer lipid membrane supplemented with fluorescently labeled phospholipids. Next, the adaptation of our platform for confocal microscopy allows us to study phase separation in ternary bilayer systems. Following, the high resolution optical capability is coupled with electrophysiology for combined measurements on a model ion channel, gramicidin, and the membrane fluidity. This dual approach allows us to study bilayer characteristics while recording the peptide activity. Our measurements reveal a decrease in thickness for gramicidin containing POPC bilayers, and the addition of NBD-PE leads to a decreased gramicidin open probability and shorter channel lifetimes. The latter effect however cannot be caused by an increase in the bilayer thickness but rather by a change in the mechanical bilayer properties, such as the monolayer curvature. Finally, no change in diffusion constant is detected for bilayer systems with and without gramicidin, indicating that gramicidin itself does not alter the fluidity.

In the future, this combined approach could reveal the influence of changes in bilayer properties on ion channel activity. For instance, the membrane properties could be changed upon addition of drugs, such as aspirin, to the buffer solution, or by supplementing the lipids with ethanol or cholesterol prior to bilayer formation.[18,35] Moreover, this dual approach allows studying single ion channel activity both using electrophysiology and fluorescent dyes, to yield ion specific information on single channel gating and to reveal fundamental processes responsible for pore formation. Finally, spontaneous bending of the bilayer is observed in our device upon evaporation. If controlled, bilayer bending would allow assessing membrane mechanical properties.

4.5 Acknowledgements

I would like to thank Ionovation GmbH for help with the confocal measurements, Hans de Boer for fabrication of the chip holder, Dr. Martin Bennink for lending the patch-amplifier, and Burcu Celikkol, Aditya Iyer, and Himanshu Chaudhary for help with the FRAP measurements.

4.6 References

1. Aidley, D. J.; Stanfield, P. R., *Ion Channels*. Cambridge University Press: Cambridge, **1996**.
2. Bretschneider, F.; Weille, J. R. d., *Introduction to Electrophysiological Methods and Instrumentation*. Elsevier: London, **2006**.
3. Tillman, T.; Cascio, M., Effects of membrane lipids on ion channel structure and function. *Cell Biochem Biophys* **2003,** *38* (2), 161-190.
4. Clegg, R. M., Förster resonance energy transfer - FRETwhat is it, why do it, and how it's done. In *Laboratory Techniques in Biochemistry and Molecular Biology, FRET and FLIM Techniques*, Gadella, T. W. J., Ed. Elsevier: Oxford, **2009**; Vol. 33.
5. Axelrod, D., Cell-substrate contacts illuminated by total internal reflection fluorescence. *The Journal of Cell Biology* **1981,** *89* (1), 141-145.
6. Veatch, W. R.; Mathies, R.; Eisenberg, M.; Stryer, L., Simultaneous fluorescence and conductance studies of planar bilayer membranes containing a highly active and fluorescent analog of gramicidin A. *Journal of Molecular Biology* **1975,** *99* (1), 75-92.
7. Ladha, S.; Mackie, A. R.; Harvey, L. J.; Clark, D. C.; Lea, E. J.; Brullemans, M.; Duclohier, H., Lateral diffusion in planar lipid bilayers: a fluorescence recovery after photobleaching investigation of its modulation by lipid composition, cholesterol, or alamethicin content and divalent cations. *Biophysical Journal* **1996,** *71* (3), 1364-1373.
8. Borisenko, V.; Lougheed, T.; Hesse, J.; Fureder-Kitzmuller, E.; Fertig, N.; Behrends, J. C.; Woolley, G. A.; Schutz, G. J., Simultaneous optical and electrical recording of single gramicidin channels. *Biophysical Journal* **2003,** *84* (1), 612-622.
9. Kendall, E. L.; Shao, C.; DeVoe, D. L., Visualizing the Growth and Dynamics of Liquid-Ordered Domains During Lipid Bilayer Folding in a Microfluidic Chip. *Small* **2012,** *8* (23), 3613-3619.
10. Honigmann, A.; Walter, C.; Erdmann, F.; Eggeling, C.; Wagner, R., Characterization of Horizontal Lipid Bilayers as a Model System to Study Lipid Phase Separation. *Biophysical Journal* **2010,** *98* (12), 2886-2894.
11. Ide, T.; Takeuchi, Y.; Yanagida, T., Development of an Experimental Apparatus for Simultaneous Observation of Optical and Electrical Signals from Single Ion Channels. *Single Molecules* **2002,** *3* (1), 33-42.

12. Heron, A. J.; Thompson, J. R.; Cronin, B.; Bayley, H.; Wallace, M. I., Simultaneous Measurement of Ionic Current and Fluorescence from Single Protein Pores. *Journal of the American Chemical Society* **2009,** *131* (5), 1652-1653.
13. White, S. H., The Physical Nature of Planar Bilayer Membranes. In *Ion Channel Reconstitution*, Miller, C., Ed. Plenum Press: New York, **1986**; pp 3-35.
14. Semrau, S.; Schmidt, T., Membrane heterogeneity - from lipid domains to curvature effects. *Soft Matter* **2009,** *5* (17), 3174-3186.
15. Veatch, S. L.; Keller, S. L., Miscibility Phase Diagrams of Giant Vesicles Containing Sphingomyelin. *Physical Review Letters* **2005,** *94* (14), 148101.
16. van Uitert, I.; Le Gac, S.; van den Berg, A., Determination of the electroporation onset of bilayer lipid membranes as a novel approach to establish ternary phase diagrams: example of the L-a-PC/SM/cholesterol system. *Soft Matter* **2010,** *6* (18), 4420-4429.
17. Fettiplace, R.; Andrews, D. M.; Haydon, D. A., The thickness, composition and structure of some lipid bilayers and natural membranes. *J. Membrain Biol.* **1971,** *5* (3), 277-296.
18. Stimberg, V. C.; Bomer, J. G.; van Uitert, I.; van den Berg, A.; Le Gac, S., High Yield, Reproducible and Quasi-Automated Bilayer Formation in a Microfluidic Format. *Small* **2013,** *9* (7), 1076-1085.
19. Nikolelis, D. P.; Krull, U. J.; Ottova, A. L.; Tien, H. T., Bilayer lipid membranes and other lipid-based methods. In *Handbook of chemical and biological sensors*, Taylor, R.; schultz, J., Eds. Institute of physics publishing: Bristol, **1996**; pp 221-256.
20. Bransburg-Zabary, S.; Kessel, A.; Gutman, M.; Ben-Tal, N., Stability of an Ion Channel in Lipid Bilayers: Implicit Solvent Model Calculations with Gramicidin. *Biochemistry* **2002,** *41* (22), 6946-6954.
21. Elliott, J. R.; Needham, D.; Dilger, J. P.; Haydon, D. A., The Effect of Bilayer Thickness and Tension on Gramicidin Single-Channel Lifetime *Biochimica Et Biophysica Acta* **1983,** *735* (1), 95-103.
22. Lundbaek, J. A.; Andersen, O. S., Spring constants for channel-induced lipid bilayer deformations estimates using gramicidin channels. *Biophysical Journal* **1999,** *76* (2), 889-895.
23. Helfrich, P.; Jakobsson, E., Calculation of deformation energies and conformations in lipid membranes containing gramicidin channels. *Biophysical Journal* **1990,** *57* (5), 1075-1084.
24. Lundbæk, J. A.; Maer, A. M.; Andersen, O. S., Lipid Bilayer Electrostatic Energy, Curvature Stress, and Assembly of Gramicidin Channels. *Biochemistry* **1997,** *36* (19), 5695-5701.
25. Lippincott-Schwartz, J.; Altan-Bonnet, N.; Patterson, G. H., Photobleaching and photoactivation: following protein dynamics in living cells. *Nature Cell Biology* **2003,** *5*, S7–S14.
26. Braga, J.; Desterro, J. M.; Carmo-Fonseca, M., Intracellular macromolecular mobility measured by fluorescence recovery after photobleaching with confocal laser scanning microscopes. *Molecular biology of the cell* **2004,** *15* (10), 4749-60.

27. Lalchev, Z. I.; Mackie, A. R., Molecular lateral diffusion in model membrane systems. *Colloids and Surfaces B: Biointerfaces* **1999,** *15* (2), 147-160.
28. Vaz, W. L. C.; Clegg, R. M.; Hallmann, D., Translational diffusion of lipids in liquid crystalline phase phosphatidylcholine multibilayers. A comparison of experiment with theory. *Biochemistry* **1985,** *24* (3), 781-786.
29. Troiano, G. C.; Stebe, K. J.; Raphael, R. M.; Tung, L., The Effects of Gramicidin on Electroporation of Lipid Bilayers. *Biophysical Journal* **1999,** *76* (6), 3150-3157.
30. Lundbaek, J. A.; Collingwood, S. A.; Ingolfsson, H. I.; Kapoor, R.; Andersen, O. S., Lipid bilayer regulation of membrane protein function: gramicidin channels as molecular force probes. *Journal of the Royal Society Interface* **2010,** *7* (44), 373-395.
31. Sawyer, D. B.; Williams, L. P.; Whaley, W. L.; Koeppe 2nd, R. E.; Andersen, O. S., Gramicidins A, B, and C form structurally equivalent ion channels. *Biophysical Journal* **1990,** *58* (5), 1207-1212.
32. Lundbaek, J. A.; Birn, P.; Girshman, J.; Hansen, A. J.; Andersen, O. S., Membrane stiffness and channel function. *Biochemistry* **1996,** *35* (12), 3825-3830.
33. Rostovtseva, T. K.; Petrache, H. I.; Kazemi, N.; Hassanzadeh, E.; Bezrukov, S. M., Interfacial Polar Interactions Affect Gramicidin Channel Kinetics. *Biophysical Journal* **2008,** *94* (4), L23-L25.
34. Lundbaek, J. A.; Andersen, O. S., Lysophospholipids modulate channel function by altering the mechanical properties of lipid bilayers. *J Gen Physiol* **1994,** *104* (4), 645-673.
35. Lundbæk, J. A.; Andersen, O. S., Cholesterol Regulation of Membrane Protein Function by Changes in Bilayer Physical Properties—An Energetic Perspective. In *Cholesterol Regulation of Ion Channels and Receptors*, John Wiley & Sons, Inc.: **2012**; pp 27-44.

Chapter 5

A multi-parametric approach to assess cholesterol-induced changes in bilayer properties and their effect on gramicidin activity

---

The proposed dual confocal and electrophysiological approach is applied to measure the relationship between bilayer properties and gramicidin activity upon addition of cholesterol (0, 15 and 40% mol). Bilayers are characterized in terms of thickness and fluidity, while at the same time, the gramicidin activity is recorded. The addition of cholesterol results in a decrease of the bilayer thickness and fluidity by a factor of ~1.2 and ~2.7, respectively, for BLMs supplemented with NBD-PE and gramicidin, and with 40% mol cholesterol. Strikingly, gramicidin pore formation is almost inhibited in presence of cholesterol, which cannot be explained by the detected changes in membrane properties. Interestingly, the gramicidin average single channel lifetime is reduced, suggesting alterations in the mechanical bilayer properties.[1]

[1] Manuscript in preparation

5.1 Introduction

The membrane composition differs between various cell types,[1] and even within a single cell, heterogeneities can be found locally in the lipid packing density and the membrane thickness depending on the nature of the phospholipids, to yield for instance microdomains.[2] The precise lipidic environment is important for the structure and proper functioning of ion channels, which are responsible for the transport of ions across the membrane, their activity being mostly associated with conformational changes.[2] Therefore, alterations in the host bilayer can modulate the ion channel activity, either directly or indirectly, by favoring or not these essential conformational changes. Direct influences involve specific interactions between (charged) lipids and proteins, causing changes in, e.g., the protein conductance,[3] while indirect effects relate to the overall membrane properties. For instance the energetic cost of bilayer deformation required for channel activation highly depends on the bilayer physical and mechanical properties such as the membrane thickness.[4] The latter is of prime importance, and a hydrophobic mismatch induced for instance by a variation in the phospholipid chain length or solvent, can influence the dynamics of a functional channel activity.[5] Finally, the membrane fluidity impacts processes involving protein-protein interactions,[2] while the packing density of the bilayers affects the equilibrium between different conformational states of proteins.[2]

One important modulator in this lipidic landscape is cholesterol.[4] Cholesterol is present in a large amount (30-50% mol) in the plasma membrane, and in lower amounts in the membranes of intracellular organelles, while it exhibits local concentration variations in a given membrane. Cholesterol affects the lipidic environment in different manners. One general mechanism relies on ordering of the phospholipids and increasing their packing density,[6] which in turn affects the bilayer thickness, fluidity, compressibility, lateral pressure profiles and the surface charge distribution.[2,6] Next, cholesterol induces phase separation phenomena in membranes, which is a key process in the formation of specific domains rich for instance in sterol and sphingolipids,[7] for which certain proteins such as G-proteins exhibit a specific affinity.[2,8] Altogether, by regulating the membrane properties, cholesterol exerts an indirect impact on ion channel activity. Next to these indirect effects, cholesterol can also have a direct influence on protein activity[9] via specific cholesterol-protein interactions, resulting in pore blocking of the ion channel[4] or alteration in the protein conformational state and subsequently in its function.[2,4]

Altogether, studying the relationship between protein activity and bilayer properties is essential to understand the regulation mechanisms of ion channels.[2] In a typical setting, the properties of an artificial bilayer are altered by changing the lipidic

composition (e.g., acyl chain length, presence and number of unsaturations, nature of the head groups, and presence of cholesterol), while the ion channel activity is recorded using electrophysiology,[10] to correlate membrane properties and ion channel activity. Gramicidin is an attractive ion channel candidate to sense these induced alterations in bilayer properties, since this peptide is highly responsive to changes in its lipidic environment,[10] and it is widely utilized as a molecular force sensor.[11] Gramicidin forms a pore upon assembly of two monomers present in the two leaflets of the bilayer. This dimerization process is influenced by the membrane properties, since it involves local deformation of the bilayer, and it is more or less favored energetically depending on the membrane thickness, fluidity and mechanical properties.[10]

In chapter 4 of this thesis, we proposed a multi-parametric measurement approach, which is implemented in a microfluidic format to correlate membrane properties and the activity of gramicidin using simultaneous confocal imaging and electrophysiological recordings. This strategy is applied here to study cholesterol-induced changes in the bilayer properties and their indirect impact on the gramicidin activity. Bilayers are formed in the microfluidic device, as before, and characterized in terms of specific capacitance and membrane thickness, using orthogonal measurements. Next, the membrane fluidity is assessed using confocal microscopy and a dedicated FRAP (Fluorescence Recovery After Photobleaching) protocol. Finally, electrophysiological measurements are carried out to characterize the gramicidin ion channel activity in terms of open probability, single channel lifetime, and conductance, and this is related to the membrane properties.

5.2 Experimental Section

5.2.1 Materials

POPC (1-palmitoyl-2-oleoyl-*sn*-glycero-3-phosphocholine) and NBD-PE (1,2-dioleoyl-*sn*-glycero-3-phosphoethanolamine-N-(7-nitro-2-1,3-benzoxadiazol-4-yl) (ammonium salt)) are purchased as solutions in chloroform from Avanti polar lipids (Alabaster, AL, USA), together with cholesterol as powder. Potassium chloride (KCl), (4-(2-hydroxyethyl)-1-piperazineethanesulfonic acid (HEPES), chloroform and gramicidin (mixture of species with ~80% gramicidin A) are purchased from Sigma Aldrich (Zwijndrecht, The Netherlands), n-decane from from Fluka (Steinheim, Germany), and ethanol from Assink Chemie (Enschede, The Netherlands). Milli-Q water (MilliQ system, Millipore, Billerica, MA, USA) is used to prepare all solutions. All experiments are carried out at room temperature.

5.2.2 Microfluidic device

The microfluidic device described in chapter 4 is used, with a thinned bottom glass substrate (~200 μm) for confocal microscopy measurements, and a microaperture of 100 μm in diameter, located at the intersection of the two microfluidic channels (100 μm deep, 300 μm wide). Thick PDMS reservoirs are bonded on top of the device to facilitate liquid handling. The complete device is placed in a custom-made chip holder that fits on the stage of a confocal microscope and the device is shielded with a faraday cage for the electrophysiological measurements.

5.2.3 Bilayer formation

The lipids (POPC, NBD-PE and/or cholesterol) are mixed as chloroform-based solutions, and the solvent is subsequently evaporated under vacuum for at least 30 min. The resulting dried lipids are dissolved in n-decane to yield a concentration of 25 mg/mL. Gramicidin is dissolved in ethanol and added to the lipid solution prior to bilayer formation (final concentration of 1 nM; peptide/lipid ratio of $\sim 3 \cdot 10^{-8}$). For control measurements without gramicidin, the same amount of ethanol is added to all lipid solutions. BLMs are formed by injecting 0.5 μL lipid solution in both channels of the device, followed by buffer solution (1 M KCl, 10 mM Hepes, pH 7.4; 30 and 20 μL in the bottom and top channel, respectively).

5.2.4 Experimental approach

The experimental approach is summarized in **Figure 5.1**. In short, POPC membranes are supplemented with 15 or 40% mol cholesterol to alter their properties,[4] and those are compared to plain POPC membranes without any cholesterol. All bilayers are characterized, as described in chapter 4, in terms of thickness and fluidity, while recording the gramicidin activity (open probability, average single channel lifetime, and conductance). For FRAP experiments, 1% mol NBD-PE (probe 1) is added to the bilayers, and 1 nM gramicidin (probe 2) for the electrophysiological measurements. First, the BLM thickness is assessed in all bilayer types (plain, one or two probes) with or without cholesterol. Next, simultaneous confocal and electrophysiological measurements are carried out using both probes (NBD-PE and gramicidin), as well as experiments with only one probe (either NBD-PE or gramicidin) as a control.

5.2.5 Specific capacitance determination

The specific capacitance (C_s) - or capacitance per surface area - is determined as described previously,[12] from the bilayer capacitance (C_m) and its surface area (A_{BLM})

(chapter 4). After BLM formation, but prior to starting the FRAP and electrophysiological measurements, the capacitance and surface area of the bilayer are assessed. The same parameters are measured as well at the end of the experiment to verify that the membrane properties remain the same throughout the whole recording time. It should be noted that no significant difference is observed over the time of the measurement, as shown in **Appendix I** for the specific capacitance of POPC BLMs with and without cholesterol. However, the C_s values utilized here for the study always correspond to the values measured at the end of the experiment.

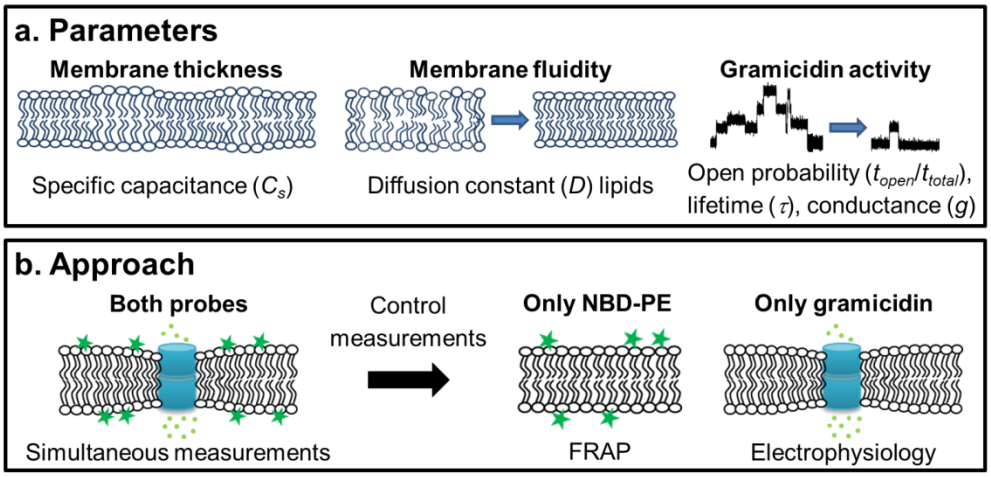

Figure 5.1. Experimental approach. a) Measurable parameters in our device are the membrane thickness, derived from the specific capacitance, the membrane fluidity, assessed in terms of phospholipid diffusion, and the gramicidin activity, determined using electrophysiology and characterized in terms of open probability, average single channel lifetime and conductance. b) Simultaneous FRAP and electrophysiological measurements are carried out with both probes (NBD-PE and gramicidin) present in the bilayers, as well as control measurements with only one probe (either NBD-PE or gramicidin).

5.2.6 Dual confocal and electrophysiological measurements

FRAP measurements

FRAP measurements are conducted using a confocal laser scanning microscope (LSM510 Zeiss, Argon laser, λ = 488 nm, Plan-Apochromat 63x/1.4 Oil DIC, LP 505 filter and HFT 488 beam splitter) and a dedicated FRAP protocol (**Appendix II**). First, the focus is adjusted to reach the highest intensity, and two regions of interest (ROIs) are defined (bleach and reference ROIs, 10 µm in diameter, distance of 15 µm in *x*-direction, same *y*-position). In total, 500 bleaching cycles are carried out (20 cycles before bleaching, bleach at 100% laser intensity with 5 iterations, bleach time of 1.322 s, and 0.22 s scan time per image), yielding ~20% of bleach and full recovery. The

diffusion constant is derived from the resulting bleaching curve using FRAPAnalyser (freeware from the University of Luxemburg, http://actinsim.uni.lu/eng). Data are corrected for the background fluorescence, which is determined using the same bleaching protocol after rupture of the bilayer. For each bilayer composition, the diffusion coefficient is measured at least twice, with a minimum of three independent bilayers prepared on different days.

Table 5.1: Gramicidin experiments. POPC bilayers are supplemented either with gramicidin only (-NBD-PE), or with gramicidin and NBD-PE (+NBD-PE). The number of experiments, the total recorded time and the number of channels measured are summarized for various concentrations of cholesterol (0, 15 and 40% mol).

	n_{exp} **(experiments)**		**Total time (s)**		$n_{channel}$ **(channels)**	
[Cholesterol]	*- NBD*	*+ NBD*	*- NBD*	*+ NBD*	*- NBD*	*+ NBD*
0% mol	4	5	1209	2327	365	368
15% mol	5	3	3239	1590	19	14
40% mol	4	4	1516	1775	16	2

Gramicidin recordings

Gramicidin activity is recorded by applying a dc voltage of 80 mV while monitoring the current response (1 kHz Lowpass Bessel filter, 10 kHz sampling rate, CV 203 BU head stage and Axopatch 200B amplifier (both Molecular devices, Sunnyvale, CA, USA)). Data are filtered and analyzed using an in-house written Matlab routine. The number of experiments, the total recording time and number of detected gramicidin channels are summarized in **Table 5.1**. For experiments without cholesterol, at least 88 s are recorded per BLM, and for cholesterol containing bilayer at least 231 s. The open probability is measured by dividing the sum of the lifetimes of all channels by the total recorded time for each experiment (t_{open}/t_{total}). The single channel lifetime is derived as described previously.[10] Shortly, the number of events measured with a certain lifetime are normalized, plotted, and fitted using Matlab. The average lifetime, τ, is derived from $N(t)/N(0) = \exp(-t/\tau)$ with N being the number of events and $N(t)$ the number of channels observed with a lifetime longer than t. For cholesterol-containing bilayers, fewer channels are detected, and therefore a smaller bin size is chosen here (bin size 0.05 s *vs.* 0.2 s in chapter 4). However, the bin size is adjusted so that no significant effect is found on the fitted value of the single channel average lifetime for bilayers without cholesterol. Furthermore, for cholesterol-free POPC

membranes, multiple channels are recorded simultaneously, and here results in a slightly underestimated value for the average single channel lifetime (**Appendix III**). Finally, the single channel conductance is derived from the amplitude of each gramicidin step and plotted as the number of events for a given conductance value (bin size 2 pS).

Combined measurements

For the combined measurements, the same protocols as before are applied. First, the capacitance and surface area are determined, and the ROIs are defined in the bilayer. Following this, combined FRAP and electrophysiological measurements are performed. After the experiment, the C_m and A_{BLM} of the bilayer are checked.

5.3 Results and Discussion

5.3.1 Specific capacitance - Bilayer thickness

The specific capacitance is derived from the capacitance C_m and the surface area A_{BLM} for bilayers with different concentrations of cholesterol (0, 15 and 40% mol), and with no, one or two probes (NBD-PE and gramicidin). The values measured for all bilayers are summarized in **Table 5.2**. Subsequently, the bilayer thickness is estimated from C_s ($d = \varepsilon_0\varepsilon_r/C_s$) using a dielectric constant ε_r equal to 2.09, as reported for phosphatidylcholine bilayers in n-decane.[13] The same ε_r value can also be used for BLMs with cholesterol, as previously discussed in the literature.[13,14] In general, the found C_s values lie here between 0.52 and 0.74 μF/cm², indicating that solvent (n-decane) is present in our bilayers.[15]

When cholesterol is added to plain POPC BLMs, C_s increases from 0.54 ± 0.02 to 0.74 ± 0.05 μF/cm² for 0 and 40% mol cholesterol (both n = 6), respectively. These results are in good agreement with previous reports, where thinning of DOPC and lecithin membranes prepared from a phospholipid solution in n-decane is found upon addition of cholesterol.[11,16] Interestingly, more often, the opposite effect is reported upon addition of cholesterol,[2, 4, 6] this being however valid for solvent-less membranes.[14] In the latter case, addition of cholesterol causes ordering of the acyl-chains of the phospholipid and an increase in bilayer thickness.[4] In solvent containing bilayers, as is the case here, the ordering of the phospholipid chains leads to the expulsion of small hydrocarbon molecules such as n-decane from the bilayer to the annulus. Thereby, the bilayer becomes thinner since less solvent is present between the two phospholipid leaflets.[17,18]

Table 5.2: Bilayer specific capacitance and thickness. The values of the specific capacitance are given in μF/cm², and the estimated values for the thickness, below and between brackets, in nm. Data are presented for POPC bilayers with 0, 15 and 40% mol cholesterol, and with no probe, one probe (1% NBD-PE or 1 nM gramicidin) and both probes (1% NBD-PE and 1 nM gramicidin). The thickness is assessed using ε_r equal to 2.09 for all conditions.[13] The error represents the standard deviation between the different experiments. a: n=3; b: n=4; c: n=5, d: n=6.

POPC BLM	Plain	+ NBD-PE (1% mol)	+ gramicidin (1 nM)	+ NBD-PE (1% mol) + gramicidin (1 nM)
0% mol Ch	0.54 ± 0.02^{d} (3.45 ± 0.16)	0.52 ± 0.10^{c} (3.65 ± 0.64)	0.65 ± 0.03^{b} (2.86 ± 0.15)	0.57 ± 0.03^{c} (3.28 ± 0.18)
15% mol Ch	0.65 ± 0.07^{c} (2.88 ± 0.30)	0.70 ± 0.14^{a} (2.69 ± 0.47)	0.64 ± 0.04^{c} (2.91 ± 0.17)	0.66 ± 0.01^{a} (2.80 ± 0.06)
40% mol Ch	0.74 ± 0.05^{d} (2.51 ± 0.17)	0.69 ± 0.04^{c} (2.69 ± 0.15)	0.69 ± 0.08^{b} (2.70 ± 0.29)	0.70 ± 0.05^{b} (2.66 ± 0.18)

The same effect on C_s is observed for bilayers supplemented with gramicidin and/or NBD-PE. Interestingly, no significant change is observed for the two cholesterol amounts tested here (15 or 40% mol), while a concentration-dependent effect would be expected.[16] Previously, a plateau in the specific capacitance value around 0.6 μF/cm² has been found for lecithin-decane bilayers with increasing cholesterol concentrations,[16] while the values in our experiment seem to saturate around ~0.7 μF/cm². For bilayers with only gramicidin, no significant change in the C_s value is observed upon addition of cholesterol. However, the presence of gramicidin already results in membrane thinning, as discussed in chapter 4, and the specific capacitance for those membranes (0.65 ± 0.03 μF/cm² ($n = 4$)) is already close to the plateau mentioned earlier, which may explain why the addition of cholesterol has no significant effect here.

5.3.2 Diffusion constant - Membrane fluidity

Following this, the membrane fluidity is assessed by determining the diffusion constant D of fluorescently tagged phospholipids NBD-PE added to bilayers supplemented or not with gramicidin, and for the herein tested cholesterol concentrations (0, 15, and 40% mol). In general, D for POPC BLMs without cholesterol is in the same range as previously reported values for suspended PC bilayers,[19,20] as already discussed in chapter 4.

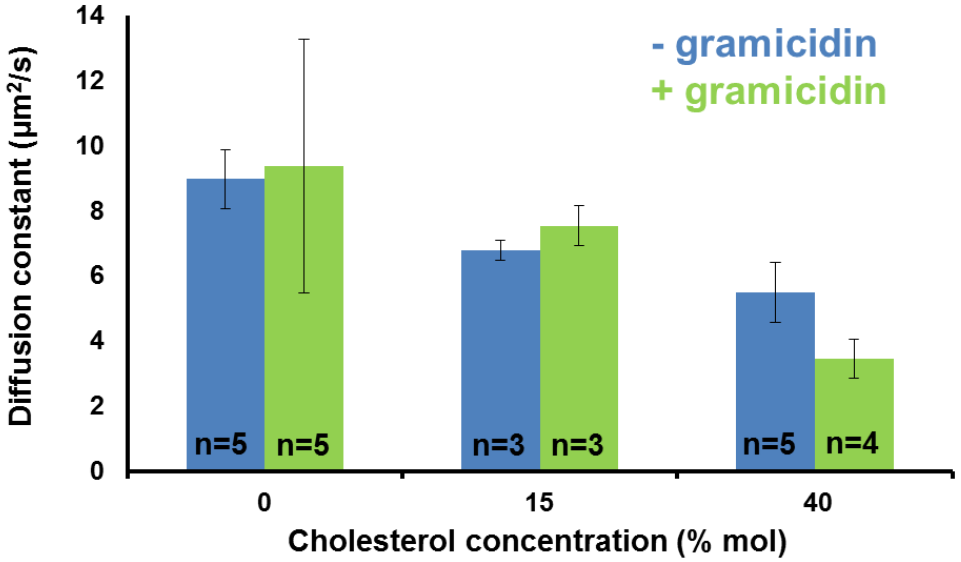

Figure 5.2. Diffusion coefficient. The diffusion coefficient (*D*) is determined in POPC BLMs supplemented with only 1% mol NBD-PE (blue) or with both 1% mol NBD-PE and 1 nM gramicidin (green), for various concentrations of cholesterol (0, 15 & 40% mol). The error bars represent the standard deviation between the different experiments (n).

Upon addition of cholesterol, *D* decreases in a cholesterol concentration dependent manner (See **Figure 5.2**), from 8.97 ± 0.90 μm²/s for 0% (n = 5), to 6.77 ± 0.31 μm²/s and 5.49 ± 0.92 μm²/s for 15% (n = 3) and 40% mol cholesterol (n = 5), respectively, for BLMs with only NBD-PE. Globally, a ~1.3-fold reduction in *D* is found for 15% mol cholesterol, against a ~1.6-fold decrease for 40% mol cholesterol. Similar variations in *D* have been observed under comparable experimental conditions for PC bilayers supplemented with various amounts of cholesterol, using the same probe (1% mol NBD-PE).[20,21] Specifically, a 1.4-fold decrease has been found for suspended bilayers (POPC with 30% mol DOPE) with 10% mol cholesterol,[21] and a ~2- to 3-fold decrease for 33% and 50% mol cholesterol,[20,21] while for pure DOPC bilayers with 50% mol cholesterol a 1.5-fold decrease has been measured.[20]

A decrease in *D* upon addition of cholesterol has been reported for BLMs above the phase transition temperature of the lipids, T_m, this effect being linked to a change in the ordering of the lipids.[22] POPC has a T_m of -2 °C (www.avantilipids.com), so that the bilayer is in the liquid disordered phase (l_d) in these experiments conducted at room temperature. When cholesterol is added to a bilayer in the l_d phase, it induces ordering of the phospholipid acyl chains and the bilayer shifts progressively to a liquid ordered phase (l_o),[23] which is characterized by a reduced fluidity. This transition from l_d to l_d/l_o can already take place around 10% mol cholesterol, which could explain the

decrease in *D* we observe for 15% mol cholesterol.[21,24] Higher amounts of cholesterol (here 40% mol) further decrease *D*, suggesting a gradual shift in membrane fluidity towards a l_o state.

In presence of gramicidin (1 nM), the same trend is observed, with a 1.2-fold and 2.7-fold decrease for 15 and 40% mol cholesterol, respectively (9.37 ± 3.88 μm²/s (n = 5), 7.54 ± 0.62 μm²/s (n = 3) and 3.46 ± 0.60 μm²/s (n = 4), for 0, 15 and 40% cholesterol, respectively). In these experiments, the peptide concentration is kept low (1 nM) so that the presence of gramicidin is not expected to influence the bilayer fluidity. Troiano et al. have reported a noticeable influence of gramicidin on the electroporation threshold of a membrane for a relatively high concentration (gramicidin/lipid ratios of ~$7 \cdot 10^{-2}$ or $2 \cdot 10^{-3}$), while no effect is observed at a ~10^{-4} gramicidin/lipid ratio, which is much higher than the concentration utilized here (gramicidin/lipid ratio of ~$3 \cdot 10^{-8}$).[25]

Finally, it should be noted that all experiments are carried out at room temperature, but without any control on the temperature in the vicinity of the bilayer. Therefore, some temperature fluctuations may happen, leading to the observed variations in the measured diffusion constant.

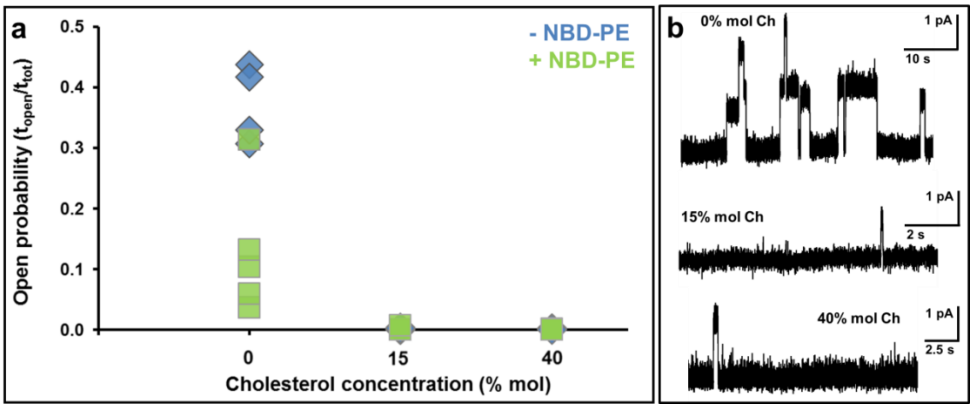

Figure 5.3. Gramicidin activity. a) The open probability is displayed for all conducted experiments for BLMs with gramicidin only (-NBD-PE) and gramicidin and NBD-PE (+NBD-PE) present for various cholesterol concentrations (0, 15, and 40% mol). b) Characteristic gramicidin recording traces are shown for BLMs with both probes present (80 mV applied, 10 kHz sampling rate, moving average filter (Matlab), window size 30) for 0, 15 and 40% mol cholesterol, from top to bottom, respectively.

5.3.3 Open probability, lifetime, conductance - Gramicidin activity

Gramicidin recordings are performed in POPC BLMs with 1 nM gramicidin (gramicidin/lipid molar ratio ~$3 \cdot 10^{-8}$), supplemented or not with NBD-PE, and with

various concentrations of cholesterol (0, 15, and 40% mol). As before in chapter 4, the gramicidin activity is analyzed in terms of open probability, average single channel lifetime and conductance.

First, the open probability, which is the sum of the open times of all channels with respect to the total recording time (t_{open}/t_{total}), is determined (**Figure 5.3)**. The results for 0% cholesterol are the same as in chapter 4, and a slightly lower gramicidin open probability is recorded for BLMs supplemented with 1% mol NBD-PE. Strikingly, in presence of cholesterol, for the conditions tested here (15 and 40% mol), the open probability drops by >98%. Interestingly, no concentration-dependent difference is observed for 15 and 40% mol cholesterol, for bilayers with and without NBD-PE. A similar drastic decrease in gramicidin activity upon addition of cholesterol has already been found by others, and 10 times more peptide was added to the lipid solution to reach comparable appearance rates.[4] In our experiments, the gramicidin/phospholipid ratio is kept constant for possible direct comparison between the different conditions, but this means that a much lower number of channels is detected (**Table 5.1**).

In a next step, the lifetime of the gramicidin channels is examined. For that purpose, the duration of each channel is measured and its occurrence plotted (See **Figure 5.4** a). In a next step, the data are normalized, fitted using Matlab and the average lifetime τ is derived from $N(t)/N(0) = \exp(-t/\tau)$ with $N(t)$ being the number of channels with a lifetime longer than t.[10] For BLMs without cholesterol, average single channel lifetimes of 1.22 and 0.74 s are determined in absence or presence of NBD-PE, respectively, as discussed in chapter 4. In absence of NBD-PE, the addition of cholesterol results in a reduction of τ to 0.20 s (n_{exp} = 5, $n_{channel}$ = 19) and 0.06 s (n_{exp} = 4, $n_{channel}$ = 16) for 15 and 40% mol cholesterol, respectively, compared to 1.22 s (n_{exp} = 4, $n_{channel}$ = 365) in absence of cholesterol. Bilayers with NBD-PE show a similar trend, as summarized in **Table 5.3**. Upon addition of 15% mol cholesterol, in NBD-PE supplemented bilayers the average single channel lifetime further decreases to 0.16 s (n_{exp} = 3, $n_{channel}$ = 14), compared to 0.74 s (n_{exp} = 5, $n_{channel}$ = 368) initially in absence of cholesterol. For 40% mol cholesterol and 1% mol NBD-PE, in total only 2 channels are detected with lifetimes of 0.02 and 0.34 s (n_{exp} = 4), which precludes any proper analysis on the average lifetime under these conditions. Finally, the addition of NBD-PE to POPC bilayers with 15% mol cholesterol does not induce any clear change in the average single channel lifetime (0.20 *vs.* 0.16 s, respectively), as occurred for cholesterol free bilayers (see chapter 4 and **Table 5.3**) A similar effect of cholesterol on the gramicidin average channel lifetime has been found by others,[11, 26,27] with a five-fold reduction in DOPC bilayers containing 66% cholesterol.[11]

Finally, the single channel conductance is determined for all experiments (**Figure 5.4** b). As already observed in chapter 4, in absence of cholesterol, the single channel

conductance does not show any particular variations in the different sets of experiments. While previous work has reported a slight reduction in the single channel conductance in the presence of cholesterol,[27] our results do not indicate any clear trend, which may be related though to the low number of channels measured in bilayers containing cholesterol.

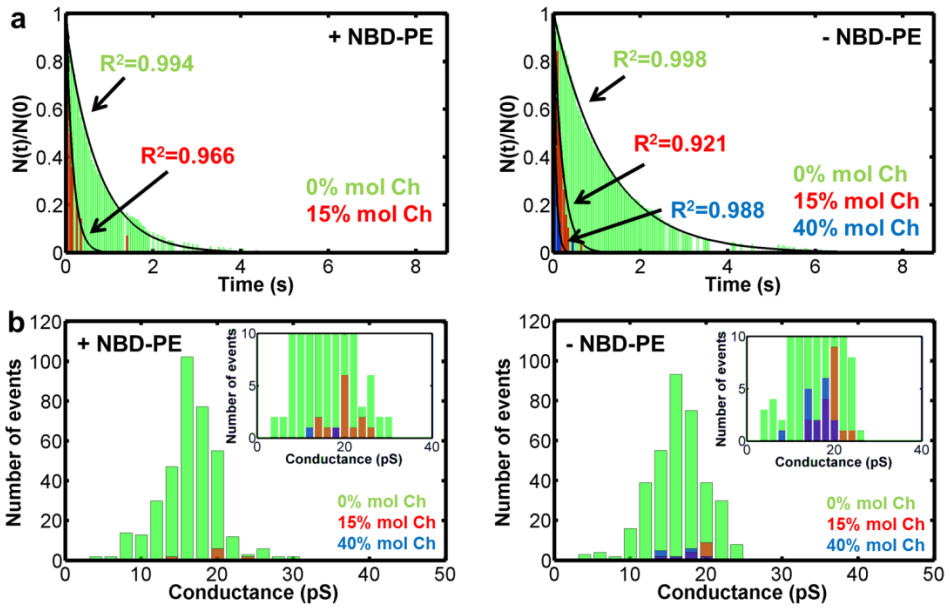

Figure 5.4. Lifetime and conductance. The normalized and fitted gramicidin single channel lifetime (a) and conductance (b) are presented for BLMs with both probes (*left*) and with only gramicidin (*right*) for cholesterol concentrations of 0, 15 and 40% mol, represented as green, red and blue bars, respectively. The inset in b) represents a zoom to visualize the conductance values for 15 and 40% mol cholesterol. Bin size lifetime: 0.05 s, bin size conductance: 2 pS.

In the following section, the results from the gramicidin measurements are discussed with respect to the bilayer properties. In our experiments, where the bilayer thickness and fluidity are assessed, two counter-acting effects are found upon addition of cholesterol. On one hand, the higher specific capacitance observed in presence of cholesterol suggests thinning of the bilayers (~3.28 *vs.* ~2.66 nm for 0 and 40% mol cholesterol, and both probes), which should lead to an increase in gramicidin open probability by reducing the hydrophobic mismatch between the length of the gramicidin pore (2.17 nm) and the bilayer thickness (see **Tables 5.3 & 5.4**).[10,26] On the other hand, the bilayers become less fluid, which should results in an overall reduction in t_{open}/t_{total}, by decreasing the probability of pore formation due to slower motion of the monomers in the monolayers of the bilayer (see **Tables 5.3 & 5.4**). At the same time, both the decrease in d and D should correlate with an increase in the average

single channel lifetime[10,11] while here, a reduction in τ is found (1.22 for 0% mol cholesterol *vs.* 0.20 and 0.06 s for 15 and 40% mol cholesterol and BLMs without NBD-PE). The effect of the bilayer thickness is expected to dominate that of the fluidity,[4] with theoretically an increase in open probability while our experimental results reveal a quasi-total loss in gramicidin activity. Furthermore, no variation in C_s is found in bilayers with only gramicidin, suggesting that these bilayers have a similar thickness compared to BLMs with both probes, and should therefore exhibit the same gramicidin activity if the thickness only would govern pore formation. However, the contrary is observed with a decrease in open probability and in the average single channel lifetime. Altogether, these results suggest, that other parameters play a major and dominant role, and are responsible for the loss in gramicidin pore formation and the reduction in τ.

Table 5.3: Summary bilayer properties and gramicidin activity. The bilayers are characterized in terms of thickness (d) and fluidity (D), whereas the gramicidin activity is presented with the open probability (t_{open}/t_{total}), and the average single channel lifetime (τ). Bilayers are formed with POPC (25 mg/mL) in n-decane, supplemented with 1 nM gramicidin and 1% mol NBD-PE or only one of the two probes present. The three values in each box, from top to bottom, correspond to BLMs with either 0, 15 or 40% mol cholesterol, respectively. The error represents the standard deviation between the different experiments. a: n = 5; b: n = 3; c: n = 4.

POPC BLM	d (nm)	D ($\mu m^2/s$)	t_{open}/t_{total}	τ (s)
+ NBD-PE (1% mol)	3.65 ± 0.64^a 2.69 ± 0.47^b 2.69 ± 0.15^a	8.97 ± 0.90^a 6.77 ± 0.31^b 5.49 ± 0.92^a	-	-
+ gramicidin (1 nM)	2.86 ± 0.15^c 2.91 ± 0.17^a 2.70 ± 0.29^c	-	0.37 ± 0.06^c $<0.004^a$ $<0.003^c$	1.22^c 0.20^a 0.06^c
+ NBD-PE (1% mol)[c] + gramicidin (1 nM)	3.28 ± 0.18^a 2.80 ± 0.06^b 2.66 ± 0.18^c	9.37 ± 3.88^a 7.54 ± 0.62^b 3.46 ± 0.60^c	0.13 ± 0.11^a $<0.007^b$ $<0.0006^c$	0.74^a 0.16^b -

Next to indirect effects whereby gramicidin activity is regulated by changes in the membrane properties, direct effects involving specific gramicidin-cholesterol interactions[28,29] via a N-term tryptophan residue found in gramicidin A have been suggested, resulting in channel inactivation.[30,31] However, more recent articles using a variety of techniques (Förster Resonance Energy Transfer, solid-state ^2H NMR, Fluorescence Quenching) have not confirmed the existence of this interaction in a bilayer environment, using either gramicidin A[32] or another Trp-flanked peptide.[33]

Altogether, the possible inhibition of gramicidin activity via that specific mechanism is controversial.[33]

The different parameters and membrane properties both influencing gramicidin activity and regulated by cholesterol are summarized in **Table 5.4**. The simultaneous decrease in both the open probability and average single channel lifetime correlates with a change in the bilayer mechanical properties, such as the bilayer elastic modulus, its stiffness, and from the introduction of a more negative monolayer curvature. In general, a variation in the average channel lifetime is an indication for changes in the bilayer stiffness.[11] Cholesterol is expected to increase the bilayer stiffness,[4, 11] which is collectively determined by the bilayer compression, bending and monolayer curvature.[11] The bending modulus and the bilayer area compression modulus have been found to increase by a factor of 3 and 4 for 50% mol cholesterol in PC BLMs, respectively.[34,35] Furthermore, cholesterol introduces a more negative monolayer curvature.[11] Altogether, in presence of cholesterol, the deformation energy for gramicidin pore formation is increased which in turn results in a lower open probability and shorter lifetime.[11]

Table 5.4. Influence of membrane properties on gramicidin activity. The influence of cholesterol on various parameters such as the bilayer thickness, fluidity, elasticity, curvature, and stiffness are summarized, as well as their effect on the gramicidin activity (open probability and lifetime) as reported in the literature (*left column*).[10] Next, the observations from our experiments are given for the bilayer properties (thickness and fluidity), as well as the changes in gramicidin activity (*middle column*).

Cholesterol effect (literature)	Gramicidin (our experiments)	Parameter
$d\downarrow$[11]$\rightarrow$ $\tau\uparrow, f\uparrow$	$d\downarrow$ or no effect $\rightarrow$ $\tau\downarrow, f\downarrow$	
$D\downarrow$[20]$\rightarrow$ $\tau\uparrow, f\downarrow$	$D\downarrow \rightarrow \tau\downarrow, f\downarrow$	d = Thickness D = Fluidity K = Elastic modulus
$K\uparrow$[4]$\rightarrow$ $\tau\downarrow, f\downarrow$	$K \rightarrow$ *not measurable*	c_0 = Curvature s = Stiffness
$c_0\downarrow$[11]$\rightarrow$ $\tau\downarrow, f\downarrow$	$c_o \rightarrow$ *not measurable*	τ = Lifetime f = Open probability
$s\uparrow$[11]$\rightarrow$ $\tau\downarrow, f\downarrow$	$s \rightarrow$ *not measurable*	

In conclusion, the presence of cholesterol in the bilayer correlates with changes in both the bilayer thickness and fluidity in our measurements. However, these changes seem not to be the dominant parameters governing gramicidin activity, and other mechanical parameters, which are not directly accessible using our experimental

approach, may play a major role such as the overall membrane stiffness. Alternatively, specific cholesterol-gramicidin interactions might take place, although this proposed mechanism is the subject of debates in the literature.[33]

5.4 Conclusion

Here, we study the effect of ion channel activity related to changes in the membrane properties caused by the addition of cholesterol. For that purpose, a combination of confocal microscopy and electrophysiological measurements is employed to monitor simultaneously the membrane properties (thickness & fluidity) and the activity of the well-established model gramicidin (open probability, average single channel lifetime, and conductance). Addition of cholesterol to the bilayer (0, 15 and 40% mol) leads to a significant decrease in bilayer thickness and a reduction in the bilayer fluidity. Unexpectedly, a drastic loss in gramicidin open probability is observed, together with a decrease in its average channel lifetimes. This significant alteration in gramicidin activity cannot be explained by the recorded moderate changes in fluidity or thickness, also since these parameters would have opposite and counter-acting effects. Collectively, these results demonstrate that parameters must be examined such as the mechanical properties of the bilayer (e.g., bilayer stiffness, compression and bending moduli, and monolayer curvature). The compression and bending moduli can be assessed for instance by aspiration of a vesicle into a micropipette.[34,35] In the future, a similar approach could be implemented in our device and on our bilayers, by controlling the bending of the membrane and correlating the applied pressure (flow-rate) and the measured bilayer deformation using confocal imaging. This proposed comprehensive measurement strategy would allow understanding the precise relationship between bilayer properties and gramicidin activity. Additionally, the proposed multi-parametric measurement scheme could be applied on other ion channels known to be sensitive to their lipidic environment[36] to identify possible non-specific effects of drugs on ion channel activity via alterations in the membrane properties, which should not be neglected in the process of drug development.[37]

5.5 Acknowledgements

I would like to thank Hans de Boer for designing and fabricating the chip holder, Martin Bennink for kindly providing the patch-clamp amplifier, and Burcu Celikkol, Aditya Iyer, and Himanshu Chaudhary for their help with the FRAP measurements.

5.6 References

1. Alberts, B., *Molecular Biology of the Cell*. Garland Publishing, Inc., New York, USA: **1989**.
2. Tillman, T.; Cascio, M., Effects of membrane lipids on ion channel structure and function. *Cell Biochem Biophys* **2003**, *38* (2), 161-190.
3. Turnheim, K.; Gruber, J.; Wachter, C.; Ruiz-Gutiérrez, V., *Membrane phospholipid composition affects function of potassium channels from rabbit colon epithelium*. **1999**; Vol. 277, p C83-C90.
4. Lundbæk, J. A.; Andersen, O. S., Cholesterol Regulation of Membrane Protein Function by Changes in Bilayer Physical Properties—An Energetic Perspective. In *Cholesterol Regulation of Ion Channels and Receptors*, John Wiley & Sons, Inc.: **2012**; pp 27-44.
5. Killian, J. A., Hydrophobic mismatch between proteins and lipids in membranes. *Biochimica et Biophysica Acta (BBA) - Reviews on Biomembranes* **1998**, *1376* (3), 401-416.
6. Kelkar, D. A.; Chattopadhyay, A., The gramicidin ion channel: A model membrane protein. *Biochimica et Biophysica Acta (BBA) - Biomembranes* **2007**, *1768* (9), 2011-2025.
7. Semrau, S.; Schmidt, T., Membrane heterogeneity - from lipid domains to curvature effects. *Soft Matter* **2009**, *5* (17), 3174-3186.
8. Grimm, M. O. W.; Zimmer, V. C.; Lehmann, J.; Grimm, H. S.; Hartmann, T., The Impact of Cholesterol, DHA, and Sphingolipids on Alzheimers Disease. *BioMed Research International* **2013**, *2013*, 16.
9. Bukiya, A. N.; Belani, J. D.; Rychnovsky, S.; Dopico, A. M., Specificity of cholesterol and analogs to modulate BK channels points to direct sterol–channel protein interactions. *The Journal of General Physiology* **2011**, *137* (1), 93-110.
10. Lundbaek, J. A.; Collingwood, S. A.; Ingolfsson, H. I.; Kapoor, R.; Andersen, O. S., Lipid bilayer regulation of membrane protein function: gramicidin channels as molecular force probes. *Journal of the Royal Society Interface* **2010**, *7* (44), 373-395.
11. Lundbaek, J. A.; Birn, P.; Girshman, J.; Hansen, A. J.; Andersen, O. S., Membrane stiffness and channel function. *Biochemistry* **1996**, *35* (12), 3825-3830.
12. Stimberg, V. C.; Bomer, J. G.; van Uitert, I.; van den Berg, A.; Le Gac, S., High Yield, Reproducible and Quasi-Automated Bilayer Formation in a Microfluidic Format. *Small* **2013**, *9* (7), 1076-1085.

13. Fettiplace, R.; Andrews, D. M.; Haydon, D. A., The thickness, composition and structure of some lipid bilayers and natural membranes. *J. Membrain Biol.* **1971**, *5* (3), 277-296.
14. Simon, S. A.; McIntosh, T. J.; Latorre, R., Influence of cholesterol on water penetration into bilayers. *Science* **1982**, *216* (4541), 65-67.
15. Nikolelis, D. P.; Krull, U. J.; Ottova, A. L.; Tien, H. T., Bilayer lipid membranes and other lipid-based methods. In *Handbook of chemical and biological sensors*, Taylor, r.; schultz, j., Eds. Institute of physics publishing: Bristol, **1996**; pp 221-256.
16. Hanai, T.; Haydon, D. A.; Taylor, J., The influence of lipid composition and of some adsorbed proteins on the capacitance of black hydrocarbon membranes. *Journal of Theoretical Biology* **1965**, *9* (3), 422-432.
17. Finol-Urdaneta, R. K.; McArthur, J. R.; Juranka, P. F.; French, R. J.; Morris, C. E., Modulation of KvAP Unitary Conductance and Gating by 1-Alkanols and Other Surface Active Agents. *Biophysical Journal* **2010**, *98* (5), 762-772.
18. Coster, H. G. L.; Laver, D. R., The effect of benzyl alcohol and cholesterol on the acyl chain order and alkane solubility of bimolecular phosphatidylcholine membranes. *Biochimica et Biophysica Acta (BBA) - Biomembranes* **1986**, *861* (0), 406-412.
19. Lalchev, Z. I.; Mackie, A. R., Molecular lateral diffusion in model membrane systems. *Colloids and Surfaces B: Biointerfaces* **1999**, *15* (2), 147-160.
20. Ladha, S.; Mackie, A. R.; Harvey, L. J.; Clark, D. C.; Lea, E. J.; Brullemans, M.; Duclohier, H., Lateral diffusion in planar lipid bilayers: a fluorescence recovery after photobleaching investigation of its modulation by lipid composition, cholesterol, or alamethicin content and divalent cations. *Biophysical Journal* **1996**, *71* (3), 1364-1373.
21. Armah, C. N.; Mackie, A. R.; Roy, C.; Price, K.; Osbourn, A. E.; Bowyer, P.; Ladha, S., The Membrane-Permeabilizing Effect of Avenacin A-1 Involves the Reorganization of Bilayer Cholesterol. *Biophysical Journal* **1999**, *76* (1), 281-290.
22. Tank, D. W.; Wu, E. S.; Meers, P. R.; Webb, W. W., Lateral diffusion of gramicidin C in phospholipid multibilayers. Effects of cholesterol and high gramicidin concentration. *Biophysical Journal* **1982**, *40* (2), 129-135.
23. Almeida, P. F. F., Thermodynamics of lipid interactions in complex bilayers. *Biochimica et Biophysica Acta (BBA) - Biomembranes* **2009**, *1788* (1), 72-85.
24. Goñi, F. M.; Alonso, A.; Bagatolli, L. A.; Brown, R. E.; Marsh, D.; Prieto, M.; Thewalt, J. L., Phase diagrams of lipid mixtures relevant to the study of membrane rafts. *Biochimica et Biophysica Acta (BBA) - Molecular and Cell Biology of Lipids* **2008**, *1781* (11–12), 665-684.

25. Troiano, G. C.; Stebe, K. J.; Raphael, R. M.; Tung, L., The Effects of Gramicidin on Electroporation of Lipid Bilayers. *Biophysical Journal* **1999**, *76* (6), 3150-3157.
26. Elliott, J. R.; Needham, D.; Dilger, J. P.; Brandt, O.; Haydon, D. A., A Quantitative Explanation of the Effects of some Alcohols on Gramicidin Single-Channel Lifetime. *Biochimica Et Biophysica Acta* **1985**, *814* (2), 401-404.
27. Pope, C. G.; Urban, B. W.; Haydon, D. A., The Influence of n-Alkanols and Cholesterol on the Duration and Conductance of Gramicidin Single Channels in Monoolein Bilayers *Biochimica et Biophysica Acta* **1982**, *688*, 279-283.
28. Gasset, M.; Killian, J. A.; Tournois, H.; de Kruijff, B., Influence of cholesterol on gramicidin-induced HII phase formation in phosphatidylcholine model membranes. *Biochimica et Biophysica Acta - Biomembranes* **1988**, *939* (1), 79-88.
29. van Duyl, B. Y.; Meeldijk, H.; Verkleij, A. J.; Rijkers, D. T. S.; Chupin, V.; de Kruijff, B.; Killian, J. A., A Synergistic Effect between Cholesterol and Tryptophan-Flanked Transmembrane Helices Modulates Membrane Curvature†. *Biochemistry* **2005**, *44* (11), 4526-4532.
30. Schagina, L. V.; Blaskó, K.; Grinfeldt, A. E.; Korchev, Y. E.; Lev, A. A., Cholesterol-dependent gramicidin A channel inactivation in red blood cell membranes and lipid bilayer membranes. *Biochimica et Biophysica Acta - Biomembranes* **1989**, *978* (1), 145-150.
31. Schagina, L. V.; Korchev, Y. E.; Grinfeldt, A. E.; Lev, A. A.; Blaskó, K., Sterol specific inactivation of gramicidin A induced membrane cation permeability. *Biochimica et Biophysica Acta - Biomembranes* **1992**, *1109* (1), 91-96.
32. Yoshida, N.; Mita, T.; Onda, M., Susceptibilities of Phospholipid Membranes Containing Cholesterol or Ergosterol to Gramicidin and its Derivative Incorporated in Lysophospholipid Micelles. *Journal of Biochemistry* **2008**, *144* (2), 167-176.
33. Holt, A.; de Almeida, R. F. M.; Nyholm, T. K. M.; Loura, L. M. S.; Daily, A. E.; Staffhorst, R. W. H. M.; Rijkers, D. T. S.; Koeppe, R. E.; Prieto, M.; Killian, J. A., Is There a Preferential Interaction between Cholesterol and Tryptophan Residues in Membrane Proteins? *Biochemistry* **2008**, *47* (8), 2638-2649.
34. Evans, E.; Rawicz, W., Entropy-driven tension and bending elasticity in condensed-fluid membranes. *Physical Review Letters* **1990**, *64* (17), 2094-2097.
35. Needham, D.; Nunn, R. S., Elastic deformation and failure of lipid bilayer membranes containing cholesterol. *Biophysical Journal* **1990**, *58* (4), 997-1009.
36. Lundbaek, J. A.; Birn, P.; Hansen, A. J.; Søgaard, R.; Nielsen, C.; Girshman, J.; Bruno, M. J.; Tape, S. E.; Egebjerg, J.; Greathouse, D. V.; Mattice, G. L.; II, R. E. K.; Andersen, O. S., Regulation of Sodium Channel Function by Bilayer Elasticity: The Importance of Hydrophobic Coupling. Effects of Micelle-

forming Amphiphiles and Cholesterol. *The Journal of General Physiology* **2004**, *123* (5), 599-621.

37. Lundbaek, J. A., Lipid bilayer-mediated regulation of ion channel function by amphiphilic drugs. *Journal of General Physiology* **2008**, *131* (5), 421-429.

Chapter 6

Multiplexed microfluidic bilayer platform

Multiplexing and automation are key aspects for high throughput drug screening platforms. In that context, two designs are proposed for multiplexing of our device, the TripleX and the Fishbone, comprising up to 4 bilayer experimentation sites. Additionally, the bilayer formation technique is adapted to reduce the number of pipetting steps, which is essential for future automation. Specifically, the lipid solution is added to one channel only - compared to both channels previously. This approach allows bilayer formation in smaller apertures (50 μm compared to 100 μm), and a larger surface area of the BLMs is observed. Although the fabrication procedures are kept the same, issues are encountered during this step, primarily for two reasons: first, the footprint of the device is larger, which proves to be an issue for the device assembly, and second, smaller apertures are tested here to eventually enhance bilayer stability, which results in less well-defined shapes and edges. Nonetheless, the two designs are tested for bilayer formation, followed by early electrophysiological recordings on gramicidin activity.[1]

[1] Manuscript in preparation

6.1 Introduction

Ion channels play a major role as targets for new drug development.[1] As an alternative to conventional cell-based screening methods, bilayer platforms have been proposed as promising tools for drug screening on ion channels, as discussed in detail in chapter 2.[2,3] Bilayer experimentation allows studying the target protein together with the effect of external physical parameters and soluble compounds on the protein function and activity in a simplified, yet highly versatile and controlled environment. In a conventional approach, artificial bilayer models are prepared in a set up comprising one vertical micro-aperture, sandwiched between two liquid compartments in which electrodes are inserted for electrophysiological measurements. This conventional set-up however, cannot meet two main requirements for drug screening on ion channels: parallelization and automation, which together bring high throughput capabilities. Additionally, the use of low volumes, resulting in cost reduction, is desired. Over the last decades, a variety of miniaturized and microfluidic devices have been proposed to address this bottleneck, leading to the development of platforms amenable for multiplexing and automation, while working with sub-µL volumes. Interestingly, another essential aspect for truly parallelized measurements is to multiplex and miniaturize the recording equipment. However, in most of the reports so far, this aspect has been largely ignored, and only Thei et al. have worked towards this goal.[4]

In a first step, most bilayer platforms are designed with one experimentation site to demonstrate the feasibility of the approach, and multiplexing is considered in a next step. Additionally, novel processes have been developed to form bilayer models in these miniaturized and microfluidic devices, due to the differences in the device geometry. Similarly, before the device can be applied for high-throughput assays, this process must be tested and upgraded towards reproducible, user-friendly and automated bilayer formation. A number of approaches for multiplexing and automation have been reported for suspended bilayers, as already widely discussed in chapter 2. Therefore, only a few key developments towards multiplexing are considered in the following.

Baaken et al. proposed a device consisting of an array with 16 cavities fabricated in SU8 on a glass substrate, these cavities including Ag/AgCl electrodes for electrophysiological measurements, and initially, bilayers were formed using the painting technique.[5] While this design is easily amenable to large-scale parallelization, the painting technique remains tedious and suffers from a lack of reproducibility. This aspect was addressed with the development of an automated approach whereby a droplet of the phospholipid solution is added above the cavities and painted in a rotary movement over the entire array with the help of a magnetically actuated mechanical arm.[6] After bilayer formation, a chlorinated silver wire was inserted in the

buffer solution above the cavity and electrophysiological measurements were carried out in parallel with a multichannel patch-clamp amplifier.[7] Takeuchi's lab reported a half microfluidic device, where one fluidic compartment was replaced by a microfluidic channel and where membranes were formed by first filling the top reservoir with buffer solution and sequentially flushing lipid, air and buffer solution through the lower microchannel, followed by applying pressure to the top reservoir which thinned down the lipid solution in the aperture to a bilayer.[8] This device was multiplexed later by simple parallelization of the experimentation site, to yield up to 96 independent systems in one single platform.[9-11] For multiplexing, the membrane formation approach was slightly altered, eliminating the air in the bottom channel and bilayer thinning was achieved spontaneously, after optimization of the dimensions of the aperture-containing substrate. However, while the initial success yield in bilayer formation was high and reached 90%, for the 96 site device, it dropped to 44%.[8,11] Morgan's lab developed a comparable half open system;[12] however, membranes were formed using the so-called air exposure technique. Briefly, the complete device was filled with buffer solution, which was subsequently removed from the upper well, followed by injection of the lipid solution onto the aperture. The well was re-filled with buffer solution, and emptied again to expose the thick lipid film across the apertures to air, and to induce thinning. Last, buffer was re-injected in the top compartment. As before, the design was upgraded to include 12 independent experimentation sites, and an attempt was made to automate membrane formation. However, the success yield for simultaneously formed bilayers remained low (50%), since the addition of buffer, in the last step of the process, to the top compartment in a timely manner was found to be challenging. In comparison, serial BLM formation in the same device gave a success yield of 80%.[13] In conclusion, for these two examples, even though the bilayer formation process could be automated, the importance of monitoring bilayer formation in terms of capacitance and surface area, besides recording ion channel activity as confirmation alone was highlighted by the authors.[11,13]

So far, we have developed a fully closed microfluidic bilayer platform with one experimentation site only. The next step towards a platform for drug screening is to examine multiplexing of the device and automation of the bilayer formation approach. For the first aspect, two designs are explored here, and in a first instance, we limit ourselves to up to four experimentation sites to assess the performance of both designs and choose the most promising one. In parallel, our bilayer formation approach is optimized to reduce the number of pipetting steps, which is essential for process automation. Additionally, the size of the aperture across which bilayers are formed is decreased to enhance the bilayer lifetime, and the bonding procedure is revisited since the multiplexed devices have a larger footprint. Preliminary

experiments focusing on bilayer characterization in these multiplexed devices equipped with smaller apertures are reported, together with ion channel measurements using the gramicidin model.

6.2 Experimental Section

6.2.1 Materials

Potassium chloride (KCl), (4-(2-hydroxyethyl)-1-piperazineethanesulfonic acid (Hepes), sulfuric acid, and gramicidin (mixture of species with ~80% gramicidin A) are purchased from Sigma Aldrich (Zwijndrecht, The Netherlands). N-decane is obtained from Fluka (Steinheim, Germany), ethanol from Assink Chemie (Enschede, The Netherlands), and hydrogen peroxide from Merck (Darmstadt, Germany). For bilayer formation, 1,2-diphytanoyl-*sn*-glycero-3-phosphocholine (DPhPC) and 1,2-dioleoyl-*sn*-glycero-3-phosphoethanolamine-N-(lissamine rhodamine B sulfonyl) (DOPE) are ordered as solutions in chloroform from Avanti Polar lipids (Alabaster, AL, USA). All aqueous solutions are prepared with deionized water (MilliQ system, Millipore, Billerica, MA, USA), and the experiments are carried out at room temperature.

6.2.2 Chip design and fabrication

The multiplexed microfluidic devices are developed along the same line as to the one-plex system in terms of key features (two microfluidic channels, intermediate layer comprising a microaperture), materials (glass and Teflon) and fabrication processes (wet-etching of the microchannels, processing of the Teflon film using dry-etching and chip-level assembly using a UV-curable glue). Two main designs are proposed. First, the Fishbone presents one common bottom channel, and four individual top channels, yielding four bilayer sites. A variant of this design, the Half-fishbone design, is considered as well, which presents the same configuration as the Fishbone, while having only two top channels associated with one common bottom channel. The second main design is the TripleX, which can be seen as the parallelization of three one-plex systems, and which comprises three independent top and bottom channels, giving in total three fully independent experimentation sites.

The chips are designed in Clewin (WieWeb software, Hengelo, The Netherlands). All designs have the same footprint of 3.5 cm x 1 cm, and the diameter and position of the fluidic inlets and outlets (reservoirs) are kept constant so that the same chip holder can be used for all designs and experiments. The center-to-center distance between the reservoirs is 6 mm, which is compatible with standard fluidic connections for

future coupling to a liquid control system. The channels are drawn in the Clewin mask with a width of 50 μm, reservoir diameters of 1000 μm, and apertures with diameters ranging from 15 to 50 μm.

The devices are fabricated as described previously in chapter 3. Shortly, the microfluidic channels are defined in the top and bottom glass substrates at the wafer scale (Borofloat 33, 100 mm diameter, 500 μm thickness) by standard wet-etching techniques. The fluidic reservoirs in the top layer are created by powder-blasting, and the features in the 12.5 μm thick Teflon FEP foil (Sabic BV Snij-Unie HiFi, Enkhuizen, The Netherlands) by reactive ion etching using a shadow mask. After wafer-scale fabrication of the three layers and dicing of the individual bottom and top glass parts, the substrates are glued together with an optical adhesive (NOA81), at the chip level. Compared to the one-plex device, the multiplexed devices have a larger footprint, which required adaptation of the bonding procedure. Before assembly, the glass substrates are cleaned as before in hot piranha solution (3:1 H_2SO_4:H_2O_2) for 10 min, rinsed thoroughly in deionized water and dried. In a next step, two droplets of NOA81 (Norland Optical Adhesive, Cranbury, NJ, USA) are spread out on a glass cover slip, subsequently spin coated (30 s at 500 rpm, 30 s at 5000 rpm) and finally pre-cured to reduce the thickness of the glue layer (45 s bottom layer, 33 s top layer, λ = 366 nm, Konrad Benda Laborgeräte, Wiesloch, Germany). Instead of using a roller to apply the glue to the glass,[14] the bottom and top glass substrates are directly placed in contact with the cover slip on which the glue has been spin-coated, the channel side facing the pre-cured glue layer, and the glass is peeled off carefully. The Teflon foil is cut to chip-size, dipped in ethanol, placed on a clean cover slip and straightened out with a roller. The ethanol evaporates and the Teflon remains flat on the cover slip, which is crucial for leakage-free bonding. A home-built system is used to align the three parts to each other (**Figure 6.1** a). First, the cover slip with the Teflon foil is placed on the table of the aligner and held in place by applying vacuum. The glue-covered bottom glass part is secured in a custom-made holder which is brought at a distance of a few centimeter above the table, with the glue-side facing down (**Figures 6.1** b,c). A stereomicroscope (4x magnification) allows aligning the apertures and reservoirs in the Teflon foil to the bottom glass substrate by moving the table in the *x*- and *y*-direction with micrometer precision. Alignment marks in the bottom glass layer help to position the apertures to the bottom channel, which must match the position of the top channels in the next step. When the apertures are properly aligned, the table is moved up until the two parts come in close contact with each other. During this step, the alignment is continuously controlled with the microscope, and adjusted if needed. The bottom glass part is manually pressed on the Teflon foil, before a short exposure to UV light (~20 s) *in situ* to secure the Teflon to the bottom glass substrate and to prevent shifting of the aligned apertures. In a next step, the glass-Teflon stack is placed on the table with the Teflon foil facing up, and the top

glass part is positioned in the holder with the glue side facing down. The top channels and reservoirs are aligned to the apertures and to the channels in the bottom layer as described above. After pressing the parts together, the device is finally cured with UV light for ~2 min.

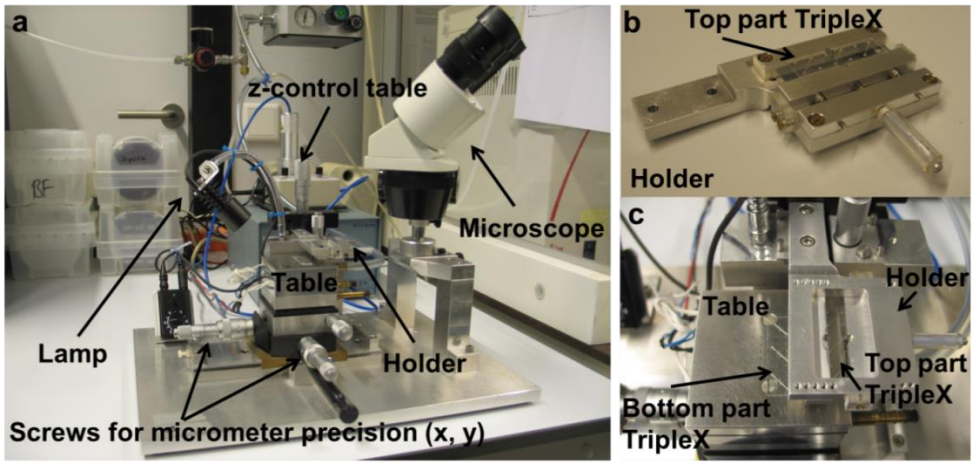

Figure 6.1. Chip aligner. a) In-house built alignment machine for the chip-level assembly, used for the bonding of the multiplexed devices. b) One glass part of the microfluidic device is placed in a holder, which is screwed on top of a table and can be moved in the *x*-, *y*-, and *z*-direction with micrometer precision (c). The other glass part is held on the table with vacuum (c). The alignment and bonding processes are continuously monitored with the help of a microscope.

6.2.3 Experimental set-up

The multiplexed device is placed in a custom-made chip holder, which is adapted to the footprint of the device, in the same manner as for the one-plex system (**Figure 6.2** a). The bottom plate houses a cavity, which fits the device, with a window allowing optical measurements. The top part includes access holes (2 mm in diameter, 7.5 mm high) for fluidic and electrical connections to the reservoirs in the chip. The chip holder fits in the stage of the microscope (Leica DMI 5000M, Rijswijk, The Netherlands), and bright field images are captured with a CCD camera (DFC310FX, Leica, Rijswijk, The Netherlands) (**Figure 6.2** b). Therefore, Ag/AgCl electrodes (Molecular devices, Sunnyvale, CA, USA), which are inserted in the reservoirs of the chip holder, are connected to a CV 203 BU headstage and an Axopatch 200b amplifier (all Molecular devices, Sunnyvale, CA, USA). Sequential electrophysiological measurements are carried out since only one patch-clamp amplifier is available, and the electrodes are shifted from one experimentation site to the other for sequential recordings. For low-noise electrical measurements, the headstage and electrodes are

shielded by a faraday cage, which is placed on top of the chip holder. Data are acquired via a LabVIEW interface and using a PCI-6259 data acquisition card (National Instruments, Austin, TX, USA).

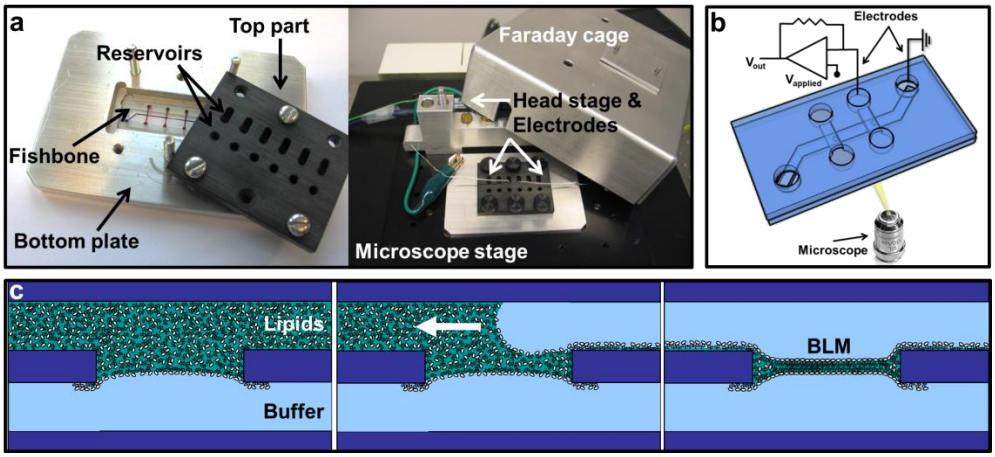

Figure 6.2. Experimental set up and bilayer formation. a) The chip holder has a cavity where the multiplexed chip is inserted, here the Fishbone device, whose channels are filled with ink for visualization purposes. The top part of the chip holder houses reservoirs for fluidic and electrical connections, the complete holder fits in the microscope stage and electrodes inserted in the reservoirs are connected to the head stage (*right*). A faraday cage is placed on top to reduce the noise during the electrophysiological recordings. b) Schematic representation of the dual optical and electrophysiological measurement scheme for the sequential measurements in a Half-fishbone device. c) Drawing of the one-sided BLM formation at the aperture (side view, not drawn to scale). First, the bottom channel is filled with buffer, and subsequently, lipid solution is introduced in the top channel (*left*). In a next step, buffer is added to the top channel to replace the lipid solution (*middle*). A BLM is formed instantaneously (*right*).

6.2.4 Bilayer experimentation and characterization

The lipids, DPhPC and fluorescently labeled DOPE, are purchased as chloroform-based solution with a concentration of 10 mg/mL and 1 mg/mL, respectively. First, the chloroform is evaporated in a vacuum chamber for at least 30 min, and the residue is re-suspended in n-decane to yield a concentration of 10 or 25 mg/mL. Two protocols are utilized here for BLM formation: the two-sided protocol described in chapter 3 and a novel one-sided protocol. In the first case, both channels are filled with 0.2 μL of lipid solution, which is subsequently replaced by buffer (1 M KCl, 10 mM Hepes, pH 7.4), 30 μL and 20 μL being added to the bottom and top channels, respectively. In the new protocol, 30 μL of the measurement buffer is injected in the bottom channel of the empty chip. In a next step, 0.3 μL of the lipid solution is pipetted in the top channel, and subsequently replaced by 20 μL of buffer, as depicted

in **Figure 6.2** c. The buffer replaces the lipid solution, and, spontaneous and instantaneous BLM formation is observed. After stabilization of the bilayer, the seal resistance (R_m) is determined by measuring the current while applying dc voltages (-30 - 30 mV, in 10 mV steps). The bilayer capacitance (C_m) is obtained from the current response of an ac voltage (50 Hz, 75 mV pp), after thorough calibration of the system with solid-state capacitors (1 - 22 pF). The capacitance values are corrected for stray capacitance measured in a chip containing a Teflon foil without aperture (2.35 ± 0.34 pF, n = 4). Simultaneously with the capacitance measurements, the surface area (A_{BLM}) of the bilayer is determined optically (bright field) using ImageJ (open source software from NIH). The specific capacitance (C_s), which is the capacitance per surface area, is calculated from the measured C_m and A_{BLM} values. For the multiplexed experiments, the bilayers are formed as described above. However, first buffer solution is added in one top channel only to initiate bilayer formation, leaving the other top channel filled with lipid solution. After the electrical characterization and measurements are finished in the first aperture, BLM formation is initiated in the next aperture by adding buffer to the second top channel. The electrodes are manually moved to the next reservoir after buffer injection, and before bilayer formation.

6.2.5 Gramicidin measurements

The gramicidin peptide is dissolved in ethanol (100 nM) and added to the lipid solution prior to BLM formation to yield a final concentration of 0.8 nM. After bilayer formation, a dc voltage of 80 mV is applied while the current response is recorded (1 kHz Lowpass Bessel filter, 10 kHz sampling rate). Data are filtered and analyzed using an in-house written Matlab routine.

6.3 Results and discussion

6.3.1 Chip design

Two different designs are proposed for multiplexing of the device: the Fishbone – and Half-fishbone- and the TripleX (**Figure 6.3**), which are discussed in detail and compared in the following (**Table 6.1**).

As described in chapter 3, we have first developed a one-plex device. This device includes two microfluidic channels - each in one glass substrate - which represent the intra- and extracellular media of the cell. These two fluidic compartments are separated by a Teflon foil comprising a microaperture across which the bilayers are formed. These key features, as well as the materials used to produce the devices (glass and Teflon), have proven to be suitable for bilayer formation and for measurements

on individual pore-forming species. Therefore, these elements are kept to develop the multiplexed chips. Furthermore, next to the multiplexing of the device, another parameter is essential for eventually large throughput experimentation, which is the development of a bilayer formation procedure, which is easily amenable to automation.

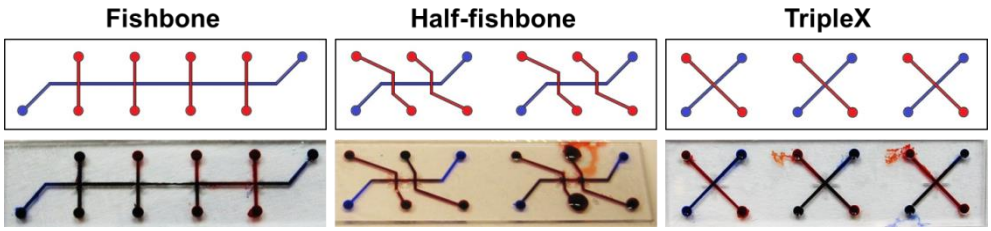

Figure 6.3. Multiplexed designs. Fishbone (*left*), Half-fishbone (*middle*), and TripleX (*right*) designs for multiplexed experiments: sketched (*Top*) and pictures of actual devices (*Bottom*), as shown in the first row. The top channels are colored in red and the bottom ones in blue (sketch), or they are filled in with corresponding inks for visualization purposes (picture). In the Half-fishbone and TripleX devices, leakage is visible around the reservoirs, revealing poor bonding.

Table 6.1. Comparison TripleX and Fishbone. The advantages and disadvantages for the TripleX and Fishbone are summarized in terms of design, measurements and experimentation ease.

	TripleX	Fishbone
Advantages	• Fully independent systems • Possibility to conduct different experiments	• Reduced number of reservoirs • Less liquid manipulation • Less electrodes needed
Disadvantages	• Larger number of reservoirs • More electrodes	• "Connected" bilayers • Risk of electrical and chemical crosstalk

Comparison TripleX and Fishbone

The Fishbone device comprises four experimentation sites, compared to three for the TripleX, while keeping the same footprint and position for the reservoirs. Furthermore, in the Fishbone device, one common bottom channel is connected to the four apertures, which would enable BLM formation in all four apertures using the one-sided protocol, with less pipetting steps than for the TripleX. For the one-sided bilayer formation, the following steps are required: (i) filling of one channel with buffer solution, (ii) injection of lipid solution in the other channel, followed by (iii) buffer solution to replace the lipids. In the TripleX device, these three steps must be

performed three times for the three independent experimentation sites, giving a total of nine pipetting steps. In the Fishbone device however, if the bottom channel is used to introduce the lipid solution, only six steps are needed in total, which results in a reduction of the pipetting steps by 30% for four instead of three bilayers. Similarly, since one channel is common, the reference electrode can be shared for all experimentation sites, and the number of electrical connections becomes lower, i.e., five electrodes for the Fishbone and six for the TripleX, for four and three bilayers, respectively. Even though the reduction in terms of fluidic connections, manipulation steps, and electrodes is not extreme for the herein presented Fishbone and TripleX designs, this factor can play a larger role for devices including more experimentation sites. For all these reasons, the Fishbone design seems to be more advantageous.
One possible limitation however with the Fishbone system is that the bilayers are somehow connected, which brings two possible issues of electrical or chemical cross talk between experimentation sites. The TripleX design appears to be a safer option in that respect, as the systems are fully independent, and the BLMs are addressed separately, so that different experiments can be performed in one device in parallel without any risk of interference.

6.3.2 Fabrication

The fabrication process for the multiplexed devices is much akin that of the one-plex devices. However, changes in feature sizes (microfluidic channels and apertures), as well as the increased footprint of the devices turned out have an impact on the fabrication success yield, as discussed below.

Microfluidic channels in the glass substrates
The width of the microfluidic channels in the glass substrates in the multiplexed chips is reduced from ~300 μm to ~190 μm compared to the one-plex design, and their depth from ~100 μm to ~50 μm. The rationale behind this alteration is to decrease the total volume of the microfluidic channels, to thereby reduce the consumption of chemicals, which is an important aspect for drug screening, since it would mean using lower amounts of drugs.

Micrometer-sized apertures in the intermediate Teflon layer
For the multiplexed systems, smaller sized apertures are designed, with diameters ranging from 15 to 50 μm, compared to 50 and 100 μm for the one-plex system. Here, the diameter of the aperture is decreased, since the bilayer stability directly relates to the aperture size,[15] and bilayer stability is essential, as discussed earlier (chapter 2) for developing a robust screening tool.

As already mentioned in chapter 3, apertures of ca. 15 µm in diameter can be realized using our dry-etching strategy in 12.5 µm thick Teflon foils. However, these apertures have a conical shape, while 100 µm sized apertures exhibit a straight profile (See **Figure 6.4** a). A tapered profile is also observed for 35 µm diameter apertures, as revealed by SEM imaging (scanning electron microscope) and WLI (White Light Interferometry) measurements, as presented in **Figures 6.4** b,c. Additionally, some apertures were found to have a less round profile (**Figure 6.4** b). Apertures with a 100 µm diameter are typically produced with an etching time of ca. 45 min while longer etching times of at least 60 min are required for smaller apertures. The increased etching time includes a cooling step since the maximum etch-time of the machine is limited to 45 min, resulting in slight shifting of the shadow masker during cooling and re-heating of the Teflon foil, which could lead to the less-defined shape. Additionally, the reduction in aperture diameter in the shadow mask limits the chance of ions to reach the edge of the feature resulting in a tapered structure. Finally, as already discussed in chapter 3 for 50 and 100 µm diameter apertures, the etched features are typically 7-8% larger than the drawn design, and 35 or 50 µm designed apertures have actual sizes of 38 ± 2 µm (n = 7) and 54 ± 1 µm (n = 2), respectively, as measured with bright field microscopy.

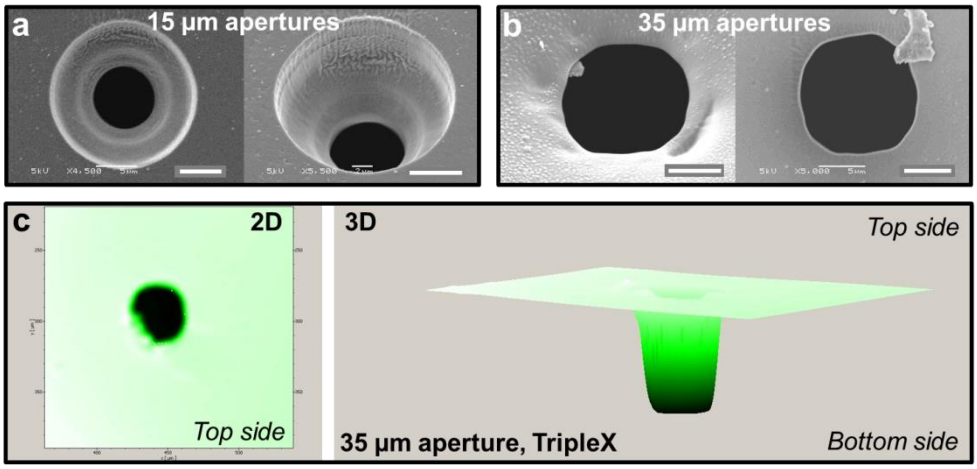

Figure 6.4. Aperture characterization. SEM images of 15 (a) and 35 (b) µm apertures etched in a 12.5 µm thick Teflon foil using dry-etching. Scale bars: 5 µm. c) 2D (*left*) and 3D (*right*) profile of a 35 µm aperture imaged with WLI. The top side is facing the shadow mask during the dry-etching process.

Bonding

The glass-Teflon-glass devices are assembled using UV-curable glue, which was applied with a roller on the glass substrate, for the one-plex systems. This approach,

which is well suited for devices with a small footprint (1 cm x 2 cm), turned out to be less suitable for larger devices (1 cm x 3.5 cm). Applying a homogenous glue layer on the glass in the latter case is more challenging, and this often leads to either leakage when the glue layer is too thin, clogging of the channels caused when the layer is too thick, or both issues being encountered for the same device. Therefore, the bonding procedure is adapted, and the devices are directly stamped onto the pre-cured glue to yield a more homogeneous layer of glue on a larger surface area. However, and as seen in **Figure 6.3**, leakage sometimes still occurs, mainly on only one extremity of the device, which proves that this alternative approach to apply the glue suffers from poor reproducibility.

The smaller channel dimensions increases the risk of clogging of the structures with glue, due to the higher capillary action in the glass channel. Therefore, in a second fabrication batch, channels are etched deeper (~130 μm compared to previously ~50 μm) and concomitantly wider (~350 μm compared to ~190 μm), to improve bonding and enhance its reproducibility.

The next challenge is the alignment of the apertures to the channels. For the multiplexed device, up to four apertures (15 - 50 μm in diameter) must be aligned in one device, which is not possible manually. Therefore, a dedicated device is built in-house for this step, to achieve alignment with micrometer precision. In the one-plex device, the 100 μm apertures are aligned to the ~300 μm wide channels with a precision of 7 ± 5 μm (n = 3), typically, using this custom aligner. In that case, the large apertures are clearly visible under the stereo-microscope in the aligner (4x magnification). The edges of smaller apertures (<50 μm) are less visible with the stereo-microscope, which makes the alignment more challenging. To facilitate this process, the position of the apertures is marked with a pen on the glass slide during the bonding procedure. Altogether, smaller apertures were aligned to the larger channels (~350 μm) with a precision of 16 ± 10 μm (35 μm aperture, n = 5). However, it must be noticed that even though the channels are wider and the aligner offers a micrometer precision, the simultaneous alignment of four different apertures in one device to both the top and bottom channels remains highly tedious. A slight displacement at one extremity of the device leads to the shift of the aperture positioned at the other end of the design.

In conclusion, a number of issues have been encountered during the fabrication of the multiplexed devices, and their assembly, compared to the one-plex devices, which were not expected since the fabrication process was the same. First, due to the increased footprint of the device, applying a homogeneous glue layer is difficult and not reproducible, although this aspect is crucial for leakage free bonding. Second, the decreased channel size increases the risk for clogging by the glue. Finally, the smaller

apertures are difficult to visualize during the bonding process, and simultaneous alignment of more experimentation sites is more tedious. For future experiments, these different key issues must be solved to increase the fabrication yield of the multiplexed devices, even more if larger devices with more experimentation sites are designed.

6.3.3 BLM formation

So far, BLM formation in the one-plex device has been achieved by filling both channels with lipid solution, which is subsequently replaced by buffer. In this technique, bilayers are formed through spontaneous and instantaneous thinning of a lipid plug deposited in the aperture into a bilayer. For the multiplexed device, the procedure for bilayer formation is slightly altered to reduce the amount of pipetting steps: only one channel is filled with the lipid solution, which is subsequently replaced by the buffer, while buffer is directly injected in the other channel at the beginning of the procedure.

As already described above, the diameter of the apertures is decreased in the multiplexed devices, to eventually enhance bilayer stability. However, the aspect ratio of the aperture (ratio between the Teflon film thickness and the aperture diameter) plays a key role for bilayer formation. For solvent-containing bilayers, the BLM is surrounded by an annulus, which stabilizes the bilayer at its edge. The shape of the annulus is defined by the angle it forms with the bilayer and with the aperture-containing substrate, as well as by the volume of the solution added to the aperture.[16] The higher aspect ratio found in smaller apertures is accompanied by a change in the shape of the annulus, and impacts the surface area of the BLM relative to the aperture size.[17] Consequently, BLM formation is first tested in one-plex devices with smaller apertures, 50 μm in diameter, and compared to devices with a 100 μm aperture previously tested, applying the initial two-sided method. Additionally, this technique is compared to the one-sided bilayer formation method.

In a first series of experiments where the influence of the aperture diameter on the bilayer formation is assessed, only the surface area of the bilayer is determined, since this is influenced by the angle of the annulus with the aperture, which is related to the aperture aspect ratio. In a second series of experiments, bilayers in the multiplexed device are fully characterized. For those experiments, DPhPC in n-decane with 1% vol fluorescently labeled DOPE is used.

Two-sided bilayer formation

The two-sided bilayer formation method is first tested in the one-plex device with apertures of ~53 μm in diameter, and compared with apertures of ~105 μm in diameter, referred to as 50 and 100 μm apertures in the following. As already mentioned in chapter 3, BLM formation is more challenging for smaller apertures (50 μm diameter) under the same conditions. Specifically, bilayer formation in devices with a 100 μm aperture and using a 25-mg/mL lipid solution gives a 100% success yield including reflushing steps (n = 45),[18] and, in that case, the measured bilayer area accounts for 55 ± 15% (n = 9) of the aperture. For a 50 μm aperture, a success yield of only 57% (4 out of 7) is recorded when using the same lipid concentration, with the bilayer forming either directly (3 out of 7) or after creation of a lipid plug that thins down into a bilayer. Sometimes, thinning of the lipid plug is not observed (2 out of 7), or the bilayer goes back to a lipid plug state after a few minutes (1 out of 7). Additionally, the bilayer area for a 50 μm aperture is dramatically smaller (7 ± 5% (n = 4), **Figure 6.5**). This decrease in surface area can be caused by the increase in the aspect ratio of the aperture, as mentioned earlier, and the subsequent change in the angle of the annulus with respect to the substrate and the bilayer.[17] Another possible explanation is that the lipid concentration is too high for the smaller aperture, hindering thereby the thinning process. Therefore, the same bilayer formation technique is applied with a lower lipid concentration. For a 50 μm aperture and using a 10 mg/mL lipid solution, the BLM formation yield becomes 67% (4 out of 6) and in two cases, first a lipid plug is formed, that eventually thins down to a bilayer after 17 and 45 min. The surface area of these bilayers becomes 15 ± 9% (n = 4) only. Altogether, these results suggest that the lipid concentration does not have a significant influence on the success yield and the surface area, and only a trend towards slightly larger surface areas and higher success yield is noticed. For 100 μm apertures, the same lipid concentration (10 mg/mL) leads to successful bilayer formation in all trials (3 out of 3, including reflushing for one bilayer), with a surface area comparable to the initial lipid concentration (44 ± 9% (n = 3) for 10 mg/mL lipid solution *vs.* 55 ± 15% (n = 9) for 25 mg/mL). Last, and importantly, spontaneous and instantaneous bilayer formation is also observed under these conditions.

One-sided bilayer formation

In a next step, the bilayer formation process is adapted by applying the lipid solution in one channel only. Spontaneous and instantaneous thinning is observed, in the same way as for the two-sided bilayer formation. For 100 μm apertures, using a 25 mg/mL lipid solution, bilayer formation is successful in all attempts, including reflushing in one case (n = 3). Interestingly, the bilayer area is greatly increased to 92 ± 2% (n = 3) compared to 55 ± 15% (n = 9) for the two-sided method. A similar result is obtained

for the 50 μm apertures using the same lipid concentration: BLM formation is successful in all attempts (n = 3, with once a reflushing step), and BLMs have a surface area of 63 ± 12% (n = 3) (See, **Figure 6.5**). For 25 mg/mL lipids, the success yield in the 50 μm aperture increases from 57% to 100% for the two- and one-sided method, respectively. Additionally, the surface area is larger for the 50 μm apertures (7 ± 5% (n = 4) *vs.* 63 ± 12% (n = 3) for the two- and one-sided approach, respectively, both with 25 mg/mL phospholipids)). Using the one-sided approach, the significant changes in BLM area and annulus suggest, that the phospholipids adopt a different organization in the aperture. To verify this hypothesis, the bilayer shape should be further investigated with for instance confocal imaging. Furthermore it would be interesting to examine the bilayer stability for the two BLM formation techniques. For now, this comparison tends to show that the one-sided technique facilitates BLM formation in smaller apertures, and additionally it leads to larger bilayer surface areas. In the rest of this chapter, the one-sided bilayer formation technique is utilized for the following step of BLM characterization, for both designs.

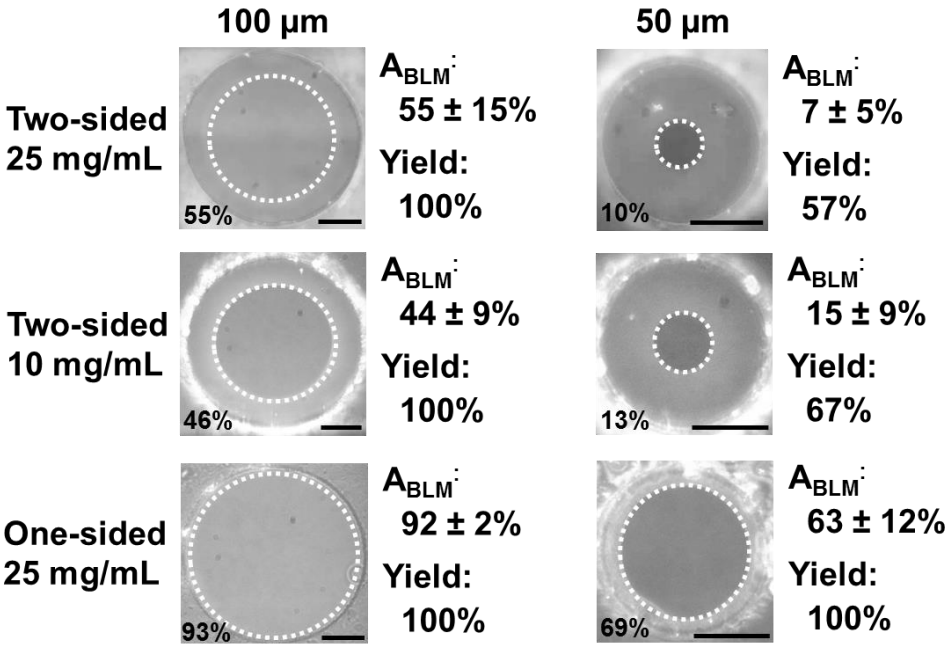

Figure 6.5. BLM formation. Summary of the results for the two-sided and one-sided BLM formation procedures using 25 and 10 mg/mL lipid solution, and for 100 and 50 μm diameter aperture. The surface area of the corresponding bilayer is presented in the left corner of the image. The success yield for bilayer formation is indicated next to the images, and includes re-flushing steps. Scale bars: 25 μm.

6.3.4 BLM characterization in the Fishbone and TripleX

The two designs, the Half-fishbone and the TripleX, are compared in terms of BLM properties, using 10 mg/mL DPhPC in n-decane. Sequential measurements are carried out, since only one patch-amplifier is available. Specifically, first one BLM is formed, and thoroughly characterized, before bilayer formation is initiated in the second experimentation site, as presented in **Figure 6.6** for the Half-fishbone device. For this reason, the lipid solution is applied in the top channels of the Half-fishbone instead of the common bottom channel, to alleviate any risk of bilayer rupture upon insertion of the electrode in the reservoirs.

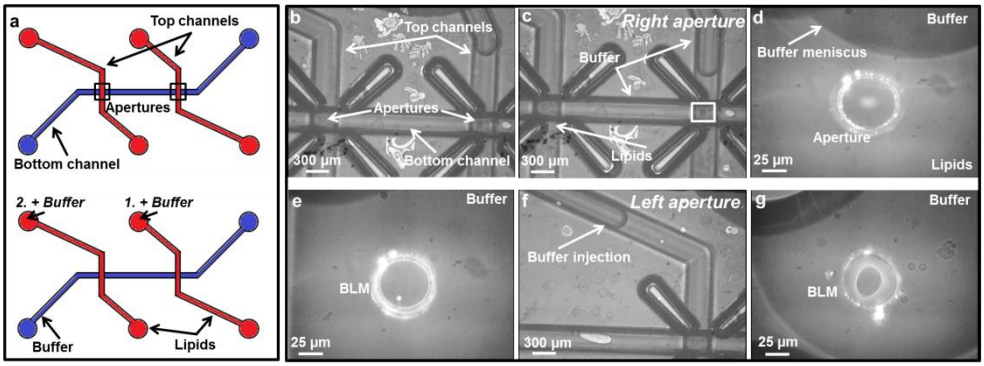

Figure 6.6. One-sided BLM formation in a Half-fishbone device. a) Bilayers are formed sequentially across two apertures, by first filling the bottom channel with buffer, and subsequently adding lipid solution to both top channels (*top*). Following this, buffer is injected in the right top channel to replace the lipid solution (b-c). d) The buffer meniscus moves across the aperture leading to spontaneous and instantaneous BLM formation (e). In the next step, buffer is added to the left top channel (*bottom* sketch & f) and bilayer formation is initiated in the left aperture following the same protocol (g).

First, measurements are performed in a TripleX device with apertures of 23 µm in diameter (actual size). However, bilayers formed in such small apertures are not clearly visible and, similarly, their capacitance values lie in the range of the stray capacitance, which is around 2.35 pF. This difficulty to monitor bilayer formation in small apertures has been reported before for aperture diameters of <1 µm[19] (electrical monitoring) and for <40 µm (optical monitoring).[9] Therefore, only apertures of >40 µm diameter are tested for the BLM characterization. Additionally, the system is calibrated with solid-state capacitors in the low pF-range to increase its sensitivity and reliability for the present measurements on smaller bilayers. Even though problems have been encountered for the device fabrication, at least one device is available for each type, with at least two good apertures for initial tests. Specifically, for the Half-fishbone design, measurements are performed on two different days using two different apertures with actual diameters of 55 and 54 µm (n = 7, n = 5, respectively),

and for the TripleX, on two apertures with actual diameters of 37 and 39 μm on different days (n = 7, n = 2, respectively). It is worth noticing that due to fabrication issues, measurements are not carried out using same aperture diameters for the two designs, which precludes direct comparison between the two designs.

In these experiments, BLMs are characterized in both designs in terms of seal resistance (R_m), capacitance (C_m), surface area (A_{BLM}) and specific capacitance (C_s). All experimental values are presented in **Figure 6.7**. From these preliminary experiments, no clear difference is observed in the bilayer characteristics for the Half-fishbone and TripleX design. For all apertures, the measured seal resistance is in the GΩ range. However, a large variation is observed in the seal values, even for bilayers formed in the same aperture, which may reflect the issues encountered to produce apertures with a well-defined shape. The capacitance lies in the low pF range, around 3.9 ± 1.6 pF for the 54 μm apertures in the Half-fishbone, and 3.5 ± 1.0 and 4.9 ± 0.5 pF for the TripleX and the 37 and 39 μm apertures, respectively. For the 55 μm aperture in the Half-fishbone device, a slightly higher capacitance of 8.8 ± 1.7 pF is observed. This value is comparable to that measured in a 53 μm aperture in the one-plex device for the one-sided BLM formation, using a 25 mg/mL DPhPC solution (8.3 ± 1.4 pF (n = 3)). The surface area of the bilayers in the Half-fishbone device is 59 ± 14 and 35 ± 10% for 55 and 54 μm apertures, respectively, and in the TripleX device the area is in the same range or slightly higher (65 ± 19 and 83 ± 2% for 37 and 39 μm apertures, respectively). From the values of the capacitance and surface area, the specific capacitance is calculated. Here, a C_s value of 0.48 ± 0.07 μF/cm² is measured in the Half-fishbone device (54 μm aperture), and, of 0.52 ± 0.12 and 0.50 ± 0.03 μF/cm² for 37 and 39 μm apertures, respectively, in the TripleX. The C_s value of the 55 μm aperture in the Half-fishbone device is slightly higher (0.64 ± 0.08 μF/cm²). In general, these values are in the same range as in the one-plex design using the one-sided BLM formation (0.60 ± 0.08 μF/cm² and 0.52 ± 0.04 μF/cm² for 53 and 105 μm apertures, respectively (both n = 3 and 25 mg/mL lipid solution)), and as expected for solvent containing bilayers (around 0.45 μF/cm²).[20]
For the TripleX device, bilayer stabilities of 15, 2 and 13 h are observed in a 37 μm aperture, which is comparable to previous results in the one-plex device (typically 10-15 h for a 100 μm aperture). A longer bilayer lifetime would have been expected due to the smaller size of the apertures but other factors such as the less-defined shape of the apertures are likely to act in the opposite direction.

In conclusion, even though different aperture diameters and system designs are tested, the bilayer characteristics in the Half-fishbone and TripleX device are not significantly different from each other in these initial experiments. Still, large deviations are observed within measurements performed on the same aperture. Therefore, additional

experiments are required for a better characterization, and before any conclusion can be drawn with respect to the design.

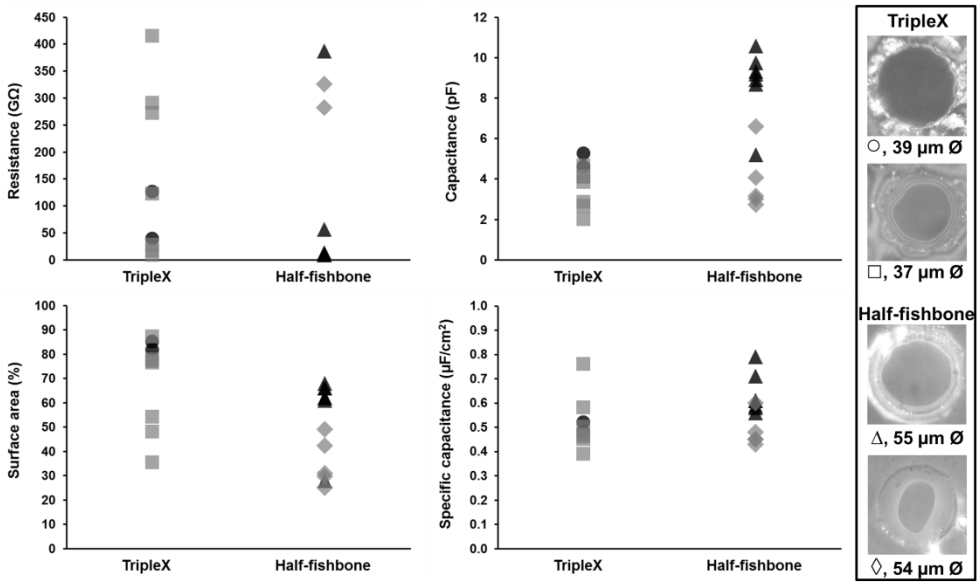

Figure 6.7. BLM characterization. The graphs summarize the values measured for the resistance (top *left*), capacitance (top *right*), surface area (bottom *left*), and specific capacitance (bottom *right*) of bilayers formed in both the TripleX and Half-fishbone device with the one-sided bilayer formation technique (10 mg/mL DPhPC in n-decane). The corresponding apertures are presented on the right, and are represented in the graph as circles or squares (both TripleX), and triangles or diamonds (both Half-fishbone).

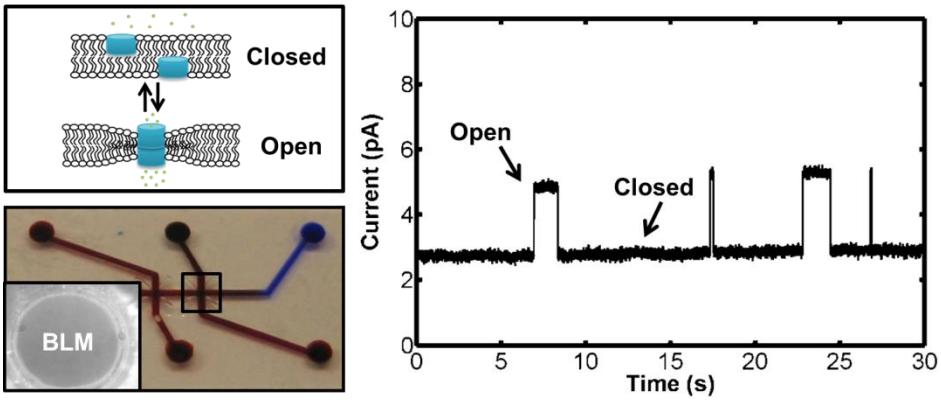

Figure 6.8. Gramicidin measurements. A first proof-of-principle experiment is performed, where gramicidin activity is recorded in the multiplexed device (*Right*). The process of pore formation is illustrated in the sketch (*Top, left*). Here, the Half-fishbone chip is utilized for the experiment (*Bottom, left*) and a DPhPC bilayer (*inset*) is formed in one aperture. (80 mV applied, 10 kHz sampling rate, moving average filter (Matlab), window size 30).

6.3.5 Gramicidin measurements

Gramicidin measurements are conducted by adding 100 nM peptide dissolved in ethanol to the lipid solution to yield a final concentration of 0.8 nM. Bilayers are formed with the one-sided approach in the Half-fishbone device and with 10 mg/mL DPhPC in n-decane. Current steps, which are characteristic for gramicidin activity, are observed, as presented in **Figure 6.8**. In total, 83 events are recorded during the complete measurement period (856 s). An average conductance of 28 ± 5 pS is determined, which is in good agreement to previous reported values under similar experimental conditions.[21] Furthermore, a noise level of 0.41 pA rms is measured, using a 10 kHz sampling rate and 1 kHz Bessel filter. In conclusion, this first proof-of-principle experiment shows good electrical resolution to measure single ion channel events in our multiplexed device.

6.4 Conclusion

In this chapter, we explore multiplexing of our microfluidic platform for BLM experimentation and proposed two different designs, the (Half-)Fishbone and the TripleX. Even though the fabrication process is kept the same for the devices, changes in the device dimensions and their internal structures (larger footprint of the devices, smaller apertures, and reduced channel dimensions) have given rise to a number of unexpected challenges for the aperture creation and assembly of the device. Consequently, the fabrication yield is much lower compared to the one-plex device, and only few devices have been tested. Nonetheless, after adaptation of the bilayer preparation protocol, and the development of a one-sided BLM formation procedure, which is better amenable to automation, BLM formation is successfully demonstrated in both designs. Furthermore, bilayers are characterized in both devices in terms of seal resistance, capacitance, surface area and specific capacitance, as before. So far, no clear difference is observed between the two designs with respect to bilayer formation and characteristics, while the resulting values are relatively spread. Finally, single gramicidin events have been successfully recorded, confirming the applicability of the platform for single protein studies. In conclusion, these preliminary results show the potential of our microfluidic platform for multiplexing and automation.

In the future, the one-sided bilayer formation approach should be tested in the (Half)fishbone device by applying the lipid solution in the common bottom channel. Additionally, the expected chemical and electrical cross-talk in the Fishbone device should be investigated in detail.

6.5 Outlook

Even though initial multiplexing of the device is demonstrated, further improvements are needed before a robust platform exists for reliable multiplexed measurements. First, the aperture size has been decreased to enhance bilayer stability. However, the fabrication of smaller apertures is found more challenging; they are less well defined, less reproducible and exhibit no vertical walls. Therefore, in the future, apertures of 50 and 100 μm diameter, which have been validated with the one-plex device, should be used to further characterize the (Half-)Fishbone and TripleX designs. Alternatively, other fabrication methods could be applied to create clean apertures with a decreased diameter. To overcome problems with the BLM formation in small apertures, a thinner hydrophobic partition could be used to keep the aspect ratio constant. Here, difficulties to verify bilayer formation with optical and electrophysiological techniques for apertures <40 μm should be taken into account. On the other hand, alternative techniques for BLM preparation could be applied for small apertures, as for instance vesicle rupturing. This approach would be interesting, also with respect to future measurements on ion channels, since the proteins can be integrated directly in the vesicles, and tedious proteoliposome fusion with the bilayer, which is conventionally implemented for the insertion of membrane proteins, could be avoided. This BLM formation technique however, would also include adaptation of the substrate material since a hydrophilic aperture surface is needed for this alternative membrane formation technique.

Furthermore, bonding the devices at the wafer scale would be highly advantageous; it would increase the efficiency, especially for large scale production, while facilitating the alignment step, if dedicated equipment present in the clean room is used.

Finally, integrating the electrodes in the device would be essential for the multiplexed platform. For now, the electrodes are physically moved between the reservoirs, as only one patch-clamp amplifier is available. Furthermore, integrated electrodes are easier to connect, can be downscaled, and facilitate automation.

6.6 Acknowledgements

I would like to thank Johan Bomer and Lennart de Vreede for their help in the clean room, Hans de Boer for the fabrication of the chip holder and the aligner, Auke Jansen for his work on the chip design and device assembly, and Adithya Sridhar for the WLI measurements.

6.7 References

1. Clare, J. J., Targeting ion channels for drug discovery. *Discovery medicine* **2010,** *9* (46), 253-260.
2. Zagnoni, M., Miniaturised technologies for the development of artificial lipid bilayer systems. *Lab on a Chip* **2012,** *12* (6), 1026-1039.
3. Kongsuphol, P.; Fang, K. B.; Ding, Z., Lipid bilayer technologies in ion channel recordings and their potential in drug screening assay. *Sensors and Actuators B: Chemical* **2013,** *185* (0), 530-542.
4. Thei, F.; Rossi, M.; Bennati, M.; Crescentini, M.; Lodesani, F.; Morgan, H.; Tartagni, M., Parallel Recording of Single Ion Channels: A Heterogeneous System Approach. *Ieee Transactions on Nanotechnology* **2010,** *9* (3), 295-312.
5. Baaken, G.; Sondermann, M.; Schlemmer, C.; Ruehe, J.; Behrends, J. C., Planar microelectrode-cavity array for high-resolution and parallel electrical recording of membrane ionic currents. *Lab on a Chip* **2008,** *8* (6), 938-944.
6. Behrends, J.; Baaken, G., Method for the automated production consisting of a molecular layer of amphiphilic molecules and a device for producing said molecular layer, International Patent WO 2012095299, **2012**.
7. Baaken, G.; Ankri, N.; Schuler, A.-K.; Ruehe, J.; Behrends, J. C., Nanopore-Based Single-Molecule Mass Spectrometry on a Lipid Membrane Microarray. *Acs Nano* **2011,** *5* (10), 8080-8088.
8. Suzuki, H.; Tabata, K. V.; Noji, H.; Takeuchi, S., Highly reproducible method of planar lipid bilayer reconstitution in polymethyl methacrylate microfluidic chip. *Langmuir* **2006,** *22* (4), 1937-1942.
9. Le Pioufle, B.; Suzuki, H.; Tabata, K. V.; Noji, H.; Takeuchi, S., Lipid bilayer microarray for parallel recording of transmembrane ion currents. *Analytical Chemistry* **2008,** *80* (1), 328-332.
10. Osaki, T.; Suzuki, H.; Le Pioufle, B.; Takeuchi, S., Multichannel Simultaneous Measurements of Single-Molecule Translocation in alpha-Hemolysin Nanopore Array. *Analytical Chemistry* **2009,** *81* (24), 9866-9870.
11. Suzuki, H.; Le Pioufle, B.; Takeuhci, S., Ninety-six-well planar lipid bilayer chip for ion channel recording Fabricated by hybrid stereolithography. *Biomedical Microdevices* **2009,** *11* (1), 17-22.
12. Sandison, M. E.; Zagnoni, M.; Morgan, H., Air-exposure technique for the formation of artificial lipid bilayers in microsystems. *Langmuir* **2007,** *23* (15), 8277-8284.
13. Zagnoni, M.; Sandison, M. E.; Morgan, H., Microfluidic array platform for simultaneous lipid bilayer membrane formation. *Biosensors & Bioelectronics* **2009,** *24* (5), 1235-1240.
14. Arayanarakool, R.; Le Gac, S.; van den Berg, A., Low-temperature, simple and fast integration technique of microfluidic chips by using a UV-curable adhesive. *Lab on a Chip* **2010,** *10* (16), 2115-2121.
15. Mayer, M.; Kriebel, J. K.; Tosteson, M. T.; Whitesides, G. M., Microfabricated teflon membranes for low-noise recordings of ion channels in planar lipid bilayers. *Biophysical Journal* **2003,** *85* (4), 2684-2695.

16. White, S. H., The Physical Nature of Planar Bilayer Membranes. In *Ion Channel Reconstitution*, Miller, C., Ed. Plenum Press: New York, **1986**; pp 3-35.
17. White, S. H., Analysis of Torus Surrounding Planar Lipid Bilayer Membranes. *Biophysical Journal* **1972,** *12* (4), 432-&.
18. Stimberg, V. C.; Bomer, J. G.; van Uitert, I.; van den Berg, A.; Le Gac, S., High Yield, Reproducible and Quasi-Automated Bilayer Formation in a Microfluidic Format. *Small* **2013,** *9* (7), 1076-1085.
19. Kawano, R.; Osaki, T.; Sasaki, H.; Takeuchi, S., A Polymer-Based Nanopore-Integrated Microfluidic Device for Generating Stable Bilayer Lipid Membranes. *Small* **2010,** *6* (19), 2100-2104.
20. Nikolelis, D. P.; Krull, U. J.; Ottova, A. L.; Tien, H. T., Bilayer lipid membranes and other lipid-based methods. In *Handbook of chemical and biological sensors*, Taylor, r.; schultz, j., Eds. Institute of physics publishing: Bristol, **1996**; pp 221-256.
21. Borisenko, V.; Lougheed, T.; Hesse, J.; Fureder-Kitzmuller, E.; Fertig, N.; Behrends, J. C.; Woolley, G. A.; Schutz, G. J., Simultaneous optical and electrical recording of single gramicidin channels. *Biophysical Journal* **2003,** *84* (1), 612-622.

Chapter 7

Technology assessment and societal embedding - Exploring innovation journeys for a microfluidic bilayer platform

---

The microfluidic bilayer platform is assessed from a technological point of view, as described in this chapter. For that purpose, a workshop is organized with participants from various backgrounds to identify possible innovation pathways, and to discuss essential factors that may play an important role in the commercialization phase. Following this, four proposed applications are selected and their innovation pathways are discussed in terms of possible hurdles and opportunities, as well as their impact on society.

7.1 Introduction

The field of nanotechnology raises hopes and expectations in many areas, such as optics, electronics, biology, medicine, or in the food, energy and environmental sector. Enabling technologies are emerging from this sector and eventually enter the market to influence areas of industry and health care.[1] In the Netherlands, nanotechnology research is currently largely funded by NanoNextNL, a consortium including more than 100 firms, universities, knowledge institutes and university medical centers, with a total funding of 250 million Euro (www.nanonext.nl). Next to fundamental and application-driven research, NanoNextNL also focusses on the ethical, legal and social aspects (ELSA) of this new technology. In this frame, graduate students are required to dedicate part of their research to RATA (Risk Analysis and Technology Assessment), to enhance their reflection on developments in the field of nanotechnology and embedding of nanotechnology in the society.[1]

In my research, I have integrated the technology assessment (TA) aspect by organizing a workshop, used as pre-screening tool to identify innovation pathways for the microfluidic bilayer platform described in this thesis. In a next step, the outcome of the workshop is analyzed and four innovation pathways are discussed in detail, in terms of opportunities, possible issues and societal impact. The preparation, organization and post-processing of this workshop is done in close collaboration with Dr. Douglas Robinson, consultant in Technology Assessment and Industrial dynamics (IFRIS-LATTS, Paris) and PostDoc (University of Utrecht) in the NanoNextNL RATA theme 1C (Technology Assessment).

In this chapter, I will shortly introduce the concept of TA, followed by a description of our approach, the preparation and organization of the workshop and finally discuss and reflect on the outcomes.

7.1.1 Technology assessment and societal embedding

While emerging technologies may offer various benefits for the society, their societal embedding becomes more and more complex as a larger number of actors, e.g., technology developers, policy makers, insurance companies, or NGOs (Non-governmental Organizations) are more actively involved in this process.[1] Public perception and acceptability of a new technology is important and plays a crucial role in determining the market success of a product, as already experienced for genetically modified food products, where fear and negative public reaction led to reserved product success.[2] One way to improve acceptance and understanding is to interact with society at an early stage of the product creation process (PCP). Technology

developers however recognize the innovation chain for PCPs as concentric circles, starting with the basic research, followed by experimental platforms and prototypes, and finally reaching the definite product. In this approach, regulations and societal embedding are only considered at the end of the PCP, which increases the risk of product failure.[2] The integration of societal embedding at an early stage of the product development process would decrease such a risk, but also leads to a dilemma: in the beginning of the process many unknowns are present in the product concept, which makes anticipation more difficult, but at the later stage, flexibility for adaptations is reduced and therefore anticipation is less effective.[2] Additionally, many actors are involved in such a PCP, which makes communication and adaptation even more challenging. Constructive Technology Assessment (CTA) takes societal aspects into account already at an early stage by applying so-called socio-technical scenarios.[1] Additionally, bridging events such as workshops can bring together various relevant actors, stimulate the communication between them, help to map possible innovation chains for an embedding technology and identify gaps that might be present.[3] The visualization of various innovation pathways for a new technology can help to specifically flesh out individual paths, and in detail identify important factors for technology transfer and commercialization, including risk assessment, regulation, and societal embedding, and finally influence and shape the dynamics of the technology development.

In our case, the process of technology development is visualized in concentric circles. However, already before the process of development starts or a definite application is chosen, a workshop with various actors is organized to look for possible innovation pathways, and to identify a number of applications. In this case, the workshop can be seen as a pre-screening tool. In a next step, specific pathways would be selected to specifically identify possible risks and to anticipate the societal impact of the chosen technology and its application.

7.1.2 Technology

The technology assessed here is the microfluidic bilayer platform described in this thesis, whose targeted application was initially drug screening on ion channel proteins. During my research, various technical aspects of this platform have been developed such as the design and fabrication of the device, a reliable protocol for bilayer formation, the coupling of the platform to various detection techniques including high resolution confocal imaging and conventional electrophysiological measurements. The potential of the platform has been demonstrated through electrophysiological measurements of protein channels at the single molecule level, simultaneous optical and confocal imaging, and by proof-of-principle experiments to observe the impact of

changes in the bilayer properties, induced by chemicals, drugs or cholesterol, on the ion channel activity. While most of these developments have been driven by the motivation to come closer towards a drug-screening platform, the questions remain whether alternative applications exist compared to the initially envisioned screening tool, as well as a possible niche in the market for this targeted application. Here, the process of CTA can help to define other routes for technology transfer and commercialization, or possibly even influence the direction of future research in terms of technological developments as well as targeted applications.

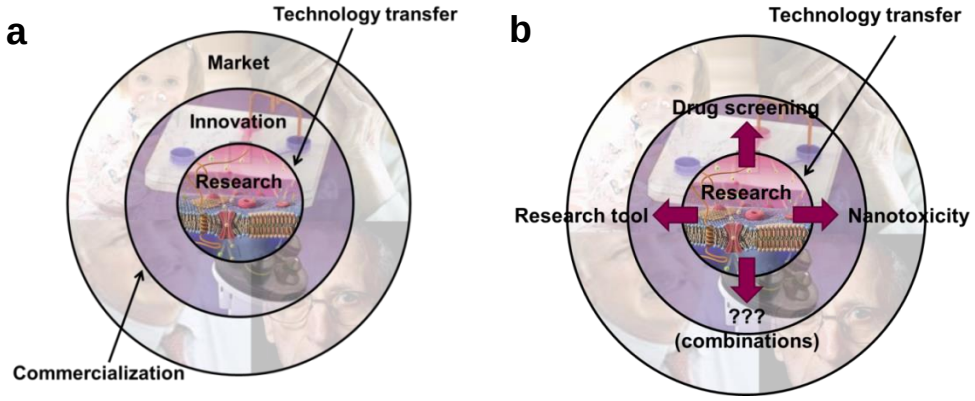

Figure 7.1. Circle diagram. a) Circle diagram representing the three layers (research, innovation and market) defined for the TA process and the interface between the different circles (technology transfer and commercialization). b) Adapted circle diagram for the microfluidic BLM platform including possible applications.

7.1.3 Circle diagram

Here, the process of product development is visualized in a "circle diagram", as shown in **Figure 7.1**. The center of the diagram shows the research, including the technical development of the platform and proof-of-principle experiments, which is in large parts described in this thesis. The second layer corresponds to the innovation phase. Here, important steps of the technology transfer must be taken into account, meaning the process to go from a research platform towards a prototype. Finally, the outer layer represents the market, including the commercialization of the technology and an evolution from a prototype towards a final product. The transition from the central circle towards the middle and sequentially to the outer circle are accompanied by issues, hurdles and opportunities, while regulations have to be taken into account. Certainly, also societal embedding needs to be taken into account during this development process. As already described in Deuten et al.,[2] a risk with this

concentric approach is the implementation of societal embedding only in the late stage of PCP. In our case, we rather use this diagram in a pre-development phase as a basis for our workshop to look at difficulties encountered when crossing the different layers, whereas the societal embedding is taken into account once a specific pathway, and more specifically a definite application, has been selected.

7.2 Exploring innovation journeys for a specific nanomedicine platform – a workshop

7.2.1 Invitation of participants

For the workshop, a list of possible participants is constructed with experts and generalists from different areas of expertise. Such a broad audience is selected to receive input on all areas of the circle diagram during the workshop. A list of all participants can be found below:

- Organizers
  - Dr. Douglas Robinson (TA expert, IFRIS-LATTS (Paris), Utrecht University)
  - Dr. Séverine Le Gac (Supervisor of the PhD student, Twente University)
  - Verena Stimberg (PhD student, Twente University)
- Researchers involved in this particular research
  - Dr. Roland Hemmler (Head technological development, Ionovation GmbH)
  - Dr. Alexander Prokofyev (PostDoc, Twente University)
- Scientists with research interests related to membranes and proteins
  - Dr. Armağan Koçer (Assistant Professor, Groningen University)
  - Dr. Martin Bennink (Assistant Professor, Twente University)
- Participants with expertise in commercialization and start-up companies
  - Henk Leeuwis (Senior Vice President Strategy and Innovation, LioniX B.V.)
  - Steven Staal (CTO, Medimate B.V.)
  - Dr. Aurel Ymeti (CTO, Ostendum R&D B.V.)
- Participants from regulations, public agencies, or involved in IP
  - Prof. Bärbel Dorbeck-Jung (Professor, IGS, Twente University)
  - Dr. Robert Geertsma (Senior Scientist/Project Leader, RIVM)
  - Dr. Leon Gielgens (Head program office NanoNextNL, STW)
  - Dr. Roy Kolkman (Intellectual Property Manager, Twente University)
- Social scientists
  - Dr. Lise Bitsch (Researcher/Lecturer, Vrije Universiteit Amsterdam)

- Dr. Dirk Stemerding (Senior researcher, Rathenau Institute)
- Prof. Harro van Lente (Professor, Utrecht University)

In total, 19 participants are invited, from which 14 agreed to join the workshop. Even though all participants were already in contact with the organizers prior to the workshop, this high level of readiness to participate shows a general interest for such activities, whereas interestingly the opposite was observed several years ago.[1]

7.2.2 Workshop preparation

During the workshop preparation, the circle diagram shown in **Figure 7.1** is defined to visualize the three-step PCP. The participants are invited by a general letter stating the goals of the workshop: i) define a road map for commercialization and societal embedding of our microfluidic bilayer platform for multiple applications, ii) discuss factors to consider including technology transfer, product development, risks, regulations and societal aspects, and finally iii) create a template for other PhD students within NanoNextNL to apply TA to their research. Additionally, a presentation is prepared with background information on the microfluidic platform and the technological elements, such as design, fabrication, measurement schemes and the application of the device for given experiments. Next to that, current collaborations and alternative applications compared to the main goal drug screening are presented.

7.2.3 Content of the workshop

After a short introduction, the workshop starts with a presentation on the targeted technology, followed by a round table discussion. In the following, first, a short summary of the presentation is given, and second, the outcome of the discussion is reported. Here, the chronological order of the discussion is adapted and rearranged to fit the construction of the circle diagram.

Presentation of the research

The main motivation of the research project is to develop a platform for drug screening on membrane proteins, as these proteins are involved in a large variety of diseases and therefore account as main targets for drug development, as discussed in the previous chapters.[4] The key feature of our platform is its suitability for combined optical and electrophysiological experimentation schemes. Combined together, they allow assessing the membrane thickness, single protein activity (electrophysiologically), and give ideas of the specific transport through a protein pore, molecular organization

of the bilayers and their properties such as the membrane fluidity (all optical/confocal). First steps towards the multiplexing of the platform are achieved and continued in a joined project, together with two companies (Micronit B.V., Ionovation GmbH). Potential other applications for our platform are presented as well: (i) a research tool for studying interactions of proteins with the membrane, as illustrated here with the example of α-synuclein abnormal aggregates involved in Parkinson's disease (collaboration initiated), and (ii) a screening tool for toxicity of nanoparticles (collaboration initiated). To visualize the three mentioned applications, the circle diagram is slightly adapted (**Figure 7.1** b), keeping still some room for further ideas.

Round table discussion: Technology transfer

The presentation is followed by a round table discussion. Here, important steps are discussed for the technology transfer from the lab to the market. The most important step is the definition of an application already early in the development process, as different markets require different strategies for commercialization. Simultaneously, potential customers should be identified. Here, it is important to determine what the customer or the market is missing and whether the gap can be bridged by the proposed technology. Finally, intimate knowledge of the daily practice in the targeted area of application is of great importance in order to find a good strategy to interfere.
Below, possible applications for our microfluidic bilayer platform are discussed in two categories, drug screening and membrane transport.

1. Targeted application: high-throughput platform for drug screening on ion channels

The development of a drug is a very long and expensive process, as illustrated in **Figure 7.2**. After identification of a target, e.g., a biomolecule or pathway responsible for a disease-specific process, a tailored activity test is developed for this target and a large compound library, previously created, is scanned in a high-throughput manner. The most promising lead compounds are further optimized and following evaluated *in silico* (with computers), *in vitro* (membrane models, cells and tissues) and *in vivo* (animals) during this preclinical testing. After packaging of the active ingredient, the compound can be tested in clinical trials. First, the drug is given to a small number of healthy volunteers, and if the drug has no severe side effects, it is tested on actual patients suffering from the targeted disease. The clinical trials, which take four to eight years, account for more than half of the total development costs. These trials on patients are governed by strict regulations, and scientific and ethical guidelines. Finally, the tests are evaluated by the FDA (Food and Drug Administration, USA) or the

EMA (European Medicines Agency, European Union), hopefully leading to the successful approval of the drug.[5]

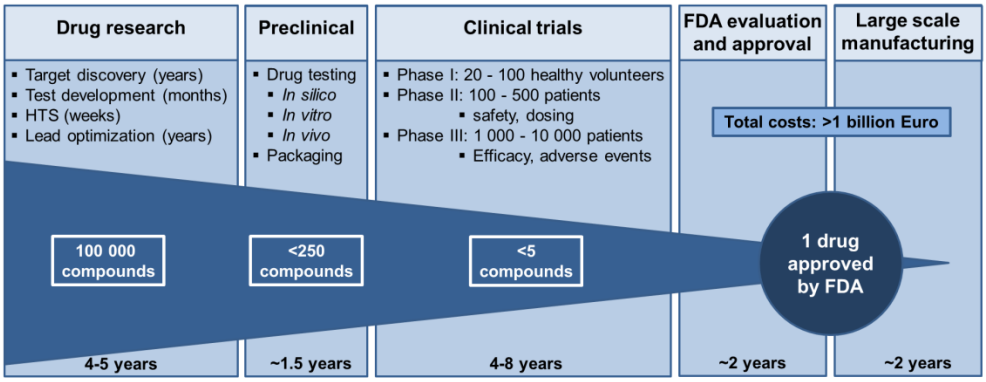

Figure 7.2. Process of drug development. For the development of a drug, first thousands of compounds are evaluated to find several interesting leads that are further optimized and tested in the lab during the preclinical phase. The most promising compounds are tested on patients in clinical trials, and finally, after FDA approval, one new drug is available for the broad society.[5]

During drug research and in the preclinical test phase, potential drug candidates targeting ion channel proteins are screened on a few established cell lines in which the specific membrane protein has been over-expressed. The interaction of the drug with the protein can be measured by various techniques as summarized in **Table 7.1**.

First, a primary screening assay is performed to discover lead chemical structures by scanning large compound libraries. In this step, a high throughput is required with a minimum of 30,000 and ideally 100,000 compounds per day.[6] For this step, mainly fluorescent assays are applied, that either are ion specific (calcium sensitive dyes) or sensitive to changes in the membrane potential. For the first one, the cells are loaded with the dye and the flux of calcium ions through the channel protein, activated by the potential drug candidate, is measured via an increase in fluorescence. The established FLIPR system (Fluorometric Imaging Plate Reader, Molecular Devices, Sunnyvale, CA) utilizes a CCD-camera to capture the fluorescent signal in a high throughput manner. To detect voltage-gated ion channels, for instance a FRET (Förster Resonance Energy Transfer) assay is applied. Here, one dye (donor) is linked to a phospholipid that inserts in the outer leaflet of the cell membrane, and another dye (acceptor) is loosely associated with the outer membrane. The dyes are located closely to each other which results in a fluorescent signal at a certain wavelength. Depolarization of the cell membrane, which can be linked to channel function, causes movement of the acceptor dye to the inner leaflet and a shift in fluorescent emission is detected. One drawback of fluorescence-based assays is that the membrane potential

is not actively controlled and additionally, it can be influenced by the negative charge of the dyes. Another problem can occur from quenchers that interfere with the fluorescence signal and distort the result, leading to a high number of false positives.[6]

After the first round of high-throughput screening (HTS), the lead compound needs to be further optimized to improve its action. In this secondary screening assay a throughput of 10 -100 compounds per day is desired. Here, patch clamp is applied, which is the golden standard for *in vitro* studies of compound activity on ion channels, even though it has a very low throughput. Manual patch clamp technique makes use of a pipette with a micrometer-sized tip diameter, which is pushed on the membrane of a cell, forming a gigaohm seal. The current that flows through individual ion channels in the membrane is measured electrophysiologically while controlling the membrane potential, yielding high-quality information on single channel behavior. Manual patch clamp allows only measuring one cell at a time, and additionally the experiment is tedious and requires a skilled operator, which results in a very low throughput and high costs. The development of automated patch clamp platforms, where the pipette is replaced by a planar substrate with arrays of microapertures, enables electrophysiological measurements with a much higher throughput and less user intervention.[6] Currently, automated patch clamp systems can achieve a throughput of 6250 compounds per day, such as the IonWorks Barracuda (Molecular Devices, Sunnyvale, CA, www.moleculardevices.com), which is promising also for primary screening.

Next to the target protein, new drug candidates must also be tested on cardiac ion channels, e.g., hERG, to exclude undesired effects on these proteins which can induce QT prolongation and eventually lead to sudden death. To assess ion channel safety, the screening assay must be of very high quality, reproducibility and reliability. The throughput of these assays is comparable to the secondary screening, and mostly the same techniques are used.[6] All of the above mentioned screening steps study the ion channel activity in the natural environment, the cell membrane. However, the cell is a complex system and other processes that are taking place in the cell can also influence this activity. Additionally, the interaction of the compound on the target is difficult to isolate as other proteins and lipids present in the cell membrane can play a role in this process. Finally, cell culture is required which is costly and time-consuming.

In this respect, our microfluidic device as a tool for drug screening on ion channels has the advantage of using a cell membrane model, which decreases the above mentioned drawbacks. However, some limitations are envisioned for our platform due to the strong competition on the market and the existing drug screening platforms. The standard technologies described above are fully developed and widely implemented, which makes it challenging to propose a directly competing product.

Specifically, this new product should exhibit better performance in terms of data quality and/or should have a higher throughput (at least 10 compounds per day) and/or be much cheaper. Only in that case, our platform would become interesting for pharmaceutical companies. Therefore, another more promising strategy would be to propose new functionalities, such as additional measurement schemes which would yield complementary and previously inaccessible information.

Table 7.1. Technologies for ion channel drug screening. Summary of various screening assays, their required throughput, suitable assay types and the resulting costs.[6]

Screening assays	Throughput	Assay type	Costs
Primary screening (HTS)	30 000 (>100 000) compounds/day	Fluorescent calcium dyes Voltage sensing dyes Membrane potential dyes	Low-medium Low-medium Medium-high
Secondary screening (hit confirmation, lead optimization)	10 – 100 compounds/day	Automated patch clamp Ion-flux assay (e.g., Rb^+) Patch clamp (single cell)	High Low Very high
Safety assessment (e.g., hERG ion channels)	10 – 100 compounds/day	Automated patch clamp Ion-flux assay (e.g., Rb^+) Patch clamp (single cell) Radioligand binding assay	High Low Very high Medium

If we compare our platform to the standard screening technologies, assuming the target protein is incorporated in our bilayer, complementary information is accessible from simultaneous confocal and electrophysiological measurements. In electrophysiological experiments, the signal of a single channel is required in order to yield high quality data on the gating mechanism. The implementation of confocal microscopy offers complementary information as it allows to optically identify, e.g., the activity of a particular channels which then can be linked to the electrical signal. The same could be applied for low conducting channels such as voltage-gated proton channels, which give a very small electrical signal (7-16 fA[7]), and additional optical information would increase the quality of the measured data. Finally, the field of stochastic sensing is mentioned, where single channels are modified to specifically detect the presence of, e.g., metal ions. In summary, the addition of high-resolution optical techniques to standard electrophysiology would not only allow generating high-quality data with complementary information but also exquisite data on, e.g., ion specificity. Alternatively, the platform could be applied for either electrical or optical measurements. Even though the competition of our platform with optical techniques

is challenging in terms of throughput, our technology could present unique advantages in terms of data quality.

1. Alternative applications: drug delivery and toxicity screening - transport across the membrane

The membrane is the first barrier every substance has to pass to enter the cell. Therefore, studying transport across the cell membrane is a very important aspect in intracellular drug delivery, but also for toxicity screening. Many drugs are developed to target intracellular biomolecules located in the cytoplasm or nucleus. However, to exert their therapeutic action they need to be transported across this impermeable barrier surrounding the cell.[8] The development of membrane-permeable drugs or dedicated packaging is thus of great importance, and good understanding of transport processes across the membrane is required for this purpose. For toxicity screening, the membrane transport of nanoparticles, or chemicals used in cosmetics, is interesting as well, but also the interaction of the compounds with the membrane and their ability to form pores or to disturb the membrane. Even though the cell membrane is the first barrier, finally the action of the drug on the complete organism must be understood, which is much more complex, as demonstrated in **Figure 7.3**. Generally, in order to understand the action of the target compound, first *in vitro* experiments on, e.g., single cells or cell cultures are performed, as these systems are rather simple and cheap compared to animal models. However, next to the transport across the cell membrane, also the transport of the substance through the body is important. Therefore in a next step, *in vivo* measurements on animal models are carried out to determine the uptake of the drug or nanoparticles by the body, and the action of metabolized products and their side effects.[9] This step is important and involves a system with a high level of complexity, that cannot be modeled *in vitro* yet, even though research on organs on chip make some first steps into that direction.[10] The results from the *in vitro* and *in vivo* experiments are then extrapolated in order to predict their action in humans. In the case of cosmetics however, animal testing has been recently banned by the EU and, therefore, alternative testing methods must be found.[11] In comparison with the currently used methods, such as cell cultures, eventually organs on chip, or animal models, our bilayer system is much more simple, which results in a less realistic testing model. On the other hand, the composition of the cell membrane influences its properties and structure, and might influence the interaction of substances with it, or transport across it. A controlled environment in terms of lipid composition and proteins, would help to understand the action of the target compound and facilitate the prediction of potential effects *in vivo*.

Toxicity screening of nanoparticles or other chemicals for, e.g., cosmetics, could be envisioned with our platform by measuring electrically or optically the influence and

interaction of these materials on and with the membrane. In this case, only the bilayer is needed and no cell. Still, the complexity and control of the system plays an important role. The bilayers can be made very simple, consisting just from one lipid species, up to a complex environment with many different and naturally relevant phospholipids, or even membrane proteins. This high level of control offers the possibility to elucidate mechanisms of the interactions of drugs or other substances with the membrane. In the field of drug development, our platform could play a role in preclinical tests as a pre-screening tool prior to cell or tissue experiments, and animal testing, where only low to medium throughput is required, but with a high quality of data. Here, the chemical-modifications of a potential drug candidate can be tested in terms of membrane transport and interactions with target proteins. In both applications no cell is needed, which makes it simpler and cheaper, and little competition is envisioned with (automated) patch-clamp techniques. However, regulatory aspects in these fields are very high, which may rise other obstacles for the transfer of our platform to the market. Additionally it is suggested, that our platform may find a niche in the market as a research tool, where throughput is less important but a variety of measurement schemes are of great interest. This functionality could be useful for instance to study the interactions of proteins with the membrane that are sensitive to the lipid composition[12] or to characterize engineered ion channels.[13]

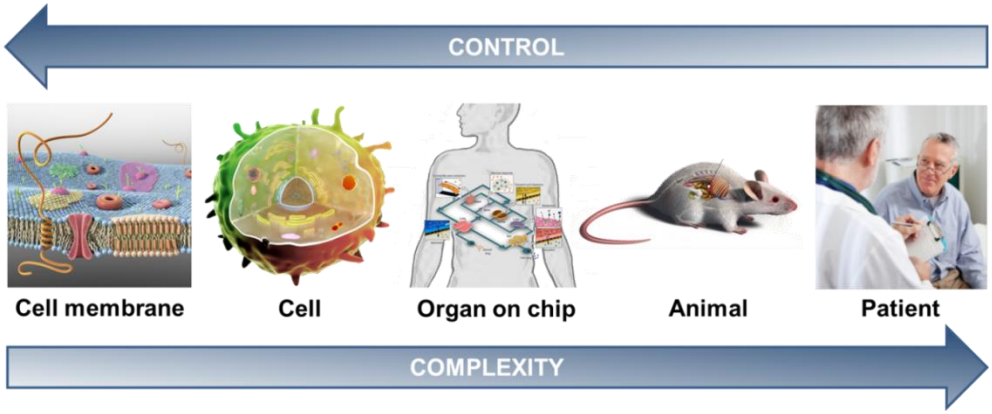

Figure 7.3. Complexity of potential models for screening of drugs, nanoparticles, or cosmetics. Potential screening models range from the cell membrane, to the complete cell (both images Nymus 3D), to organs on chip (internet)[14], to animal models (Nymus 3D), and finally to the patient (Bayer).[5] The more realistic the model, the higher the complexity of the system, and the lower the level of control.

Round table discussion: Commercialization

In a next step, the commercialization, the transition from a prototype towards the market, is discussed. Here, it is important to look at the bigger scope and not to only sell the platform but also, e.g., a new diagnostic procedure as in the case of the lithium

sensor of Medimate B.V. An important aspect in general is to get intimate knowledge of the targeted sector, e.g., of pharmaceutical companies and their needs. However, in this market it is difficult to get insider information, so that additional information of possible required applications can be gained by interacting with other companies in this field.

Additionally, funding is a very important aspect. Until the final product is on the market and money can be earned, the financial situation should be arranged, whereas the financial support is different depending on the application (research tool or commercial platform). For researchers, there are possibilities to apply for grants to financially support start-up businesses such as the Dutch valorization grant or a European grant. The last one includes, e.g., proof of concept experiments, IP screening, and the development of a business plan. In general it is advised to analyze the financial costs for different applications: e.g., electrophysiological measurements are relatively expensive, but maybe cheaper compared to confocal imaging. This means that tradeoffs must be made in terms of costs, resources and/or information content. However, many measurements can already be done with a conventional (fluorescence) microscope, which would still be an added value compared to conventional techniques but a "cheap" alternative to confocal microscopy.

Next to finance, IP plays an important role in the PCP, and should be considered already from the start and at least when steps are taken towards commercialization. Additionally, it can be used to increase the interest in the product. The technology in our microfluidic platform is not very complicated and might be difficult to protect, which could lead to problems when looking for investors and increases the risk for competition of other companies.
Finally, TA is mentioned in the process of commercialization, which helps to define gaps between different innovation pathways, identify customers and competitors, and analyze the risks that might be involved. Additionally, the application of TA might increase the chance to receive financial support from grants or private investors.

Technology roadmap
Mostly, a technology roadmap consists of three levels: technology, products/applications and markets. The construction of a roadmap is an approach that is applied in the business community, and it gives an overview of various paths a specific technology could evolve to in time, including alternative products and markets. The different layers are displayed graphically on top of each other, going from technology towards the market in the y-direction. The x-axis displays the time. The various technologies, products and markets are connected to each other by arrows, while the different levels can still influence each other.[15]

During our workshop, such a technology roadmap has been filled in, as shown in **Figure 7.4**, using the outcome from the discussion. However, horizontally this map is not aligned in time as many of the routes are still unclear and difficult to predict. Therefore, this figure consists of a "vision map" rather than a roadmap. During the construction in the workshop, a fourth layer for functionalities is added to the map.

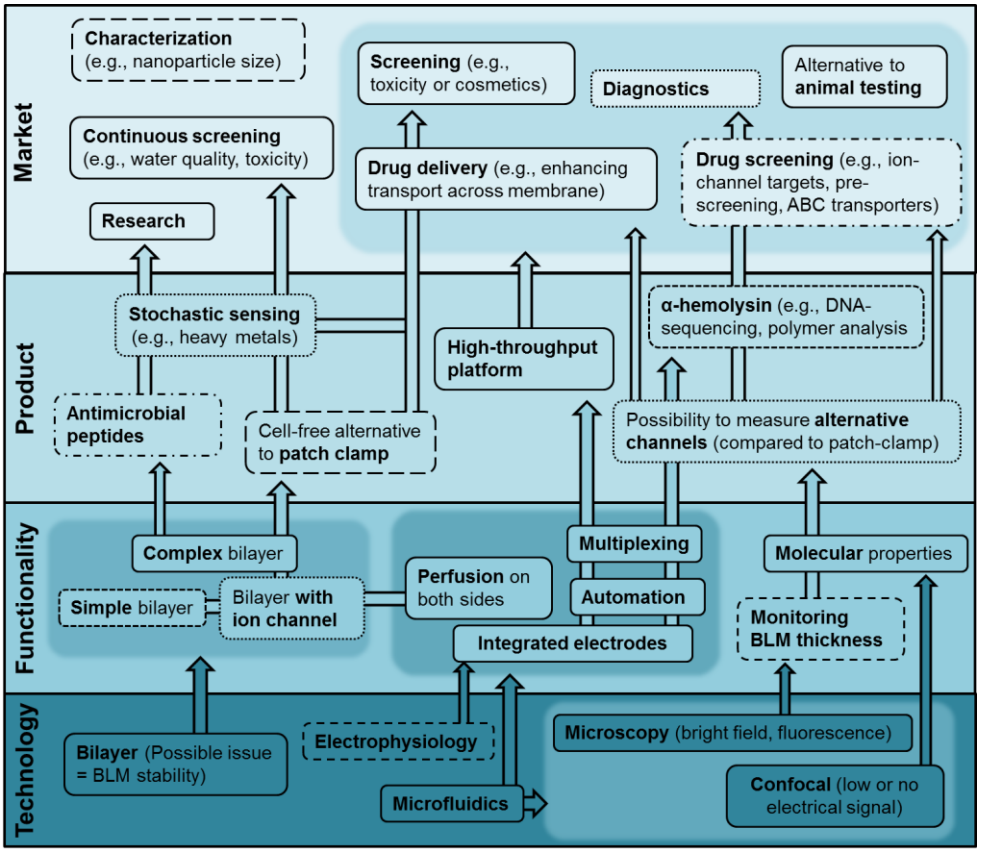

Figure 7.4. Vision map. Technology vision map for a microfluidic bilayer platform. The map is separated in four different layers of technologies, functionalities, products or markets. Each layer is filled with different boxes that are connected to each other or between the different layers. Colored backgrounds in the different layers indicate clusters of boxes and large arrows show connections to several boxes whereas small arrows connect only to one box. To make it more visual, several connections are also indicated by the same border-type of the boxes.

The technologies for our platform are the bilayer, electrophysiology, microfluidics and conventional as well as confocal microscopy. Typically, bilayer technology is linked with electrophysiology. In our platform however, the combination of bilayer experimentation with microfluidics is well suited for bright, fluorescence and confocal

microscopy as additional measurement schemes, due to the horizontal arrangement of the aperture. Next to that, microfluidics brings about various functionalities: multiplexing, automation and integrated electrodes, as well as perfusion of buffer solution on both sides of the membrane. The technology of bilayer formation also enables different functionalities: simple bilayers can be formed, as well as bilayers with a complex lipid composition or with proteins. The optical technologies allow determining, in combination with standard electrophysiological measurements the bilayer thickness, and give information on molecular membrane properties. Functionalities offered by microfluidics, such as the potential for automation, integration and multiplexing are essential for a high throughput platform. Such a system could affect many markets as, e.g., (drug) screening, drug delivery, diagnostics or the replacement of animal testing but also become a α-hemolysin-based sequencing platforms that might be useful as well for diagnostics. The different bilayer functionalities, combined with the perfusion, provide the possibility for a cell-free alternative to the standard patch clamp technique and could be useful for, e.g., continuous screening applications or characterization tools. The control of the bilayer environment can be of interest for studying the influence of the membrane composition on drugs, nanoparticles and for toxicity tests. The optical functionalities offer the possibility to measure channels that are not assessable by patch clamp experimentation, and therefore offer an alternative approach for drug screening or diagnostics. One important technical issue mentioned during the workshop concerns the bilayer stability, which is a crucial factor for long term measurements. In order to increase this parameter, smaller apertures could be used, and in this case bilayer formation would be possible also by collapsing vesicles or cells, which directly contain proteins.

7.3 Discussion

7.3.1 Workshop

The goals of the workshop to find alternative applications, to define routes for commercialization and societal embedding, to indicate factors that might influence technology transfer and product development, and to identify possible risks and regulations have been largely reached.

The initial application drug screening on membrane proteins is discussed in detail and many factors are indicated that potentially lead to risks in the technology transfer and/or commercialization process. On one hand, our bilayer platform will experience difficulties in competing with conventional cell-based drug screening platforms on the

market such as automated patch clamp technique, as they are implemented standard tools and already achieve high throughput. On the other hand, many regulatory aspects are required which must be taken into account during product development. One aspect here is the reliability of our bilayer platform to predict effects of drugs in the human, which is generally tested in more complex and realistic models such as animals, cells and tissues. The last point also accounts for the replacement of animal models in general for nanoparticle toxicity or cosmetic screening. Furthermore, possible risks are mentioned for IP protection, as the technology in our platform is not very complex. Finally, the financial aspect should be considered in terms of optical or electrical measurements, while choosing an application.

Next to possible risks, also alternative applications are defined. Targeting the same customer, the pharmaceutical industry, the platform could eventually be applied for drug testing during preclinical studies, which requires less throughput, or for studying drug delivery, or generally transport processes across the membrane. Alternatively, the technology could be commercialized as a research tool for, e.g., universities, including the offer to carry out measurements for customers. In a later stage, the research tool could be further commercialized with as target customer, e.g., the pharmaceutical industry. Finally, products are envisioned using various bilayer functionalities or by implementing optical measurements to target, e.g., alternative proteins, or to monitor the bilayer thickness which could be an interesting parameter for membrane research.

Additionally, a vision map is constructed with the results from the discussion indicating different routes for commercialization from various technologies towards a larger number of markets. During the workshop, the role of TA is shortly discussed, however the societal embedding is left out. In this early stage, where not even an application is defined yet, it is difficult to anticipate about possible impacts on society. However, it is important to consider it once a specific innovation path has been chosen.

Moreover, during the workshop all participants contributed actively to the discussion, and the broad range of backgrounds of the participants allowed many different aspects to be discussed.

7.3.2 Vision map

A vision map is drawn during the workshop with ideas from the discussion. The lower layers (technology and functionality) are filled in immediately. During the map construction, more ideas for possible applications (products and markets) are mentioned, but also concerns about possible cost effects are expressed. Interestingly, the microfluidic format is compatible with additional technologies such as high resolution imaging, and enables new functionalities (e.g., automation and multiplexing), and opens up new products and markets (e.g., screening platforms).

Therefore, it seems that the use of microfluidics would have a great impact from a commercial point of view.

As many different innovation pathways are displayed in the vision map, the next step requires to pick one or several routes defined in the roadmap and to analyze these routes in depth. Specifically, potential customers and markets should be defined, and the final potential product should be compared to existing products on the market, as well as to competitors. Next to literature research, this in-depth analysis could be carried out with additional workshops, interviews with various actors and landscape mapping scenarios.[16] In our case, the route towards a high-throughput platform for drug screening could be chosen, as this is our initial target application. Alternatively, a bilayer application could be chosen without proteins for the screening of nanoparticle toxicity or to study the passive transport across the membrane. Finally, an application using optical features could be selected, such as the use of our platform as a research tool.

7.3.3 Innovation journeys

As already mentioned above, after the definition of various innovation pathways the analysis of individual routes should be carried out. Here, different layers and factors like research, industry, regulations and society are linked to each other, as shown in a very simplified form in **Figure 7.5**. The innovation journey can start with the research that is translated into a product, to eventually reach the society. Alternatively, the research can be triggered by a demand in the society, new funding or regulatory regulations, or by the industry. In the following, several examples of these different innovation journeys for our bilayer platform are discussed, inspired by the vision map created during the workshop, and summarized in **Table 7.2**.

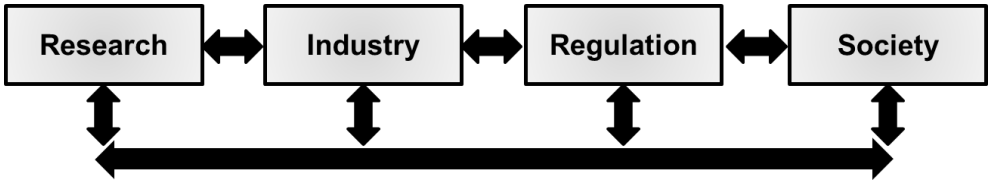

Figure 7.5. Simplified innovation chain model. The various dimensions, research, industry, regulation and society, which are connected in a linear model, can influence each other.

Table 7.2. Innovation pathways for the bilayer platform. Various different application areas (drug screening, nanoparticle toxicity, cosmetics and research) are analyzed in different dimensions such as technological considerations, commercial interest, regulations and risk management, and societal embedding. (N.A. = not available)

	Technological considerations	**Commercial interest**	**Regulations**	**Societal embedding**
Drug screening	*BLM with proteins* Optical and/or electrophysiological techniques	*Preclinical testing*: Improved efficiency, and reduced costs compared to implemented techniques	Regulatory framework already exists	N.A.
Nanoparticle toxicity	*Variable BLM composition* Optical (confocal)/ electrophysiological techniques	*Pre-screening*: Transport of particles across the membrane to predict potential toxicity	New accreditations needed	Growing concern for nanotoxicity
Cosmetics	*BLM without proteins* Fluorescence and electrophysiological techniques	*Pre-screening*: Membrane permeation, improved testing compared to current methods	Enforced in the EU	Demand for reduced or no animal testing
Research	*All variations of BLMs* High-resolution optical and electrophysiological measurements	*Research*: Platform for universities or research institutes and departments	N.A.	N.A.

Drug screening

Existing drug screening platforms are established in the process of drug development, as already discussed in detail above. Our platform could probably best be implemented in the secondary screening process, where usually the patch clamp technique is applied, and where throughput is less important than data quality. From the commercial point of view, an interest is expected, if our platform would give a faster or more reliable outcome, meaning that the platform would increase the process in efficiency and/or reduce costs. The regulations for the process are already established, which would dictate the development of the platform towards a product. As a drug screening tool, the platform would probably have little or no direct effect

on the society. In the complete process, our platform would be involved in the preclinical phase, together with other techniques, such as computer simulations, cell studies and/or animal testing. The final drug however, is only approved after passing several phases of clinical trials. The failure of an approved drug would not directly be related to our platform, as it is one part of a long process, but it could turn into a negative public perception of drug development processes in general and as a result lead to a change in regulations and safety standards, as already experienced before. In the late 1950s for instance, thalidomide has been given as a drug to pregnant women against morning thickness, but side effects caused horrible birth defects, which raised public concern about drug safety and triggered the development of new regulations and toxicity tests for drugs and chemicals.[17] On the other hand, if the platform would facilitate the prediction of successful drugs candidates and minimize animal testing, the societal acceptance for drug development in general could be improved. The implementation of the platform as pre-screening tool depends on its impact on the drug development process itself. If the platform helps to identify compounds that pass all phases of the clinical trial in a better way compared to the conventional techniques, the pharmaceutical companies would save a lot of money, as the last phases account for most of the development costs of a drug. Additionally, good drug candidates would reduce the number of side effects experienced by the patients in the clinical trial.

Nanoparticle toxicity

The implementation of our platform as a tool for nanoparticle toxicity screening, could be triggered, on one hand, from a growing concern in society about the toxicity of nanomaterials, and, on the other hand, from new regulations that are needed in order to characterize, test and screen these materials. Nanoparticles are made from various materials and come in all kinds of shapes, sizes and with various surface charges. Therefore, also the toxicity of different types of nanoparticles might not be the same. In order to test nanoparticle toxicity, new tools are required preferably minimizing animal testing. A very important part is the thorough characterization of the various types of particles in terms of physical and chemical properties but also the analysis of their pharmacokinetics, such as absorption, distribution, metabolism and excretion.[9] Here, our bilayer platform could be used as a pre-screening tool to study the interaction of various types of nanoparticles on the membrane, as well as their transport across it. De Planque et al. already demonstrated the suitability of a simple bilayer system for measuring electrophysiologically membrane disturbance by nanoparticles.[18] Additionally, the influence of the lipid composition on adsorption and permeability could be investigated to better understand the nanoparticle-membrane interaction and to predict particle toxicity.[19] In a next step during toxicity screening, the particles can be tested on full organisms to determine their distribution,

metabolism and excretion. Here, the development of organs on chip models are promising, especially as an alternative to animal testing. The use of our bilayer platform as a pre-screening tool could thus give a first indication whether a particular nanoparticle is potentially dangerous, and therefore decrease the number of compounds that are tested on more complex models. In general, the reliability is an important aspect for nanoparticle toxicity screening, also with respect to public acceptance. False positive measurements during safety screening, where nanoparticles are claimed to be safe but eventually turn out to be toxic to humans or the environment, can have a tremendous impact on society. Such a case could raise public concern for nanoparticles in general, even though only this particular type of particle, e.g., with a positive charge and from a certain material, is really toxic. Also, the public acceptance of nanoparticle-containing products could be reduced and influence the complete market. Furthermore, nanoparticles represent one type of product from the emerging field of nanotechnology, and carry the name "nano". If a public concern about nanoparticles expands, this could also influence other nanotechnology products even though they are not related to nanoparticles, neither are potentially dangerous. If the screening process however is reliable and the nanoparticles that are claimed safe are harmless, this could also increase the public acceptance for nanoparticles, and eventually for nanotechnology in general. Additionally to new screening platforms, also the regulations for nanoparticle toxicity screening must be reliable and should be evaluated, as existing regulations might not be applicable for nanoparticles. Here, legal uncertainty in the regulations can lead to a public distrust.[20] Even though there is a requirement for nanoparticle toxicity screening from the society and regulatory agencies, a diffused demand is visible for the industry. As potential business models, particle screening could be offered by a company as a service for large firms that produce these materials and probably need to prove that their products are safe. On the other hand, the platform can be sold to large companies to test the toxicity of their products in-house.

Cosmetics

To ensure safety of cosmetic products, their toxicity is conventionally tested on animals - experiments that are often poorly predictive as their toxicity is either over- or underestimated or simply cannot be translated reliably to humans.[17] Long term studies to estimate the potential of a chemical to cause cancer can take up to five years and require 400 rats. The false positive rate however lies at 90%.[17] In the last years, the public approval of animal testing is drastically decreasing in various countries in Europe[21] and animal rights activists such as for instance PETA (People for the Ethical Treatment of Animals, www.peta.org) or Proefdiervrij (www.proefdiervrij.nl) demand the prohibition of animal tests. The growing public concern as well as the unpredictability of these tests has led to the ban of animal models for testing

cosmetics in the EU and India from mid-2013 on,[22,23] which leads to a high demand for alternative testing methods. In the EU, the 3R-strategy of refinement, reduction and replacement is applied, with the goal to provide alternative tests with equivalent information compared to the *in vivo* models.[11] Due to the complexity of a complete organism, no valid *in vitro* replacement method is available for animal toxicity studies at the moment. In various fields however, substitutive tests already exist, for instance to evaluate cosmetics in terms of skin corrosion and irritation, dermal absorption, or mutagenicity. Our bilayer platform could be envisioned for studying the membrane permeability, which would give an indication on for instance the oral absorption.[11] Currently, the membrane transport can be studied with *in vitro* assays such as the Caco-2 cell monolayers or the parallel artificial membrane permeability assay (PAMPA). The Caco-2 assay consists of a cell monolayer, grown on a porous and thin substrate separating two stacked microwell plates, and the transport of the substance or drug from one to the other compartment is analyzed. This technique is applied to study passive and active transport across the cell membrane, as well as paracellular transport between the cells. The reproducibility however is not ideal and additionally, the assay is rather time intensive, as it can take up to 30 days to prepare stable and confluent cell monolayers.[24] In the PAMPA a similar approach is used, but instead of cells a lipid bilayer is formed from phospholipid solution in solvent on the filter between two compartments. This assay is much quicker compared to the Caco-2 assay, but only measures passive transport. In both cases, the transport is analyzed with UV spectroscopy, or liquid chromatography combined with mass spectrometry.[24] Here, our bilayer platform could have advantages compared to PAMPA, as our BLMs are formed across an aperture without any additional filter substrate present, that could influence the measurements. Furthermore, optical or electrical measurements can be performed giving the opportunity to measure *in situ* the transport across the membrane online by, for instance, using fluorescent labels and monitoring the fluorescence intensity in one compartment over time. Alternatively, the combination of our platform with conventional analytical techniques such as mass spectrometry could be an option as well. Commercially, this application could be interesting, if the bilayer platform could decrease the time and/or costs of the permeability studies. Here, a similar product could be used to test the transport across membranes for cosmetics, but also for nanoparticle toxicity, and drug screening, which increases market possibilities. Alternatively, computational methods are increasingly applied and combined with fundamental research. First, specific functions or pathways are analyzed in the lab and the resulting data is fed into an *in silico* model.[22] Here, the membrane penetration and interactions could be studied with our platform, and the results can be further investigated with computational techniques. As in the previous example, our platform would serve as pre-screening tool in a chain of various technologies. In Europe, the society is interested in products that are tested without

using animals, and therefore, the platform will have a good impact if it reduces the amount of animal testing. In China however, consumers are not as much concerned about animal tested products, but are more interested in the price or the brand.[23] On top of that, in China, animal testing is mandatory for new cosmetic products, which creates a dilemma for large cosmetic companies as they need to apply alternative methods for the European, and animal tests for the Chinese market.[23] The validation of new *in vitro* procedures in other countries could help to convince Chinese agencies to use alternative models as well, and therefore further increase the public acceptance of such platforms and the tested products.

Research

Finally, it is envisioned that our platform could be applied as a research tool. As already mentioned earlier, the combination of optical and electrophysiological techniques can yield complementary data that can be applied to study the influence of membrane properties on ion channel function or the effect of new materials (nanoparticles), proteins or drugs on the membrane. Here, for instance the alteration of membrane properties induced by non-specific drug effects would be an interesting research topic, especially for pharmaceutical companies. As a pure research platform, no regulations must be taken into account, which might facilitate commercialization, targeting universities, research institutes or research departments in companies as potential customers. For this application, at the moment no effect on the society is anticipated.

In conclusion, various innovation journeys can be chosen for one technology, as shown in **Table 7.2**, that are driven by different aspects. For drug screening the platform would be implemented in an existing chain, whereas for nanoparticle toxicity screening and cosmetic testing a new concern or demand, either in the society or in the regulatory landscape, creates the need for alternative screening platforms. After selecting various pathways from the vision map for further analysis, the next step would be to interact with knowledgeable actors in the different sectors to find interactions and missing links, for example by conducting interviews.[16] Based on **Table 7.2**, it would be interesting to find interviewees that are familiar with the technological points involved for a certain application, potential customers with a broad knowledge of the targeted market (e.g., pharmaceutical industry for drug screening), people from regulatory agencies that are familiar with the regulations and risks in the market, and finally non-government organizations or for instance journalists that have a good impression of the societal perception of a certain technology. After conducting interviews, a more precise scripting exercise can be performed to further predict hurdles and possibilities for our platform in a particular innovation chain.

7.3.4 Reflections

As a PhD student focusing on the development of one particular technology, it is an interesting experience to have a look at the process of bringing this technology to the market, even if the commercialization is not concretely targeted. Specifically, the workshop has been a great tool to identify important aspects for this journey. Even though the focus here is not directly placed on one particular application, the motivation of the project is to develop a drug screening platform for ion channels, and much input is obtained on potential hurdles and possibilities for its commercialization. The construction of a vision map helped to identify valuable technological aspects in this platform, such as the microfluidic format which offers many possibilities and leads to a number of applications. The comparison of the technology to existing platforms on the market is a very important task, which brings the system into perspective and reveals that the optical and especially confocal aspects are advantageous. Finally, it is a good exercise to think about the impact this particular technology may have on society, even though the platform only seems to have indirect effects.

Opportunities and tensions

As already mentioned above, the selected innovation pathways should be further analyzed in depths by conducting interviews to reveal concrete opportunities and possible hurdles. This step cannot be performed within this TA exercise due to the limited time available, however, a short discussion about possible opportunities and tensions for the four applications shown in **Table 7.2**, as well as future directions are shortly described below.

Although a number of risks were envisioned in this workshop for our platform to be applied as a drug screening tool on ion channels, the application of cell-free platforms for this purpose is promising, as recently acknowledged in the literature, showing opportunities for our device.[25] In the process of drug screening, our platform would be applied in early stages of drug research or in the secondary screening where lead compounds are optimized and tested. Conventionally, patch clamp is used in this step, and even though it has some drawbacks, it is the gold standard for ion channel studies. At the moment, bilayer platforms still need further improvement to fulfill the requirements of a drug screening platform on ion channels in terms of reliable and reproducible insertion of biologically relevant ion channels in the membrane, fast perfusion, high bilayer stabilities, as well as automation and parallelization.[26] On the other hand, for fundamental research in the early stage the high level of control and data quality offered by our platform could lead to new opportunities in this phase. In order to target the drug screening market, first a number of technological developments are required to fulfil the needs of pharmaceutical companies for such a

platform. Specifically, the throughput of the measurements must be increased in combination with automation of the bilayer formation and experimentation schemes, faster buffer perfusion must be integrated, as well as the reliable insertion of biologically relevant membrane proteins, and parallel electrophysiological measurements. So far, the multiplexing of our platform is only demonstrated, and water-soluble proteins are used for proof-of-principle experiments. For these technical improvements, the communication with pharmaceutical companies is extremely important to receive specific knowledge on the technological requirements they expect, such as protein targets, the number of experimentation sites that are acceptable, and the final costs they are willing to pay. Additionally, information is needed on the required regulations and standards that the platform must fulfil.

In contrast to the drug screening sector, replacement of animal testing for cosmetic products is now mandatory, which requires the development of alternative methods. Additionally, the screening of nanoparticle toxicity is becoming more important and new platforms and testing procedures are needed. Both demands create a niche in the market where our platform could play a role. As already discussed previously, it would be possible to apply our device to study the interaction or transport of substances with and across the membrane. In this case, in an early screening step, only a bilayer is needed, and the insertion of proteins is not per se required which would make the targeted product less complex. Since the two applications have similar requirements, both markets can be targeted which increases the market volume and the number of potential customers. A potential risk in this application could come from the large amount of regulations and extensive validations that the platform needs to go through in order to ensure toxicity information that can be translated to humans.[17] Additionally, high throughput screening would probably be preferred, which is not yet at a level to compete with cell based methods. Furthermore, for long term toxicity studies the stability of the BLMs must be increased which requires a few more technological development steps. Here again, the interaction with knowledgeable players in the particular market is of great importance. To define the required technological developments, future customers must be interviewed to get information on for instance the number of experimentation sites, the preferred bilayer stability, or the complexity of the system in terms of lipid composition and proteins in the bilayer. Furthermore, the desired characterization schemes, as for instance electrophysiological or optical techniques, should be investigated and matched with the resources of the customer. Additionally, cooperation with regulatory agencies is important already early in the commercialization process to implement possible requirements.

In general, for all the above mentioned screening applications, our platform would play a role in the research or pre-screening process and would be used in combination with other *in vitro* models (cells, tissues, organs on chip), since the combination of a

number of techniques is general practice and therefore should not create any additional hurdles.[17,22]

Finally, the platform is envisioned as a research tool. Here, the combination of high-resolution optical and electrophysiological techniques would be of great advantage for fundamental studies in terms of information content but also in terms of competition with other platforms. Membrane property studies as well as research on permeability or interaction of a molecule across or with the membrane would only require a model bilayer which decreases product complexity. A reliable protocol for protein insertion can still be developed in a later stage. At first, the platform could be marketed as a research tool, targeting universities or research institutes as customers. This could take place in collaboration with research groups, and via national and international funded research projects and grants, that stimulate product development, and additionally, would secure the first step of financial support. Moreover, no regulations are required for this application which makes the initial product development much easier and the market launching time shorter. Even though the product development might be more straight-forward, technological adaptations are still required such as the large scale assembly of the device and production of a customized chip holder. Again, intimate knowledge about the research practices and available equipment is crucial for the technology transfer. After development of a research platform, the same tool could be interesting as well for the R&D departments of for instance pharmaceutical companies, and the market can be extended at a later stage. Here, it would be good to keep such a step in mind, so that adaptations needed to fulfill their standards and regulations can be taken into account at an early stage.

In summary, the commercialization of our platform as a research tool seems to me the most feasible at this moment, even though all innovation pathways must be analyzed in more depth for a more detailed picture. Here, the transfer of the technology towards a prototype still requires technological developments, however, basic steps such as the wafer-scale fabrication, chip packaging and connection are also important for the other application areas. If these developments can be achieved in the frame of a grant, the financial support is secured for the first phase, and additionally, the close collaboration with research groups, which are potential customers, could facilitate the innovation process. Furthermore, successful validation and commercialization of our platform as a research tool, could also raise interest from the other markets, such as cosmetic and toxicity screening, or the research departments of pharmaceutical companies, as reported before.[16]

In conclusion, as a PhD student, the implementation of TA helped me to have a broader look at my project and at the technology, how it could be used and where it

eventually could be implemented. I could imagine that in general such an exercise could help to focus research and technological developments. Such a simplified chain model could be applied as a skeleton for scientists to place their technology into perspective and to foresee problems that might occur.

7.4 Conclusion and Outlook

As demonstrated in this chapter, our workshop is suitable as a pre-screening tool to gather information on (alternative) applications and commercialization pathways in a broad way, and this information can be used in a next step to focus on specific routes. The goals set for our workshop have been largely achieved, with as main visual result a vision map displaying various innovation pathways. One risk involved in this pre-screening approach is that the societal embedding is left out. Therefore, an important step is still the analysis of various innovation paths, especially with a focus on societal embedding.

Generally, technology assessment (or risk analysis) implemented into a PhD research project can be seen as a good opportunity to increase the reflexivity of researchers both, on their own research and on its impact on society. However, if RATA is implemented in e.g., a PhD research project, especially as a requirement, additional time should be reserved in the program that can be dedicated to this part. In my case, the workshop was organized within a short period of time, which is only possible with assistance from an expert in this particular field.

7.5 Acknowledgements

First, I would like to thank Dr. Douglas Robinson for many fruitful discussions and his support during preparation, organization and post-processing of the workshop. I also would like to thank all participants of the workshop for the active discussion, their input and for sharing their knowledge. Finally, I would like to thank Dr. Séverine Le Gac for bringing me in contact with Douglas and for supporting me throughout the complete process, even though it is not the main topic of my PhD research.

7.6 References

1. A. Rip, H. v. L., Bridging the Gap Between Innovation and ELSA: The TA Program in the Dutch Nano-R&D Program NanoNed. *Nanoethics* **2013,** *7*, 7-16.
2. J. Deuten, A. R., J. Jelsma, Societal Embedding and Product Creation Management. *Technology Analysis & Strategic Management* **1997,** *9*, 131-148.

3. A. Rip, H. t. K., Constructive technology assessment and socio-technical scenarios, Volume 1: Presenting Futures. In *The Yearbook of Nanotechnology in Society*, E. Fisher, C. S., J.M. Wetmore, Ed. Springer: Berlin, **2008**; pp 49-70.
4. Filmore, D., It's a GPCR world. *Modern Drug Discovery* **2004,** *7* (11), 24-28.
5. BayerPharmaAG From Molecules to Medicine. A Journey through Research and Development. . (accessed 27.05.14).
6. Zheng, W.; Spencer, R. H.; Kiss, L., High throughput assay technologies for ion channel drug discovery. *Assay and Drug Development Technologies* **2004,** *2* (5), 543-552.
7. Cherny, V. V.; Murphy, R.; Sokolov, V.; Levis, R. A.; DeCoursey, T. E., Properties of Single Voltage-gated Proton Channels in Human Eosinophils Estimated by Noise Analysis and by Direct Measurement. *The Journal of General Physiology* **2003,** *121* (6), 615-628.
8. Gupta, B.; Levchenko, T. S.; Torchilin, V. P., Intracellular delivery of large molecules and small particles by cell-penetrating proteins and peptides. *Advanced Drug Delivery Reviews* **2005,** *57* (4), 637-651.
9. Fischer, H. C.; Chan, W. C. W., Nanotoxicity: the growing need for in vivo study. *Current Opinion in Biotechnology* **2007,** *18* (6), 565-571.
10. van de Stolpe, A.; den Toonder, J., Workshop meeting report Organs-on-Chips: human disease models. *Lab on a Chip* **2013,** *13* (18), 3449-3470.
11. Safety, S. C. o. C., The Sccs's Notes Of Guidance For The Testing Of Cosmetic Substances And Their Safety Evaluation - 8th revision. Commision, E., Ed. SCCS 17th plenary meeting, 11 December 2012, **2012**.
12. van Rooijen, B. D.; Claessens, M. M. A. E.; Subramaniam, V., Lipid bilayer disruption by oligomeric α-synuclein depends on bilayer charge and accessibility of the hydrophobic core. *Biochimica et Biophysica Acta (BBA) - Biomembranes* **2009,** *1788* (6), 1271-1278.
13. Koçer, A.; Walko, M.; Meijberg, W.; Feringa, B. L., A Light-Actuated Nanovalve Derived from a Channel Protein. *Science* **2005,** *309* (5735), 755-758.
14. http://en.wikipedia.org/wiki/Organ-on-a-chip#mediaviewer/File:Conceptual_Schematic_of_a_Human-on-a-Chip.jpg (accessed 19.06.2014).
15. H. van Lente, J. v. T., A Combined Roadmapping-Cluster Approach For Emerging Technologies. *International Journal of Foresight and Innovation Policy* **2007,** *3*, 121-138.
16. D. den Boer, A. R., S. Speller, Scripting possible futures of nanotechnologies: A methodology that enhances reflexivity. *Technology in Society* **2009,** *31*, 295-304.
17. Abbott, A., Animal testing: More than a cosmetic change. *Nature* **2005,** *438* (7065), 144-146.
18. de Planque, M. R. R.; Aghdaei, S.; Roose, T.; Morgan, H., Electrophysiological Characterization of Membrane Disruption by Nanoparticles. *ACS Nano* **2011,** *5* (5), 3599-3606.

19. Li, S.; Malmstadt, N., Deformation and poration of lipid bilayer membranes by cationic nanoparticles. *Soft Matter* **2013,** *9* (20), 4969-4976.
20. Trisolino, A., Nanomedicine: Building a Bridge Between Science and Law. *NanoEthics* **2014**, 1-23.
21. von Roten, F. C., Public perceptions of animal experimentation across Europe. *Public Understanding of Science* **2013,** *22* (6), 691-703.
22. Mone, G., New Models in Cosmetics Replacing Animal Testing. *Communications of the ACM* **2014,** *57* (4), 20-21.
23. Lin, L., An Ugly Dilemma for Beauty Companies. *Bloomberg Businessweek* **2013,** (4348), 31-32.
24. Orsi, M.; Essex, J. W., Chapter 4 Passive Permeation Across Lipid Bilayers: a Literature Review. In *Molecular Simulations and Biomembranes: From Biophysics to Function*, The Royal Society of Chemistry: **2010**; pp 76-90.
25. Farre, C.; Fertig, N., HTS techniques for patch clamp-based ion channel screening – advances and economy. *Expert Opinion on Drug Discovery* **2012,** *7* (6), 515-524.
26. Kongsuphol, P.; Fang, K. B.; Ding, Z., Lipid bilayer technologies in ion channel recordings and their potential in drug screening assay. *Sensors and Actuators B: Chemical* **2013,** *185* (0), 530-542.

Summary and outlook

In this final chapter, a brief summary on the content of each chapter is given, together with the main results and conclusion. Subsequently, potential improvements are suggested that are required towards a drug screening platform, and additional experimentation schemes are proposed.

8.1 Summary

In this thesis, a microfluidic device for bilayer experimentation is developed, potential applications are explored, and its utilization for drug screening on ion channels is discussed.

In the last decade, miniaturization aspects and microfluidics have received increasing attention for bilayer experimentation. A number of systems have been reported, using various types of membrane models, including suspended bilayer lipid membranes (BLMs) or droplet interface bilayers (DIBs). These systems have shown potential for automation and multiplexing, as well as for commercial purposes (e.g., www.ionovation.com, www.nanion.de, www.librede.com). One particular promising application and one of the driving forces for the development of these miniaturized bilayer platforms, is drug screening on ion channels, as discussed in detail in chapter 2. Ion channels are involved in a number of diseases, which makes them attractive targets for the development of new drugs. Additionally, upon decision of the FDA, drugs must now be tested on cardiac ion channels, such as hERG, for safety reasons.[1] For both safety as well as drug effect assessment purposes, dedicated high-throughput screening assays and platforms are required. Current techniques for drug screening on ion channels lack from either low sensitivity and reliability (e.g., fluorescence-based assays), or lower throughput and high costs (manual and automated patch clamp). In that context, microfluidic bilayer platforms have emerged as an attractive alternative, since they do not require any dedicated environment, such as cell culture facilities, and they allow studying ion channels in a highly controlled and tunable environment, while reducing the volumes of the reagents and the overall cost of the assay. So far, first attempts for automation, multiplexing and parallel electrophysiological measurements have been described using this microfluidic approach, and platforms have been validated through preliminary drug screening experiments on ion channels.[2-4] Even though further development is required, these first examples clearly reveal the potential of microfluidic bilayer platforms for future application in the field of drug screening.

In this thesis, an alternative miniaturized platform is proposed for the formation of suspended bilayers in a fully microfluidic environment. This closed device includes two microfluidic channels, etched in two glass substrates, and separated by a Teflon foil. The latter Teflon layer possesses a microaperture, which is located at the channel intersection, where bilayers are formed. BLMs are prepared by successive flushing of lipid and buffer solutions through the microfluidic channels. A lipid plug is left in the aperture, which spontaneously and instantaneously thins into a bilayer with no intervention of the experimenter. This quasi-automated approach gives a high success yield of ~100% for formation of the membrane, and the process can be monitored in

the device both optically and electrically. The bilayer lipid composition is varied, and bilayers characterized in depth, using a combination of optical (bright field) and electrophysiological techniques. Next, the activity of ion channel or pore-forming species (gramicidin and α-hemolysin) is recorded in the microfluidic platform, with a single ion channel resolution. Finally, the potential of the platform for drug screening is illustrated by a gramicidin-based assay, where changes in the membrane environment upon addition of ethanol or aspirin, are sensed by recording variations in the gramicidin activity (chapter 3).

In a next step, the device is adapted to be compatible with high-resolution imaging. For that purpose, the bottom glass substrate is thinned down to yield a thickness comparable with a cover slip for confocal microscopy measurements. This capability is exploited to visualize phase separation in a membrane prepared from a ternary lipid mixture (L-α-phosphatidylcholine, sphingomyelin and cholesterol). Next, the potential of the platform for multi-parametric measurements is demonstrated, and a combination of electrophysiology and confocal microscopy is applied to study POPC bilayers supplemented with two probes (gramicidin and/or fluorescently labeled lipids, NBD-PE). The bilayers are characterized in terms of thickness and lipid diffusion (e.g., fluidity), while the gramicidin activity is recorded. These combined measurements reveal interesting findings: while NBD-PE has no effect on the bilayer thickness, gramicidin induces thinning of the membrane, most probably by squeezing out the solvent entrapped in the bilayer, upon pore formation. This effect is not observed when both probes are present in the system. Additionally, an overall decrease in gramicidin activity is detected, suggesting that NBD-PE has some influence on the mechanical bilayer properties, and hinders pore formation. Conversely, no influence of gramicidin on the membrane fluidity could be observed (chapter 4).

Next, this combined measurement approach is further applied in a setting where membrane properties are altered by the addition of cholesterol (15 and 40% mol), to investigate the influence of membrane properties on ion channel activity. As before, the bilayer thickness and fluidity are assessed, while recording the gramicidin activity. The specific capacitance increases upon addition of cholesterol, suggesting thinning of the bilayer, while the lipid diffusion is reduced in a cholesterol concentration dependent manner. Unexpectedly, the gramicidin activity (pore formation rate) drops when cholesterol is present in the bilayers, which cannot be explained by the reduction in fluidity alone. At the same time, the single channel lifetime becomes shorter, while both the measured decrease in BLM thickness and fluidity are expected to cause the opposite. Collectively, these results suggest that other parameters, such as the bilayer mechanical membrane properties - which cannot be accessed in our device

- are altered upon addition of cholesterol and play an important role to modulate the gramicidin activity (chapter 5).

For its application in drug screening, the platform must be improved, with respect to two main features, which are the automation and multiplexing of the experiments. Multiplexing is examined with two different designs, the Fishbone and TripleX that contain so far up to four bilayer experimentation sites. Furthermore, the technique for bilayer formation is adapted to reduce the number of pipetting steps, which is essential for future automation. Specifically, the lipid solution is applied only in one of the two channels - compared to both channels previously. This approach allows bilayer formation as well in smaller apertures (50 μm compared to 100 μm), and larger BLMs are obtained. The fabrication of the multiplexed platform is more challenging, primarily for two reasons: first, the footprint of the device is greater, which proves to be an issue for assembly of the device; and second, the apertures, whose size is made smaller to eventually enhance bilayer stability, do not exhibit anymore their well-defined shape. However, the two designs are tested for bilayer formation, followed by early electrophysiological recordings on gramicidin activity (chapter 6).

In parallel, a technology assessment exercise is performed for the herein presented microfluidic bilayer platform; a workshop is organized with participants from various backgrounds, to identify possible routes for commercialization of the platform and to discuss its possible societal impact (chapter 7). In terms of commercialization, a number of possible issues are mentioned, including regulatory requirements, and obvious competition with existing and well-established automated patch clamp systems. Therefore, the bilayer microfluidic platform could more likely be implemented as a tool to investigate the transport across membranes, interaction of nanoparticles with membranes for toxicity screening, and maybe for cosmetic testing. For all these applications, the platform would be part of a complex screening process, so that the proposed technology is unlikely to have any direct influence on the society. Alternatively, the platform could be highly interesting for researchers in academia or pharmaceutical companies, due to its unique multi-parametric characterization capability.

8.2 Outlook

The experiments described in this thesis primarily highlight the versatility of the herein developed microfluidic bilayer platform. However, before the initial goal of drug screening on ion channels is reached, various key elements remain to be addressed. For instance, the insertion of biologically relevant ion channels in the bilayer must still be demonstrated; perfusion of the solutions on both sides of the membrane, without

endangering its stability, must be implemented; and temperature control on chip is required. On other aspects, next to alternative applications envisioned in chapter 7, the suitability of the platform for combined confocal and electrophysiological measurement schemes is highly attractive for other applications, as discussed below.

A first and essential step is to insert biologically relevant ion channels in the bilayer. So far, only gramicidin and α-hemolysin have been utilized in our experiments, and they have been either added to the lipid solution prior to bilayer formation, or to the buffer solution, from which they spontaneously self-insert. Biologically relevant ion channels, on which drugs are eventually tested, as for instance the ryanodine receptor (RyR) or hERG, must be either kept in a hydrophobic and functional environment, such as proteoliposomes, which are subsequently fused with the bilayer, or solubilized with detergents. Proteoliposome fusion, which has been tested in this work without any success, is highly challenging.[5] Conventionally, the proteoliposomes are delivered manually close to the bilayer in order to initiate fusion, followed by stirring of the solution. In our closed microfluidic device, the proteoliposomes are added to the liquid reservoirs and flow is induced by hydrostatic pressure to transport the liposomes to the aperture. In the microfluidic channels however, no mixing or active transport takes place, which might make it more difficult for the proteoliposomes to actually reach the bilayer, and additionally, the risk of liposome adsorption to the channel walls is high. Furthermore, proteoliposome fusion is promoted in the presence of an osmotic gradient across the membrane, this gradient inducing swelling of the vesicles, which might influence bilayer stability.

Another highly important aspect for ion channel experimentation and drug screening is the fast and reliable exchange of buffer solution in the microfluidic channels without membrane rupture. Ideally, only one ion channel is reconstituted in the BLM, which means fusion of only one liposome containing one protein. To favor this situation, directly after fusion is detected, the *cis* reservoir, where the vesicles are added must be perfused quickly to remove the osmotic gradient and the remaining vesicles. For studying the effect of drugs on ion channels, perfusion is also required, to introduce the drugs on one side of the bilayer.[6] In general, the perfusion system must be chosen depending on the targeted application. For instance, pipetting robotic systems could be used; they would facilitate automation of the liquid handling while avoiding the presence of tubing and connections that are present in a conventional pumping system (e.g., syringe pumps). Obviously, fast perfusion is easier to implement in a closed system. On other aspects, flow control in the channels would be highly advantageous for assessing membrane mechanical properties such as the membrane tension, by determining the amount of bending of the membrane in the aperture using confocal microscopy, as already observed upon buffer evaporation

(chapter 4). If flow is applied in a controlled way, the BLM mechanical properties could be assessed, and correlated to the gramicidin activity. So far, we have focused on other membrane properties, such as their thickness and fluidity and their relationship with gramicidin activity. However, our results suggest an important contribution of mechanical properties, which would be interesting to test in the future by performing membrane tension measurements in our platform.

Finally, the implementation of a temperature control in the device is important, since the outcome of biological processes is frequently temperature dependent, as for instance diffusion phenomena in the membrane and in solution, and the lipidic organization.[7,8] Additionally, certain ion channels such as hERG have been shown to exhibit different responses to drugs depending on the temperature.[9] For now, all experiments reported in this thesis have been performed at room temperature, which is not physiologically relevant.[9]

As already shortly mentioned above, the unique combination of confocal and electrophysiological measurements, which is possible in our platform, is very powerful for a number of studies. So far, we have utilized this capability for diffusion measurements using FRAP, together with ion channel recordings on gramicidin activity. However, in a next step, the same approach could be applied to visualize the interactions between soluble or membrane compounds and ion channels by using FRET (Förster Resonance Energy Transfer), in combination with electrophysiological measurements.[10] This dual approach would yield additional information on the pore formation process by optically detecting the binding of the target, inducing conformational changes in the protein, while electrophysiologically recording the ion channel activity. Additionally, ion transport across the bilayer could be assessed optically by utilizing ion sensitive dyes.[11] The ryanodine receptor (RyR), which is an intracellular calcium channel involved in cardiovascular diseases and which is a target for anti-arrhythmia drugs,[12] is conventionally studied either in its natural environment, in the membrane of a cell, or using conventional bilayer set-ups, since RyR is present in an intracellular membrane, which is not easily accessible for the patch clamp technique. RyR activity is measured in a cell by visualizing the Ca^{2+} flux across the membrane using ion sensitive dyes and confocal microscopy.[13] However, as the cell is a very complex system, the different proteins present in the cell membrane, and the rich cytosolic and luminal solutions have an impact on the mechanisms of Ca^{2+} signaling and on their reaction to drugs and chemical stimuli. Additionally, neighboring RyR channels might influence each other.[13] As a result, extra information on the single channel level in a controlled environment is essential to get closer insight into the channel behavior. These single channel measurements are typically carried out by reconstituting the RyR channel into a bilayer system, which reveals its opening and closing behavior. However, the results of the cell and single channel studies cannot

directly be compared to get "the big picture",[12] since the experimental conditions for both measurements are different, and additionally, signals from RyR clusters are detected in the cell membrane,[13] while single ion channels are measured using electrophysiology. In that context, the availability of a platform combining both measurement approaches - electrophysiology and high-resolution confocal microscopy - would provide a unique opportunity to correlate optical and electrophysiological recordings, and would bring a better insight into understanding the RyR channel.

In summary, the microfluidic bilayer platform described in this thesis does have a potential to become a drug-screening tool on ion channels in the future, although a number of developments are still required before this goal is actually reached. Furthermore, the system is highly versatile and suitable for multi-parametric experiments, which is a key-asset to study fundamental biophysical processes.

8.3 References

1. Xu, J.; Wang, X.; Ensign, B.; Li, M.; Wu, L.; Guia, A.; Xu, J., Ion-channel assay technologies: quo vadis? *Drug Discovery Today* **2001,** *6* (24), 1278-1287.
2. Kongsuphol, P.; Fang, K. B.; Ding, Z., Lipid bilayer technologies in ion channel recordings and their potential in drug screening assay. *Sensors and Actuators B: Chemical* **2013,** *185* (0), 530-542.
3. Steller, L.; Kreir, M.; Salzer, R., Natural and artificial ion channels for biosensing platforms. *Anal Bioanal Chem* **2012,** *402* (1), 209-230.
4. Zagnoni, M., Miniaturised technologies for the development of artificial lipid bilayer systems. *Lab on a Chip* **2012,** *12* (6), 1026-1039.
5. *Ion Channel Reconstitution*. Plenum Press: New York, **1986**.
6. Dunlop, J.; Bowlby, M.; Peri, R.; Vasilyev, D.; Arias, R., High-throughput electrophysiology: an emerging paradigm for ion-channel screening and physiology. *Nat Rev Drug Discov* **2008,** *7* (4), 358-368.
7. Honigmann, A.; Walter, C.; Erdmann, F.; Eggeling, C.; Wagner, R., Characterization of Horizontal Lipid Bilayers as a Model System to Study Lipid Phase Separation. *Biophysical Journal* **2010,** *98* (12), 2886-2894.
8. Tank, D. W.; Wu, E. S.; Meers, P. R.; Webb, W. W., Lateral diffusion of gramicidin C in phospholipid multibilayers. Effects of cholesterol and high gramicidin concentration. *Biophysical Journal* **1982,** *40* (2), 129-135.
9. Stoelzle, S.; Obergrussberger, A.; Bruggemann, A.; Haarmann, C.; George, M.; Kettenhofen, R. F.; Fertig, N., State-of-the-art automated patch clamp devices: Heat activation, action potentials and high throughput in ion channel screening. *Frontiers in Pharmacology* **2011,** *2*.
10. Borisenko, V.; Lougheed, T.; Hesse, J.; Fureder-Kitzmuller, E.; Fertig, N.; Behrends, J. C.; Woolley, G. A.; Schutz, G. J., Simultaneous optical and

electrical recording of single gramicidin channels. *Biophysical Journal* **2003,** *84* (1), 612-622.

11. Harriss, L. M.; Cronin, B.; Thompson, J. R.; Wallace, M. I., Imaging Multiple Conductance States in an Alamethicin Pore. *Journal of the American Chemical Society* **2011,** *133* (37), 14507-14509.
12. Zhou, Q.; Xiao, J. M.; Jiang, D. W.; Wang, R. W.; Vembaiyan, K.; Wang, A. X.; Smith, C. D.; Xie, C. H.; Chen, W. Q.; Zhang, J. Q.; Tian, X. X.; Jones, P. P.; Zhong, X. W.; Guo, A.; Chen, H. Y.; Zhang, L.; Zhu, W. Z.; Yang, D. M.; Li, X. D.; Chen, J.; Gillis, A. M.; Duff, H. J.; Cheng, H. P.; Feldman, A. M.; Song, L. S.; Fill, M.; Back, T. G.; Chen, S. R. W., Carvedilol and its new analogs suppress arrhythmogenic store overload-induced Ca2+ release. *Nat. Med.* **2011,** *17* (8), 1003-U126.
13. Porta, M.; Zima, A. V.; Nani, A.; Diaz-Sylvester, P. L.; Copello, J. A.; Ramos-Franco, J.; Blatter, L. A.; Fill, M., Single Ryanodine Receptor Channel Basis of Caffeine's Action on Ca2+ Sparks. *Biophysical Journal* **2011,** *100* (4), 931-938.

Appendix I

Capacitance measurements

1. Capacitance correction

For the capacitance measurements, a triangular wave (50 Hz, 75 mV pp) is applied, and the resulting current response (ideally a square wave, **Figure 1** a) is recorded using a LabView interface. First, the system is calibrated using solid state capacitors (1 to 56 pF) and the bilayer capacitance is derived from the resulting calibration curve by determining the amplitude of the square wave.

The capacitance values are corrected for possible leakage currents, which add a resistive component to the capacitance curve and lead to distorted tips, as shown in **Figure 1** b. To correct for this effect, the mean current values of the distorted tips are utilized to receive the amplitude of the curve (**Figure 1** b), and the capacitance is calculated as before.

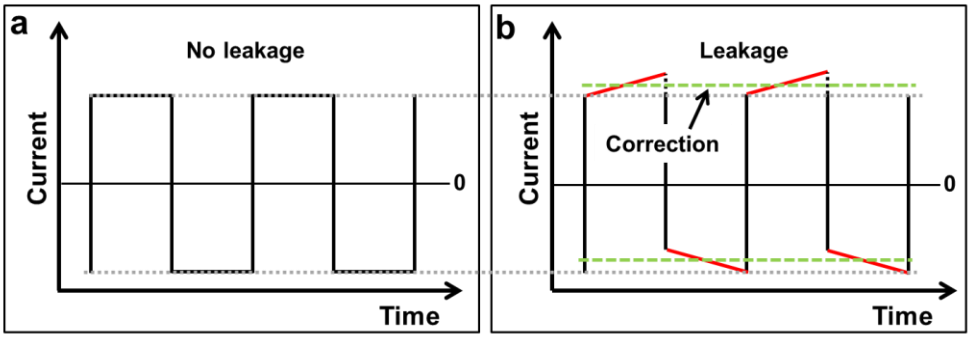

Figure 1. Capacitance correction. a) The response of the bilayer to the triangular wave is recorded using a labview interface, which typically is a square wave. b) The distorted tips (red) are caused by the presence of a leakage current. To correct for this, the mean value of the tips, here defined by the green lines, is taken as amplitude to calculate the actual capacitance.

2. Specific capacitance

In chapter 5, POPC BLMs (25 mg/mL in n-decane) with various concentrations of cholesterol (0, 15 and 40% mol) are utilized. To demonstrate that the specific capacitance is stable over the time course of one experiment, C_s is monitored for all plain POPC bilayers without and with cholesterol over ~30 min, as shown in **Figure 2**.

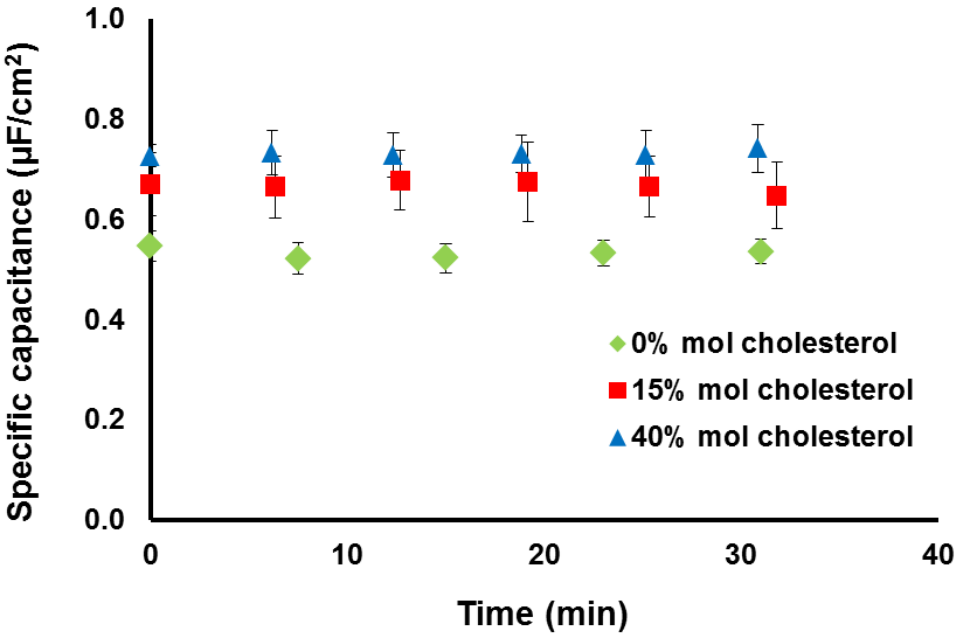

Figure 2. Specific capacitance. The specific capacitance for plain POPC BLMs is measured over time, for various cholesterol concentrations (0, 15, and 40% mol). For all conditions, error bars as standard deviation (n = 6 for 0 and 40% mol, n = 5 for 15% mol).

Appendix II

FRAP measurements

1. Regions of interest

After bilayer formation and before starting the FRAP experiments, a picture is taken at the center of the bilayer with a zoom of 3.5 (63x/1.4 oil DIC objective). Two regions of interest (ROIs) are drawn on this image, each with a 15 µm diameter and with a distance of 10 µm in the *x*-direction, as shown in **Figure 1**. The *y*-position of both ROIs is the same, to keep the scan time as small as possible. For the bleaching, one region is selected as bleach ROI and the other as reference ROI. Prior to the experiment, the focus is adjusted to yield the highest fluorescent intensity. During the experiment, the intensity of both ROIs is recorded by scanning from top to bottom in a line scan mode. The scanning of both ROIs is called one "cycle". For the analysis, the average intensity for each ROI is calculated per cycle.

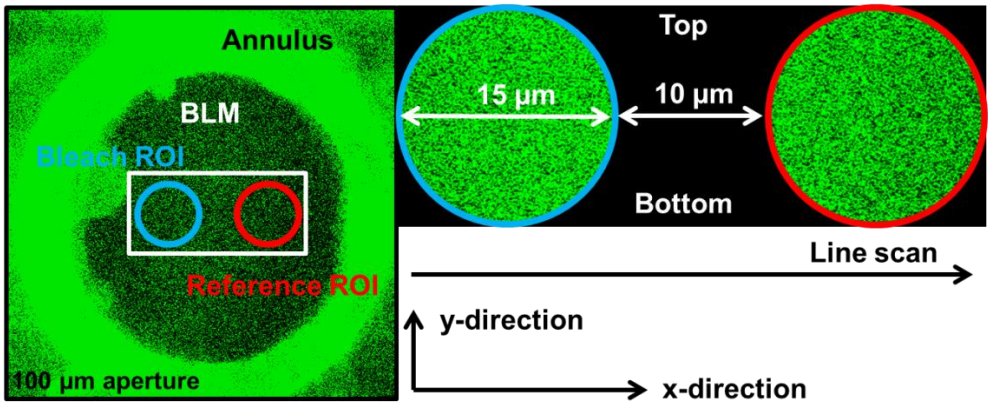

Figure 1. Regions of interest (ROIs). Bleach and reference ROIs are defined in the center of the bilayer, and the intensity is recorded by scanning from top to bottom in a line scan mode.

2. Bleaching protocol

For the FRAP experiments, the intensity of both ROIs is recorded over time, with a scan time of 0.22 s per cycle, and a total recording of 500 cycles (including bleaching), while one cycle includes the imaging of both ROIs. During the scanning, the laser intensity (I_{laser}) of the Argon laser (λ = 488 nm) is set to 0.5%. First, 20 cycles are

recorded to capture the fluorescence intensity before bleaching (pre-bleach, laser intensity of 0.5%), as shown in **Figure 2**. Following this, the bleach ROI is illuminated with an increased laser intensity of 100% to photobleach this region, while the reference ROI is not imaged. To increase the amount of bleach, 5 iterations are carried out leading to a total bleach time of 1.32 s. The bleaching step is not included in the total number of cycles. After bleaching, the remaining 480 cycles are recorded for both ROIs with a laser intensity set at 0.5%. The lipid molecules which are freely diffusing in the bilayer, replenish the bleach area with a rate depending on their mobility, resulting in a progressive recovery of the fluorescent intensity in the bleach ROI. The recovery rate is related to the diffusion of the phospholipids in the membrane. After the experiment, the bilayer is ruptured and the same protocol is repeated to determine the background fluorescence. For each BLM, the bleaching is carried out at least twice.

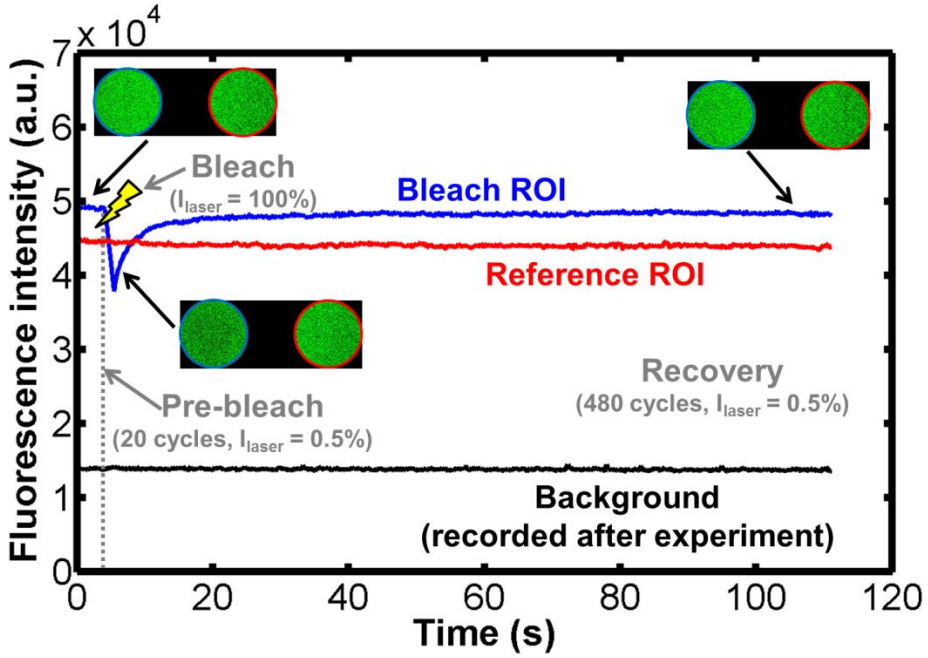

Figure 2. Bleaching protocol. First, the fluorescent intensity of the bleach and reference ROI is recorded for 20 cycles (pre-bleach). The fluorescence of the bleach ROI is reduced with a high intensity laser pulse (bleach), and the recovery is recorded for 480 cycles (recovery). The background fluorescence is measured after rupturing of the bilayer after the experiment.

3. Data analysis

Data of the FRAP experiments are analyzed with the software FRAPAnalyser (freeware from the University of Luxemburg, http://actinsim.uni.lu/eng). First, the

FRAP curve is normalized with respect to the reference ROI and the background measurement. Therefore, the following equation is applied, whereas I_{ref} and I_{frap} are the average intensities of the reference and bleach ROI, respectively. I_{back} corresponds to the background fluorescence. The subscript *_pre* represents the average intensity for the bleach and reference ROIs before bleaching and after subtraction of the background. Here, the background fluorescence cannot be recorded during the experiment, and is only determined after membrane rupture. The resulting normalized curve is shown in **Figure 3**.

$$I_{norm}(t) = \frac{I_{ref\_pre}}{I_{ref}(t) - I_{back}(t)} * \frac{I_{frap}(t) - I_{back}(t)}{I_{frap\_pre}}$$

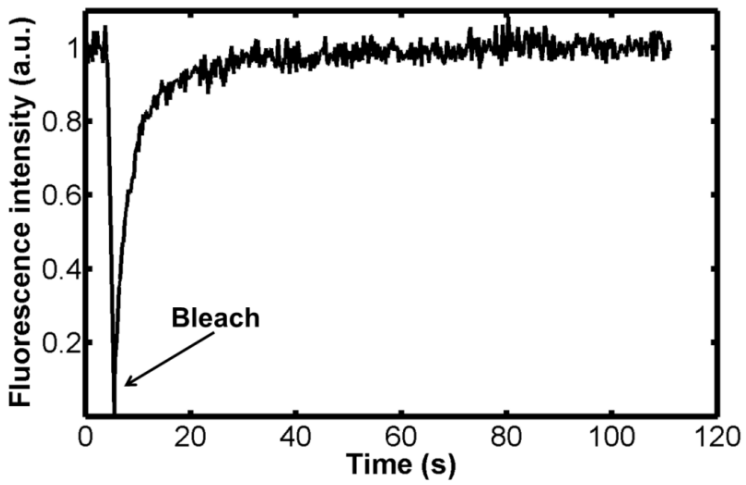

Figure 3. Normalized FRAP curve. After the experiment, the fluorescence intensity is normalized with respect to the reference ROI and the background measurement.

After the normalization of the curve, the software is used to determine the diffusion constant, and mobile and immobile fractions by fitting the curve. Therefore, the diffusion model for a circular spot is used, as shown below.[1]

$$\mathrm{FRAP(t)} = a_0 + a_1 * e^{\frac{\tau}{2(t-t_{bleach})}} * \left(I_0\left(\frac{\tau}{2(t-t_{bleach})}\right) + I_1\left(\frac{\tau}{2(t-t_{bleach})}\right)\right)$$

Here, $\tau = \frac{w^2}{D}$, and $I_0(x)$ and $I_1(x)$ are modified Bessel functions. D is the diffusion constant, w the radius of the bleach spot, a_0 and a_1 are normalizing coefficients which account for non-zero intensity at the bleach moment and incomplete recovery.[2]

4. References

1. D.M. Soumpasis, Theoretical Analysis of Fluorescence Photobleaching Recovery Experiments, *Biophysical Journal*, **1983**, 41, 95-97.
2. FRAPAnalyser, User Manual, University of Luxembourg, **2009**.

Appendix III

Gramicidin analysis

Gramicidin is dissolved in ethanol (100 nM) and added to the lipid solution prior to bilayer formation to yield a final concentration of 1 nM. After BLM formation, the gramicidin activity is recorded by applying a dc voltage of +80 mV while monitoring the current response (1 kHz Lowpass Bessel filter, 10 kHz sampling rate) with a patch clamp set up (CV 203 BU head stage and Axopatch 200B amplifier (both Molecular devices, Sunnyvale, CA, USA)). Data are acquired using a LabView interface and a PCI-6259 data acquisition board (National Instruments, Austin, TX, USA), and are analyzed using an in-house written Matlab routine after filtering with a moving average filter.

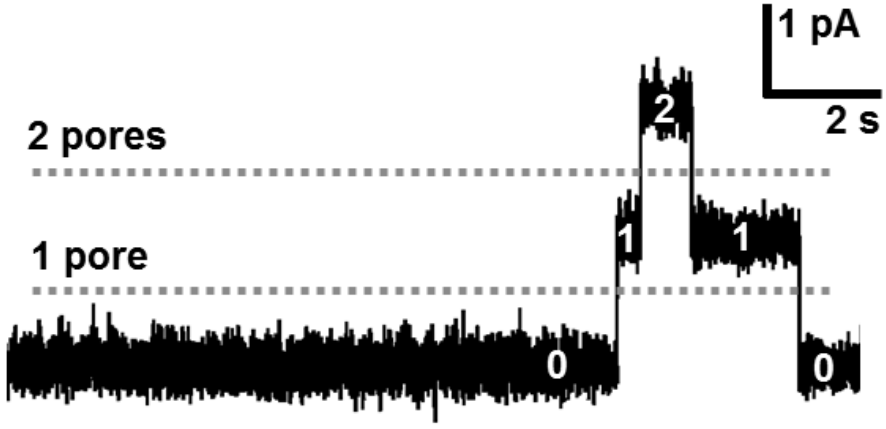

Figure 1. Gramicidin analysis. Snapshot of a gramicidin recording with multiple pores opened simultaneously. The grey lines illustrate the manually set thresholds to assign the measured current to the number of simultaneously open pores. The current below the first threshold belongs to 0 pores, the current above the first threshold to 1 pore, and the current above the second threshold to 2 pores. Recording from a POPC lipid bilayer (25 mg/mL in n-decane) with 1 nM gramicidin, (+80 mV applied, 1 kHz Lowpass Bessel filter, 10 kHz sampling rate) and filtered with a moving average filter in Matlab (window size 50).

The pore formation process gives rise to transient steps in the recorded current, and in certain bilayer types, multiple pores are opened simultaneously (**Figure 1**). To analyze the different current steps, a threshold, shown by the grey lines, is set manually for each experiment in the Matlab routine, to determine whether the recorded current belongs to no pore (0), 1 pore (1), 2 pores (2) or more pores. In the

following, each data point is analyzed and assigned to a certain category in a matrix. For instance, if the current is below the first threshold, the data point is assigned to the category 0, if it is above this threshold, it is assigned to category 1. It should be noted, that the threshold itself is not used as the current value, since not all events are expected to have the same amplitude as a mixture of gramicidin (A, B, and C) is applied. If one data point cannot be assigned to the previous category (e.g, 0 pores), a new category is opened in the matrix (e.g., 1 pore). Finally, all data points from one category are averaged and the length of this category and the corresponding current value are summarized in a new matrix. To determine the amplitude from one pore, the difference between two following current levels is calculated and added to the matrix (**Table 1**). These values are utilized for further analysis.

Table 1. Gramicidin analysis. Categories are defined by a manually set threshold, representing the number of pores simultaneously detected (0, 1 or 2). The open time and the amplitude of each event are assigned to a certain category, placed in a matrix, and used for further analysis.

# pore	**0**	**1**	**2**	**1**	**0**
Open time (s)	10.56	0.39	0.88	1.82	1.78
Pore amplitude (pA)	-	1.36	1.33	1.35	-

For the open probability (t_{open}/t_{total}), the complete time of all open channels (the open time of the categories 1, 2, etc.) is divided by the total recording time (all categories including 0).

The channel lifetime is determined by plotting the number of events for various lifetimes in a histogram taking into account each pore event. The lifetimes are normalized and fitted using Matlab with $N(t)/N(0) = \exp(-t/\tau)$ with N being the number of events and $N(t)$ the number of channels observed with a lifetime longer than t. The average single channel lifetime, τ, is derived from the fit. It should be noted here, that for BLMs where multiple channels simultaneously occur, this approach doesn't take into account the disassembly rate of the pores, and therefore the calculated lifetime is expected to give an underestimated value for the average single channel lifetime.

Finally, the single channel conductance is derived from the height of each pore and plotted as the number of events for a certain conductance value.

Samenvatting

In dit proefschrift wordt de ontwikkeling van een microfluïdische chip voor het maken van kunstmatige celmembranen, bilayer lipid membranes (BLMs), beschreven. Daarnaast wordt de mogelijke toepassing van deze chip voor het ontwikkelen en testen van medicijnen aan ionkanalen besproken.

Ionkanalen zijn eiwitten in het membraan van een cel en verantwoordelijk voor het passieve en selectieve transport van ionen door het celmembraan. Deze eiwitten zijn belangrijk voor fundamentele functies in het lichaam die ervoor zorgen dat we kunnen bewegen, voelen, leren en denken. Mutaties in ionkanaal genen kunnen dus ernstige ziektes veroorzaken, bijvoorbeeld Taaislijmziekte, Epilepsie of Hartritmestoornis. Daardoor zijn deze eiwitten belangrijke doelwitten voor medicijnen en op het moment werken ~13% van de geneesmiddelen op ionkanalen.

Alhoewel deze eiwitten belangrijk zijn voor het ontwikkelen van medicijnen zijn de huidige platformen en procedures niet optimaal. Aan de ene kant worden technieken toegepast waar de ionenstroom door eiwitten indirect wordt gemeten, met bijvoorbeeld fluorescentie. Hierdoor kan een hoge throughput worden bereikt maar deze gaat gepaard met een lage resolutie en nauwkeurigheid. Als alternatief wordt de patch clamp techniek gebruikt waar de stroom van ionen direct door enkele ionkanalen gemeten wordt. Deze techniek levert gedetailleerde informatie over de eigenschappen van een specifiek eiwitkanaal, maar vereist een ervaren experimentator, is tijdsintensief en daardoor heel duur. In de laatste jaren is deze methode verder ontwikkeld naar de geautomatiseerde patch clamp techniek, waardoor gedetailleerde informatie kan worden verkregen met een hogere capaciteit. Alhoewel de bovengenoemde methodes belangrijke informatie leveren hebben ze een gezamenlijke nadeel: ze werken met cellen, waarvoor een speciale werkomgeving nodig is. Dit is niet het geval voor kunstmatige celmembranen waardoor ze een veelbelovende alternatief zijn om medicijnen aan ionkanalen te testen vergeleken met de bovengenoemde procedures. De conventionele BLM opstelling bestaat uit twee mL-reservoirs die gescheiden worden door een hydrofoob materiaal met een kleine opening voor het membraan. In de laatste jaren is veel onderzoek gedaan om de conventionele BLM opstelling te converteren naar een microfluïdisch systeem. Het werken met kleinere volumes levert een kostenbesparing op - een belangrijk punt voor drug screening. Bovendien zorgen de kleine structuren voor stabielere membranen en snellere processen. De oriëntatie van de opening is vaak horizontaal waardoor ook optische analysemethoden makkelijk kunnen worden toegepast. De voor- en nadelen van de huidige methodes voor drug screening en de ontwikkeling van microfluïdische chips en hun potentieel voor deze toepassing zijn besproken in hoofdstuk 2.

In de erop volgende hoofdstukken wordt een alternatieve microfluïdische chip voorgesteld om vrijstaande BLMs te maken. Deze chip bestaat uit twee microfluïdische kanalen die gefabriceerd zijn in glas en uit een micro-opening in een Teflon folie welke zich bevindt bij de intersectie van de twee kanalen (hoofdstuk 3). Het membraan wordt gevormd door het spoelen van een vet- en een waterige oplossing door de kanalen en de formatie gebeurt meteen en spontaan met een hoge succesratio (~100%). Het proces kan zowel elektrisch worden gemeten met capaciteitsmetingen als optisch met een microscoop waarbij de oppervlakte van het membraan bepaald wordt. Door deze combinatie van elektrische en optische technieken toe te passen kunnen membranen met verschillende composities worden gekarakteriseerd. Elektrofysiologische metingen aan enkele model eiwitten zoals α-hemolysin en gramicidine laten zien dat met de metingen een hoge elektrische resolutie bereikt kan worden. Uiteindelijk, om het potentieel van de platform voor het testen van medicijnen te laten zien, zijn metingen gedaan aan gramicidine waarbij de activiteit van dit peptide is bestudeerd na de verandering van de membraaneigenschappen door toevoeging van verschillende chemicaliën (ethanol en Acetylsalicylzuur).

De chip beschreven in het vorige hoofdstuk is verder aangepast voor optische metingen met een hogere resolutie (hoofdstuk 4). Hiervoor wordt de onderste glas laag geslepen tot een dikte van ~200 μm zodat de chip geschikt is voor confocale metingen. Om deze functionaliteit te testen worden membranen van een vet mengsel (L-α-phosphatidylcholine, sphingomyelin en cholesterol) gemaakt dat microdomeinen vormt welke zichtbaar zijn met een confocale microscoop. In de volgende stap wordt de confocale optie gecombineerd met elektrofysiologische metingen om POPC membranen te bestuderen die verrijkt zijn met gramicidine en/of fluorescerend gelabelde NBD-PE. De dikte en de vloeibaarheid van de membranen zijn gekarakteriseerd en tegelijkertijd wordt de activiteit van gramicidine gemeten. Deze gecombineerde metingen laten zien dat NBD-PE geen invloed heeft op de dikte van de membranen, terwijl gramicidine het membraan dunner maakt, waarschijnlijk door het verwijderen van oplosmiddel (n-decaan) tussen de twee lagen van de BLM. Dit effect is niet zichtbaar voor membranen die gramicidine en NBD-PE bevatten, wat erop wijst dat NBD-PE een invloed heeft op andere membraaneigenschappen en wat ook te zien is in de gramicidine metingen. De vloeibaarheid van het membraan wordt niet beïnvloed door het peptide zelf.

In hoofdstuk 5 wordt de gecombineerde experimentele opzet toegepast om de invloed van verschillende concentraties cholesterol (15 en 40% mol) op de eigenschappen van het membraan te bepalen en uiteindelijk de verandering van de functie van ionkanalen te meten door dezelfde parameters te karakteriseren als boven beschreven (dikte, vloeibaarheid en gramicidine activiteit). De resultaten suggereren dat de toevoeging

van cholesterol het membraan dunner maakt terwijl de vloeibaarheid afneemt. Het is interessant om op te merken dat de formatie van gramicidine poriën bijna verdwenen is in membranen met cholesterol en ook de levensduur van de poriën is gereduceerd, wat niet alleen te verklaren is met de verandering in de hier gemeten membraan eigenschappen (dikte en vloeibaarheid). Daarom wordt aangenomen dat cholesterol andere eigenschappen zoals de elasticiteit of kromming van het membraan verandert die op het moment nog niet kunnen worden gemeten in onze chip.

Voor het bovengenoemde doel, het testen van medicijnen aan ionkanalen, moet de chip geschikt zijn voor geautomatiseerde en geparallelliseerde metingen. Om een eerste stap in deze richting te zetten, zijn twee nieuwe designs ontworpen voor het maken van maximaal vier membranen tegelijkertijd: de TripleX en Fishbone. Bovendien is de techniek om membranen te maken aangepast zodat minder pipetteerstappen nodig zijn door de vetoplossing maar in één kanaal aan te brengen in plaats van beide kanalen, wat uiteindelijk een voordeel voor automatisering is. Deze methode is getest in een kleinere opening (50 μm in plaats van 100 μm) en laat zien dat een groter membraanoppervlakte verkregen wordt met deze methode. Hoewel de fabricagestappen dezelfde zijn vergeleken met de bovengenoemde enkele chip, is het bonden van de geparallelliseerde chips moeilijker door de vergrootte oppervlakte. Verder resulteert het maken van kleinere openingen in minder strakke randen, wat een nadeel is voor het vormen van de membranen. Door deze uitdagingen zijn alleen voorlopige tests gedaan met beide designs, en een enkele meting van gramicidine welke wel laat zien dat ook deze chips een goede elektrische resolutie hebben om enkele poriën te kunnen detecteren (hoofdstuk 6).

Het laatste gedeelte van dit proefschrift, hoofdstuk 7, beschrijft de technology-assessment van onze microfluïdische chip. Hiervoor werd een workshop georganiseerd met deelnemers van verschillende vakrichtingen om de mogelijkheden voor commercialisering van ons platform te bespreken en om over alternatieve toepassingen te discussiëren. Voor het ontwikkelen van een product worden een aantal uitdagingen verwacht zoals regelgevingen die gelden voor verschillende toepassingen en concurrentie van bestaande technieken en bedrijven op het gebied van medicijnontwikkeling. Als alternatief voor het testen van medicijnen aan ionkanalen zou de chip ook gebruikt kunnen worden om naar het transport door het membraan te kijken voor toxiciteitstests van nanodeeltjes of voor het testen van cosmetica. Voor alle toepassingen zou onze chip terechtkomen in een keten van verschillende meetmethodes waardoor het effect van deze technologie op de maatschappij niet direct te herkennen is. Verder wordt ook de mogelijkheid besproken om onze chip te gebruiken als onderzoekstool voor universiteiten of onderzoeksafdelingen in farmaceutische bedrijven.

Dit proefschrift wordt afgesloten met een samenvatting en aanbevelingen voor de toekomst (hoofdstuk 8).

List of publications

Journal articles

First author:

Stimberg et al., "High Yield, Reproducible and Quasi-Automated Bilayer Formation in a Microfluidic Format", 2013, Small, 9, 7, 1076–1085. **Cover article** (**Chapter 3**)

Stimberg et al., "Miniaturized lipid bilayer platforms: promising tools for drug screening on ion channels", Manuscript in preparation. (**Chapter 2**)

Stimberg et al., "Comprehensive measurement approach combining confocal microscopy and electrophysiology to elucidate lipid-ion channel interactions in a microfluidic format.", Manuscript in preparation. (**Chapter 4**)

Stimberg et al., "Simultaneous confocal and electrophysiological recordings to assess cholesterol-induced changes in bilayer properties and their effect on gramicidin single channel properties", Manuscript in preparation. (**Chapter 5**)

Second author:

Prokofyev et al., "Multiplexed microfluidic bilayer platform for studies on membrane proteins", Manuscript in preparation. (based on **Chapter 6**)

Conference proceedings

Stimberg et al., "BLM experimentation and opto-electrical characterization in microchips. Towards an integrated platform for drug screening on membrane proteins." Proceedings of MicroTAS 2010, Groningen (The Netherlands), 830-832.

Stimberg et al., "Integrated microfluidic platform for fundamental bilayer studies and experimentation on single pore-forming species." Proceedings of MicroTAS 2011, Seattle (WA, USA), 1400-1402.

Stimberg et al., "Simultaneous confocal and electrophysiological assessment of membrane properties and ion channel activity in a microfluidic format – a powerful

combination for drug development", Proceedings of MicroTAS 2014, San Antonio (TX, USA).

Prokofyev et al., "Multiplexed microfluidic platform for electrophysiological measurements on ion channels in a functional environment", Proceedings of MicroTAS 2014, San Antonio (TX, USA).

Oral presentations

"Studying the impact of membrane properties on ion channel activity in a microfluidic format – an important aspect in drug development." NanoBio-Europe 2014, Münster (NRW, Germany), 2-4 June 2014.

"Multiplexed Microfluidic Device for Bilayer Experimentation and Drug Screening Assays on Membrane Proteins." 56th Annual Meeting of the Biophysical Society 2012, San Diego (CA, USA), 25-29 February 2012.

"Integrated microfluidic platform for studies on membrane proteins and drug screening assays." MicroNano conference 2011, Epe (The Netherlands), 15-16 November 2011.

"Integrated microfluidic platform for fundamental bilayer studies and experimentation on single pore-forming species." MicroTAS 2011, Seattle (WA, USA), 2-6 October 2011.

"Integrated microfluidic platform for studies on membrane proteins and drug screening assays." 55th Annual Meeting of the Biophysical Society 2011, Baltimore (MD, USA), 5-9 March 2011.

"BLM experimentation and opto-electrical characterization in microchips. Towards an integrated platform for drug screening on membrane proteins." NanoBioTech, Montreux (Switzerland), 15-17 November 2010.

Lectures

"Exploring innovation pathways for nanomedicine platforms." Presentation at the NanoNextNL Board Meeting for the midterm review, Utrecht (The Netherlands), 13 March 2014.

"Microfluidic platform for bilayer experimentation - Application to monitor membrane dynamics using confocal microscopy combined with electrophysiological measurements of gramicidin activity." SRO meeting Nanomedicine, MESA+, University of Twente (The Netherlands), 16 January 2014.

"Microfluidic platform for bilayer experimentation and drug screening on membrane proteins." Presentation for the NanoNextNL Supervisory Board Meeting, Utrecht (The Netherlands), 20 November 2013.

"Versatile microfluidic platform for bilayer experimentation." SRO meeting Enabling Technologies, MESA+, University of Twente (The Netherlands), 10 April 2013.

"Microfluidic platform for drug screening on membrane proteins." Journal club presentation, visiting the lab of Prof. Michael Fill and Dr. Dirk Gillespie. Rush University Medical Center, Chicago (IL, USA), 10 October 2011.

"Integrated microfluidic platform for bilayer studies and experimentation on single pore-forming species." MESA+ day, University of Twente (The Netherlands), 27 September 2011.

Posters

"Probing Simultaneously Membrane Dynamics and Protein Activity in Suspended Bilayers in a Microfluidic Format." 58th Annual Meeting of the Biophysical Society 2014, San Francisco (CA, USA), 15-19 February 2014.

"Integrated microfluidic platform for fundamental bilayer studies and experimentation on single pore-forming species." Dutch meeting on Molecular and Cellular Biophysics, Veldhoven (The Netherlands), 1-2 October 2012.

"BLM experimentation and opto-electrical characterization in microchips. Towards an integrated platform for drug screening on membrane proteins." NanoBioTech, Montreux (Switzerland), 14-16 November 2011.

"BLM experimentation and opto-electrical characterization in microchips. Towards an integrated platform for drug screening on membrane proteins." MicroTAS 2010, Groningen (The Netherlands), 3-7 October 2010.

Acknowledgements

Yes, you have reached the right page – welcome to my acknowledgements! After four years I am writing the final section of my thesis, the one that is most widely read. And this is not surprising, because during the last few years I received much help and support from so many people: without you I could not have finished this book, thank you so much!

Specifically, I would like to start by thanking you, Albert, for giving me the opportunity to do my PhD in the BIOS Lab-on-a-chip group. Your ideas and suggestions during our meetings were always helpful and stimulating. BIOS is a great group to work in and I like to think back to our "uitjes", the workweeks and the yearly mountain biking tours finishing with a BBQ at your place.

Séverine, you were my daily supervisor during the last four years, and I am so grateful for everything you have done for me – without your help this book would not exist. Your door was always open to discuss experiments, new results, and all problems and challenges that I faced during this time. Time and again you motivated and inspired me, leaving space for my own creativity while guiding where necessary. Thanks for the time you spent helping practice my presentations, correcting my writing, and for your pep-talks in between. I learned a lot from you! Next to working with you, I also like to think back to the trips we took together to Osnabrück, Bielefeld, the US (and Mexico ☺), and Switzerland, and to the evenings in the city center, talking, joking and enjoying nice beers.

Great thanks also goes to our technicians. Hans, we first met in the Biochip group, long time ago. I am simply amazed by the gadgets you make, which you create so quickly after only one short discussion and from a very vague drawing. Johan, thanks for the time you spent in the clean room fabricating my chips, developing such a great technique to produce apertures and for your support and patience in teaching me these fabrication steps. Jan v. N., you were always helpful for introductions, when new filters were needed for the microscope and for helping with computer problems. Eddy, additionally to our "gezellig" talks in Dutch and German, your door was always open for questions and you took the time to help finding an answer, thanks. Paul, your support in the lab is highly appreciated, same as your good mood and our German conversations ☺. Next, I would like to thank Ad and Wouter O., for taking the time to answer all questions regarding electrical problems and for clarifying many things. Mathieu, you introduced me to Matlab and wrote a large part of my program for data analysis. Thank you so much for spending time on this, patiently answering all

my questions and explaining it in a very clear way. Alexander, you taught me a lot about electrophysiology and our discussions were very helpful. Jan E., I had a great time with the nanoteam. It is so much fun to see the expression on the kids' faces when you tell them about nanotechnology! Hermine, there were so many things that needed to be arranged and organized - thank you for always taking care of this.

During the last years, I spent many hours behind my computer. Luckily, this also meant having nice conversations, serious discussions and a lot of fun with my office mates: Susan (thanks for correcting my Dutch summary), Andries (I really enjoyed "Germanischen-Freitag" ☺), Lonneke, Laura, Anis, and Songyue. Justyna, thanks for the long talks about life, work, and traveling, it felt so good at the end of a working day. Thank you also for agreeing to be my paranymph! Also, together with you, Lennart and Guillaume, I had the privilege to organize one of the BIOS workweeks which was an amazing experience and so much fun! Adithya, we had a lot of fun, during outings, pub-quizzes (as thunder bunnies ☺), lunch breaks, and conferences. Thanks for being my other paranymph!

The time at BIOS was "ontzettend gezellig", especially through the many evenings in the city center, dinners, BIOScope movie nights, Friday afternoon talks and drinks, sport events, and many helpful and interesting discussions, conversations and laughs. Thanks to all past and present members of the BIOS group for this unforgettable time: Allison, Arpita, Bjorn, Burcu, Edwin, Egbert, Evelien, Fleur, Floor, Floris, Henriette, Iris, Jean-Philippe, Karel, Lingling, Liza, Loan, Loes, Maarten, Maria-Andrea, Marinke, Masood, Miguel, Mingliang, Natalia, Paul V., Pavel, Rik, Rerngchai, Rogier S., Rogier V., Rosa, Sertan, Sourav, Stefan, Trieu, Wei-Shu, Wesley, Wouter S., Yanbo, Yawar, Yusuf, and Zhenxia. I would also like to thank my students, Auke and Lucas, for your help.

Next to BIOS, I got much help from the NBP group. Martin, thanks for lending me the patch amplifier for the combined confocal and electrophysiological measurements. Burcu and Aditya, you answered so many questions I had about FRAP, you were a great help. Himanshu, you always took time to help me with the confocal and I really enjoyed our coffee breaks, thanks.

I would also like to thank Roland and Karsten from Ionovation GmbH. Our lunches and dinners at the Biophysical meetings were always fun, as well as the visits to Osnabrück. Roland, thank you for all the time you spent with me in the lab, answering all questions and helping me to improve my "lab-German". Marco T. and Federico, thanks for the discussions about electrical measurements and the multiplexing, here in Enschede and in Cesena. Mike and Dirk from the Rush University Medical Center, thanks for the opportunity to visit your lab and for all the things you taught me about

the Ryanodine receptor, even though it has not worked yet – I hope you will manage soon to measure it in our devices!

Douglas, thank you so much for your help with my TA chapter and for the nice discussions. I really enjoyed our meetings at "Bagels & Beans", each time learning much more about TA, and how to look at my work from a different perspective. It was a great experience to organize the workshop with you!

Next to the help from colleagues, I had a lot of support from my friends. A special thanks goes to "my girls", Astrid, Caro, Eva, Helen, Janin, Jenny, Mareike, Rachel, Resi, and Steffi for always being there, for our wonderful meetings which are just great like always, no matter how long we haven't seen each other, for so many laughs, and parties. You are the best friends I could wish for! Thanks also to my other friends from home and for the great times we had together, going camping or visiting each other for New Year's, for all the nice messages in the last months and for your continuous interest in my work!

Finally, without the support of my family I wouldn't be where I am now. Birgit, Uli, Annette, Michi, Ronja und Lenter (naja, quasi Familie ☺): vielen Dank für euer Interesse und eure Unterstützung die letzten Jahre und für die vielen lieben Berichte und Gedanken, besonders in den letzten Monaten. Simon, auch wenn wir uns nicht so oft sehen, die langen (Konzert-)Abende in Münster, Düsseldorf oder Enschede waren wunderbar zum Entspannen! Vielen Dank auch für deine Hilfe beim Cover. Mama und Papa, ihr habt mich immer unterstützt in allem was ich machen wollte und immer an mich geglaubt. Eure bedingungslose Liebe hat mich zu dem Menschen gemacht der ich heute bin – vielen Dank dafür! Last, but definitely not least: Stephan. Die letzten Monate waren nicht immer einfach für dich. Immer und immer wieder hast du es geschafft mich wieder aufzubauen, du hast mir neue Energie und Motivation gegeben, du hast mir den Rücken gestärkt, immer an mich geglaubt und mich immer wieder zum Lachen gebracht. Bei dir zu sein und in deinen Armen zu weinen und zu lachen ist das schönste was es gibt - ich liebe dich!

Love,

Verena